Role of hypoxia in the regulation of the microRNA-containing RNA-induced silencing complex

A dissertation

submitted by

Connie Wu

In partial fulfillment of the requirements

for the degree of

Doctor of Philosophy

in

Biochemistry

TUFTS UNIVERSITY

Sackler School of Graduate Biomedical Sciences

February 2012

ADVISER: Dr. Akiko Hata

LIST OF ABBREVIATIONS

17-AAG	17-allylamino-17-demethoxygeldanamycin
Ago	Argonaute
ALK	Activin-receptor-like kinases
ANOVA	Analysis of variation
ARNT	Aryl hydrocarbon receptor nuclear translocator
bHLH	Basic helix-loop-helix
BMP	Bone morphogenetic protein
bp	Basepairs
BRF1	Butyrate response factor-1
CBP	Cyclic AMP-responsive element binding protein–binding protein
ChIP	Chromatin immunoprecipitation
ChIP-on-chip	Chromatin immunoprecipitation-on-genomic DNA microarray chip
CNN	Calponin
co-IP	Co-immunoprecipitation

C-P4H	Collagen prolyl 4-hydroxylase
C-P4H(I)	Type I collagen prolyl 4-hydroxylase
CPEB	Cytoplasmic polyadenylation-element-binding protein
DAPI	4'-6-Diamidino-2-phenylindole
DGCR8	DiGeorge syndrome critical region gene 8
DMEM	Dulbecco's modified Eagle media
DMSO	Dimethyl sulfoxide
DOCK7	Dedicator of cytokinesis 7
dsRBD	Double stranded RNA binding domain
EGF	Epidermal growth factor
EGFR	Epidermal growth factor receptor
eIF2α	Eukaryotic translation initiation factor 2α
EPO	Erythropoietin
ER	Endoplasmic reticulum
ERK	Elk-related tyrosine kinase
FBS	Fetal bovine serum
FITC	Fluorescein isothiocyanate

FMRP	Fragile X mental retardation protein
FXR1	Fragile X mental retardation-related protein 1
G3BP	GTPase activating protein (SH3 domain) binding protein
GA	Geldanamycin
GDFs	Growth and differentiation factors
GFP	Green fluorescent protein
GLUT1	Glucose transporter 1
Grb2	Growth factor receptor-bound protein 2
GST	Glutathione S-transferase
h	Hour
HIF	Hypoxia-inducible factor
hnRNP	Heterogeneous nuclear ribonucleoprotein
HREs	Hypoxia response elements
Hsp	Heat shock protein
IP	Immunoprecipitation
IPAH	Idiopathic pulmonary arterial hypertension
KLF4	Krüppel-like factor 4

KSRP	KH domain-containing RBP
MAPK	Mitogen-activated protein kinase
MAPKAPK2	MAPK-activated protein kinase 2
MID	Middle
miRNA/ miR	MicroRNA
mLin41	Mouse homologue of lin-41
mRNP	Messenger ribonucleoprotein
MRTF	Myocardin-related transcription factor
NHL	Ncl-1, HT2A and Lin-41
nt	Nucleotides
O_2	Molecular oxygen
PABP-1	Poly(A)-binding protein 1
PACT	Protein kinase R-activating protein
PAH	Pulmonary arterial hypertension
PARG	Poly(ADP-ribose) glycohydrolase
PARP-13	Poly(ADP-ribose) polymerase-13
PAs	Pulmonary arteries

PAS	Per-ARNT-Sim
PASMCs	Pulmonary artery smooth muscle cells
PAZ	Piwi Argonaute Zwille
P-bodies	Processing bodies
PDCD4	Programmed cell death protein 4
PDGF	Platelet derived growth factor
PDGFR	Platelet derived growth factor receptor
PEI	Polyethylenimine
PES	2-phenylethynesulfonamide
PHD	Prolyl hydroxylase domain
PI3K	Phosphatidylinositol 3-kinase
PIWI	P-element-induced wimpy testis
PKC	Protein kinase C
PLC-γ	Phospholipase C-γ
PMR1	Polysomal ribonuclease 1
pre-miRNA/ pre-miR	Precursor microRNA
pri-miRNA/ pri-miR	Primary microRNA transcript

qRT-PCR	Quantitative reverse transcription polymerase chain
RACK1	Receptor of activated C-kinase
RBPs	RNA-binding proteins
RISC	RNA-induced silencing complex
RLC	RISC loading complex
RNA pol II	RNA polymerase II
R-Smad	Receptor-regulated Smad
SBE	Smad binding element
SCF	Stem cell factor
SH3	Src-homology 3
shRNA	Short hairpin RNA
siRNA	Small interfering RNA
SMA	Smooth muscle α-actin
SMC	Smooth muscle cell
Sm-GM2	Smooth muscle growth medium-2
SM-MHC	Smooth muscle myosin heavy chain
TβRI	TGF-β receptor I

TβRII	TGF-β receptor II
TCE	TGF-β control element
TFIIB	Transcription factor IIB
TGF-β	Transforming growth factor-β
TIA-1	T-cell intracellular antigen-1
TIAR	TIA-1-related protein
TLDA	TaqMan low density array
TRBP	TAR RNA binding protein
Trim	Tripartite motif
TTP	Tristetraprolin
USF	Upstream stimulatory factor
UTR	Untranslated region
VEGF	Vascular endothelial growth factor
VHL	von Hippel-Lindau
WT	Wild-type

ABSTRACT

Hypoxia plays a major role in the pathobiology of pulmonary arterial hypertension (PAH), a disease characterized by obstructive remodeling of the small pulmonary arteries (PAs). Acute hypoxia results in the selective constriction of PAs and elevation of pulmonary arterial pressure, while chronic exposure to hypoxia induces structural and functional changes to the pulmonary vasculature. The mechanisms underlying these pulmonary vascular changes induced by hypoxia are not entirely understood. The finding that the levels of various microRNAs (miRNAs) are altered during the development of PAH induced by chronic hypoxia in rats suggests that changes in miRNA expression in response to hypoxia may play a role in PAH development. However, the mechanisms by which hypoxia regulates miRNAs and the miRNA pathway have not been fully elucidated.

In this study, we show that hypoxia upregulates the protein levels of Argonaute2 (Ago2), a key component of the RNA-induced silencing complex (RISC). We found that the increase in Ago2 protein levels under hypoxia occurs post-transcriptionally and involves the hydroxylation of Ago2 by type I collagen prolyl 4-hydroxylase (C-P4H(I)). Hydroxylation of Ago2 is also important for its localization to stress granules and its increased association with heat shock protein 90, whose activity is crucial for miRNA loading into the RISC, under hypoxia. We further demonstrate that hydroxylation of Ago2 is critical for the increase in RISC activity and the post-transcriptional elevation of miRNA levels under hypoxia. Finally, we present evidence

that similar to hypoxia, transforming growth factor-β (TGF-β) also induces the protein levels of Ago2.

The work described here reveals that hypoxia can modulate the expression of core protein components of the miRNA pathway and provides a novel mechanism of miRNA regulation by hypoxia through C-P4H(I)-mediated hydroxylation of Ago2. Thus, we present an alternative mechanism for modulating gene expression under hypoxia by post-translational modification of Ago2. In addition, given that our lab has previously shown that the TGF-β pathway regulates miRNA biogenesis at the transcriptional level and by facilitating Drosha-mediated miRNA processing, the results in this thesis suggest a novel regulation of miRNA biogenesis/activity by the TGF-β pathway via increasing Ago2 stability and modulating RISC activity.

ACKNOWLEDGMENTS

I would like to express my deepest gratitude and appreciation to my mentor, Dr. Akiko Hata. This work would not have been possible without her careful guidance, intellectual support, unwavering encouragement, and invaluable advice throughout the years. She has provided an excellent learning environment and has taught me how to think critically and analytically. I have learned from her example how to be a good scientist, and I am truly grateful for everything that she has taught me, both scientifically and personally. I have thoroughly enjoyed my time in her lab, which has allowed me to become a better scientist and a better person. Her positivity, passion, and enthusiasm for science have been and will always be a constant source of motivation and inspiration for me. I am very thankful to have her as my mentor.

I would like to thank the lab members, who are all truly amazing, and I feel extremely fortunate to have been surrounded by such incredible people. They have all really made a difference, and I will cherish the friendships that I have formed with them over the years. From my first days rotating in the lab until now, Brandi has always been there to help me learn techniques and guide me through my experiments. She has been a great teacher to me, and her dedication pushed me to work harder everyday. MC and Nicole have also provided much support when I was getting started in the lab. I would like to thank them for sharing their experiences and wisdom with me. I would also like to extend my gratitude to Giorgio for making me think more carefully and deeply about my results and for all the helpful insights during lab meetings. Hara and Dahai have given me much advice as well, and I learned a lot from them. I would like to thank Aaron,

Peter, Jem, and Alix for making the lab a fun place to be and for their technical expertise and hard work in ensuring that the lab runs smoothly. My thanks also goes out to Jon for being a good companion and labmate. I would like to thank our newest group members Sunghwan, Justin, Matt, and Nisha as well. Last but not least, I would like to send a big thank you to Jessica and Tomo for helping me with the stress granule experiments in this project and giving me an opportunity to learn how to teach. I really appreciate all the time and efforts that they have put into this study, much of which would have been impossible without their help.

I would like to acknowledge the members of my thesis committee, Dr. Larry Feig, Dr. John Kyriakis, and Dr. Claire Moore, for all their stimulating discussions, guidance, and counsel over the years. Their constructive criticisms and insightful feedbacks were invaluable in helping me to improve this work. I would like to thank Dr. Donald Bloch for taking time out of his schedule to serve as my outside examiner and for being a great collaborator. Dr. Bloch has educated me about stress granules and provided me with tremendous amount of help, advice, and reagents. I would also like to thank my other collaborators Dr. Eric Lai and, especially, Dr. Hank Qi for sharing their precious reagents and advice. Dr. Qi was instrumental to the initiation of this project, and I appreciate all the support that he has given me. The generosity and expertise of all my collaborators helped push my project forward in ways I could not have done myself.

I would like to thank my fantastic friends Colleen, Hiroko, Susan, Le, Kevin, Hoang, and Wendy for lending me their ears and keeping my life outside of lab fun and

interesting. Finally, I must thank my parents for always standing by me and believing in me. I am forever grateful for the unconditional love and support that they have given me.

TABLE OF CONTENTS

LIST OF FIGURES

Role of hypoxia in the regulation of the microRNA-containing RNA-induced silencing complex

A dissertation

submitted by

Connie Wu

In partial fulfillment of the requirements

for the degree of

Doctor of Philosophy

in

Biochemistry

TUFTS UNIVERSITY

Sackler School of Graduate Biomedical Sciences

February 2012

ADVISER: Dr. Akiko Hata

CHAPTER I. INTRODUCTION.

1.1 Pulmonary arterial hypertension and the vasculature.

Pulmonary arterial hypertension (PAH) is a disease characterized by obstructive remodeling of the small pulmonary arteries (PAs) [1-3]. This vascular remodeling involves increased proliferation, hypertrophy, and migration of pulmonary artery smooth muscle cells (PASMCs) as well as decreased apoptosis and enhanced production of extracellular matrix proteins [4]. Together, these changes lead to thickening of the vascular smooth muscle layer, increased muscularization of the pulmonary artery, and thickening and fibrosis of the intima, reducing the diameter of the lumen and increasing pulmonary vascular resistance [4, 5] (**Fig 1.1**). As a result, pulmonary arterial pressure is progressively elevated, which ultimately leads to right ventricular heart failure and death [4].

Although the incidence of PAH is relatively low (about 7.6 cases per million people), mortality rates are high (15% within 1 year after diagnosis, 50% within 5 years after diagnosis), and there is currently no cure for PAH, other than a heart/lung transplantation [6]. Drugs such as Bosentan (an endothelin-1 receptor antagonist), Sildenafil (an inhibitor of phosphodiesterase-5), and prostacyclin analogues have been shown to exhibit vasodilator and anti-proliferative effects and are approved therapies for PAH; however, these drugs cannot reverse PAH and do not improve survival [1]. Thus, it is crucial to have a better understanding of the molecular mechanisms underlying the pathogenesis of PAH to develop novel and effective treatments for PAH.

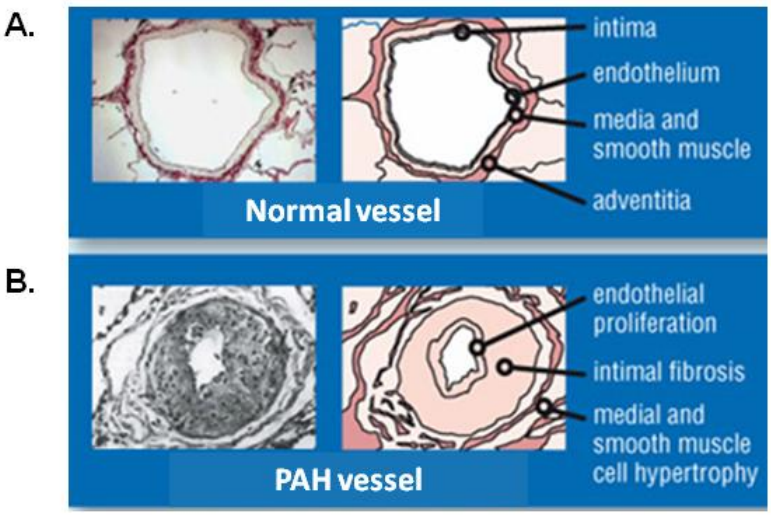

Figure. 1.1 Abnormal vascular morphology in PAH. **A.** Cross-section of a normal arteriole with the structure of a typical vessel. **B.** Cross-section of an arteriole from a PAH patient showing increased proliferation and hypertrophy of endothelial and smooth muscle cells, thickening of the medial layer, and thickening and fibrosis of the intima, greatly reducing the diameter of the lumen. Adapted from www.pah-info.com.

Pulmonary artery smooth muscle cells (PASMCs)

PASMCs are vascular smooth muscle cells (SMCs) that comprise the medial layer of blood vessels [4]. The medial layer is one of the three layers that makes up all blood vessels and is the middle layer located in between the other two layers. The media is composed of several layers of vascular SMCs that can contract and relax and elastic connective tissue that can stretch and recoil, thus providing elasticity and strength to the vessel [7]. The innermost layer of the vessel is known as the intima, which has direct contact with the lumen and is composed of a single layer of endothelial cells as well as extracellular matrix. The endothelial cells function as a barrier between the blood and the medial layer, regulating the selective passage of substances into and out of the bloodstream [8]. Endothelial cells can also affect the proliferation and migration of the underlying vascular SMCs by producing signaling molecules, such as nitric oxide, and growth factors, such as transforming growth factor-β (TGF-β) and platelet-derived growth factor (PDGF) [4]. The outermost layer of the vessel is called the adventitia, which is a thin layer of connective tissue that serves to protect and hold the vessel in place [7]. Our lab is particularly interested in studying PASMCs not only because of their important contribution to pulmonary artery remodeling and the resulting PAH, but also because of their unique ability to undergo phenotypic switching.

Vascular SMCs, such as PASMCs, are not terminally differentiated cells and thus exhibit phenotypic plasticity, in which they can modulate their phenotype between a "differentiated" (also known as "contractile") state and a "dedifferentiated" (also known as "synthetic") state [9] (**Fig 1.2**). The "differentiated" state is characterized by decreased

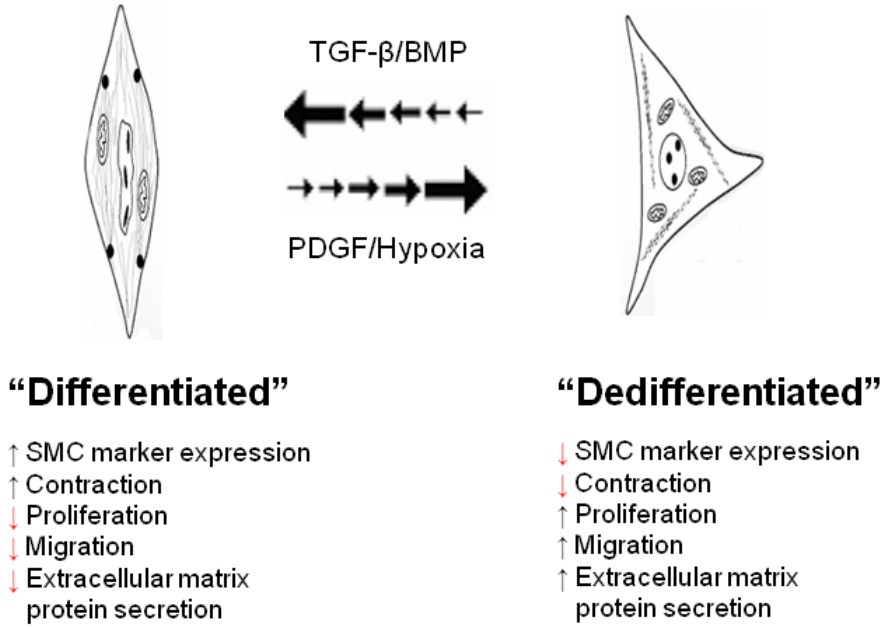

Figure. 1.2 Phenotypic plasticity of vascular SMCs. Vascular SMCs are not terminally differentiated and can undergo phenotypic switching between a "differentiated" state and a "dedifferentiated" state. The "differentiated" state is characterized by decreased proliferation, migration, and extracellular matrix protein secretion and increased expression of contractile proteins. On the other hand, the "dedifferentiated" state is characterized by increased proliferation, migration, and extracellular matrix protein secretion and decreased contractile gene expression. TGF-β and BMP promote the "differentiated" state, while PDGF and hypoxia promote the "dedifferentiated" state. Adapted from [9].

proliferation, migration, and extracellular matrix protein secretion and increased expression of contractile proteins (such as smooth muscle α-actin (SMA) [10-12], smooth muscle myosin heavy chain (SM-MHC) [13-15], h1-calponin (CNN) [16-18], and SM22α [17, 19]), ion channels as well as signaling molecules [20]. On the other hand, the "dedifferentiated" state is characterized by increased proliferation, migration, and extracellular matrix protein secretion and decreased contractile gene expression [9].

The genes encoding the contractile proteins mentioned above are often used as SMC differentiation markers. Given its abundant expression in differentiated SMCs and the fact that it is the earliest known protein to be expressed during the development of SMCs, SMA is the most commonly used marker [9, 11]. The expression levels of these markers can also be indicative of the relative degree of differentiation of the SMCs; for example, higher level of SMA expression indicates a more differentiated SMC [20]. In addition, expression of SM22α and SM-MHC is associated with more mature, fully differentiated SMCs [20]. It is important to note that although these genes are considered to be SMC differentiation markers, studies have shown that they can be expressed in other non-SMCs as well [4, 9]. Most of the markers mentioned above have been demonstrated to be transiently expressed in cell types other than SMCs during development, tissue repair, or disease [9]. During normal development, skeletal and cardiac muscle express SMA [21]. Additionally, endothelial cells have been reported to express SMA during the process of vascular remodeling and in response to TGF-β treatment [22, 23]. Thus, the markers identified above are not entirely SMC-specific.

Nevertheless, it is known that the expression of many of these marker genes is much more abundant in fully differentiated SMCs compared to other cell types [9].

Normally, PASMCs in the adult lung vasculature are mainly in the differentiated state, given their role in blood vessel contraction and maintenance of blood vessel tone and integrity [4]. However, during the development of the vasculature or in response to vascular injury, the SMCs dedifferentiate and increase their proliferation, migration, and secretion of extracellular matrix proteins, such as elastin, proteoglycans, and collagen, to promote blood vessel formation or the repair of the vessel [9]. Exposure to stimuli such as hypoxia or PDGF, which will be described in more detail in the next section, can also induce SMCs to dedifferentiate. Once the injury is resolved or the stimuli are removed, healthy SMCs switch back to the differentiated phenotype, thus demonstrating the reversibility of the phenotypic switching process [9]. Although the ability of SMCs to modulate their phenotype is physiologically beneficial and provides a survival advantage, deregulation of this phenotypic modulation can lead to obstructive vascular remodeling, such as that seen in PAH, and the development of diseases, such as atherosclerosis, hypertension, restenosis, asthma, and obstructive bladder disease [9].

1.2 Factors involved in PAH pathobiology and their effects on PASMCs.

A number of signaling molecules, growth factors, and inflammatory cytokines and chemokines have been identified to play a role in the initiation and/or progression of PAH through their effects on PASMCs [4]. They are often produced and secreted from the endothelial cells of the intima and affect the hypertrophy, proliferation, or migration of PASMCs [4]. In particular, this thesis will focus on the roles of TGF-β, bone

morphogenetic protein (BMP), PDGF, and hypoxia. TGF-β and BMP have been shown to inhibit the proliferation of PASMCs, while PDGF promotes PASMC proliferation and migration [4]. In addition, exposure to hypoxia has been reported to stimulate the proliferation of PASMCs [4]. Each of these factors will be discussed in more detail below.

TGF-β superfamily of ligands

The TGF-β superfamily is a large group of ligands that regulate a variety of biological processes, such as differentiation, migration, proliferation, apoptosis, extracellular matrix production, and vascular function [24, 25]. Members of the TGF-β superfamily include 3 TGF-β isoforms (TGF-β1, TGF-β2, and TGF-β3), more than 20 BMPs, nodal, 4 activins, and 11 growth and differentiation factors (GDFs) [26-28] (**Fig 1.3**). Based on sequence homology and their downstream signal effects, these ligands are divided into two major branches of the TGF-β superfamily: the TGF-β subfamily, which consists of TGF-βs, activins, and nodal, and the BMP subfamily, which comprises of BMPs and GDFs [29]. All members of the TGF-β superfamily are first made as inactive precursors, which are subsequently activated through dimerization and proteolytic cleavage of their pro-domains [24]. There are two types of TGF-β superfamily receptors: type I and type II receptors, both of which are serine/threonine transmembrane kinases. Seven type I (activin-receptor-like kinases (ALKs) 1-7) and five type II (TGF-βRII, ActRII, ActRIIB, BMPR-II, and AMHR-II) receptors are known to exist [30, 31]. Activated ligands of the TGF-β superfamily bind to preformed type II receptor dimers,

TGF-β superfamily of ligands

Subgroup	Name	Alternative names
TGFβ	TGFβ1	
	TGFβ2	
	TGFβ3	
BMP2/4	BMP2	BMP2A
	BMP4	BMP2B
BMP5/6/7	BMP5	
	BMP6	Vg1-related sequence (Vgr1)
	BMP7	OP-1
	BMP8A	OP-2
	BMP8B	OP-3
GDF1	GDF1	
	GDF3	Vgr2
GDF5/6/7	GDF5	Cartilage-derived morphogenetic protein-1 (CDMP1)
	GDF6	CDMP2, BMP13
	GDF7	BMP12
BMP3	BMP3	Osteogenin
	BMP3b	GDF10, Sumitomo-BIP
BMP9/10	BMP9	GDF2
	BMP10	
GDF9	GDF9	
	GDF9b	BMP15
	GDF15	BMP-placenta, PLAB, prostate-derived factor (PDF), macrophage inhibiting cytokine-1 (MIC-1)
GDF8	GDF8	Myostatin
	GDF11	BMP11
Activins	Activin A	
	Activin B	
	Activin AB	
Inhibins	Inhibin A	
	Inhibin B	
Nodal	Nodal	
Lefty	Lefty1	LeftyA, endometrial bleeding associated factor (EBAF)
	Lefty2	LeftyB
MIS	MIS	Mullerian inhibiting substance

Figure. 1.3 Members of the TGF-β superfamily of ligands. The TGF-β superfamily of ligands consists of TGF-βs, BMPs, GDFs, activins, inhibins, nodal, lefty proteins, and MIS. Alternative names of the ligands are provided. Adapted from [28].

which then recruit preformed type I receptor dimers to form a heterotetrameric receptor complex. Once this complex is formed, the constitutively active type II receptor phosphorylates and thus activates the type I receptor. Upon activation, the type I receptor recruits and phosphorylates receptor-regulated Smad signal transducers (R-Smads) [31]. R-Smads include Smads 1, 2, 3, 5, and 8; TGF-β subfamily ligands lead to the phosphorylation of Smads 2 and 3, whereas BMP subfamily ligands lead to the phosphorylation of Smads 1, 5, and 8 [32]. Phosphorylated R-Smads associate with the common Smad (Smad 4) and translocate to the nucleus. In the nucleus, the R-Smad/Smad 4 complex interacts with additional factors, such as transcription factors, co-activators, co-repressors, and chromatin remodeling complexes, to activate or repress target gene expression [26, 33-35] (**Fig 1.4**).

Studies from our lab as well as others have shown that TGF-β1 and BMP4 promote the differentiation of vascular SMCs. Treatment of vascular SMCs with TGF-β1 reduces their proliferation and migration and also induces the expression of SMA, CNN, SM22α, and SM-MHC, which are all markers of SMC differentiation [36, 37]. Similar to TGF-β1, treatment of PASMCs with BMP4 stimulates the expression of the contractile proteins SMA, CNN, and SM22α [38]. In addition, PDGF-mediated decrease in the expression of SMA is suppressed in the presence of TGF-β1 or BMP4 treatment, thus suggesting that TGF-β1 and BMP4 help maintain the differentiated state of PASMCs [38]. The mechanisms by which TGF-β and BMP mediate vascular SMC differentiation are not completely understood. Promoter analysis of the SMA and SM22α genes reveals the presence of a TGF-β control element (TCE) that is critical for

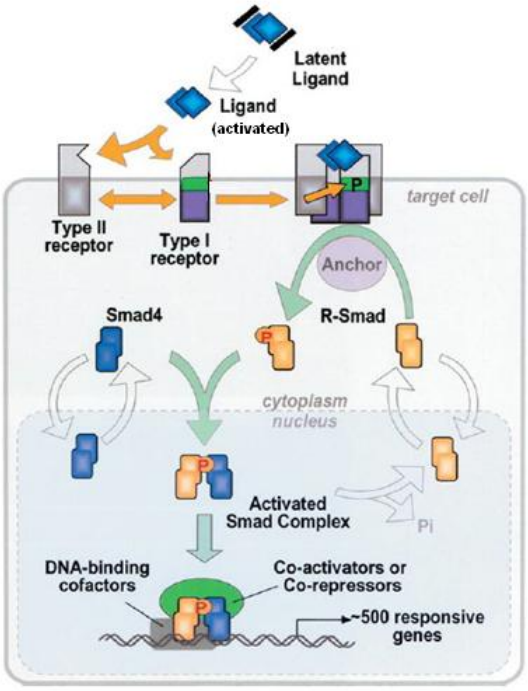

Figure. 1.4 TGF-β superfamily signaling pathway. Ligands of the TGF-β superfamily are first made as latent precursors, which are subsequently activated through dimerization and proteolytic cleavage. Activated ligands then bind to preformed type II receptor dimers, which then recruit preformed type I receptor dimers to form a heterotetrameric receptor complex. The constitutively active type II receptor phosphorylates and thus activates the type I receptor. Upon activation, the type I receptor recruits and phosphorylates R-Smads, which associate with Smad 4 and translocate to the nucleus to activate or repress target gene expression. Adapted from [31].

TGF-β-mediated induction [36]. Interestingly, Krüppel-like factor 4 (KLF4), a zinc finger transcription factor that strongly represses vascular SMC contractile gene transcription, can bind to the TCE, and studies have found that TGF-β treatment transcriptionally and post-transcriptionally reduces the expression of KLF4 [39, 40]. Together these results suggest that the TGF-β mediated induction of SMC differentiation could be in part mediated by the downregulation of KLF4, which would relieve its repressive effect on SMC markers. Additionally, our lab has shown that treatment of PASMCs with BMP4 activates the RhoA/ROCK signaling pathway and increases the accumulation of myocardin-related transcription factors (MRTF-A and MRTF-B) in the nucleus, where MRTF-A and MRTF-B are recruited to the promoter of SMA [38]. MRTF-A and MRTF-B are transcriptional co-activators that are known to play a role in the transcriptional activation of many SMC-specific genes [38, 41].

Besides modulating the expression of protein-coding genes, studies from our lab demonstrate that TGF-β/BMP can regulate the levels of small non-coding RNAs, such as microRNAs (miRNAs), to promote SMC differentiation. Specifically, we found that TGF-β1 and BMP4 post-transcriptionally upregulate miR-21, which in turn represses programmed cell death 4 (PDCD4), an inhibitor of the SMC contractile genes SMA, CNN, and SM22α, thus resulting in the induction of SMC differentiation [42]. Recently, our lab showed that TGF-β1 and BMP4 can also increase the levels of miR-143 and miR-145, two miRNAs that have been implicated to play crucial roles in SMC differentiation [43, 44]. We found that TGF-β1 and BMP4 transcriptionally activate the expression of miR-143 and miR-145, which in turn represses KLF4, the negative regulator of SMC

contractile gene transcription [43]. These results provide another mechanism by which TGF-β and BMP promote SMC differentiation. Thus, it is clear that multiple mechanisms underlie the effect of TGF-β/BMP on the expression of SMC differentiation markers in vascular SMCs.

The role of TGF-β signaling in PAH is highlighted by the finding of mutations in the gene encoding BMPR-II in 70% of familial PAH and 10%–30% of idiopathic PAH (IPAH) cases [45-47]. Studies have also found that the expression of BMPR-II is decreased in the pulmonary vasculature of IPAH patients with no identifiable BMPR-II mutation [48]. In addition, mice carrying a heterozygous mutation of BMPR-II develop PAH, with the characteristic thickening of PAs and increases in pulmonary arterial pressure and pulmonary vascular resistance [49]. Furthermore, decreased expression of BMP type I and type II receptors is observed in animal models of PAH [50, 51]. Thus, these data suggest that altered TGF-β signaling, particularly BMP signaling, may contribute to the development of PAH. Given the important role of BMP in promoting SMC differentiation, it is reasonable to speculate that decreased BMP signaling would reduce the expression of SMC markers and lead to the dedifferentiation of PASMCs, which would contribute to pulmonary vascular remodeling and PAH development. It is also possible that the vascular remodeling associated with BMPR-II mutation creates a hypoxic environment in the PAs due to pulmonary arterial obstruction. As a result, this may produce a feedforward mechanism to promote further thickening and remodeling of the PAs and contribute to PAH development, since chronic hypoxia is a well-known inducer of PASMC proliferation and pulmonary vascular remodeling [52]. Although

mutations in BMPR-II can lead to the development of PAH, it is important to note that BMPR-II mutations do not always result in PAH, and carriers of BMPR-II mutations can be asymptomatic, thus suggesting that other genetic and/or environmental factors may also be needed for the development of PAH [53].

PDGF

In mammals, four different PDGF polypeptides exist: PDGF-A, PDGF-B, PDGF-C, and PDGF-D [54]. To generate the functionally active form of PDGF, these polypeptides dimerize with each other through disulfide bonds to form the homodimers PDGF-AA, PDGF-BB, PDGF-CC, and PDGF-DD or the heterodimer PDGF-AB [54]. These PDGF dimers interact with cell surface receptor tyrosine kinases [54]. There are two types of PDGF receptors: PDGFR-α and PDGFR-β [55]. Similar to the PDGF polypeptides, dimerization is essential for the formation of functionally active PDGF receptors (PDGFR-$\alpha\alpha$, PDGFR-$\beta\beta$, or PDGFR-$\alpha\beta$) [54]. Upon binding by PDGF dimers, PDGF receptors dimerize and undergo autophosphorylation at tyrosine residues [56]. This phosphorylation not only enhances the intrinsic protein tyrosine kinase activity, but also results in the generation of docking sites for adaptor proteins (such as phospholipase C gamma (PLCγ), growth factor receptor-bound protein 2 (Grb2), Src, or Shc), which can then activate various signaling pathways (such as the phosphatidylinositol 3-kinase (PI3K)/Akt, Ras/extracellular signal-regulated (Erk1/2) mitogen-activated protein kinase (MAPK), or protein kinase C (PKC) pathway) (**Fig 1.5**). The signaling pathways activated by PDGF often promote cell proliferation and migration [54, 57-59].

Indeed, *in vitro* studies on cultured PASMCs have shown that PDGF treatment promotes the proliferation and migration of PASMCs and that the PDGF receptor inhibitor, imatinib, strongly inhibits the PDGF-mediated increase in proliferation and migration [60-62]. Besides regulating proliferation and migration, PDGF treatment of vascular SMCs also decreases the expression of SMC differentiation markers, such as CNN, SMA, SM-MHC, and SM22α [63-65]. Although the mechanisms by which PDGF induces PASMC proliferation and migration and represses SMC markers are not fully understood, studies from our lab demonstrate that miRNAs may play a role. In particular, we found that in PASMCs, PDGF transcriptionally upregulates miR-221, which in turn targets p27Kip1 and c-Kit [66]. Downregulation of the cell cycle inhibitor p27Kip1 results in increased cell proliferation, while repression of c-Kit reduces the expression of myocardin, a potent transcriptional co-activator of SMC gene transcription, thus leading to decreased expression of SMC markers [66]. Moreover, Western blot analysis shows that PDGF treatment increases the expression of KLF4, a repressor of vascular SMC contractile gene transcription, and decreases the expression of SMC markers in vascular SMCs [67]. Various other molecular mechanisms have also been proposed to underlie the effect of PDGF on the expression of SMC differentiation markers in vascular SMCs [68-73].

Consistent with the *in vitro* studies, increased expression and activity of components of the PDGF signaling pathway have also been observed *in vivo* in the chronic hypoxia animal model of PAH. Western blot analysis of lung samples from mice exposed to chronic hypoxia reveals that the protein levels of PDGFR-β and its

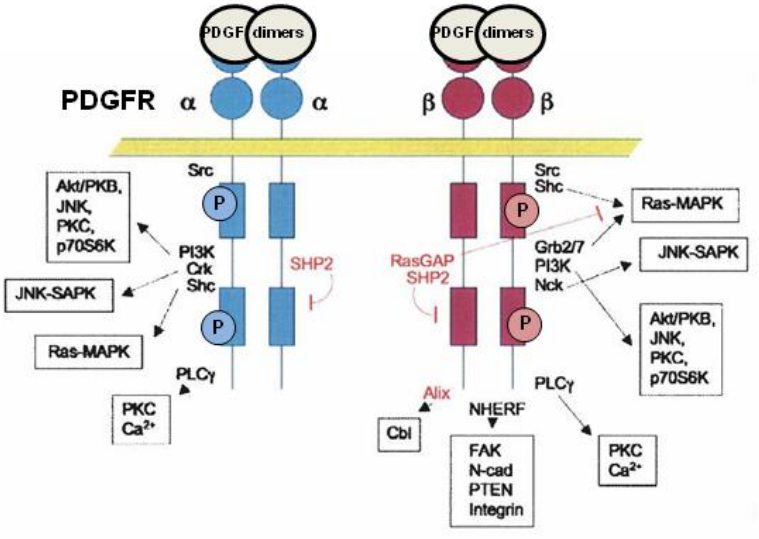

Figure. 1.5 PDGF signaling pathway. Upon binding by PDGF dimers, PDGF receptors (PDGFR-α and PDGFR-β) dimerize and undergo autophosphorylation at tyrosine residues. Such phosphorylation results in the generation of docking sites for adaptor proteins (such as PLCγ, Grb2, Src, or Shc), which can then activate various signaling pathways (such as the Akt, Ras-MAPK, or PKC pathway). Adapted from [57].

phosphorylated (i.e. activated) form are significantly upregulated and that imatinib treatment is able to reduce the protein levels of phospho-PDGFR-β [61]. Treatment of the hypoxic mice with imatinib also reduces the muscularization of PAs [61], thus suggesting that the PDGF pathway is involved in pulmonary artery remodeling and the development of PAH. Consistent with these results, Western blot analysis of lung samples from patients with IPAH also indicates an increase in the protein levels of PDGFR-β and its phosphorylated form compared to healthy controls [61]. In addition, qRT-PCR analysis demonstrates that the mRNA levels of PDGF-A, PDGF-B, PDGFR-α, and PDGFR-β are upregulated in the small PAs of IPAH patients compared to controls [60]. Immunohistochemical staining shows that PDGF-A, PDGF-B, PDGFR-α, and PDGFR-β are expressed in the PASMCs as well as the endothelial cells of these small PAs [60]. Together, the *in vitro* and *in vivo* findings suggest that the effect of PDGF on PASMC proliferation and migration could play a role in the development of PAH. In fact, clinical trials using imatinib in PAH treatment have begun and are currently still ongoing [74].

Hypoxia

Chronic exposure to hypoxia is known to be one of the causes of PAH [1, 75]. Given that hypoxia naturally occurs at high altitudes, PAH is a disease that is commonly reported in high-altitude residents, such as those living 2,500 meters above sea level [76]. PAH is also associated with chronic hypoxia lung diseases, such as chronic obstructive pulmonary disease, asthma, cystic fibrosis, and bronchiectasis [52]. Moreover, rodents exposed to chronic hypoxia are often used as animal models of PAH [77]. Similar to the

phenotype of human PAH, rats or mice treated with chronic hypoxia exhibit pulmonary vasoconstriction and pulmonary vasculature remodeling, in which PASMCs dedifferentiate and become more proliferative, hypertrophic, and migratory, leading to increased thickening of the media and muscularization of PAs [77]. After two weeks of hypoxia treatment, rats develop PAH with the characteristic increase in pulmonary artery pressure as seen in human PAH [77]. It is well-accepted that chronic hypoxia results in PASMC proliferation *in vivo* [52]; however, much contradicting results have been presented in the scientific literature about the effect of acute hypoxia (i.e. 0–10% O_2 for 4–24 h) on PASMC proliferation *in vitro* [52]. Some studies show that acute hypoxia promotes the proliferation of PASMCs [78-82], while other studies report that hypoxia inhibits or reduces the proliferation of PASMCs [83-86]. It is speculated that these contradictory findings could be due to differences in the severity of the hypoxia treatment, variations in the seeding density of PASMCs in experimental culture plates, and/or differences in the concentration of serum in the cell culture media [52].

Despite the controversy about the effects of hypoxia on PASMC proliferation *in vitro*, several mechanisms have been proposed to underlie the hypoxia-mediated increase in the proliferation of PASMCs. Studies have found that hypoxia reduces potassium currents ($I_{K(V)}$) in PASMCs, leading to the depolarization of the membrane [87-89]. As a result of the depolarization, voltage-dependent calcium channels open and Ca^{2+} enters the cell, resulting in an increase in the intracellular calcium concentration. The elevated Ca^{2+} level induces vasoconstriction and stimulates PASMC proliferation [87-89]. Studies have also reported that hypoxia triggers pulmonary artery endothelial cells to produce factors such as endothelin, serotonin, PDGF, and interleukin 6, all of

which have been shown to promote the proliferation or migration of PASMCs [90]. In addition, recent studies have reported that hypoxia regulates the expression of various miRNAs in PASMCs. Exposure of human PASMCs to 24 h of hypoxia results in a 2-fold increase in the expression levels of several miRNAs, such as miR-21, miR-107, miR-151, miR-22, miR-20, and miR-214, compared to normoxic controls [91]. In particular, miR-21 is shown to play an important role in the hypoxia-mediated induction of PASMC proliferation and migration. The increase in PASMC proliferation and migration in response to hypoxia is significantly reduced when miR-21 is knocked down using antisense oligonucleotides [91]. Hypoxia-mediated regulation of miRNA expression is observed *in vivo* in the chronic hypoxia animal model of PAH as well. Results from our lab show that lungs from rats treated with chronic hypoxia exhibit increased levels of miR-24 and miR-221 compared to normoxic controls [92]. Additionally, fluorescence *in situ* hybridization analysis of PAs from rats exposed to chronic hypoxia reveals that miR-24 levels are upregulated in the medial layer, which comprises SMCs, compared to normoxic controls [92]. Other studies have also examined the expression levels of various lung miRNAs during the development of PAH induced by chronic hypoxia in rats [93]. It was found that while the levels of certain miRNAs, such as miR-145, did not change over time, the levels of other miRNAs, such as miR-451 and miR-322, were strongly upregulated over time in the hypoxic samples compared to the normoxic controls [93]. There were also miRNAs, such as miR-30c and miR-22, whose expression levels decreased over time in the hypoxic samples compared to the normoxic controls [93]. Interestingly, unlike the results from the *in vitro* studies on hypoxia-treated PASMCs [91], miR-21 levels were not significantly changed compared

to the normoxic controls [93]. This difference could be due to the fact that the lung contains many other cell types besides PASMCs, which could all contribute to the changes in miRNA expression. The differences in the severity and duration of the hypoxia treatment could also result in differential modulation of miRNA expression. Nevertheless, these results together suggest that changes in miRNA levels in response to hypoxia may play a role in the development of PAH in part by affecting the proliferation or migration of PASMCs.

Moreover, hypoxia increases the production of extracellular matrix components, such as collagen (types I, III, IV, VI, VIII, and XIII), fibronectin, elastin, and laminin, which can regulate the proliferation and migration of vascular SMCs [94, 95]. Types I and IV collagen as well as laminin have been implicated to inhibit vascular SMC proliferation and promote the "differentiated" state of SMCs [96]. On the other hand, fibronectin has been shown to promote the "dedifferentiated" state and increase vascular SMC proliferation [97, 98]. The increase in collagen synthesis in response to hypoxia is mediated by the induction of collagen prolyl 4-hydroxylase (C-P4H), an enzyme which plays a critical role in the maturation and secretion of collagen [99].

1.3 Collagen prolyl 4-hydroxylase.

C-P4H is a member of the evolutionarily conserved non-heme-Fe(II) and 2-oxoglutarate-dependent dioxygenase superfamily [100]. All enzymes of this superfamily use iron (Fe(II)), 2-oxoglutarate, ascorbic acid, and molecular oxygen (O_2) to catalyze hydroxylation reactions, in which one oxygen atom from O_2 is incorporated into the substrate as a hydroxy group, while the other oxygen atom is incorportated into 2-

oxoglutarate, resulting in the production of succinate and CO_2 [101]. Although ascorbic acid is one of the cofactors for the enzymatic reaction, many cycles of the reaction can be completed even in the absence of ascorbic acid [102], thus suggesting that ascorbic acid is not required for catalytic activity. However, ascorbic acid does help enhance the catalytic reaction by maintaining the oxidation state of iron in the Fe^{2+} state [103, 104].

C-P4H is an endoplasmic reticulum (ER) tetrameric enzyme composed of two α- and two β-subunits ($\alpha_2\beta_2$) [100, 105]. The β-subunit is also known as protein disulfide isomerase (PDI), which is an enzyme that catalyzes the formation, breakage, and rearrangement of disulfide bonds [106-109]. Three different isoforms of the α-subunit exist, and they are designated as α(I), α(II), and α(III) [110-113]. Each of these isoforms can associate with the β-subunit to form an active C-P4H enzyme. Type I C-P4H (C-P4H(I)) is composed of two α(I)- and two β-subunits ($[\alpha(I)]_2\beta_2$), type II C-P4H (C-P4H(II)) is composed of two α(II)- and two β-subunits ($[\alpha(II)]_2\beta_2$), and type III C-P4H (C-P4H(III)) is composed of two α(III)- and two β-subunits ($[\alpha(III)]_2\beta_2$) [110-113]. Type I C-P4H is usually the major form that is found in the majority of cell types and tissues, whereas type II C-P4H is the predominant form in endothelial cells, cells in epithelial structures, chondrocytes, and osteoblasts [114, 115]. As for type III C-P4H, its expression is the highest in the adult liver, fetal skin, and placenta [112, 113].

The C-P4H-α subunit contains the majority of the catalytic active site and thus is largely responsible for enzymatic activity [100, 105]. On the other hand, the β subunit is constitutively expressed and is thought to serve several functions in the C-P4H enzyme complex. The β subunit has a signal sequence (Lys-Asp-Glu-Leu, also known as the

KDEL sequence) located at its C-terminus, and this sequence is absence from the α-subunit [100, 105]. The KDEL sequence is a well-known ER retention signal that is necessary and sufficient for retaining proteins within the ER lumen [116]. Thus, since the C-P4H enzyme localizes to the lumen of the ER, the β-subunit could be important for retaining the enzyme complex within the ER lumen [100, 105]. In addition, studies have found that the α-subunit forms insoluble aggregates upon dissociation from the enzyme complex [100, 105]. Expression of the α-subunit itself in a baculovirus expression system or in an *in vitro* translation system also results in the formation of insoluble aggregates that lack C-P4H activity [117, 118]. These results suggest that the β-subunits in the C-P4H enzyme complex exhibit chaperone functions to prevent the misfolding and aggregation of the α-subunits.

Since the C-P4H-α subunit is the catalytic subunit and is also rate-limiting during the formation of the active enzyme [119], the activity of C-P4H can be effectively controlled by regulating the expression of the α-subunit. Several factors have been shown to modulate the expression of the α-subunit. As will be discussed in more detail in chapters II and IV, hypoxia upregulates C-P4H-α(I) at both the transcriptional and post-transcriptional levels [120, 121], and TGF-β1 increases the transcription of the gene encoding C-P4H-α(I) [122]. Given the fact that the α-subunit harbors most of the catalytic activity, the hypoxia-mediated induction of C-P4H-α(I) expression would be expected to be associated with an increase in the activity of the C-P4H(I) enzyme under hypoxia. Indeed, studies have found that hypoxia increases the activity of C-P4H(I) [104, 123, 124]. Fibroblasts treated with 24 h of hypoxia exhibit increased C-P4H(I) activity,

about 4-fold increase compared to normoxia, and an enhanced degree of proline hydroxylation in newly synthesized collagen [123]. In addition, treatment of fibroblasts with hypoxia upregulates the levels of hydroxyproline residue secreted from the cells [104]. Thus, hypoxia stimulates not only the expression, but also the activity of the C-P4H(I) enzyme.

C-P4H hydroxylates procollagens at proline residues that are located in the -X-Pro-Gly triplet, where X represents any amino acid [100, 105]. Besides procollagens, C-P4H has also been shown to hydroxylate other non-collagen proteins that contain the X-Pro-Gly triplet, such as apoproteins, pulmonary surfactant, the 18S form of acetylcholinesterases, and the complement protein C1q [99]. In addition, C-P4H can hydroxylate proline residues in the -X-Pro-Ala triplet, which is found in C1q and type IV collagen [119]. Prolyl hydroxylation of procollagens occurs in the ER after the procollagen polypeptide chains are synthesized and is crucial for the folding of the polypeptide chains into a stable triple-helical conformation [104, 125]. The triple-helical trimers are then secreted into the extracellular space, where their ends are proteolytically cleaved and subsequent polymerization and deposition of the collagen trimers occur [104]. As a result, in the absence of prolyl hydroxylation, such as when the activity of C-P4H is inhibited, unstable collagen will be generated and is rapidly degraded in the cell, thus leading to a reduction in the production and secretion of collagen [126]. On the other hand, studies have shown that overexpressing C-P4H-α(I) will lead to excess collagen production [127]. Interestingly, recent studies have found that protein components of the miRNA pathway, specifically the Argonaute proteins, also contain X-

Pro-Gly and X-Pro-Ala triplets [119]. As will be discussed in more detail in section 1.6 and in chapter II, Argonaute proteins are shown to be direct substrates of C-P4H(I), which can hydroxylate the Argonaute proteins at specific proline residues [119]. These findings suggest a possible connection between hydroxylation and modulation of miRNA activity.

1.4 The hypoxic response.

In response to hypoxia, mammalian cells activate transcriptional and post-transcriptional processes to regulate the expression of various genes that are critical for cell survival and adaptation to low oxygen levels [128]. The transcriptional response to hypoxia is mainly mediated by the hypoxia-inducible factor (HIF) family of transcription factors [129], while the post-transcriptional response involves the actions of RNA-binding proteins (RBPs) and miRNAs [128]. Activation of these processes plays a role not only in the physiological response to hypoxia, but also in the pathogenesis of different disorders, such as PAH [1, 75] and cancer [130]. Having a greater mechanistic understanding of these transcriptional and post-transcriptional processes could lead to the identification of novel therapeutic targets and the development of better therapies for these diseases.

Transcriptional control of the hypoxic response

Hypoxia-inducible factors (HIFs) are a family of transcription factors composed of two subunits: an oxygen-regulated α-subunit (HIF-1α, HIF-2α, or HIF-3α) and a constitutively expressed β-subunit (HIF-1β, also known as aryl hydrocarbon receptor

nuclear translocator (ARNT), ARNT2, or ARNT3) [131-134]. Heterodimerization can occur between any of the α- and β- subunits. Each of the α- and β-subunits contains a Per-ARNT-Sim (PAS) domain, which mediates the heterodimerization of the two subunits, and a basic helix-loop-helix (bHLH) domain, which is important for DNA binding [129]. In addition to the PAS and bHLH domains, HIF-1α and HIF-2α have two transactivation domains (the N-terminal transactivation domain and the C-terminal transactivation domain) that allow the two α-subunits to activate transcription when bound to DNA [135]. Although all three isoforms of HIFα are upregulated by hypoxia, studies show that there are differences in the expression pattern and functions of the three isoforms [136]. HIF-1α is ubiquitously expressed, whereas the expression of HIF-2α is restricted to the endothelium, kidney, lung, heart, and small intestine [137]. Even though a common set of target genes is activated by both HIF-1α and HIF-2α, genes that are distinctly activated by HIF-1α or HIF-2α have also been identified [136]. In addition, unlike HIF-1α and HIF-2α, not much is known about the function of HIF-3α. However, interestingly, studies have found that when the HIF-3α transcript undergoes alternative splicing, the inhibitory PAS domain protein is produced and negatively regulates the HIF response by binding HIF-1α, thus forming a transcriptionally inactive complex [138]. Out of the three HIFα isoforms, HIF-1α is the most well-studied and will be the focus in the sections below.

Oxygen-dependent regulation of the HIF-1α-subunit involves the prolyl hydroxylation of the HIF-1α-subunit by the prolyl hydroxylase domain (PHD) proteins, also known as HIF prolyl hydroxylases [139, 140]. Similar to C-P4H, the PHD proteins

are members of the non-heme-Fe(II) and 2-oxoglutarate-dependent dioxygenase superfamily [101]. Thus, the PHD proteins use iron (Fe(II)), 2-oxoglutarate, ascorbic acid, and molecular oxygen (O_2) to catalyze hydroxylation reactions, in which one oxygen atom from O_2 is incorporated into the substrate as a hydroxy group, while the other oxygen atom is incorportated into 2-oxoglutarate, resulting in the production of succinate and CO_2 [101]. In mammals, three different PHD isoforms exist: PHD1 (also known as HPH3 in humans), PHD2 (also known as HPH2 in humans), and PHD3 (also known as HPH1 in humans) [139, 140]. Although all three isoforms can hydroxylate the HIFα subunits, studies have reported that PHD2 has a greater effect on HIF-1α than HIF-2α and that PHD3 has more influence on HIF-2α than HIF-1α, thus suggesting that the PHD isoforms do show some degree of substrate selectivity [141]. In addition, the three isoforms exhibit differences with respect to their subcellular localization and tissue distribution. While PHD3 is found in either the cytoplasm or nucleus, PHD1 and PHD2 are mainly localized to the nucleus and cytoplasm, respectively [101]. Also, PHD1 is highly expressed in the testis and lowly expressed in the heart, whereas PHD2 and PHD3 both have high levels of expression in the heart [101]. As a result of the different tissue expression patterns, the relative contributions of the three PHD isoforms in regulating the HIFα-subunit will differ depending on the cellular context.

Under normoxia, the PHDs hydroxylate HIF-1α at specific proline residues (Pro564 and Pro402 in humans) that are located in the sequence motif Leu-X-X-Leu-Ala-Pro, where X represents any amino acid. This motif is conserved between HIF-1α and HIF-2α and also among the different HIF isoforms from various species [142]. Prolyl

hydroxylation of HIF-1α results in the recognition of HIF-1α by the von Hippel-Lindau (VHL) protein, which is a component of the E3 ubiquitin ligase complex and functions in substrate recognition [143-145]. The interaction between the VHL protein and HIF-1α is dependent on prolyl hydroxylation, for the VHL protein binds to the same proline residues that are hydroxylated by the PHDs [146, 147]; hydroxylation of the HIF-1α proline residues promotes hydrogen bonding between HIF-1α and the VHL protein, thus increasing the affinity of the VHL protein for HIF-1α [148-150]. Once HIF-1α binds to the VHL-E3 ubiquitin ligase complex, HIF-1α becomes polyubiquitinated and subjected to proteasomal degradation (**Fig 1.6**). As a result, HIF-1α is maintained at low levels and has a half-life <5 min under normoxia [151].

Since O_2 is required for PHD activity, the activity of the PHDs is inhibited under hypoxia. Consequently, HIF-1α is no longer hydroxylated and is not targeted by the VHL protein for proteasomal degradation, thus allowing the levels of HIF-1α to accumulate in the cell. HIF-1α heterodimerizes with HIF-1β and translocates to the nucleus via nuclear localization signals present in HIF-1α [152] (**Fig 1.6**). It is interesting to note that although both the PHDs and C-P4H(I) require O_2 for activity, hypoxia inhibits the activity of the PHDs but not C-P4H(I). Although the increase in C-P4H(I) activity under hypoxia may appear paradoxical, a distinguishing feature between the PHDs and C-P4H(I) is that the K_m value for O_2 of the PHDs is much higher than that of C-P4H(I) [153]. The K_m values of the PHDs are slightly above the dissolved O_2 concentration in the atmosphere, ranging from 230 μM to 250 μM, whereas C-P4H(I) has a K_m for O_2 of only 40 μM [153]. Thus, the PHDs have a lower affinity for O_2 compared

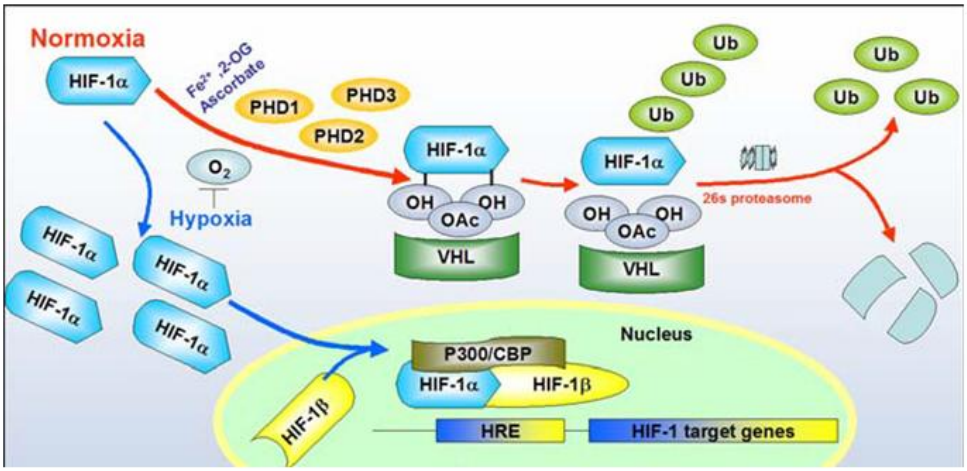

Figure. 1.6 HIF-1 signaling pathway. Under normoxia (indicated by red arrows), HIF-1α is hydroxylated by the PHDs at specific proline residues. Prolyl hydroxylation of HIF-1α promotes its binding to the VHL-E3 ubiquitin ligase complex, thus leading to its ubiquitination and proteasomal degradation. Under hypoxia (indicated by blue arrows), the activity of the PHDs is inhibited. As a result, HIF-1α is no longer hydroxylated and is not recruited to the VHL complex for degradation, allowing the levels of HIF-1α to accumulate in the cell. HIF-1α heterodimerizes with HIF-1β and translocates to the nucleus. In the nucleus, the HIF-1α-HIF-1β complex activates target gene expression by binding to a specific consensus sequence known as the HRE and by recruiting co-activators, such as p300 and CBP. Adapted from [101].

to C-P4H(I). Their different K_m values for O_2 could play a role in the differential regulation of their activities under hypoxia. Even though the O_2 concentration is low under hypoxia, C-P4H(I) would still be active because of its relatively high oxygen affinity. Maintenance of C-P4H(I) activity under hypoxia correlates with the hypoxia-mediated increase in collagen production [94, 95]. Moreover, as mentioned previously, hypoxia increases the expression of C-P4H-α(I), the subunit harboring most of the C-P4H(I) catalytic activity [120, 121]. The relatively high O_2 affinity of C-P4H(I) together with the hypoxia-mediated induction of C-P4Hα(I) could result in enhanced substrate hydroxylation under hypoxia.

Once in the nucleus, the HIF-1α-HIF-1β complex activates the expression of various genes by binding to specific consensus sequences known as hypoxia response elements (HREs) found within the promoter regions of the genes [154, 155] and by recruiting co-activators, such as the histone acetyltransferases cyclic AMP-responsive element binding protein–binding protein (CBP) and p300 [156] (**Fig 1.6**). These co-activators can in turn recruit additional co-activators, such as steroid receptor co-activator, transcription intermediary factor-2, and redox effector factor-1 [136, 156-159]. The recruitment of co-activators is essential for HIF-mediated activation of transcription. It is thought that the co-activators help stabilize the RNA polymerase II transcription initiation complex and that the histone acetyltransferase activity of the co-activators facilitates gene expression by rendering the DNA of the target gene more accessible to RNA polymerase II [136]. Although binding of the HIF-1α-HIF-1β complex to target genes often leads to transcription activation, HIF-1 proteins have also been shown to

negatively regulate gene expression [160, 161]. Thus, HIF-1 regulation of gene expression can lead to both activation and repression of target genes.

HIF-1 activates the expression of a wide range of genes that are critical for cell survival and hypoxia tolerance (**Fig 1.7**). Genes coding for erythropoietin (EPO) and vascular endothelial growth factor (VEGF) are among some of the genes activated by HIF-1. EPO is a hormone that increases the production of red blood cells, thereby enhancing the ability of the blood to carry oxygen [162], and VEGF is a well-known growth factor that stimulates the production of new blood vessels to increase oxygen supply [163, 164]. Genes encoding glucose transporters, such as glucose transporter 1 (GLUT1), and enzymes involved in glycolysis are also upregulated by HIF-1. Induction of these genes is important because oxidative phosphorylation decreases when the levels of oxygen are low and glycolysis becomes the main pathway for producing ATP [134, 163, 165]. Many additional HIF-1 target genes controlling cell growth, cell division, and cell survival have been identified over the years. Interestingly, recent studies have shown that HIF-1 not only regulates protein-coding genes, but it can also stimulate the expression of miRNA genes, such as miR-210 [128] (**Fig 1.7**). Promoter analysis and chromatin immunoprecipitation (ChIP) studies show that similar to protein-coding genes, the promoter of miR-210 contains a HRE to which HIF-1α binds and activates transcription [166]. miR-210 is identified by many studies to be one of the most robustly and consistently upregulated miRNAs in response to hypoxia and thus is considered to be a reliable marker of hypoxia [167-173]. As will be discussed in more detail below, the induction of miRNAs provides an additional, post-transcriptional way to modulate gene

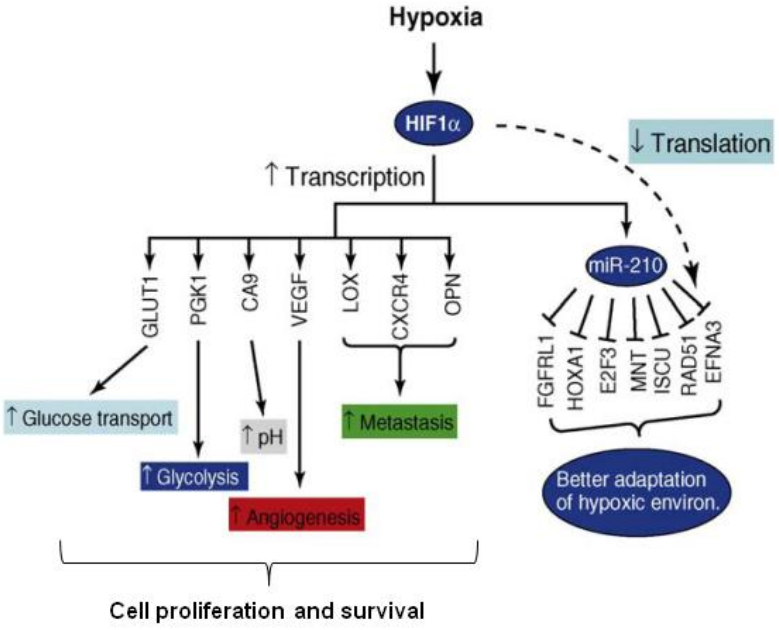

Figure. 1.7 HIF-1 target genes. HIF-1α increases the transcription of both protein-coding and miRNA genes that are critical for cell survival and hypoxia tolerance. Genes coding for GLUT1 and VEGF are among some of the genes activated by HIF-1α under hypoxia. HIF-1α-regulated miR-210 is one of the most robustly and consistently induced miRNAs in response to hypoxia. Through the increase in miR-210, the expression of miR-210 target genes is indirectly repressed by HIF-1α. Adapted from [155].

expression during hypoxia [128]. Approximately 5% of the human genome is thought to be regulated by HIF-1 [174], yet it is important to note that the exact set of genes activated by HIF-1 in response to hypoxia will depend on the cell type.

Post-transcriptional control of the hypoxic response

Except for the activation of selective genes that are crucial for cell survival and maintaining oxygen homeostasis, transcription is largely suppressed under hypoxia [175, 176]. However, post-transcriptional mechanisms still exist to regulate mRNAs at the level of mRNA turnover or at the translational level [128]. These post-transcriptional mechanisms are mediated through RBPs and miRNAs, which interact with the mRNAs to decrease or increase mRNA stability or mRNA translation [128]. It is important to note that mRNAs transcriptionally induced by HIF-1, such as VEGF and GLUT1 mRNAs, can be regulated at the post-transcriptional level as well [128]. Thus, together with HIF-1-mediated transcriptional regulation of gene expression, post-transcriptional mechanisms to modulate gene expression give rise to diverse and specific responses to hypoxia.

Post-transcriptional mechanisms to decrease the stability of mRNAs involve the recruitment of mRNAs to structures or complexes that promote mRNA degradation, such as the RNA-induced silencing complex (RISC), the exosome, and processing (P)-bodies [128]. miRNAs within RISC complexes can bind to specific target mRNAs and promote the degradation of the mRNAs via mechanisms that will be discussed in section 1.5. RBPs that promote mRNA decay, such as heterogeneous nuclear ribonucleoprotein D (hnRNP D), TTP (tristetraprolin), BRF1 (butyrate response factor-1), and KSRP (KH domain-containing RBP), recruit mRNAs to the multi-protein exosome complex, where

the mRNAs undergo 3’ to 5’ degradation [128]. Last but not least, RBPs can also recruit mRNAs to structures in the cytoplasm called P-bodies. P-bodies are a type of non-membranous RNA granule that are present in actively growing cells in the absence of stress, and their formation can be rapidly induced in the presence of arsenite [177]. Although the mechanism by which P-bodies are assembled is not fully understood, it is clear that the assembly of P-bodies does not require the stress-induced phosphorylation of eukaryotic translation initiation factor 2α (eIF2α), which is unlike the closely related class of RNA granule, the stress granules, described below [178, 179]. Time-lapse video microscopy studies reveal that the position of P-bodies within the cytoplasm is not fixed; P-bodies can move dynamically in the cytoplasm without altering their size or shape [179, 180]. P-bodies are considered to be sites of mRNA decay, for they mainly contain components of the mRNA decapping machinery (such as the Dcp1p/Dcp2p decapping enzyme, the Lsm1p-7p complex, Dhh1p/RCK/p54, and the 5’ to 3’ exonuclease Xrn1p) and the CCR4/POP2/NOT deadenylase complex [181]. Interestingly, miRNAs and Argonaute proteins have also been reported to accumulate in P-bodies, thus suggesting that P-bodies may play a role in miRNA-mediated gene repression [182, 183].

Other than promoting mRNA degradation, RBPs (such as Hu proteins, NF90, nucleolin, polypyrimidine tract-binding protein, and heterogeneous ribonucleoprotein) can also enhance the stability of mRNAs. These "stabilizing RBPs" usually increase the half-lives of mRNAs by competing with other RBPs or miRNAs that promote mRNA degradation for binding to the target mRNAs [128]. Besides inhibiting the binding of these degradation-promoting factors, some "stabilizing RBPs," such as the

polypyrimidine tract-binding protein, have been suggested to increase mRNA stability by promoting polyadenylation [128, 184]. The addition of poly(A) tails to mRNAs is known to enhance the stability of the mRNAs by protecting the mRNAs from being degraded by nucleases that are present in the cell [185].

Similar to the global repression of transcription, translation is generally suppressed under hypoxia, except for the upregulation of certain proteins that are crucial for conferring hypoxia tolerance [128]. In response to hypoxia and other types of stress, eIF2α becomes phosphorylated at a specific serine residue (Ser51) [186]. eIF2α is a GTP-binding protein that is part of the eIF2/GTP/Met-tRNA ternary complex, which plays a role in the cap-dependent initiation of translation [186]. When eIF2α is phosphorylated, GDP/GTP exchange is inhibited, thus preventing the formation of active eIF2/GTP/Met-tRNA ternary complexes and inhibiting the assembly of 48S pre-initiation complexes [186, 187]. As a result, stalled initiation complexes are formed on mRNAs and translation initiation is inhibited, leading to a global repression of translation. Other than eIF2α phosphorylation, numerous studies have shown that miRNAs can also mediate the repression of mRNA translation via mechanisms that will be discussed in section 1.5 [188-192].

Another mechanism by which mRNA translation is inhibited under hypoxia involves the recruitment of mRNAs to cytoplasmic structures known as stress granules [193]. Stress granules are another type of non-membranous RNA granule, ranging from 0.1 to 2 μm in size, that are rapidly assembled within the cytoplasm when cells are exposed to different kinds of stress, such as hypoxia, UV damage, heat shock, osmotic

stress, oxidative stress, and translation initiation inhibition [177, 194]. Once the stress is relieved, stress granules gradually disassemble and disappear, so their appearance is transient. Thus, unlike the P-bodies discussed above, stress granules are not observed in the absence of stress [179]. Moreover, time-lapse video microscopy studies reveal that stress granules are dynamic structures that can fuse and divide, often changing shape [178]. Similar to P-bodies, stress granules have been identified in a variety of organisms, such as protozoa, plants, yeast, worms, and mammals, including humans [194].

The assembly of stress granules is often induced by the phosphorylation of eIF2α (**Fig 1.8**) [179]. eIF2α phosphorylation leads to the formation of stalled initiation complexes on mRNAs, as mentioned above, as well as polysome disassembly, in which actively translating or elongating ribosomes "run off" mRNA transcripts [179]. The resultant transcripts, now devoid of polysomes, are each bound by distinct RBPs, such as T-cell intracellular antigen-1 (TIA-1), TIA-1-related protein (TIAR), TTP, fragile X mental retardation protein (FMRP), and GTPase activating protein (SH3 domain) binding protein (G3BP) [195-197]. These RBPs tend to self-aggregate, thus forming oligomeric complexes, which are subsequently crosslinked by the poly(A)-binding protein 1 (PABP-1) that is bound to the mRNA poly(A) tails [179]. Crosslinking of the oligomers results in the formation of microscopically visible stress granules [179] (**Fig 1.8**). Based on fluorescence recovery after photobleaching experiments, which show that most RBPs reside in stress granules for only a limited amount of time (on the order of seconds to minutes) [198], it is proposed that instead of acting as sites of long-term storage, stress granules are sites where the messenger ribonucleoprotein (mRNP) complexes are specifically sorted for degradation, storage, or re-initiation of translation [179]. For

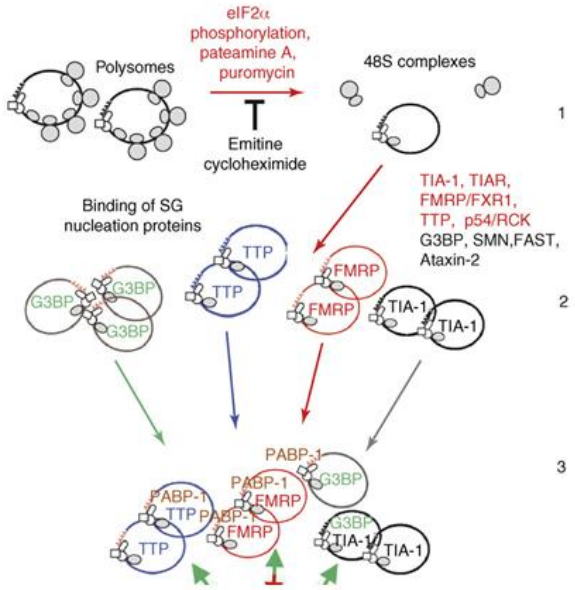

Figure. 1.8 Stress granule assembly. **(1)** The assembly of stress granules can be induced by phosphorylation of eIF2α or translation inhibitors such as pateamine A or puromycin. All of these stimuli lead to the formation of stalled initiation complexes on mRNAs and polysome disassembly. **(2)** The mRNA transcripts, now devoid of polysomes, are each bound by distinct RBPs, such as TIA-1, TTP, FMRP, and G3BP. These RBPs self-aggregate, thus forming oligomeric complexes, **(3)** which are subsequently crosslinked by PABP-1. Crosslinking of the oligomers results in the formation of microscopically visible stress granules. Drugs which stabilize polysomes, such as the translation elongation inhibitors emetine or cycloheximide, promote stress granule disassembly. Adapted from [179].

example, mRNAs bound to RBPs that promote mRNA destabilization will be targeted for degradation or decay, while mRNAs bound to “stabilizing RBPs” will be selected for storage within the stress granule itself or elsewhere in the cell [179]. In particular, it is thought that specific stress-granule-associated RBPs, such as TTP and BRF1, can shuttle mRNAs targeted for decay between stress granules and P-bodies. Live-cell microscopy studies show that when TTP or BRF1 was overexpressed, stress granules and P-bodies became more stably tethered together, thus supporting the idea that TTP or BRF1 binds to target mRNAs in stress granules and mediates the transfer of these mRNAs to P-bodies for decay [178, 179]. Interestingly, it is recently discovered that other than mRNAs and RBPs, stress granules also contain miRNAs and Argonaute proteins, thus suggesting that stress granules may be involved in miRNA-mediated gene repression [199]. However, the exact function of miRNAs and Argonaute proteins within stress granules is unclear and is an active area of research.

RBPs involved in enhancing the translation of mRNAs under hypoxia include HuR, nucleolin, hnRNP A18, and cytoplasmic polyadenylation-element-binding protein (CPEB) [128]. Similar to the "stabilizing RBPs" mentioned above, these RBPs can upregulate mRNA translation by competing with other RBPs or miRNAs that promote translational repression for binding to the target mRNAs [128]. In particular, hypoxia has been shown to increase the protein levels of nucleolin, which enhances C-P4H-α(I) mRNA translation by binding to both the 5'UTR and 3'UTR of the mRNA transcript. By interacting with the 5' and 3'UTRs, nucleolin helps bring the two ends together, forming a closed loop mRNA which can be translated more efficiently [121]. Moreover, studies have reported that in a process called "post-transcriptional derepression," the inhibitory

actions of some RBPs on translation can be relieved under hypoxia, thus leading to increased mRNA translation [128]. Overall, these post-transcriptional mechanisms work together with transcriptional mechanisms of gene expression regulation to help ensure that genes critical for cell survival and adaptation in response to hypoxia are expressed, while non-critical genes are repressed.

1.5 microRNAs.

miRNAs are evolutionarily conserved, small (21–24nt), non-coding single-stranded RNAs that post-transcriptionally regulate gene expression [200]. Since the discovery of the first miRNA, *lin-4*, in *C. elegans* in 1993 [201], hundreds of miRNAs have been identified in organisms ranging from viruses to plants, flies, fish, frogs, and mammals, including humans. The number of identified miRNAs continues to grow, and currently, more than 1,400 miRNAs have been discovered in the human genome (miRBase release 17, April 2011). miRNAs exhibit time- and tissue-specific expression patterns and function in many different biological processes, such as cell differentiation, cell proliferation, cell death, metabolism, transposon silencing, and antiviral defense [200, 202, 203]. Given the importance of miRNAs in physiological processes, it is not surprising that abnormal miRNA expression has been linked to developmental abnormalities as well as human diseases, such as cancer and cardiovascular disease [204]. Although more than a decade has passed since the first miRNA was discovered and a great deal of progress has been made in our understanding of miRNA biogenesis and activity, our knowledge about these small, non-coding regulatory molecules is still far from complete. In particular, the regulation of miRNA expression and function is poorly

understood. In addition, the exact mechanisms by which various miRNAs modulate disease pathogenesis remain to be elucidated.

Overview of miRNA biogenesis

The biogenesis of a miRNA begins with the transcription of the miRNA gene into a long primary miRNA transcript (pri-miRNA) [200, 205] (**Fig 1.9**). After the pri-miRNA is made, it is processed by the nuclear RNase III enzyme Drosha into a ~60–100nt hairpin-shaped precursor miRNA (pre-miRNA) [200, 205]. The pre-miRNA is then exported out of the nucleus into the cytoplasm by exportin-5 and is subsequently processed into a ~22nt duplex miRNA by a cytoplasmic RNase III enzyme called Dicer [200, 205]. The duplex miRNA is loaded onto an Argonaute (Ago) protein, forming the miRNA-containing RISC. The two strands of the duplex are separated, and strand selection occurs, in which one of the strands (the passenger strand) is degraded, while the other strand (the guide strand) becomes the mature single-stranded miRNA (~22nt) [200, 205]. The mature miRNA remains bound to the Ago protein and regulates gene expression by associating with partially complementary sequences usually found in the 3'UTR of target mRNAs to cause either translational inhibition or mRNA degradation [200, 205] (**Fig 1.9**). Each of these steps in the miRNA biogenesis pathway will be discussed in more detail below.

miRNA transcription

miRNAs are endogenously produced from their own genes, which are located throughout the genome. About 50% of miRNAs are expressed from intergenic, non-

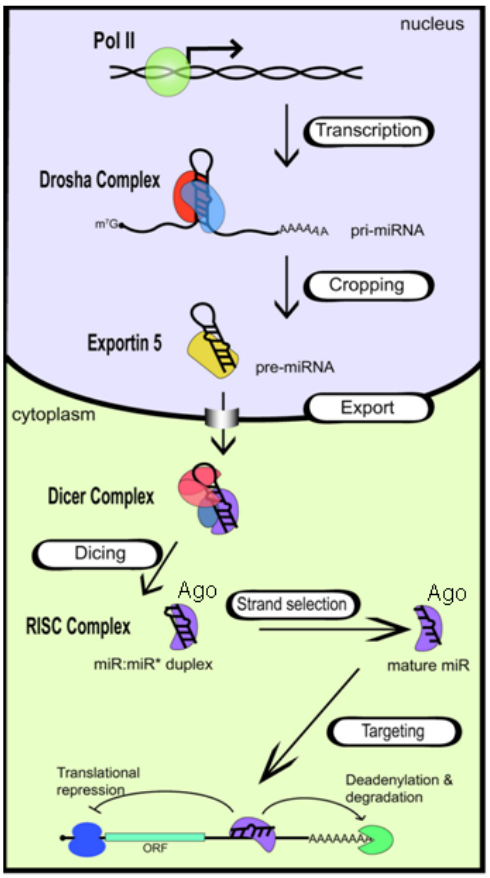

Figure. 1.9 miRNA biogenesis pathway. The biogenesis of a miRNA begins with the transcription of the miRNA gene, usually by RNA pol II, into a pri-miRNA. The pri-miRNA is then processed by the RNase III enzyme Drosha into a hairpin-shaped pre-miRNA. Following export from the nucleus into the cytoplasm by exportin-5, the pre-miRNA is processed by another RNase III enzyme, Dicer, into a duplex miRNA. The duplex miRNA is then loaded onto an Ago protein, forming the RISC complex. One of the strands of the duplex is selected to become the mature miRNA, which remains bound to Ago and regulates gene expression by associating with partially complementary sequences usually found in the 3'UTR of target mRNAs to cause either translational inhibition or mRNA degradation. Adapted from [205].

protein-coding regions, while others are encoded in intragenic regions within the introns of protein-coding genes [206, 207]. In addition, miRNA genes tend to be clustered together in the genome and transcribed as polycistronic transcripts [208]. These miRNA clusters have been found to contain anywhere from 2 to 19 miRNA genes arranged in tandem in close proximity [209]. Clustered miRNAs can have a high degree of sequence similarity to each other and can also exhibit similar expression patterns [208].

Although a few miRNA genes, such as those associated with Alu repeats, have been reported to be transcribed by RNA polymerase III, the majority of miRNA genes are transcribed by RNA polymerase II (RNA pol II) [210, 211]. RNA pol II transcription results in the generation of a long primary miRNA transcript (usually several kilobases in length), containing a 5' 7-methyl guanylate cap and a 3' poly(A) tail, similar to RNA pol II-transcribed mRNAs [200, 212, 213]. Given the fact that miRNA genes are transcribed by RNA pol II, it is not surprising that a number of RNA pol II-associated transcription factors, such as c-Myc and p53, has been demonstrated to regulate the transcription of miRNA genes [214]. The promoters of miRNA genes contain conserved transcription factor binding motifs to which transcription factors can bind and either activate or repress miRNA expression [215, 216]. Besides transcription factor binding motifs, nucleosome positioning and chromatin immunoprecipitation-on-genomic DNA microarray chip (ChIP-on-chip) analysis of human miRNA promoters reveal that miRNA promoters exhibit other features that are similar to, or even the same as, those found in protein-coding genes, such as the presence of CpG islands, TATA box, transcription factor IIB (TFIIB) recognition elements, initiator elements, and histone modifications [211, 217]. Thus, the transcription of miRNA genes can be regulated similarly to that of protein-

coding genes. In fact, miRNA gene transcription is known to be a main regulatory point in the miRNA biogenesis pathway to control the expression levels of miRNAs [218].

Pri-miRNA processing

The structure of a typical human pri-miRNA consists of a ~33nt double-stranded stem, a terminal loop, and two single-stranded RNA segments that flank both sides of the stem-loop [200, 219]. Processing of the pri-miRNA involves cleavage at the stem by the nuclear RNase III enzyme Drosha and its interacting partner DiGeorge syndrome critical region gene 8 protein (DGCR8) [200, 219]. Although Drosha contains two RNase domains that can cleave the 5' and 3' strands of the pri-miRNA stem-loop, DGCR8 is still an essential cofactor for Drosha activity [220]. When DGCR8 was knocked out in mouse embryonic stem cells, neither the pre-miRNA nor mature miRNA products were observed for the miRNAs that were examined [221]. In addition, *in vitro* pri-miRNA processing assays show that purified Drosha is unable to process pri-miRNAs efficiently; however, when supplemented with recombinant DGCR8 protein, Drosha is able to efficiently process pri-miRNAs [220]. Taken together, these results indicate that DGCR8, along with Drosha, plays an important role in the processing of pri-miRNAs to pre-miRNAs. DGCR8 has two double-stranded RNA binding domains (dsRBDs) that bind directly to the pri-miRNA at the junction between the single-stranded RNA and the stem of the stem-loop [200]. This precise positioning of DGCR8 on the pri-miRNA is thought to help determine the site of Drosha cleavage, for Drosha has been shown to cleave ~11 basepairs (bp) away from the junction between the single-stranded RNA and the double-stranded stem [222, 223]. Cleavage of the pri-miRNA by Drosha results in

the generation of a ~60–100nt hairpin-shaped pre-miRNA containing a 2nt 3' overhang, which is a characteristic feature of RNase III-mediated cleavage [224].

Drosha and DGCR8 are not the only proteins that are thought to be involved in the processing of pri-miRNAs. In fact, gel filtration chromatography of nuclear extracts reveals that Drosha is part of a large pri-miRNA processing complex called the "Microprocessor complex," which weighs ~650kDa in humans [220, 225]. Given the large size of this complex, it is plausible that other factors, besides Drosha and DGCR8, are present to facilitate pri-miRNA processing. Indeed, several accessory proteins have been identified, such as Fus, EWSR1, multiple hnRNP proteins, and the RNA helicases p68 (DDX5) and p72 (DDX17) [226]. Additionally, our lab has found that the Smad signal transducer proteins are recruited in a complex with p68 to pri-miR-21 upon TGF-β or BMP stimulation to enhance the Drosha-mediated processing of pri-miR-21 to pre-miR-21 [42].

Pre-miRNA export, pre-miRNA processing, and RISC formation

Once the pre-miRNA is generated, it is exported from the nucleus into the cytoplasm by interacting with the RanGTP-dependent nuclear export receptor, exportin-5 [227-229]. Similar to other nuclear export processes, exportin-5 interacts with the pre-miRNA as well as the GTP bound Ran in the nucleus and passes through the nuclear pore complex into the cytoplasm. Once it reaches the cytoplasm, GTP is hydrolyzed, thus resulting in the release of the pre-miRNA from exportin-5 [227-229]. The importance of exportin-5 in miRNA biogenesis is highlighted by the fact that knockdown of exportin-5 by RNA interference leads to a reduction in the levels of mature miRNAs [228]. Studies

have found that recognition of the pre-miRNA by exportin-5 is sequence independent [230]. Instead, successful interaction with exportin-5 requires the presence of a >14bp double-stranded RNA stem and a 3'overhang of 1–8nt in the pre-miRNA [229, 231]. These specific requirements provide a way for the cell to ensure that only pre-miRNAs that are correctly processed are exported from the nucleus.

Following nuclear export, the pre-miRNA undergoes cleavage near the terminal loop by a cytoplasmic RNase III enzyme called Dicer, resulting in the generation of a ~22nt double-stranded miRNA [200, 219]. The importance of Dicer in the biogenesis of miRNAs is demonstrated by the fact that knocking down Dicer reduces the expression levels of mature miRNAs [232, 233]. Unlike Drosha, which is conserved only in animals [234-236], Dicer is a highly conserved protein that is present in almost all eukaryotes [237]. Besides the two RNase III domains and the dsRBD, which are also found in Drosha, Dicer contains additional domains, such as the DExD/H-box helicase domain and the Piwi Argonaute Zwille (PAZ) domain [237]. Although the function of the DExD/H-box RNA helicase domain is unclear, crystallographic structural studies on the Dicer protein from *Giardia intestinalis* reveal that the PAZ domain anchors the 3' overhangs of double-stranded RNAs and is connected to the two RNase III catalytic domains via a long protein extension [238]. The distance separating the PAZ domain and the RNase III domains approximates the length of the cleavage product, thus allowing Dicer to cleave at a fixed distance from the 3' overhangs that were generated by Drosha cleavage [238]. The 3' overhangs were long thought to be the main structural feature that was recognized by Dicer; however, recent studies have shown that Dicer not only binds to the 3' overhangs, but it can also bind to the 5'-phosphate end of the double-stranded

RNA substrates via a newly identified "5' pocket" of its PAZ domain [239]. In this "5' counting model," Dicer cleaves at a fixed distance from the 5' phosphate end of the double-stranded RNA [239]. Hence, it is currently proposed that Dicer interacts with both the 5' phosphate end and 3' overhangs to ensure efficient and accurate processing of the pre-miRNA [239].

Recently, several studies have reported that not all pre-miRNAs depend on Dicer for their processing, thus uncovering the presence of a non-canonical Dicer-independent miRNA biogenesis pathway [240-242]. It is found that unlike other pre-miRNAs, which associate with Dicer to undergo processing, pre-miR-451 is directly loaded into Ago2 and depends on the catalytic activity of Ago2 for its cleavage [240-242]. Closer examination of pre-miR-451 reveals notable differences between its structure and that of most pre-miRNAs. First of all, only 17bp are present in the stem region of the pre-miR-451 hairpin [240, 241]. In order to be efficiently cleaved by Dicer, more than 19bp must be present in the stem of a pre-miRNA [243]; thus, the stem of pre-miR-451 is too short for Dicer-mediated processing [240, 241]. Indeed, *in vitro* assays demonstrate that Dicer cannot process pre-miR-451 into its mature miR-451 form [241]. Also, the depletion of Dicer in embryonic stem cells had no effect on the levels of miR-451, while the levels of other miRNAs were significantly reduced [241]. These results indicate that the maturation of miR-451 does not require Dicer. On the other hand, the levels of miR-451 were greatly decreased in mice expressing a catalytically inactive form of Ago2 compared to wild-type animals [241], suggesting that the endonuclease activity of Ago2 is involved in the biogenesis of miR-451. The processing of pre-miR-451 into its mature form by Ago2 was confirmed through *in vitro* assays [241]. Another important

difference between miR-451 and other miRNAs is that the mature miR-451 sequence is not confined to the stem of pre-miR-451, but instead it also encompasses the loop region of the hairpin [240-242]. Interestingly, replacing the sequence of mature miR-451 in the pre-miR-451 hairpin with that of other Dicer-dependent miRNAs, while maintaing the structure and length of the hairpin, resulted in Ago2-dependent processing of these other miRNAs [240, 242]. These findings suggest that Ago2 may recognize a certain secondary structure of pre-miRNA hairpins, and the presence of this structure will determine whether processing of the pre-miRNA will require Ago2. As mentioned previously, miR-451 is one of the miRNAs that was significantly upregulated during PAH development induced by chronic hypoxia in rats [93]. Given the unique requirement of Ago2 in the processing of pre-miR-451, it is intriguing to speculate that hypoxia may upregulate the levels and/or activity of Ago2, which could lead to the increased miR-451 levels observed under hypoxia.

Similar to Drosha, Dicer is also known to associate with interacting proteins, such as TAR RNA binding protein (TRBP; also known as TARBP2) and protein kinase R-activating protein (PACT; also known as PRKRA) [244, 245]. However, unlike the case of Drosha, where DGCR8 is essential for efficient Drosha processing activity [220], TRBP and PACT are not required for the processing activity of Dicer. *In vitro* RNA processing assays show that recombinant Dicer can effectively process pre-miRNAs into the expected double-stranded miRNA products [246, 247]. The association of Dicer with TRBP and PACT is thought to enhance the stability of the Dicer protein and facilitate the processing of pre-miRNAs [244, 245]. It has also been proposed that TRBP and PACT play a role in the formation of the RISC [244, 245, 248].

The current model for RISC formation indicates that the RISC loading complex (RLC) mediates RISC assembly. In humans, the RLC is comprised of Dicer, TRBP and/or PACT, and an Ago protein. Once Dicer cleaves the pre-miRNA, the double-stranded miRNA product is released, and one end of this miRNA duplex (the more stable end) interacts with TRBP in the RLC, while the other end of the duplex is bound to an Ago protein [245, 246, 249-251]. The two strands of the miRNA duplex are then separated into the functional guide strand, which is destined to become the mature miRNA and remains bound to the Ago protein, and the passenger (miRNA*) strand, which is degraded [200]. Recent studies have revealed that the Hsc70/Hsp90 chaperone complex plays a crucial role in the RISC-loading process, in which miRNA duplexes are loaded into Ago proteins [252]. Based on the crystal structures of Ago proteins that are currently available, it is evident that small RNA duplexes are too bulky to be accommodated in Ago proteins without any conformational changes [253-257]. Thus, it is proposed that the Hsc70/Hsp90 chaperone complex uses ATP to mediate conformational changes in Ago proteins, thereby facilitating the loading of miRNA duplexes into Ago [252]. Furthermore, studies have shown that the endonuclease activity of Ago2 allows Ago2 to cleave the passenger strand of some miRNA duplexes to facilitate the unwinding of the duplexes [258-261]. However, since not all of the Ago proteins have endonuclease activity, RNA helicases are also thought to be involved in the unwinding and removal of the passenger strand of other miRNA duplexes [200, 219]. Regardless of the mechanism by which the miRNA duplex is unwound, the active mature RISC is comprised of a single-stranded mature miRNA bound to an Ago protein [200, 219].

miRNA-mediated gene regulation

miRNA-mediated gene regulation involves miRNA-target mRNA recognition through the association of the miRNA with the RISC. The main components of the multi-protein RISC complex are the Ago proteins [262]. There are three subgroups of Ago proteins, categorized based on sequence homology: the Ago subfamily, the Piwi subfamily, and the Wago clade which is specific to worms [263-265]. Ago proteins are conserved throughout evolution and many organisms express more than one Ago protein. Humans have eight Ago proteins: four Ago subfamily proteins (Ago1–4) and four Piwi subfamily proteins (HIWI, HIWI2, HIWI3, and HILI) [265, 266]. The Piwi subfamily proteins are mainly found in germ cells and interact with piRNAs to function in germline/stem cell maintenance and transposon silencing [266, 267]. On the other hand, Ago subfamily proteins are more ubiquitously expressed and can interact with either miRNAs or small interfering RNAs (siRNAs) [268].

Three characteristic domains are present in the Ago subfamily proteins: the PAZ domain, the Middle (MID) domain, and the PIWI (P-element-induced wimpy testis) domain. Crystallographic structural studies on the Ago proteins from archaea and bacteria reveal that the PAZ domain interacts with the 3'-end of the small RNA [255, 256, 269, 270], while the 5'-end is bound by the MID domain [253-256, 271]. Interestingly, although the structure of the PIWI domain is similar to that of bacterial RNase H, not all Ago proteins exhibit RNA endonuclease cleavage activity [272]. Of the four human Ago subfamily proteins, only Ago2 has detectable endonuclease activity [272]. Studies have shown that the endonuclease activity of Ago2 not only facilitates the unwinding of some miRNA duplexes [258-261], but it also allows Ago2 to cleave a

target mRNA that is perfectly complementary to the small RNA [268, 273]. As a result of this unique cleavage activity, Ago2 is considered to play an important role in miRNA biogenesis and miRNA-mediated gene repression.

miRNAs act as guides to direct the Ago protein within the RISC to fully or partially complementary sequences on target mRNAs via Watson-Crick base-pairing [274]. These sequences are usually found in the 3'UTR of target mRNAs, but studies have reveal that they can also occur in the 5'UTR or even in the coding region of target mRNAs [275, 276]. The region on the miRNA that is thought to be important for target recognition is the "seed region," comprising of nt 2–7 at the 5'-end of the miRNA [277]. Base-pairing between the 3'-end of the miRNA and target mRNA has also been documented and can play a role in target recognition, especially when the base-pairing between the "seed region" and the target mRNA is weak [274]. Since complete sequence complementarity is not required between the miRNA and its target mRNA, each miRNA has the potential to target many different regions on the same mRNA or multiple different mRNAs, thus making the identification of bona fide miRNA targets difficult. In fact, transcriptomic and proteomic studies have shown that a single miRNA can regulate the levels of hundreds of target mRNAs as well as the amount of protein synthesized from these transcripts [278, 279]. Although the degree of repression on the individual targets is relatively small [278, 279], these small changes can together result in a major effect on gene expression.

The exact mechanism by which miRNAs regulate gene expression is controversial and has been an area of intense research over the years. Early miRNA studies, specifically with the let-7 miRNA, suggest that miRNAs repress mRNA translation

without affecting the levels of mRNAs [188, 202]. However, recent studies have found that besides inhibiting mRNA translation, miRNAs can alter the levels of target mRNAs [280]. Interestingly, these studies reveal that mRNA destabilization is often associated with target mRNAs that are strongly repressed, while translational repression is commonly seen for target mRNAs that are modestly repressed (<33%) [280]. Currently, miRNAs are thought to regulate gene expression by several different mechanisms. Perfect complementarity between the miRNA and its target mRNA promotes Ago2-mediated mRNA endonucleolytic cleavage, whereas partially complementary miRNA-target mRNA pairs lead to repression of gene expression at the level of translation or mRNA stability [274].

Various mechanisms by which miRNAs repress translation have been proposed (**Fig 1.10**), including inhibition of translation initiation, inhibition of translation elongation, co-translational degradation of the newly synthesized polypeptide chain, premature dissociation of the ribosome or ribosome drop-off, and sequestration of mRNAs in P-bodies [188-192]. Ago proteins have also been implicated in miRNA-mediated translational repression [281]. Studies have found that the MID domain of Ago proteins contains a motif that resembles the m^7G cap-binding domain of eIF4E, thus allowing Ago2 to displace eIF4E from the cap structure of mRNAs by competing with eIF4E for binding to the cap [282] (**Fig 1.10**). Since binding of eIF4E to the cap is crucial for initiating translation of most mRNAs, the displacement of eIF4E from the cap would lead to translation repression [282]. In addition, Ago proteins could inhibit translation by preventing the association of the large ribosomal subunit with the small ribosomal subunit [283] (**Fig 1.10**). Moreover, studies have shown that miRNAs can

promote the deadenylation and decapping of target mRNAs through the recruitment of the CAF1-CCR4-NOT deadenylase complex and the DCP2 decapping enzyme by the RISC [284, 285], thus leading to the destabilization of target mRNAs (**Fig 1.10**).

Although miRNAs are usually associated with repressing the translation of their target mRNAs, recent reports have shown that miRNAs can also enhance mRNA translation under certain conditions [286, 287]. When cells are arrested at the G_1 phase after serum-starvation, miR-369-3 could stimulate the translation of a reporter mRNA that contains the 3'UTR of tumor necrosis factor-α [286]. It is found that during G_1 phase arrest, the miRNA-Ago complex recruits the RNA binding protein fragile X mental retardation-related protein 1 (FXR1) to the target mRNA, and the interaction between FXR1 and Ago2 is necessary for enhancing mRNA translation [287]. However, the exact mechanism by which FXR1 and the miRNA-Ago complex stimulate translation is unclear [287]. These findings suggest that proteins recruited to the target mRNA by the miRNA-Ago complex play an important role in determining the outcome of the miRNA-target mRNA association. Depending on the cellular context, different proteins will be available or accessible, thus determining which proteins will be recruited by the miRNA-Ago complex to the target mRNA and whether translational repression or activation occurs.

1.6 Regulation of Argonaute proteins.

As mentioned in the previous section, a potential point of regulation in the miRNA pathway is at the level of transcription. Studies from our lab and others have shown that another possible control point is at the post-transcriptional level, such as

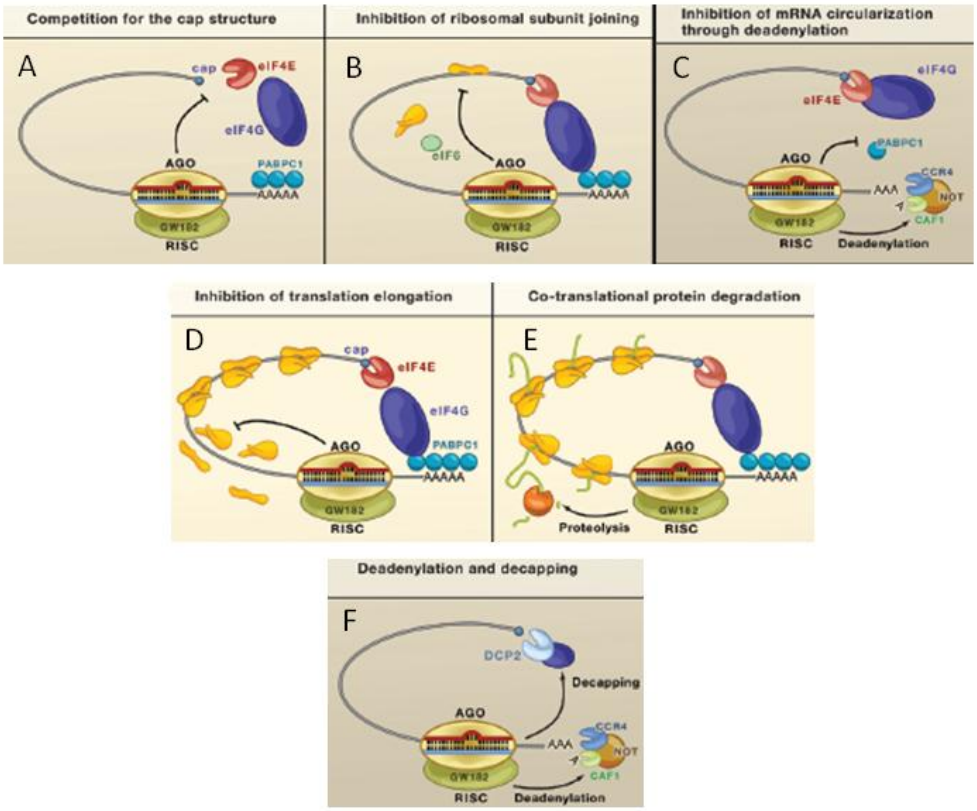

Figure. 1.10 Proposed mechanisms of miRNA-mediated gene repression. miRNAs are thought to repress gene expression by several different mechanisms. miRNA-mediated gene repression can occur at the translational level by inhibiting translation initiation **(A-C)**, inhibiting translation elongation **(D)**, or promoting co-translational degradation of the newly synthesized polypeptide chain **(E)**. miRNAs can also induce the deadenylation and decapping of target mRNAs through the recruitment of the deadenylase complex and decapping enzyme **(F)**. Adapted from [281].

during the processing of the pri-miRNA to the pre-miRNA [42, 288-290]. Moreover, several studies over the past few years have indicated that core proteins of the miRNA pathway, such as the Ago proteins, can undergo post-translational modifications, which can modulate protein stability and/or function and subsequently affect miRNA activity [291, 292]. Phosphorylation, ubiquitination, poly(ADP) ribosylation, and, most importantly, hydroxylation, are the types of post-translational modifications that have been identified in Ago proteins thus far.

The first report of post-translational modification of Ago2 appeared three years ago, demonstrating that human Ago2 can be subjected to phosphorylation [293]. Proteomic analyses reveal the presence of a phosphorylation site at serine 387 (Ser387) in Ago2 [293]. This residue is also found to be conserved in Ago1 and Ago4, but not Ago3 [293], thus suggesting that Ago1 and Ago4 may be similarly phosphorylated at Ser387 as well. Interestingly, phosphorylation of Ago2 at Ser387 is significantly upregulated ~6–8-fold upon arsenite treatment [293]. Arsenite-mediated increase in Ago2 Ser387 phosphorylation is suppressed in the presence of a p38 MAPK inhibitor, SB203580 [293]. On the other hand, addition of anisomycin, a p38 activator, is sufficient to increase Ser387 phosphorylation of Ago2 [293]. Taken together, these results imply that arsenite-induced activation of p38 MAPK plays a role in the upregulation of Ago2 Ser387 phosphorylation under arsenite treatment. Studies suggest that instead of phosphorylating Ago2 directly, p38 MAPK activates the kinase MAPK-activated protein kinase 2 (MAPKAPK2), which then phosphorylates Ago2 [293]. Since many other types of cellular stress, such as heat shock, UV irradiation, and osmotic stress, are known to activate p38 MAPK [294, 295], it will be intriguing to investigate whether these other

stress stimuli can also induce the phosphorylation of Ago2. Moreover, immunofluorescence experiments show that mutation of Ser387 to alanine reduces the P-body localization of Ago2 compared to wild-type (WT) Ago2 [293]. SB203580 treatment also decreases the association of Ago2 with P-bodies [293], thus suggesting that Ser387 phosphorylation of Ago2 by the p38 MAPK signaling pathway is important for the localization of Ago2 to P-bodies; however, the functional significance of Ago2 P-body localization is currently unclear and is an active area of investigation.

Further studies on the phosphorylation of Ago2 demonstrate that in addition to the phosphorylation site at Ser387, Ago2 can also be phosphorylated at tyrosine 529 (Tyr529) [296]. Tyr529 is found to be conserved among the other 3 human Ago proteins (Ago1, 3, and 4) as well as in the Ago proteins from other species, such as *M. musculus* (Ago2), *D. melanogaster* (Ago1 and Ago2), and *C. elegans* (Alg2), suggesting the functional importance of this residue [296]. To examine the role of Tyr529 phosphorylation in regulating Ago2 activity, the Tyr529 residue of Ago2 was mutated to glutamate (Y529E). The negatively charged glutamate is thought to mimic the negative charge of phosphorylated Tyr529 [296]. Mutating Tyr529 to glutamate decreased the cleavage activity of Ago2 as well as its ability to interact wih endogenous mRNA targets, thus indicating that Ago2 function is adversely affected by the phosphorylation of Tyr529 [296]. Structural studies reveal that Tyr529 of Ago2 is located in the region of the MID domain that is involved in binding of the 5'-phosphate ends of miRNAs and siRNAs [296]. It has been proposed that Tyr529 faciliates the binding of small RNAs through stacking interaction of its aromatic ring with the nucleotide base and the formation of a hydrogen bond between its hydroxyl group and the 5' phosphate oxygen atom [253, 254,

296]. Tyr529-to-glutamate mutation or Tyr529 phosphorylation is expected to abolish both the stacking and hydrogen bond interactions and create a repulsive force between the negative charges, thereby inhibiting the binding of the miRNA or siRNA to Ago2 [296]. Indeed, the Y529E mutant Ago2 showed reduced binding to a 5' phosphorylated single-stranded siRNA compared to WT Ago2 [296]. Together, these results suggest that phosphorylation of Tyr529 interferes with the binding of small RNAs to Ago2, which subsequently impairs Ago2-target mRNA interaction and the cleavage activity of Ago2. Since regulation of Tyr529 phosphorylation may provide an opportunity for the cell to regulate the activity of Ago2 and miRNAs in general, it will be interesting to determine whether this phosphorylation can be regulated by physiological stimuli or cellular signaling pathways.

Besides phosphorylation, Ago2 can also be ubiquitinated. Through co-immunoprecipitation (co-IP) experiments, the mouse homologue of lin-41 (mLin41) protein is found to interact with Ago2 as well as Ago1 and Ago4 [297]. Lin-41 is an evolutionarily conserved protein that is composed of a tripartite motif (Trim) domain, a filamin homology domain, and an Ncl-1, HT2A and Lin-41 (NHL) domain [298]. Given that proteins containing a Trim domain often have E3 ubiquitin ligase activity [299], the ubiquitination activity of mLin41 is examined. Studies show that mLin41 exhibits auto-ubiquitination activity and is also able to ubiquitinate Ago2 both *in vitro* and *in vivo* [297]. Co-expression of Ago2 and mLin41, but not a mutant mLin41 containing mutations in its Trim domain, induced the ubiquitination of Ago2 [297]. Overexpression of mLin41 also downregulated the protein levels of Ago2 and decreased miRNA-

mediated reporter silencing [297]. Additionally, siRNA-mediated knockdown of the endogenous expression of mLin41 decreased the amount of ubiquitinated Ago2 and increased Ago2 protein levels, while overexpression of mLin41 reduced the protein levels of Ago2 [297]. These results suggest that mLin41 regulates Ago2 stability, and consequently miRNA activity, by mediating the ubiquitination and subsequent degradation of Ago2 [297]. Thus, post-translational modification of Ago2 not only affects the subcellular localization and activity of Ago2, but it can also modulate the stability of the Ago2 protein.

Moreover, recent reports demonstrate that Ago2 can undergo poly(ADP-ribosylation) [300]. Poly(ADP-ribose) modification of all four human Ago proteins (Ago1–4) was detected in unstressed cells, and this modification increased significantly when cells were treated with a translation initiation inhibitor [300], thus suggesting that poly(ADP-ribosylation) of Ago proteins is induced upon stress conditions. Luciferase reporter experiments showed that miRNA-mediated reporter silencing was relieved upon treatment with translation initiation inhibitors or with arsenite [300]. Similar to treatment with stress stimuli, overexpression of poly(ADP-ribose) polymerase-13 (PARP-13) relieved miRNA-mediated reporter silencing as well [300]. Co-IP experiments revealed that PARP-13 associates with Ago2 in the presence and absence of stress [300]. In addition, siRNA-mediated knockdown of poly(ADP-ribose) glycohydrolase (PARG) upregulated Ago2 poly(ADP-ribosylation) and relieved miRNA-mediated reporter silencing [300]. Taken together, these results suggest that stress-induced poly(ADP-ribosylation) of Ago2 by PARP-13 reduces miRNA-mediated gene silencing. It is speculated that the increased poly(ADP-ribose) modification electrostatically interferes

with or sterically hinders miRNA-target mRNA interaction, thereby relieving miRNA-mediated gene repression [300]. Interestingly, poly(ADP-ribosylation) of glyceraldehyde-3-phosphate dehydrogenase has been recently reported to be increased under hypoxic conditions in renal epithelial cells [301]. This finding suggests that similar to translation initiation inhibitors, hypoxia can also induce poly(ADP-ribosylation); thus, it will be intriguing to investigate whether poly(ADP-ribosylation) of Ago proteins is increased under hypoxia and whether this modification affects the protein expression and/or activity of Ago proteins under hypoxia.

Last but not least, Ago2 has been documented to be prolyl 4-hydroxylated by the C-P4H(I) enzyme [119]. As will be discussed in more detail in chapter II, Ago2 interacts with C-P4H(I) and is hydroxylated at a specific proline (Pro) residue, Pro700 [119]. Studies show that unlike ubiquitination, which leads to the degradation of Ago2 [297], prolyl hydroxylation of Ago2 increases the stability of the Ago2 protein [119]. Similar to Ser387 phosphorylation [293], Pro700 hydroxylation of Ago2 is also found to promote the localization of Ago2 to P-bodies [119]. However, contrary to poly(ADP-ribosylation) of Ago2, which results in reduced miRNA-mediated gene silencing [300], downregulation of C-P4H(I) decreases siRNA-mediated RISC activity, thus suggesting that hydroxylation of Ago2 is important for siRNA-mediated gene silencing [119]. Altogether, these results indicate that different post-translational modifications of Ago2 have distinct effects on the stability, subcellular localization, and activity of the Ago2 protein.

1.7 Significance of the project and specific aims.

Although much is known about the biogenesis of miRNAs, the molecular mechanisms by which miRNA biogenesis or activity is modulated are still poorly understood. The fact that miRNAs frequently exhibit time- and tissue-specific expression patterns [202, 203] suggests that different mechanisms must exist to regulate the expression of miRNAs or the protein components of the miRNA pathway so that miRNAs can be expressed at the right place and time. Having a precise spatiotemporal regulation of miRNA expression is important because miRNAs function in many different biological processes, such as cell differentiation, cell proliferation, and cell death [200]. Loss of this precise regulation of miRNA expression will disrupt normal cellular activity and can lead to human diseases, such as cancer and cardiovascular disease [204, 302, 303]. The finding that C-P4H(I)-mediated hydroxylation of Ago2 enhances the stability of Ago2 [119] provides insights into one mechanism by which protein components of the miRNA pathway, specifically the Ago proteins, are regulated. However, important questions still remain unanswered, such as whether this hydroxylation can be modulated by physiological stimuli and whether this hydroxylation can affect the activity of Ago2. Since Ago2 plays an important role in the maturation and activity of miRNAs, further elucidation of the mechanisms of Ago2 regulation would provide additional insights into miRNA biogenesis/activity regulation, which would have implications in enhancing our understanding of normal physiological as well as disease processes.

As mentioned previously, the α-subunit is the catalytic subunit of C-P4H(I) responsible for the majority of the enzymatic activity and is known to be regulated by

various stimuli, such as hypoxia and TGF-β1, both of which upregulate the expression of C-P4H-α(I) [120-122]. Given the recent study on C-P4H(I)-mediated hydroxylation of Ago2 [119], it is plausible that hypoxia and TGF-β1 can modulate Ago2 through their induction of C-P4H-α(I) expression. However, to date, the effects of these stimuli on Ago proteins have not been investigated. Studies have shown that hypoxia modulates the levels of miRNAs [93, 167, 168], yet not much is known about the mechanisms underlying the changes in miRNA levels in response to hypoxia. Investigating the regulation of Ago2 by hypoxia may provide a better understanding of the effects of hypoxia on the miRNA pathway and may reveal a novel mechanism of miRNA regulation by hypoxia. Since chronic hypoxia is a known cause of PAH and miRNA expression is found to be deregulated in hypoxia-treated PASMCs and also during the development of PAH in rats induced by chronic hypoxia [91, 93], elucidation of the mechanism by which hypoxia affects Ago2 and the miRNA pathway may provide new mechanistic insights into the pathogenesis of PAH. The identification of Ago2 as a hypoxia-regulated protein could provide a new molecular target for the design of targeted therapies for PAH.

We hypothesize that the induction of C-P4H(I) in response to hypoxia or TGF-β will upregulate Ago2 via C-P4H(I)-mediated hydroxylation of Ago2. Hypoxia-induced C-P4H(I)-mediated hydroxylation of Ago2 will lead to increased Ago2 activity, elevated levels of miRNAs, and enhanced miRNA-mediated gene repression. To test this hypothesis, we developed the following specific aims:

i) **Elucidate the mechanism by which hypoxia regulates Ago2 in PASMCs.**

ii) **Investigate the biological significance of hypoxia-mediated regulation of Ago2 in PASMCs.**

iii) **Examine the role of TGF-β and BMP in the regulation of Ago2 in PASMCs.**

CHAPTER II. HYPOXIA UPREGULATES AGO2 PROTEIN LEVELS VIA C-P4H(I)-MEDIATED PROLYL HYDROXYLATION OF AGO2 IN PASMCS.

INTRODUCTION

2.1 C-P4H(I)-mediated prolyl 4-hydroxylation of Ago2.

Recent studies have revealed that the stability of Ago2 is regulated by a specific type of post-translational modification called prolyl 4-hydroxylation [119]. Through co-IP experiments, Qi *et al*. show that Ago2 associates with both the α- and β-subunits of C-P4H(I) [119]. Association between C-P4H-α(I) and Ago4 is also detected [119]. *In vitro* hydroxylation assays demonstrate that purified recombinant human C-P4H(I) can hydroxylate all four of the human Ago proteins (Ago1–4), thus indicating that all four Ago proteins are substrates of the enzyme [119]. However, compared to Ago1 and 3, Ago2 and 4 show a greater degree of hydroxylation in the *in vitro* hydroxylation assays [119]. This finding is consistent with the results obtained from the co-IP experiments, where association between C-P4H-α(I) and Ago2 or Ago4 is observed, but not much association between C-P4H-α(I) and Ago1 or Ago3 is seen [119]. Interestingly, neither of the three PHD proteins (PHD1–3) is able to hydroxylate the Ago proteins *in vitro* [119], suggesting that the hydroxylation of Ago proteins is specifically mediated by C-P4H(I). Mass spectrometric analysis of Ago2 identified the presence of a hydroxylation site at proline 700 (Pro700) [119]. As mentioned previously in chapter I, C-P4H(I) is an

enzyme that catalyzes the hydroxylation of specific proline residues in its substrates, which include procollagens and non-collagen proteins [99, 100, 105]. Although several non-collagen proteins have been identified to be hydroxylated by C-P4H(I) [99], the report by Qi *et al*. [119] is the first to show that protein components of the miRNA pathway can also be subjected to hydroxylation by C-P4H(I).

Furthermore, Qi *et al*. demonstrate that knocking down either the α- or β-subunit of C-P4H(I) using short hairpin RNA (shRNA) reduces the steady state protein levels of Ago2 compared to the control [119]. Although the Ago2 protein levels are decreased, the mRNA levels of Ago2 are not affected by the knockdown, thus suggesting that the stability of Ago2 may be regulated by C-P4H(I) [119]. Indeed, cycloheximide (an inhibitor of *de novo* protein biosynthesis) experiments in cells in which either the α- or β-subunit of C-P4H(I) is knocked down using shRNA reveal that the half-life of Ago2 is reduced in the knocked down cells ($t_{1/2}$ ~8 h) compared to the control ($t_{1/2}$ >10 h) [119]. Mutating the Pro700 hydroxylation site of Ago2 to alanine (P700A) also reduces the half-life of Ago2 ($t_{1/2}$ ~6 h) compared to WT Ago2 ($t_{1/2}$ >10 h), as indicated by cycloheximide experiments [119]. Together, the results suggest that C-P4H(I)-mediated hydroxylation of Ago2 at Pro700 plays a role in regulating Ago2 stability. Interestingly, the stability of the other Ago proteins, Ago1 and Ago3, is not significantly affected by the mutation of Pro700 to alanine, thus indicating that the Pro700 hydroxylation site is specifically important for regulating the stability of Ago2 [119].

2.2 Hypoxia-mediated upregulation of C-P4H-α(I).

Hypoxia is a well-known stimulus that increases the expression of C-P4H-α(I). In fact, C-P4H-α(I) is one of the target genes of HIF-1. Analysis of the promoter of C-P4H-α(I) reveals the presence of a HRE, which is a consensus sequence to which the HIF-1α-HIF-1β complex is known to bind [104]. By performing electrophoretic mobility shift assays, Takahashi *et al*. show that HIF-1α interacts with the HRE identified in C-P4H-α(I). Addition of an anti-HIF-1α monoclonal antibody results in a supershift of the C-P4H-α(I)-HRE probe complex [104]. Luciferase reporter assays also demonstrate that hypoxia exposure enhances the luciferase expression from a luciferase reporter construct in which a region of the C-P4H-α(I) promoter containing the HRE was cloned in front of the luciferase gene [104]. In addition, the hypoxia-mediated induction of C-P4H-α(I) mRNA levels is completely inhibited in cells defective in the production of HIF-1β [104]. Thus, together, these results suggest that under hypoxia, the HIF-1α-HIF-1β complex binds to the HRE in the C-P4H-α(I) gene promoter and activates the transcription of C-P4H-α(I), leading to an increase in the mRNA levels of C-P4H-α(I).

Besides upregulating C-P4H-α(I) at the transcriptional level, hypoxia can also induce the expression of C-P4H-α(I) at the post-transcriptional level. As described previously, studies have found that hypoxia increases the protein levels of the RNA-binding protein, nucleolin, which interacts with both the 5'UTR and 3'UTR of the C-P4H-α(I) mRNA transcript [121]. Nucleolin directly binds to an AU-rich element (UAAAUC or AAAUCU) in the 5'UTR, while the interaction of nucleolin with the 3'UTR is indirect and is thought to be mediated by protein/protein interaction between nucleolin and another RNA-binding protein that binds to the 3'-UTR [121]. Fahling *et al*. proposes that

the interaction of nucleolin with both the 5'UTR and 3'UTR enhances the translation of the C-P4H-α(I) mRNA by facilitating the formation of the closed loop mRNA structure, which is known to be translated more efficiently [121, 304].

Given the stimulatory effects of hypoxia on C-P4H-α(I) and the importance of C-P4H(I) in regulating the stability of Ago2, we hypothesize that hypoxic exposure of PASMCs will lead to increases in Ago2 protein levels by upregulating C-P4H(I) and that the C-P4H(I) Pro700 hydroxylation site of Ago2 will be important to the hypoxia-mediated increase in Ago2. Thus, the results in this chapter address our **first specific aim, to elucidate the mechanism by which hypoxia regulates Ago2 in PASMCs.**

RESULTS

2.3 Hypoxia increases the protein levels of Ago2.

To examine whether hypoxia regulates the protein expression of Ago2, human PASMCs were exposed to normoxia or hypoxia (95% N_2, 5% CO_2) for 24 h, and total cell lysates were prepared and subjected to Western blot analysis. Twenty-four hours of hypoxia significantly increased the protein levels of Ago2 compared to normoxia (**Fig 2.1 A**). The protein expression of two other key proteins of the miRNA biogenesis pathway, Drosha and Dicer, was also examined in these cell lysates. Interestingly, unlike Ago2, the protein levels of Drosha and Dicer decreased after 24 h of hypoxia compared to normoxia (**Fig 2.1 A**). These results suggest that there is some degree of specificity for the increase in Ago2 under hypoxia. In addition to examining the effect of hypoxia on

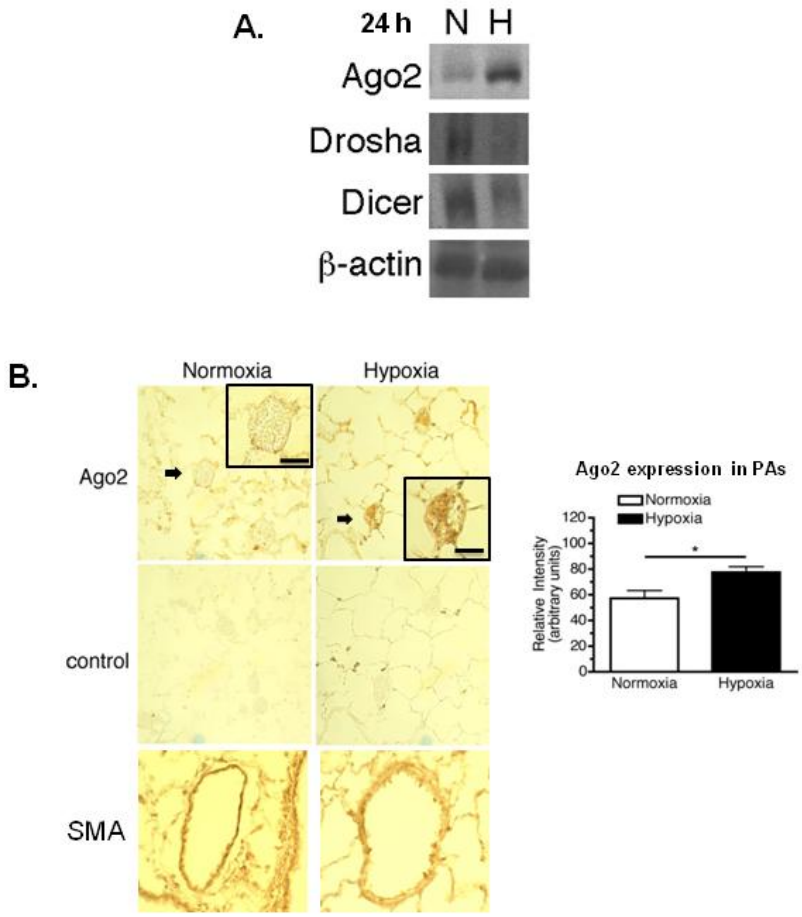

Figure. 2.1 Hypoxia upregulates Ago2 protein levels *in vitro* and *in vivo*. **A.** Total cell lysates were prepared from PASMCs exposed to normoxia (N) or hypoxia (H) for 24 h and were subjected to immunoblot analysis with anti-Ago2, anti-Dicer, anti-Drosha, or anti-β-actin (loading control) antibodies. **B.** Lung sections from rats treated with 17-day hypoxia or normoxia were subjected to immunohistochemical staining with anti-Ago2 or anti-smooth muscle α-actin (SMA) antibodies (brown, x400). Staining without the primary antibodies was performed as a control. Arrowheads indicate pulmonary arteries (PAs), and the insets in the panel are enlargements of the indicated PAs. Scale bars, 25 μm (left panel). Relative expression of Ago2 in the PAs was quantitated using ImageJ (n=3) (right panel). *p<0.05.

Ago2 protein levels in PASMCs cultured *in vitro*, hypoxia-mediated regulation of Ago2 was also investigated *in vivo* in the chronic hypoxia rat model of PAH. Following 17-days of normoxia or hypoxia treatment, rats were sacrificed, and lung sections were prepared and subjected to immunohistochemical staining for Ago2. Remodeling of PAs, which is characteristic of chronic hypoxia treatment, was observed under hypoxia, as indicated by the thickening of the medial wall shown in the SMA staining (**Fig 2.1 B)**. Elevated levels of the Ago2 protein were also evident in PAs after treatment with hypoxia (**Fig 2.1 B, arrowheads**). Thus, hypoxia treatment leads to increased Ago2 protein levels *in vitro* as well as *in vivo*.

A time course experiment was performed to determine how quickly the Ago2 protein is upregulated by hypoxia. In this experiment, human PASMCs were exposed to normoxia or hypoxia for 0.5 h, 1h, 4 h, 18 h, or 24 h, and total cell lysates were prepared and subjected to Western blot analysis. At the early time points (0.5 h and 1 h), hypoxia did not have much effect on the protein levels of Ago2; hypoxia-mediated increase in Ago2 was only observed during the later time points (4 h, 18 h, and 24 h) (**Fig 2.2 A**). Given the fact that 4 Ago subfamily proteins are present in humans, the protein expression of the other 3 members of the Ago protein subfamily (Ago1, 3, and 4) was also examined in the time course experiment to see whether hypoxia has a similar effect on the other Ago proteins. Unlike Ago2, which showed more than a 2-fold increase in protein levels after 4 h of hypoxia, Ago1, 3, and 4 exhibited a much weaker increase after 4 h of hypoxia (**Fig 2.2 B**). Moreover, 18 h and 24 h of hypoxia had much weaker effects on the protein levels of Ago1, 3, and 4 (**Fig 2.2 B**) compared to Ago2. Thus, of the 4

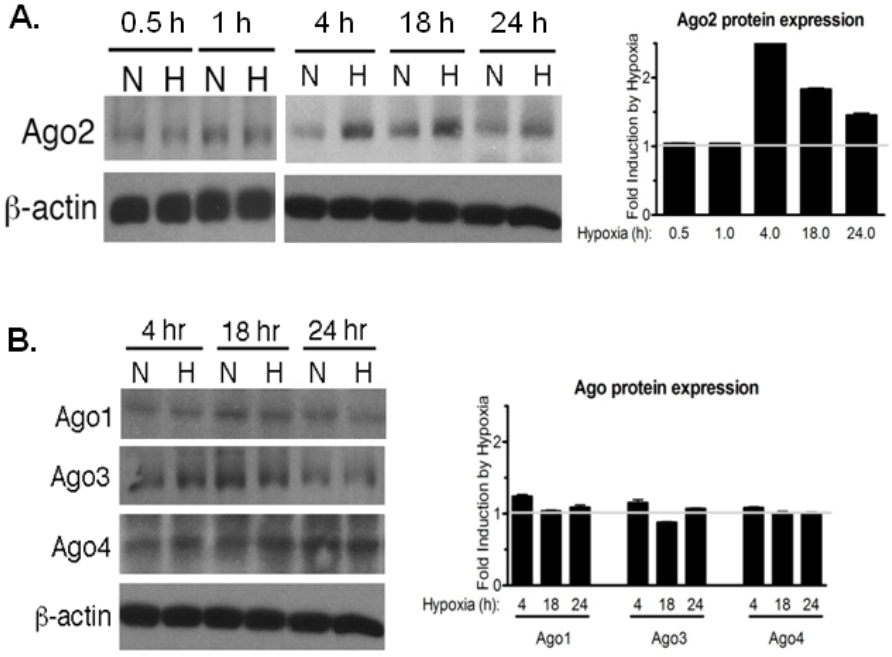

Figure. 2.2 Ago2 is the most prominently upregulated Ago protein under hypoxia. **A.** Total cell lysates were prepared from PASMCs exposed to normoxia (N) or hypoxia (H) for 0.5, 1, 4, 18, or 24 h and were subjected to immunoblot analysis with anti-Ago2 or anti-β-actin (loading control) antibodies (left panel). By densitometry, relative amounts of Ago2 protein normalized to β-actin were quantitated, and the results presented are the average of three independent experiments (n=3). Fold induction (hypoxia/normoxia) is presented (right panel). **B.** Total cell lysates were prepared from PASMCs exposed to normoxia (N) or hypoxia (H) for 4, 18, or 24 h and were subjected to immunoblot analysis with anti-Ago1, 3, or 4 or anti-β-actin (loading control) antibodies (left panel). By densitometry, relative amounts of Ago proteins normalized to β-actin were quantitated, and the results presented are the average of three independent experiments (n=3). Fold induction (hypoxia/normoxia) is presented (right panel).

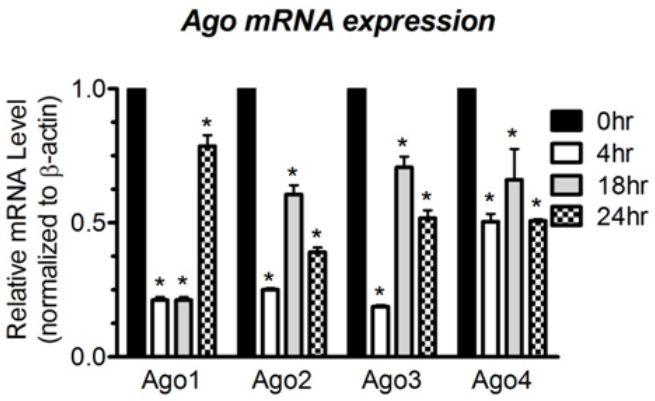

Figure. 2.3 Hypoxia decreases the mRNA levels of Ago1-4. Total RNAs were prepared from PASMCs exposed to normoxia or hypoxia for 4, 18, or 24 h and were subjected to qRT-PCR analysis of Ago1-4 mRNAs. Relative levels of mRNA expression normalized to β-actin were quantitated and are presented. *p<0.05.

Ago subfamily proteins that are present in humans, Ago2 is the most prominently upregulated by hypoxia at all the time points examined.

Total RNAs were also prepared from the time course experiment and were subjected to qRT-PCR analysis of Ago1–4. Despite the increase in Ago2 protein levels after 4 h, 18 h, and 24 h of hypoxia, hypoxia decreased the mRNA levels of Ago2, as well as that of the other Agos, by ~40–70% during these time points **(Fig 2.3**). These results indicate that hypoxia most likely upregulates Ago2 through a post-transcriptional mechanism.

2.4 Upregulation of Ago2 protein levels upon hypoxia treatment is mediated by the C-P4H(I) enzyme.

Given that previous studies have found that hydroxylation of Ago2 at Pro700 by the C-P4H(I) enzyme enhances the stability of Ago2 [119], we investigated whether C-P4H(I) may play a role in the increase in Ago2 protein levels under hypoxia. First, the protein and mRNA expression of C-P4H-α(I) and C-P4H-β were examined in human PASMCs exposed to normoxia or hypoxia for 0.5 h, 1 h, 4 h, 18 h, or 24 h. Hypoxia-mediated increase in the protein levels of C-P4H-α(I) was detected as early as 1 h after hypoxia (**Fig 2.4 A**), suggesting that C-P4H(I) may mediate the accumulation of Ago2 upon hypoxia treatment. The mRNA levels of C-P4H-α(I) and C-P4H-β were also upregulated after 1 h, 4 h, 18 h, and 24 h of hypoxia (**Fig 2.4 B**). These results are consistent with previous reports demonstrating that hypoxia upregulates C-P4H-α(I) and C-P4H-β at both the protein and mRNA levels [120, 121, 305].

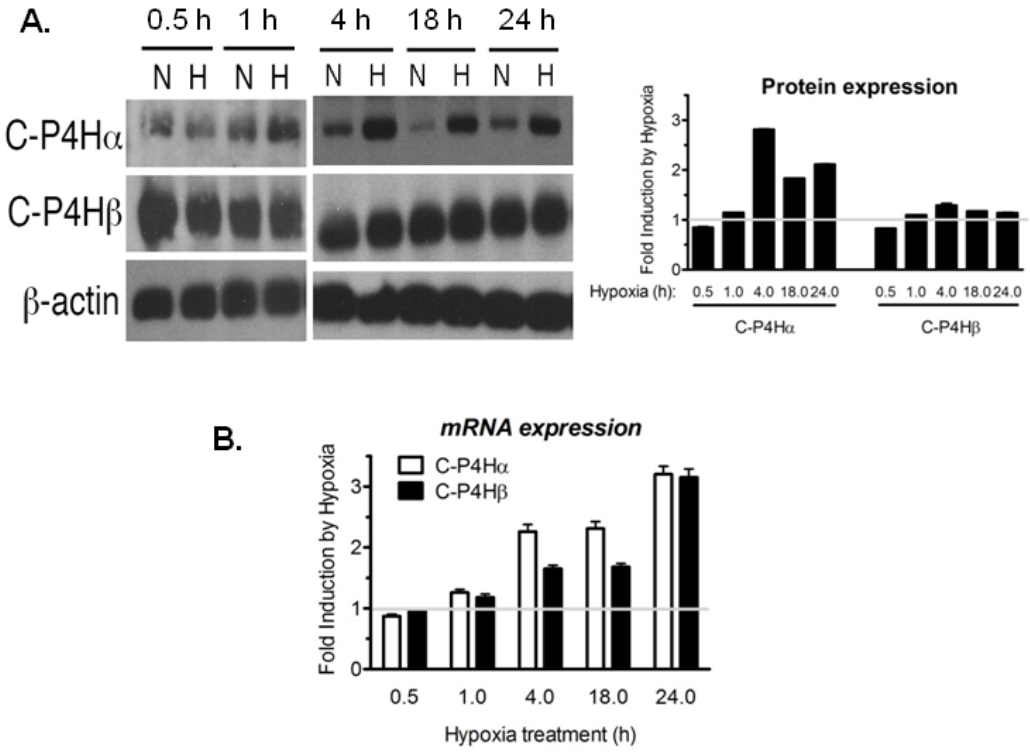

Figure. 2.4 Hypoxia increases the mRNA and protein levels of C-P4H(I). **A.** Total cell lysates were prepared from PASMCs exposed to normoxia (N) or hypoxia (H) for 0.5, 1, 4, 18, or 24 h and were subjected to immunoblot analysis with anti-C-P4Hα, anti-C-P4Hβ, or anti-β-actin (loading control) antibodies (left panel). By densitometry, relative amounts of C-P4H(I) proteins normalized to β-actin were quantitated, and the results presented are the average of three independent experiments (n=3). Fold induction (hypoxia/normoxia) is presented (right panel). **B.** Total RNAs were extracted from the cells used in **A.** and were subjected to qRT-PCR analysis of C-P4Hα and C-P4Hβ mRNAs. The relative levels of mRNA expression normalized to β-actin were quantitated. Fold induction (hypoxia/normoxia) is presented.

To determine whether the increase in Ago2 protein levels under hypoxia is mediated by the C-P4H(I) enzyme, the activity of C-P4H(I) in human PASMCs was knocked down by using siRNA against the α-subunit of C-P4H(I) (si-P4H-α) prior to treating the cells with hypoxia for 24 h. Of the two subunits of C-P4H(I), the α-subunit contains the majority of the catalytic active site and is known to be rate-limiting during the formation of the active enzyme [100, 105, 119]. Thus, knocking down C-P4H-α(I) should abolish most of the activity of C-P4H(I). Transfection of si-P4H-α reduced endogenous C-P4H-α(I) mRNA expression to ~3% of that of the si-Control (**Fig 2.5 A**), while endogenous C-P4H-α(I) protein expression in the si-P4Hα cells was reduced to ~20% of that of the si-Control (**Fig 2.5 B**). As expected, the protein levels of Ago2 increased after 24 h of hypoxia in the si-Control cells coincident with increases in the protein levels of C-P4H-α(I) (**Fig 2.5 B**). However, the knockdown of C-P4H-α(I) prevented the induction of Ago2 protein levels in response to hypoxia (**Fig 2.5 B**), thus suggesting that C-P4H(I) mediates the accumulation of Ago2 under hypoxia, most probably by promoting the hydroxylation of Ago2.

2.5 Hypoxia upregulates Ago2 protein levels through Pro700 hydroxylation of Ago2.

To confirm the importance of C-P4H(I)-mediated prolyl hydroxylation in the hypoxia-mediated upregulation of Ago2, human osteosarcoma U2OS cells were transfected with an empty vector (mock), a wild-type (WT) Ago2, or a P700A mutant (mut) Ago2 expression construct and exposed to 24 h of normoxia or hypoxia. The mutant Ago2 contains a Pro700-to-alanine mutation and thus can no longer be

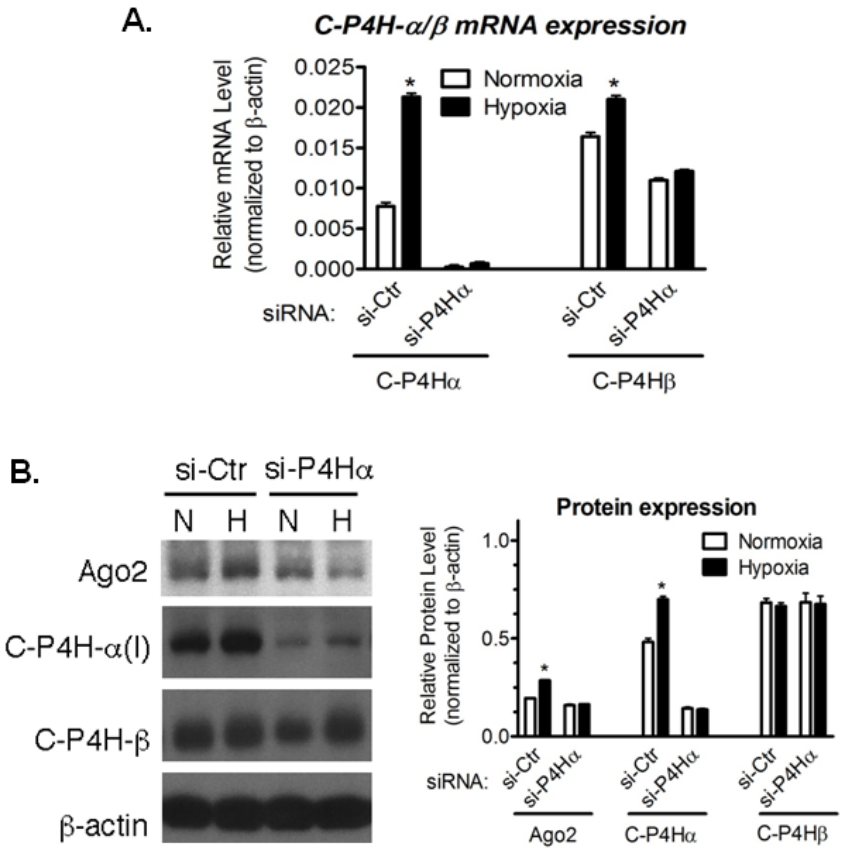

Figure. 2.5 Knockdown of C-P4H-α(I) prevents the hypoxia-mediated increase in Ago2 protein levels. **A.** PASMCs were transfected with siRNA against C-P4Hα (si-P4Hα) or non-targeting control (si-Ctr) for 48 h prior to treatment with normoxia (N) or hypoxia (H) for 24 h. Total RNAs were extracted from the cells and were subjected to qRT-PCR analysis. Relative C-P4Hα/β mRNA levels normalized to β-actin were quantitated and are presented. *p<0.05. **B.** Total cell lysates were prepared from the cells used in **A.** and were subjected to immunoblot analysis using anti-Ago2, anti-C-P4Hα(I), anti-C-P4Hβ, or anti-β-actin (loading control) antibodies (left panel). By densitometry, relative amounts of Ago2 and C-P4H(I) proteins normalized to β-actin were quantitated, and the results presented are the average of three independent experiments (n=3) (right panel). *p<0.05.

hydroxylated by C-P4H(I) at this position [119]. U2OS cells were utilized in this experiment because PASMCs are not readily transfectable. Although U2OS cells were used, the protein levels of endogenous Ago2 still increased after 24 h of hypoxia in the mock-transfected cells coincident with increases in the protein and mRNA levels of C-P4H-α(I) (**Fig 2.6 A and B**), similar to the results obtained with human PASMCs. These findings suggest that the hypoxia effect on Ago2 is not a cell-type-specific phenomenon. Interestingly, I found that 24 h of hypoxia increased the protein levels of exogenous WT Ago2, but not the P700A mut Ago2 (**Fig 2.6 A**), thus supporting our hypothesis that the C-P4H(I) Pro700 hydroxylation site of Ago2 plays an important role in the hypoxia-mediated accumulation of Ago2.

DISCUSSION

2.6 Hypoxia regulates the protein levels of Ago2.

Several studies have shown that hypoxia modulates the expression levels of miRNAs in various types of cells, ranging from cancer cell lines to primary smooth muscle cells [91, 168]; however, not much is known about the mechanisms underlying the changes in miRNA levels under hypoxia. Studies have reported that HIF-mediated activation of miRNA gene expression plays a role in regulating the levels of some miRNAs under hypoxia. The most well known HIF-1 target miRNA gene is miR-210, one of the most robustly and consistently upregulated miRNAs in response to hypoxia [167-173]. Promoter analysis and ChIP studies show that the promoter of miR-210 contains a HRE to which HIF-1α directly binds and activates transcription [166]. Besides miR-210, miR-26b and miR-181c are also identified as hypoxia-regulated

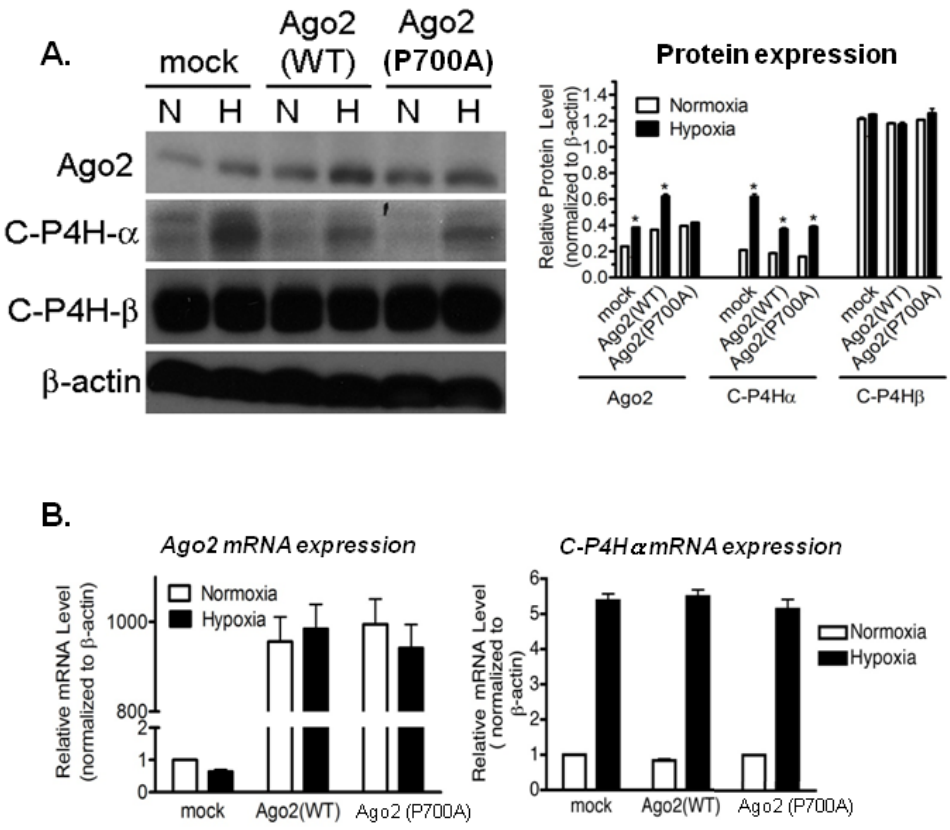

Figure. 2.6 Hypoxia increases protein levels of exogenous WT Ago2, but not P700A mutant Ago2. **A.** U2OS cells were transfected with vector (mock), wild type (WT) Ago2, or Pro700A mutant (P700A) Ago2 cDNA construct, followed by treatment with normoxia (N) or hypoxia (H) for 24 h. Relative levels of Ago2 or C-P4H(I) proteins normalized to β-actin were examined by immunoblot (left panel) and quantitated by densitometry (right panel). The quantification results presented are the average of three independent experiments (n=3). *p<0.05. **B.** Total RNAs were prepared from the cells used in **A.** and were subjected to qRT-PCR analysis. Relative mRNA levels of Ago2 (left panel) and C-P4Hα (right panel) normalized to β-actin were quantitated and are presented.

miRNAs that contain HREs in their promoters, and their expression is similarly upregulated by HIF [168].

The fact that hypoxia upregulates a wide range of miRNAs, those that are HIF-regulated as well as those that are not under the control of HIF [306], indicates that HIF-mediated induction of miRNA transcription is not the only mechanism to regulate miRNAs under hypoxia. Since hypoxia has a global effect on miRNA expression, it is reasonable to speculate that hypoxia may regulate the expression or function of core components of the miRNA pathway, such as Drosha, Dicer, and Ago proteins, and thus lead to global changes in miRNA levels. The importance of these core components of the miRNA pathway in regulating miRNA expression has been demonstrated by studies looking at the effect of knocking down these core proteins on miRNA biogenesis [224, 233]. The siRNA-mediated downregulation of Drosha resulted in decreased levels of pre-miRNAs and mature miRNAs, while pri-miRNA levels were significantly increased in the cell [224]. In addition, siRNA inhibition of Dicer reduced the levels of mature let-7 and elevated the levels of pre-let-7 [233]. These results suggest that these core proteins are rate-limiting in the miRNA biogenesis pathway.

In this chapter, I showed that hypoxia elevates the protein levels of Ago2, a key component of the RISC that plays an important role in the biogenesis and activity of miRNAs [258-262, 268, 273]. It is interesting that of the 4 Ago subfamily proteins that are present in humans, Ago2 was the most strongly upregulated by hypoxia. Unlike the other three Ago proteins, Ago2 exhibits endonuclease activity [272]; thus, the prominent upregulation of Ago2 upon hypoxia treatment may suggest that the endonuclease activity

of Ago2 is particularly important during the hypoxic response. Furthermore, it is especially interesting that the levels of two key miRNA biogenesis enzymes, Drosha and Dicer, were reduced upon hypoxia treatment. Hypoxia-mediated reduction of Dicer is not only seen *in vitro* in cultured cells, but has also been reported *in vivo* in the lungs of chronic hypoxia-treated rats [93]. Hypoxia treatment also decreased the mRNA levels of Dicer in rat pulmonary artery fibroblasts [93]. These results suggest that hypoxia-mediated downregulation of Dicer is not cell-type specific. It is intriguing to speculate that the increased levels of Ago2 under hypoxia may serve as a compensatory mechanism for the reduced amount of Drosha and Dicer in the cell. Given the fact that hypoxia has been reported to increase the levels of miRNAs, some of which have been shown to be important for mediating hypoxia-induced cell processes, such as proliferation and migration [91], increased levels of Ago2 may help to stabilize miRNA levels and may also help to augment miRNA-mediated gene regulation under hypoxia. Studies have indicated that the total levels of Ago proteins within the cell may be important in regulating the levels of mature miRNAs. Overexpression of human Ago2, as well as Ago1, 3, and 4, has been shown to increase the levels of mature miRNAs [261], while knocking out Ago2 in mouse embryonic fibroblasts reduces the levels of mature miRNAs [261]. Moreover, a recent study demonstrates that Ago proteins can post-transcriptionally upregulate miRNA levels by enhancing the stability of miRNAs [307]. When Ago2 or any of the other 3 Ago proteins is overexpressed, miRNA degradation is reduced and miRNA half-life is correspondingly increased [307].

Although I did not observe significant differences in the regulation of Ago2 by hypoxia between human PASMCs and U2OS cells, it should be noted that a previous

study found that exposure of primary term human trophoblasts to 24 h of hypoxia did not significantly change the mRNA or protein levels of Ago2 compared to normoxia [308]. This contradictory finding could be due to differences in the experimental conditions employed, such as variations in the seeding density of cells or in the components of the hypoxic gas mixture. Nevertheless, it is intriguing to speculate that the fact that hypoxia-mediated upregulation of Ago2 is seen PASMCs and U2OS cells could indicate that this mechanism of Ago2 regulation is particularly relevant to disease processes that these cell-types participate in, such as PAH and cancer, both of which are diseases that hypoxia is known to play an important role in.

2.7 Hypoxia-mediated increase in Ago2 protein levels is dependent on C-P4H(I).

In this chapter, I showed that the increase in Ago2 protein levels under hypoxia is mediated by the C-P4H(I) enzyme. The fact that knocking down the catalytic α-subunit of C-P4H(I) and mutating the C-P4H(I) Pro700 hydroxylation site to alanine prevented the hypoxia-mediated accumulation of Ago2 suggests that the hydroxylation activity of C-P4H(I) is important for elevating Ago2 protein levels under hypoxia. Although we currently do not have direct evidence that hypoxia induces the hydroxylation of Ago2, it is plausible that hypoxia would increase Ago2 hydroxylation. Previous studies have demonstrated that hypoxia induces the activity of C-P4H(I) as well as increases the expression of C-P4H-α(I), the catalytic subunit of the enzyme, at both the transcriptional and post-transcriptional levels [104, 120, 121, 123, 124]. As a result, we would expect to see an enhanced degree of prolyl hydroxylation of Ago2 under

hypoxia. Since hydroxylation has been previously shown to increase the stability of Ago2 [119], an increase in Ago2 hydroxylation would enhance the stability of Ago2 and result in elevated Ago2 protein levels under hypoxia. Thus, my results address the possibility that hydroxylation of Ago proteins can be modulated in response to physiological stimuli. Here, we propose that hypoxia upregulates Ago2 by promoting the C-P4H(I)-mediated hydroxylation of Ago2. In the future, it will be important to confirm the increase in Ago2 hydroxylation under hypoxia by performing mass spectrometry on Ago2 purified from cells exposed to normoxia or hypoxia. Alternatively, an antibody specific to the Pro700 hydroxylation site of Ago2 could be generated and could be used to show that Pro700 of Ago2 is hydroxylated to a greater extent under hypoxia compared to normoxia.

The finding that hypoxia regulates Ago2 protein levels through C-P4H(I)-mediated prolyl hydroxylation reveals another post-transcriptional mechanism by which hypoxia regulates the expression of proteins. A similar instance in which prolyl hydroxylation regulates protein stability is seen for the HIF proteins. However, instead of enhancing the stability of HIFs, prolyl hydroxylation promotes the degradation of the HIF proteins [151, 152, 309-311]. Additionally, hydroxylation of the HIF proteins is mediated by the cytosolic PHD proteins, rather than by C-P4H(I), which is located in the ER [142]. Moreover, hypoxia inhibits the hydroxylation of HIFs, while our results suggest that hypoxia appears to promote the hydroxylation of Ago2. Nevertheless, it is intriguing that the same type of post-translational modification can lead to different effects on protein stability depending on the identity of the target protein.

My results suggest that the Pro700 hydroxylation site is important in the hypoxia-mediated upregulation of Ago2. In the previous study by Qi *et al.*, mass spectrometric analysis of Ago2 under normoxic conditions only detected a hydroxylation site at Pro700 [119]; however, this analysis does not exclude the possibility that other proline residues of Ago2 may be hydroxylated in response to hypoxia. As reported by Qi *et al.*, Ago2 has three -X-Pro-Gly triplets (119–121, 522–524, 699–701) which are predicted to be hydroxylated by C-P4H(I) [119]. These motifs are found to be conserved among the other 3 human Ago proteins (Ago1, 3, and 4) and also in Ago proteins from other species, such as *M. musculus*, *D. melanogaster* (Ago1), and *C. elegans* (Alg1), suggesting that these motifs are functionally important [119]. Thus, it is possible that hypoxia promotes the hydroxylation of Pro700 as well as these other Pro residues to mediate the increase in Ago2 protein levels. Also, as mentioned by Qi *et al*. [119], the hydroxylation sites may be cell-type specific. In the original study, 293ET cells were used to determine the hydroxylation sites in Ago2; thus, it is plausible that other hydroxylation sites, besides Pro700, are found in human PASMCs.

2.8 Acknowledgments and publication status.

All experiments described in this chapter were planned and analyzed by C. Wu and A. Hata. N. Hill performed the rat hypoxia experiment and provided slides for analysis. T. Uchimura and A. Weisman performed the immunohistochemical staining of the hypoxia-treated rat lung sections. All other experiments were performed by C. Wu. All results are published in Wu C, So J, Davis-Dusenbery BN, Qi HH, Bloch DB, Shi Y, Lagna G, Hata A. *Hypoxia potentiates microRNA-mediated gene silencing through post-*

translational modification of Argonaute2. Mol Cell Biol 2011 Dec;31(23):4760-74. See the attached appendix.

CHAPTER III. HYPOXIA-INDUCED PROLYL HYDROXYLATION OF AGO2 REGULATES AGO2 SUBCELLULAR LOCALIZATION, ASSOCIATION WITH HSP90, ACTIVITY, AND miRNA LEVELS.

INTRODUCTION

3.1 Localization of Ago proteins to stress granules in response to stress.

When cells are exposed to stress, such as hypoxia, UV damage, heat shock, and oxidative stress, non-membranous RNA granules called stress granules are rapidly assembled within the cytoplasm [177, 194]. Interestingly, studies by Leung *et al.* reveal that Ago proteins localize to these newly formed stress granules in response to stress [199]. By performing immunofluorescence studies, Leung *et al*. found that in unstressed cells, Ago proteins (Ago1–4) are mostly diffusely localized to the cytoplasm, with a small percentage present in cytoplasmic structures called P-bodies [199]. However, when cells experience oxidative stress (e.g. arsenite) or translation initiation inhibition (e.g. hippuristanol), Ago proteins are also found to localize to stress granules [199]. In addition, luciferase reporter mRNAs containing miRNA binding sites and the well-characterized siCXCR4 siRNA (which is known to target the endogenous CXCR4 mRNA with a perfectly complementary binding site but can also function as a miRNA by targeting other mRNAs with partially complementary sites [312]) are shown to localize to stress granules upon arsenite or hippuristanol treatment [199]. In particular, quantitative analyses reveal that the signal intensity of siCXCR4 is ~1.5-fold greater at stress granules compared to the surrounding cytoplasm, suggesting that small RNAs accumulate in stress

granules in response to stress [199]. Together, these results indicate that stress granules contain not only Ago proteins, but also small RNAs (siRNAs and miRNAs) and target mRNAs; thus, it has been proposed that stress granules might be sites involved in miRNA-mediated gene repression [177].

Furthermore, Leung *et al*. demonstrate that localization of Ago2 to stress granules is dependent on the presence of miRNAs. When Dicer-deficient cells, which were confirmed to be deficient in endogenous mature miRNAs, were treated with hippuristanol, localization of Ago2 to stress granules was no longer observed [199]. However, when exogenous miRNAs were transfected into these Dicer-deficient cells, Ago2 localization to stress granules was again detected upon hippuristanol treatment [199]. Thus, the localization of Ago2 to stress granules appears to be a regulated process. Interestingly, Qi *et al*. have noted that knocking down either C-P4H-α(I) or C-P4H-β using shRNA reduces the localization of Ago2 to P-bodies, marked by the P-body component Dcp1a [119]. The P700A mutant Ago2, in which the Pro700 hydroxylation site is mutated to alanine, also shows reduced localization to P-bodies compared to WT Ago2 [119], implying that Ago2 localization to P-bodies is also regulated and that Pro700 hydroxylation promotes the localization of Ago2 to P-bodies. Similar to hydroxylation, studies by Zeng *et al*. indicate that phosphorylation of Ago2 is important for the localization of Ago2 to P-bodies as well. Mutation of Ser387 to alanine reduces the P-body localization of Ago2 compared to WT Ago2 [293]. Thus, post-translational modifications appear to play an important role in the localization of Ago2 to P-bodies. Given the similarities between P-bodies and stress granules, it is plausible that post-

translational modifications, such as hydroxylation, can also regulate the localization of Ago2 to stress granules.

We hypothesize that similar to arsenite and hippuristanol, hypoxia induces the localization of Ago2 to stress granules and that C-P4H(I)-mediated hydroxylation of Ago2 at Pro700 facilitates the association of Ago2 with stress granules.

3.2 Heat shock protein 90.

Heat shock protein 90 (Hsp90) is a member of a large group of proteins called heat shock proteins (Hsps), whose expression is induced in response to heat stress [313]. Out of all the Hsps, Hsp90 is one of the most highly conserved Hsp and is found in organisms ranging from bacteria to mammals [313]. Although Hsp90 is a key player in the protective response to heat stress, it has a variety of important functions outside of the heat shock response as well. Hsp90 is a constitutively expressed molecular chaperone that is located in the cytosol and also in the ER of eukaryotes [313]. Hsp90 is an abundant protein comprising ~1–2% of total soluble protein levels in the cytoplasm [314]. As a molecular chaperone, Hsp90 helps certain proteins, known as client proteins, fold, mature, and adopt their active stable conformation by using energy generated from the hydrolysis of ATP [315]. Hsp90 also plays a role in breaking up protein aggregates and in refolding denatured proteins under stress conditions [316]. In the case of terminally misfolded proteins, Hsp90 can target these proteins for degradation by interacting with the ubiquitin-proteasome system [317-320]. In addition, Hsp90 facilitates the translocation of client proteins to proper locations in the cell by interacting with translocation machineries [321]. Interestingly, several studies have revealed that

components of the miRNA pathway, specifically Ago2, are also client proteins of Hsp90, thus suggesting that Hsp90 may play a role in miRNA-mediated gene repression [252, 322-324].

3.3 Regulation of the Ago2 protein by Hsp90.

In one of the early studies on Ago2, Tahbaz *et al*. reported that Ago2 interacts with Hsp90 as well as several Hsp90 binding proteins [322]. By performing affinity purification experiments with glutathione S-transferase (GST)-Ago2 fusion proteins, Tahbaz *et al.* found that Hsp90 co-purified with full-length Ago2 and the N-terminal 323 amino acids of Ago2, but not with the C-terminal 309 amino acids, the PIWI domain, or the PAZ domain of Ago2 [322]. Co-purification of the Ago2 N-terminal region and the Hsp90 co-chaperones p23, Hop, Hsp70, and Hdj-2 was also observed [322]. These results suggest that the N-terminal region of Ago2 mediates the interaction with Hsp90 and its co-chaperones. When Hsp90 was inhibited with geldanamycin (GA), a well-known inhibitor of the ATPase activity of Hsp90 [325], newly synthesized Ago2 was degraded more quickly than in the absence of the inhibitor, as indicated by pulse-chase experiments in Cos cells [322]. Treatment of normal rat kidney cells with GA also decreased the steady state levels of the Ago2 protein compared to the control [322]. Taken together, these findings suggest that Hsp90 interacts with Ago2 and is important for stabilizing nascent Ago2 proteins. Since Hsp90 is a component of the stress response, it will be interesting to investigate whether the interaction between Hsp90 and Ago2 can be regulated by stress or other physiological stimuli.

Besides regulating the stability of Ago2, the activity of Hsp90 has been recently shown to be important for the localization of Ago2 to stress granules upon exposure to stress. Pare *et al*. performed live-cell imaging experiments and found that when HeLa cells were treated with the Hsp90 ATPase activity inhibitor GA, formation of TIA-positive stress granules was still observed upon hippuristanol treatment, but the colocalization between Ago2 and stress granules was reduced compared to the absence of the inhibitor [324]. These results suggest that Hsp90 activity is not crucial for stress granule formation in response to stress; however, it is important for the association of Ago2 with stress granules. It will be intriguing to investigate whether Hsp90 activity plays a role in the localization of Ago2 to stress granules induced by other types of stress and to determine the exact mechanism by which the activity of Hsp90 mediates the association of Ago2 with stress granules.

Moreover, recent studies by Iwasaki *et al.* demonstrate that the activity of the Hsc70/Hsp90 chaperone complex is crucial for the loading of siRNA or miRNA duplexes into Ago proteins [252]. Iwasaki *et al.* employed cell-free RISC assembly systems to examine the role of the Hsc70/Hsp90 chaperone complex in RISC assembly. In these cell-free systems, immunopurified endogenous human Ago2 was incubated with radiolabeled siRNA or miRNA duplexes in the presence or absence of an Hsp70 or Hsp90 family protein inhibitor [252]. The Hsp70 inhibitor 2-phenylethynesulfonamide (PES), which inhibits the interaction between Hsp70 and its client proteins [326], and the Hsp90 inhibitor 17-allylamino-17-demethoxygeldanamycin (17-AAG), a derivative of GA which inhibits the ATPase activity of Hsp90 [327], were utilized. A native agarose gel system was also used to separate pre-RISCs, containing duplex RNAs loaded into

Ago, and mature RISCs, containing unwound single-stranded RNAs loaded into Ago [252]. Iwasaki *et al*. found that pre-RISC formation was significantly reduced in the presence of PES or 17-AAG; however, neither of the inhibitors affected the formation of mature RISC from the pre-RISC, thus suggesting that the activity of the Hsp70/Hsp90 complex is not required for the unwinding of RNA duplexes within Ago2 [252]. Consistent with these results, target cleavage assays showed that the introduction of PES or 17-AGG prior to RISC assembly reduced the target cleavage activity of endogenous human Ago2, while the target cleavage activity was not affected when the inhibitors were introduced after RISC assembly [252]. Together, these results suggest that the activity of the Hsp70/Hsp90 chaperone complex is required for the loading of small RNA duplexes into Ago2, which is important for subsequent target mRNA cleavage. Although endogenous levels of mature miRNAs were not examined in the study by Iwasaki *et al*. [252], it is reasonable to speculate that the activity of the Hsp70/Hsp90 chaperone complex also plays an important role in the generation of mature miRNAs, since RISC-loading is a key final step in the miRNA biogenesis pathway.

Given the importance of the Hsp90 chaperone complex in the stress response and the role of Hsp90 in regulating various aspects of Ago2, we hypothesize that hypoxia may modulate the interaction between Hsp90 and Ago2. Since the activity of Hsp90 is critical for the loading of small RNA duplexes into Ago2, changes in the Hsp90-Ago2 interaction under hypoxia may lead to alterations in mature miRNA levels and Ago2 activity. Together, the results in this chapter address our **second specific aim, to investigate the biological significance of hypoxia-mediated regulation of Ago2 in PASMCs.**

RESULTS

3.4 Ago2 localizes to stress granules upon hypoxia treatment.

Previous studies have reported that Ago2 and the other 3 Ago proteins (Ago1, 3, and 4) localize to stress granules upon arsenite or hippuristanol treatment [199]; however, to date, no studies have specifically looked at the effect of hypoxia on the subcellular localization of Ago2 or any of the other Ago proteins. To examine whether hypoxia has a similar effect on the localization of Ago2 as the other stress stimuli, human PASMCs were exposed to normoxia or hypoxia and then subjected to immunofluorescence staining with antibodies against Ago2, C-P4H-β, and TIA-1 (a well-known stress granule marker [177]). Under normoxia, Ago2 was mainly localized to the cytoplasm and showed a diffuse pattern of staining (**Fig 3.1 A**). Similar to Ago2, C-P4H-β was also localized to the cytoplasm under normoxia and showed a pattern that is characteristic for ER staining (**Fig 3.1 A**). Consistent with previous findings by Qi *et al*. [119], strong colocalization between Ago2 and C-P4H-β was observed in the cytoplasm under normoxia (**Fig 3.1 A**). Exposing the cells to 3 h of hypoxia induced the formation of stress granules, which are marked by TIA-1 and appear as punctate foci in the cytoplasm (**Fig 3.1 B**). Ago2 was found to accumulate in these stress granules under hypoxia, thus suggesting that hypoxia induces Ago2 to translocate to stress granules (**Fig 3.1 B**). Similar results were obtained for U2OS cells (data not shown). Interestingly, no colocalization between C-P4H-β and TIA-1-positive stress granules was observed in human PASMCs exposed to 3 h of hypoxia (**Fig 3.2**). The staining pattern of C-P4H-β

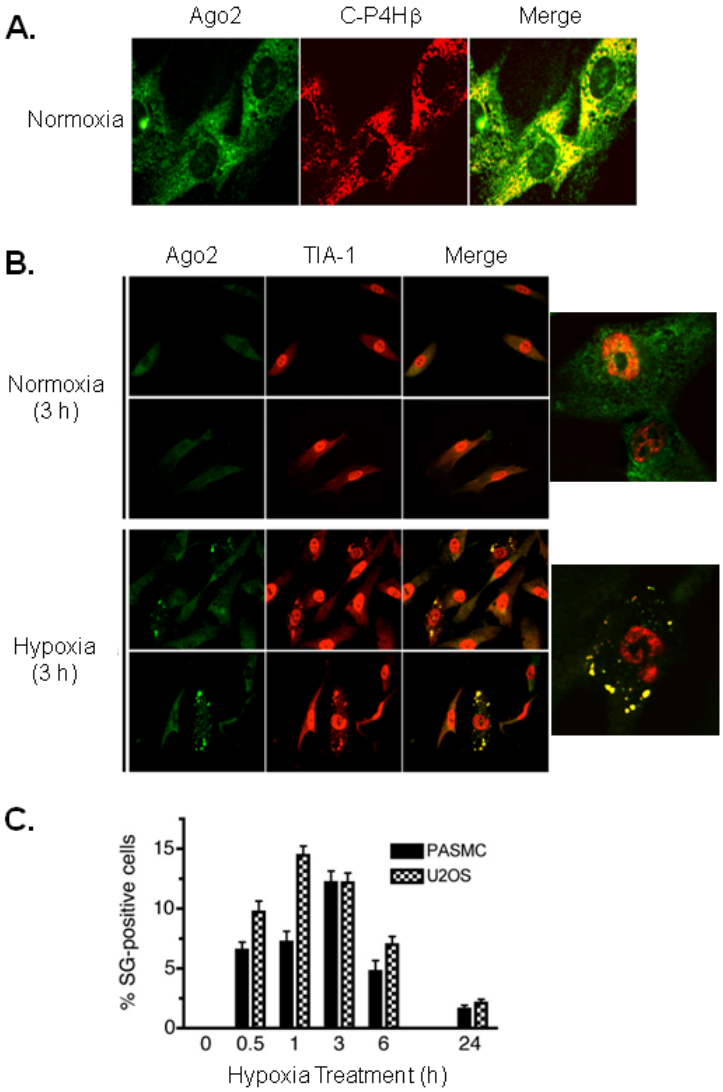

Figure. 3.1 Hypoxia induces stress granule formation and promotes the localization of Ago2 to stress granules. **A.** PASMCs were subjected to immunofluorescence staining with FITC-Ago2 antibodies (green) and rhodamin-C-P4Hβ antibodies (red) under normoxia. **B.** PASMCs exposed to normoxia or hypoxia for 3 h were subjected to immunofluorescence staining with FITC-Ago2 antibodies (green) and rhodamin-TIA-1 antibodies (red). **C.** Quantification of cells containing stress granules (SGs) after treatment with hypoxia for the indicated periods of time is presented. Approximately 200 cells from at least ten independent fields were counted for each time point, and SG-positive cells are presented as a percentage of the total population.

under hypoxia was similar to that under normoxia (**Fig 3.2**). These results indicate that C-P4H-β does not localize to stress granules upon hypoxia treatment and that the hypoxia-induced translocation to stress granules is specific for Ago2.

A time course experiment was also performed to determine how quickly hypoxia induces the formation of stress granules. Quantitative analysis reveals that stress granules were observed in ~5–10% of PASMCs and U2OS cells as early as 30 min after hypoxia (**Fig 3.1 C**). The percentage of stress-granule-positive cells continued to increase, reaching ~10–15% after 3 h of hypoxia and then gradually declined (**Fig 3.1 C**). Together, these results indicate that similar to other stress stimuli, such as arsenite or hippuristanol treatment, hypoxia induces the rapid formation of stress granules and promotes the localization of Ago2 to stress granules.

3.5 Ago2 localization to stress granules upon hypoxia treatment is mediated by Pro700 hydroxylation of Ago2.

To investigate the potential role of C-P4H(I)-mediated prolyl hydroxylation in the localization of Ago2 to stress granules under hypoxia, U2OS cells were transfected with an empty vector (mock), a Flag-tagged WT Ago2, or a Flag-tagged P700A mut Ago2, containing the Pro700-to-alanine mutation, expression construct and exposed to 3 h of normoxia or hypoxia. The cells were then subjected to immunofluorescence staining with antibodies against Flag and TIA-1. U2OS cells were utilized in this experiment because PASMCs are not readily transfectable. The 3 h time point was chosen in order to maximize the percentage of cells that form stress granules upon hypoxia treatment. Similar to endogenous Ago2, Flag-tagged WT and P700A mut Ago2 were mainly

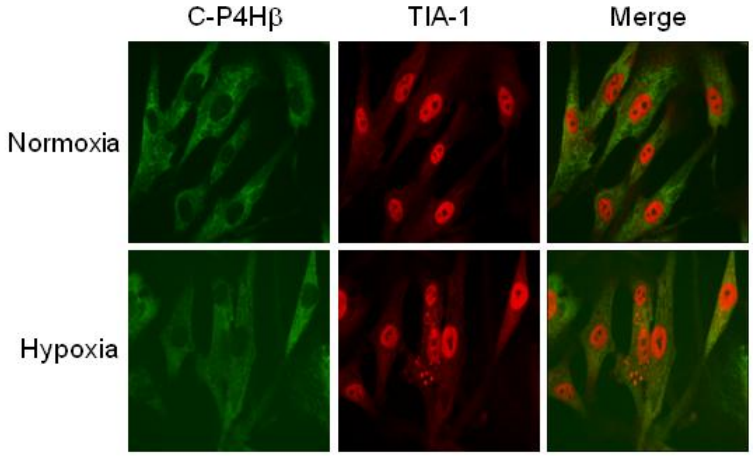

Figure. 3.2 C-P4Hβ does not localize to stress granules upon hypoxia treatment. PASMCs exposed to normoxia or hypoxia for 3 h were subjected to immunofluorescence staining with FITC-C-P4Hβ antibodies (green) and rhodamin-TIA-1 antibodies (red).

localized to the cytoplasm and showed a diffuse pattern of staining under normoxia (**Fig 3.3**). Hypoxia exposure induced the formation of stress granules, marked by TIA-1, in both the Flag-tagged WT and P700A mut Ago2 transfected cells (**Fig 3.3**). However, while strong colocalization was observed between Flag-tagged WT Ago2 and stress granules, this colocalization was greatly reduced for Flag-tagged P700A mut Ago2 (**Fig 3.3**). These results suggest that C-P4H(I)-mediated hydroxylation of Ago2 at Pro700 promotes the localization of Ago2 to stress granules upon hypoxia, probably by enhancing the translocation of Ago2 to stress granules or by stabilizing the association between Ago2 and stress granules.

3.6 Hypoxia promotes the association between Ago2 and Hsp90.

To examine whether hypoxia regulates the interaction between Ago2 and Hsp90, human PASMCs were exposed to normoxia or hypoxia for 24 h. Total cell lysates were prepared and immunoprecipitated with anti-Hsp90 antibody, followed by Western blot analysis with anti-Ago2 antibody. Consistent with the findings of Tahbaz *et al*. [322], Ago2 associated with Hsp90 under normoxia (**Fig 3.4**). Interestingly, hypoxia treatment significantly increased the association between Ago2 and Hsp90 compared to normoxia (**Fig 3.4**). Since my results in chapter II suggest that hypoxia may induce the hydroxylation of Ago2, we wondered whether hydroxylation by the C-P4H(I) enzyme plays a role in the interaction between Ago2 and Hsp90. The activity of C-P4H(I) was knocked down in PASMCs by using siRNA against C-P4H-α(I), the catalytic subunit of C-P4H(I), and the cells were then exposed to normoxia or hypoxia for 24 h. Total cell lysates were immunoprecipitated with anti-Ago2 antibody, followed by Western blot

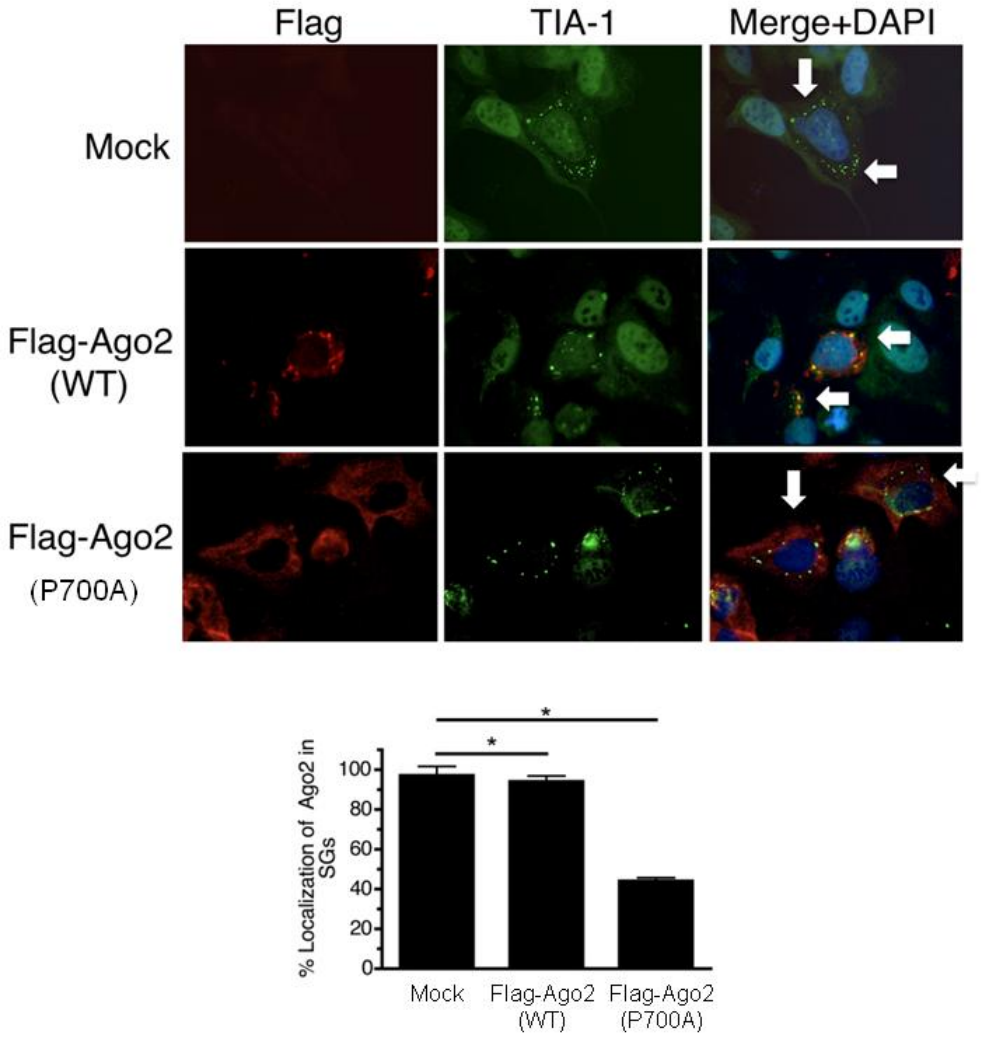

Figure. 3.3 WT Ago2 localizes to stress granules under hypoxia, but not P700A mutant Ago2. U2OS cells were transfected with vector (mock), Flag-tagged Ago2 (WT), or Flag-tagged Pro700A mutant Ago2 (P700A) cDNA construct, followed by treatment with hypoxia for 3 h. Cells were then subjected to immunofluorescence staining with rhodamin-Flag antibodies (red) and FITC-TIA-1 antibodies (green). TIA-1-positive stress granules are indicated by white arrows (upper panel). Quantification of the percentage of Ago2 localized in stress granules (SGs) for each condition is presented (lower panel). Mock refers to the localization of endogenous Ago2. Approximately 70 SGs in at least three cells were examined for each condition. *p<0.05.

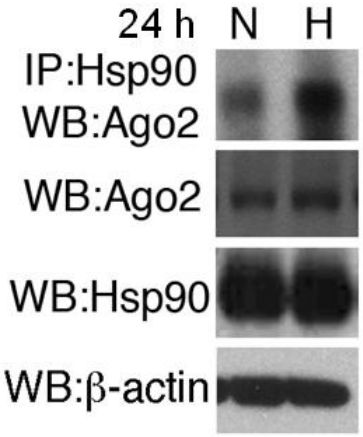

Figure. 3.4 Hypoxia promotes the interaction between Ago2 and Hsp90. Total cell lysates were prepared from PASMCs exposed to normoxia (N) or hypoxia (H) for 24 h and were subjected to immunoprecipitation with anti-Hsp90 antibody and immunoblotted with anti-Ago2 antibody. Total cell lysates were also subjected to immunoblot analysis with anti-Ago2, anti-Hsp90, or anti-β-actin (loading control) antibodies.

analysis with anti-Hsp90 antibody. As expected, the association between Hsp90 and Ago2 increased after 24 h of hypoxia in the si-Control cells (**Fig 3.5 A**). However, the knockdown of C-P4H-α(I) prevented the hypoxia-induced Hsp90-Ago2 interaction (**Fig 3.5 A**), thus suggesting that C-P4H(I) mediates the increased association of Hsp90 with Ago2 under hypoxia, probably through the prolyl hydroxylation of Ago2.

3.7 Hypoxia-induced Hsp90-Ago2 interaction is mediated by Pro700 hydroxylation of Ago2.

To confirm the importance of C-P4H(I)-mediated prolyl hydroxylation in the hypoxia-induced Hsp90-Ago2 interaction, U2OS cells were transfected with an empty vector (mock), a Flag-tagged WT Ago2, or a Flag-tagged P700A mut Ago2 expression construct and exposed to 24 h of normoxia or hypoxia. Total cell lysates were immunoprecipitated with anti-Flag antibody, followed by Western blot analysis with anti-Hsp90 antibody. Hsp90 associated with WT Ago2 under normoxia (**Fig 3.5 B**); however, unlike the experiments with endogenous Ago2, there was no increase in the association between Hsp90 and WT Ago2 after 24 h of hypoxia (**Fig 3.5 B**). This lack of increase in the association upon hypoxia could be due to the fact that WT Ago2 was highly overexpressed, so the hypoxia-induced increase in association may not be able to be detected. Although Hsp90 still associated with P700A mut Ago2 under normoxia and hypoxia, this association was much weaker compared to the association with WT Ago2 (**Fig 3.5 B**), therefore suggesting that C-P4H(I)-mediated Pro700 hydroxylation of Ago2 is important for the interaction between Ago2 and Hsp90. The Pro700 residue is located in the PIWI domain of Ago2 [119]. Although *in vitro* studies by Tahbaz *et al*. found that

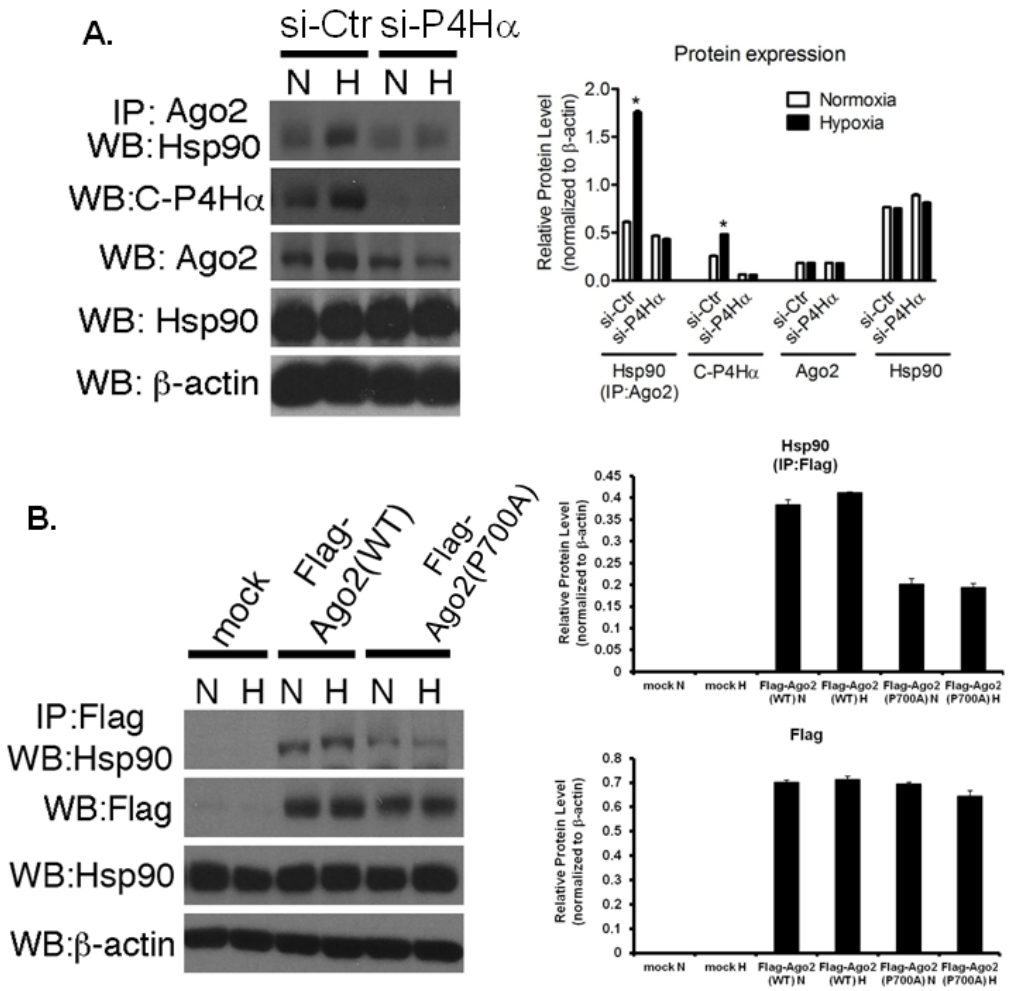

Figure. 3.5 C-P4H(I)-mediated Pro700 hydroxylation of Ago2 is important for the hypoxia-induced Ago2-Hsp90 interaction. **A.** PASMCs were transfected with siRNA against C-P4Hα(I) (si-P4Hα) or non-targeting control (si-Ctr) siRNA for 48 h, followed by treatment with normoxia (N) or hypoxia (H) for 24 h. Total cell lysates were prepared from the cells and were subjected to immunoprecipitation with anti-Ago2 antibody and immunoblotted with anti-Hsp90 antibody. Total cell lysates were also subjected to immunoblot analysis with anti-C-P4Hα, anti-Ago2, anti-Hsp90, or anti-β-actin (loading control) antibodies (left panel). Relative amounts of Hsp90, C-P4Hα, and Ago2 proteins normalized to β-actin were quantitated by densitometry, and the results presented are the average of three independent experiments (n=3) (right panel). **B.** U2OS cells were transfected with vector (mock), Flag-tagged Ago2 (WT), or Flag-tagged Pro700A mutant Ago2 (P700A) cDNA construct, followed by treatment with normoxia (N) or hypoxia (H) for 24 h. Total cell lysates were prepared and were subjected to immunoprecipitation with anti-Flag antibody, followed by immunoblot with anti-Hsp90 antibody. Total cell lysates were also subjected to immunoblot analysis with anti-Flag (for Ago2), anti-Hsp90, or anti-β-actin (loading control) antibodies (left panel). Relative amounts of Hsp90 and Flag proteins normalized to β-actin were quantitated by densitometry, and the results presented are the average of three independent experiments (n=3) (right panel).

Hsp90 primarily interacted with the N-terminal 323 amino acids of Ago2 and that no interaction was detected with the PIWI domain [322], this finding does not exclude the possibility that *in vivo*, the N-terminal region of Ago2 cooperates with hydroxylated Pro700 to create an binding interface between Ago2 and Hsp90.

3.8 Hypoxia upregulates Ago2 activities.

Given that the interaction between Ago2 and Hsp90 is increased upon hypoxia and that the activity of Hsp90 is important for RISC loading [252], we hypothesized that hypoxia may lead to increases in RISC activity. To test this hypothesis, we used U2OS stable cell lines expressing a GFP reporter, in which a perfectly complementary sequence for let-7 was inserted in the 3'UTR of the GFP gene (GFP-let-7 sensor) (**Fig 3.6 A**). These U2OS stable cell lines were exposed to normoxia or hypoxia for 24 h, and total RNAs were prepared and subjected to qRT-PCR analysis. Hypoxia treatment decreased the mRNA levels of the GFP-let-7-sensor compared to normoxia (**Fig 3.6 A**), but did not have a significant effect on the endogenous levels of let-7a (**Fig 3.6 B**), indicating that the decreased GFP-let-7 mRNA levels were not due to an increase in the levels of let-7a. These results suggest that hypoxia increased the let-7-RISC activity, probably through its effects on Ago2. As expected, hypoxia increased the mRNA levels of C-P4H-α(I) and C-P4H-β compared to normoxia (**Fig 3.6 A**). Similar to the results obtained with human PASMCs, hypoxia did not increase the mRNA levels of Ago2 (**Fig 3.6 A**). However, Western blot analysis of the total cell lysates prepared from these cells did show that hypoxia increased the protein levels of Ago2 as well as C-P4H-α(I), and C-P4H-β (data

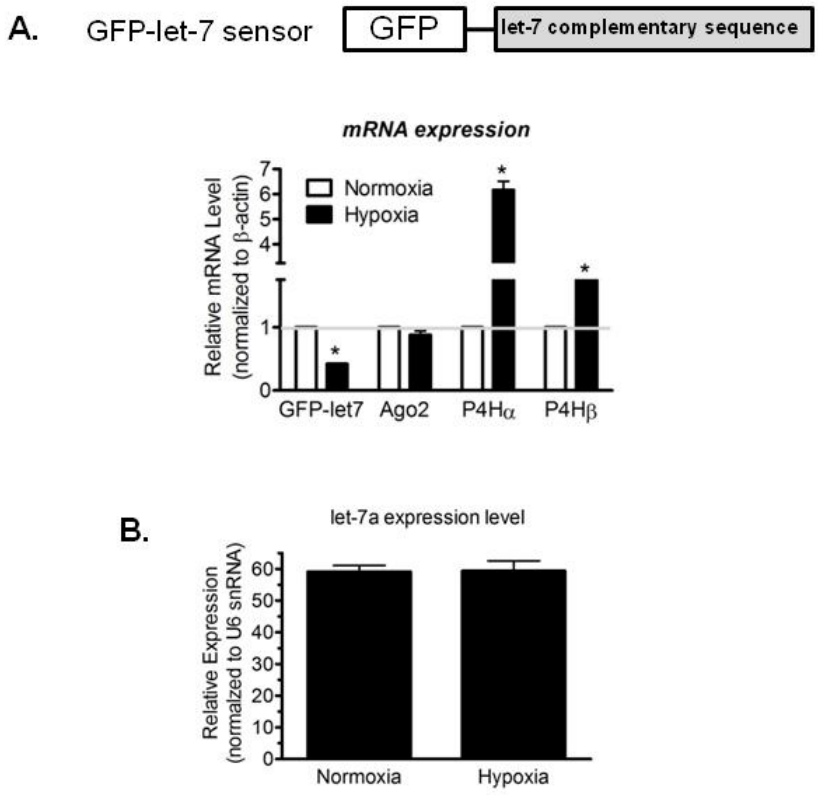

Figure. 3.6 Hypoxia increases RISC activity. **A.** Total RNAs were prepared from U2OS cell line stably expressing the GFP-let-7 sensor construct (upper panel) exposed to normoxia or hypoxia for 24 h and were subjected to qRT-PCR analysis of GFP-let-7, Ago2, C-P4Hα, and C-P4Hβ mRNAs. Relative levels of mRNA expression normalized to β-actin were quantitated and are presented by setting the expression levels of normoxia to 1 (lower panel). *p<0.05. **B.** miRNA analysis was conducted in the same cells used in **A.** Relative expression levels of let-7a normalized to U6 snRNA were quantitated and are presented.

not shown), thus suggesting that the hypoxia effect on Ago2 in these U2OS stable cell lines is similar to that in PASMCs.

To examine whether prolyl hydroxylation of Ago2 plays a role in the hypoxia-mediated increase in RISC activity, U2OS stable cell lines expressing the GFP-let-7 sensor were transfected with an empty vector (mock), a WT Ago2, or a P700A mut Ago2 expression construct and exposed to 24 h of normoxia or hypoxia. Total RNAs were prepared and subjected to qRT-PCR analysis of the GFP-let-7 mRNA. As expected, in the mock-transfected cells, hypoxia decreased the mRNA levels of the GFP-let-7 sensor compared to normoxia, suggesting that the let-7-RISC activity was increased by hypoxia (**Fig 3.7**). Similar to the mock-transfected cells, hypoxia also reduced the GFP-let-7 mRNA levels in the WT Ago2 expressing cells; however, this hypoxia-mediated decrease in GFP-let-7 mRNA expression was not observed in the P700A mut Ago2 expressing cells (**Fig 3.7**), suggesting that Pro700 hydroxylation of Ago2 by the C-P4H(I) enzyme is important for the hypoxia-mediated increase in RISC activity. Given that endogenous WT Ago2 is still present in the P700A mut Ago2 expressing cells, the lack of decrease in GFP-let-7 mRNA levels observed under hypoxia in these cells could suggest the possibility that the P700A mut Ago2 may act as a dominant negative and interfere with the RISC activity of the endogenous Ago2 under hypoxia. Interestingly, expression of either WT Ago2 or P700A mut Ago2 under normoxia decreased the GFP-let-7 mRNA levels compared to mock-transfected cells under normoxia (**Fig 3.7**). Together, these results suggest that although Pro700 hydroxylation of Ago2 is not required for RISC activity, it plays a critical role in mediating the increase in RISC activity under hypoxia.

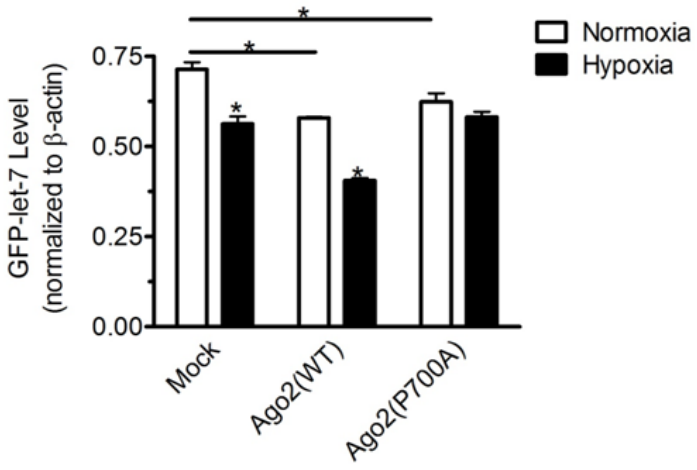

Figure. 3.7 Hypoxia-mediated increase in RISC activity is suppressed in the presence of P700A mutant Ago2. U2OS cell line stably expressing GFP-let-7 was transfected with vector (mock), wild-type Ago2 (WT), or Pro700A mutant Ago2 (P700A) cDNA construct and then exposed to normoxia or hypoxia for 24 h. Total RNAs were prepared from the cells and were subjected to qRT-PCR analysis. Relative expression of the GFP-let-7 mRNA was quantitated and is presented after normalization to β-actin. *$p<0.05$.

Besides functioning in the RISC, Ago2 has recently been demonstrated to participate in pre-miRNA processing, specifically in the cleavage of pre-miR-451 to mature miR-451 [240, 241]. Given the effects of hypoxia on Ago2, we wondered whether hypoxia could increase this Dicer-like processing activity of Ago2. U2OS cells were transfected with an empty vector (mock) or a miR-144/451 expression construct [242], encoding both pre-miR-144 and pre-miR-451 (**Fig 3.8 A**). In the mock-transfected cells, endogenous levels of miR-451 were upregulated by ~2-fold upon hypoxia treatment (**Fig 3.8 B**). Overexpression of the miR-144/451 construct resulted in a greater than 2,000-fold increase in miR-451 levels under normoxia compared to that of the mock (**Fig 3.8 B**), presumably due to the Ago2-mediated cleavage of exogenous pre-miR-451 to mature miR-451. Similar to the mock-transfected cells, the levels of miR-451 were further upregulated by hypoxia in the miR-144/451 overexpressing cells (**Fig 3.8 B**). The hypoxia-mediated increase was specific to miR-451, for the levels of miR-144 were not upregulated by hypoxia in the miR-144/451 overexpressing cells (**Fig 3.8 B**). Thus, these results suggest that hypoxia induces the miR-451 processing activity of Ago2. To confirm the importance of Ago2 in the generation of mature miR-451 from the miR-144/451 construct, the endogenous expression of Ago2 in U2OS cells was knocked down by using siRNA (si-Ago2), followed by the transfection of either an empty vector (mock) or the miR-144/451 expression construct. The cells were subsequently exposed to normoxia or hypoxia for 24 h. Transfection of si-Ago2 reduced the endogenous Ago2 mRNA expression (**Fig 3.9 A**) and the endogenous Ago2 protein expression (**Fig 3.9 B**). The knockdown of Ago2 reduced the basal level of miR-451 as well as the hypoxia-induced level of miR-451 (**Fig 3.9 C**), thus indicating that Ago2 plays a critical role in

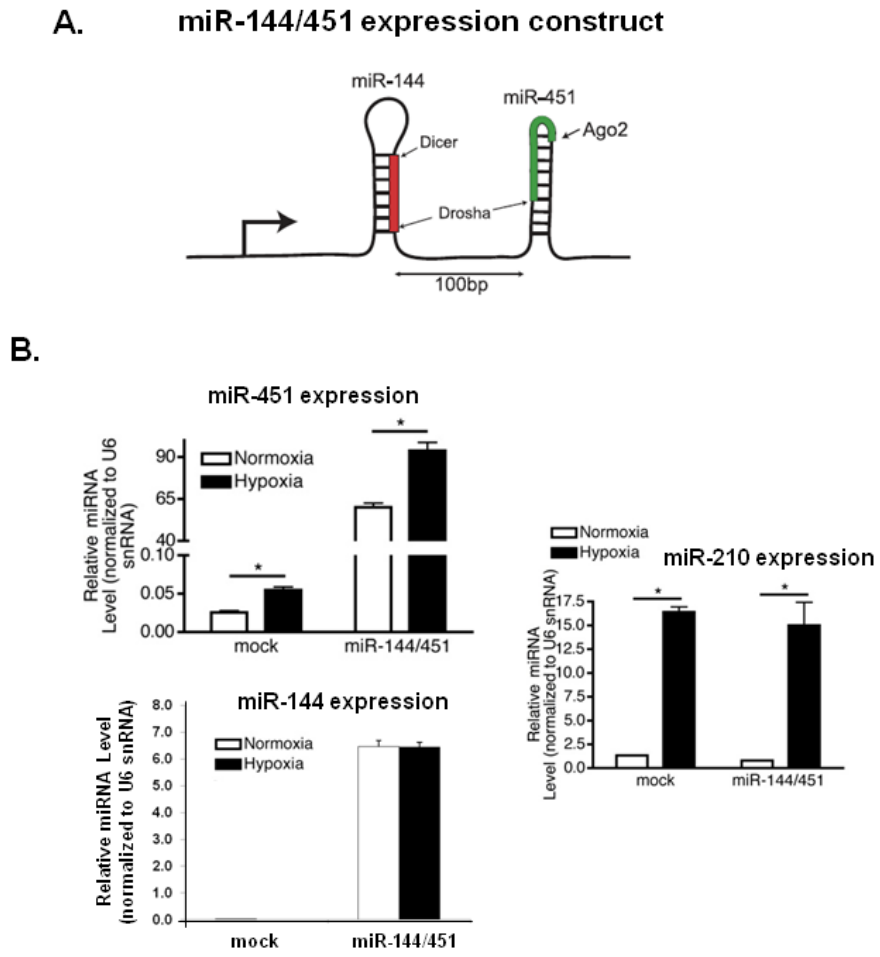

Figure. 3.8 Hypoxia induces the miR-451 processing activity of Ago2. A. Schematic of the miR-144/451 expression construct. Mature miR-144 is highlighted in red, and mature miR-451 is highlighted in green. **B.** U2OS cells were transfected with vector (mock) or miR-144/451 construct and then exposed to normoxia or hypoxia for 24 h. Total RNAs were prepared from the cells and were subjected to qRT-PCR analysis. Relative levels of miR-451, miR-144, or miR-210 normalized to U6 snRNA were quantitated and are presented. *p<0.05.

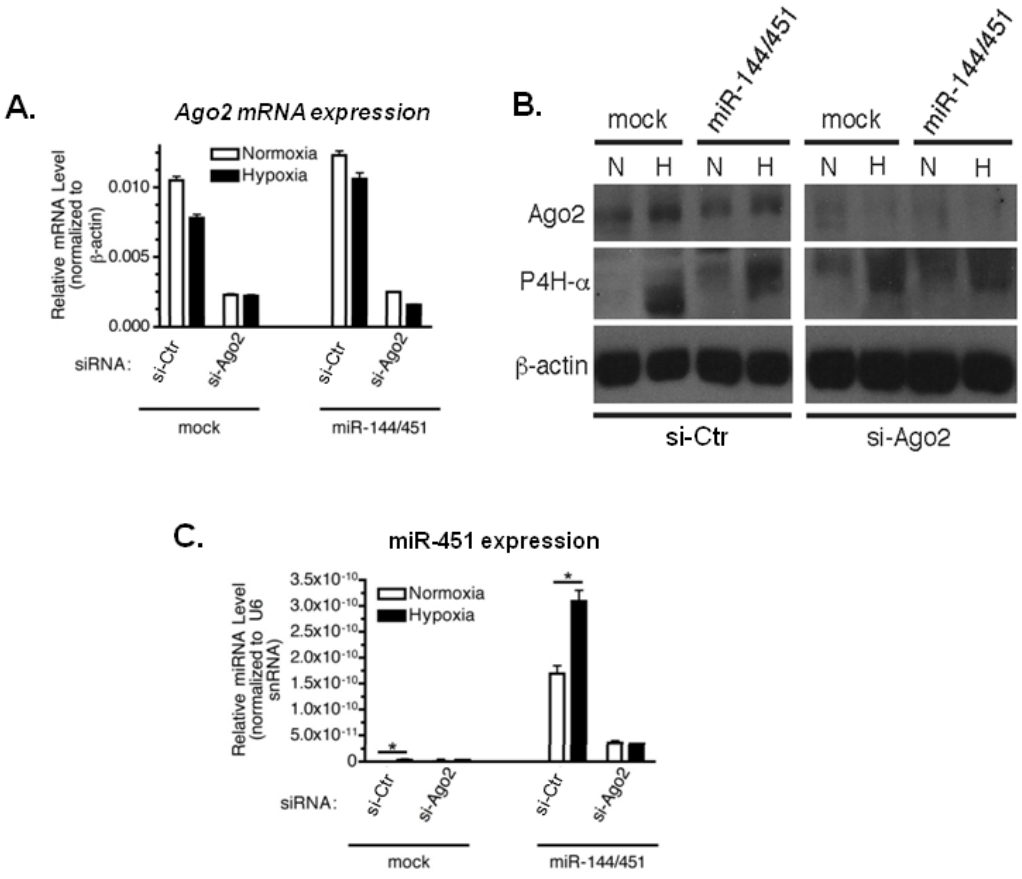

Figure. 3.9 Ago2 is essential for the maturation of miR-451 from the miR-144/451 expression construct. U2OS cells were transfected with control siRNA (si-Ctr) or siRNA against Ago2 (si-Ago2) and vector (mock) or miR-144/451 construct, followed by exposure to normoxia (N) or hypoxia (H) for 24 h. qRT-PCR analysis (**A.**) and immunoblot analysis (**B.**) were performed to confirm downregulation of Ago2 by siRNA. miRNA analysis was also conducted, and relative levels of miR-451 normalized to U6 snRNA were quantitated and are presented (**C.**). *p<0.05.

the maturation of miR-451. Altogether, these results suggest that hypoxia stimulates the RISC activity and Dicer-like processing activity of Ago2, most likely by promoting the increase in Ago2 protein levels and/or the association of Ago2 with Hsp90.

3.9 Hypoxia post-transcriptionally increases the expression levels of miRNAs.

To investigate whether hypoxia affects miRNA expression, we performed a miRNA microarray analysis on human PASMCs exposed to 24 h of normoxia or hypoxia. The analysis revealed that out of a total of 292 miRNAs that were successfully amplified, 37% (107 miRNAs) were found to be induced by hypoxia at least 1.5-fold compared to normoxia (**Fig 3.10**). Interestingly, siRNA-mediated knockdown of C-P4H-α(I) completely abolished or suppressed the hypoxia-mediated induction of 94% (101 miRNAs) of the 107 miRNAs (**Fig 3.10**), indicating that hydroxylation by C-P4H(I) could be involved in the upregulation of miRNAs under hypoxia, presumably through its effects on the Ago2 protein. We performed qRT-PCR analysis to validate the hypoxia-mediated induction of 14 of the miRNAs, which were found to be increased by ~1.3- to 4-fold under hypoxia (**Fig 3.11 A**). Consistent with previous reports [167-173], we observed that miR-210 was one of the most robustly upregulated miRNAs after hypoxia treatment (**Fig 3.11 A**).

Since miRNAs can promote the mRNA degradation of their target mRNAs, we looked at whether the hypoxia-mediated increase in miRNAs had any effect on target mRNA expression levels. Among the miRNAs that were found to be upregulated by hypoxia, we chose to look at specific mRNA targets of miR-21 and miR-221/miR-222, for these miRNAs have been well-characterized in PASMCs by our lab. Total RNAs

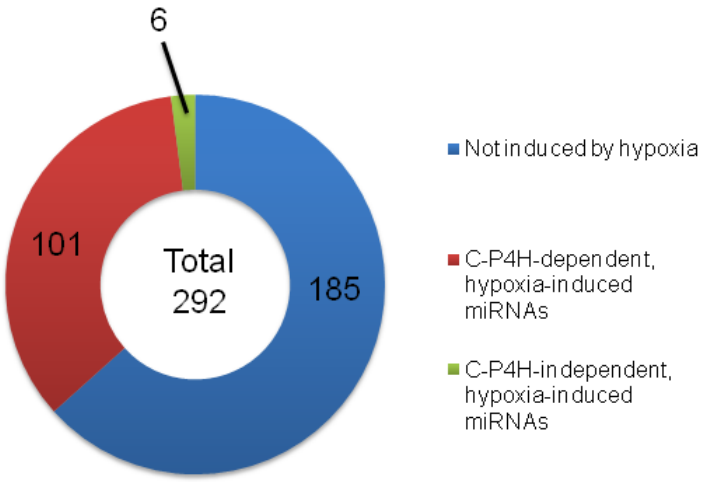

Figure. 3.10 miRNA expression profiling analysis in PASMCs. Among 292 miRNAs detected in PASMCs, 107 miRNAs were induced ≥1.5-fold upon hypoxia treatment for 24 h. Among the 107 hypoxia-induced miRNAs, 101 miRNAs were no longer induced or had reduced induction by hypoxia when C-P4Hα was downregulated (C-P4H-dependent, shown in red). Only 6 miRNAs were induced by hypoxia at a similar level in the cell downregulated in C-P4Hα (C-P4H-independent, shown in green).

were prepared from human PASMCs exposed to normoxia or hypoxia for 24 h and were subjected to qRT-PCR analysis of PDCD4, Dock7, and Sprouty2 (which are validated targets of miR-21) [328] and c-kit (which is a validated target of miR-221 and miR-222) [66]. The mRNA levels of PDCD4, Dock7, Sprouty2, and c-kit were all downregulated after 24 h of hypoxia treatment (**Fig 3.11 B**), consistent with the hypoxia-mediated upregulation of miR-21 and miR-221/miR-222 (**Fig 3.11 A**).

Examination of the primary transcript expression of some of the hypoxia-induced miRNAs showed that except for the primary transcript of miR-210 (pri-miR-210), hypoxia did not increase the levels of pri-miR-21, pri-miR-24-1, pri-miR-222, or pri-miR-23a (**Fig 3.11 C**). Thus, these results suggest that the miRNAs are upregulated by hypoxia through a post-transcriptional mechanism. The hypoxia-mediated increase in the levels of pri-miR-210 (**Fig 3.11 C**) is consistent with the findings of previous studies which demonstrate that miR-210 is upregulated at the transcriptional level by HIF-1 under hypoxia [128, 166].

3.10 Hypoxia upregulates miRNAs through Ago2 and C-P4H(I)-mediated hydroxylation.

To examine whether Ago2 plays a role in the hypoxia-mediated elevation of miRNAs, the endogenous expression of Ago2 in human PASMCs was knocked down by using siRNA (si-Ago2) prior to treating the cells with normoxia or hypoxia for 24 h. Transfection of si-Ago2 reduced endogenous Ago2 mRNA expression to ~30% of that of the si-Control (**Fig 3.12 A**). The endogenous Ago2 protein expression in the si-Ago2 cells was reduced by ~50% compared to the si-Control (**Fig 3.12 B**). As expected, the

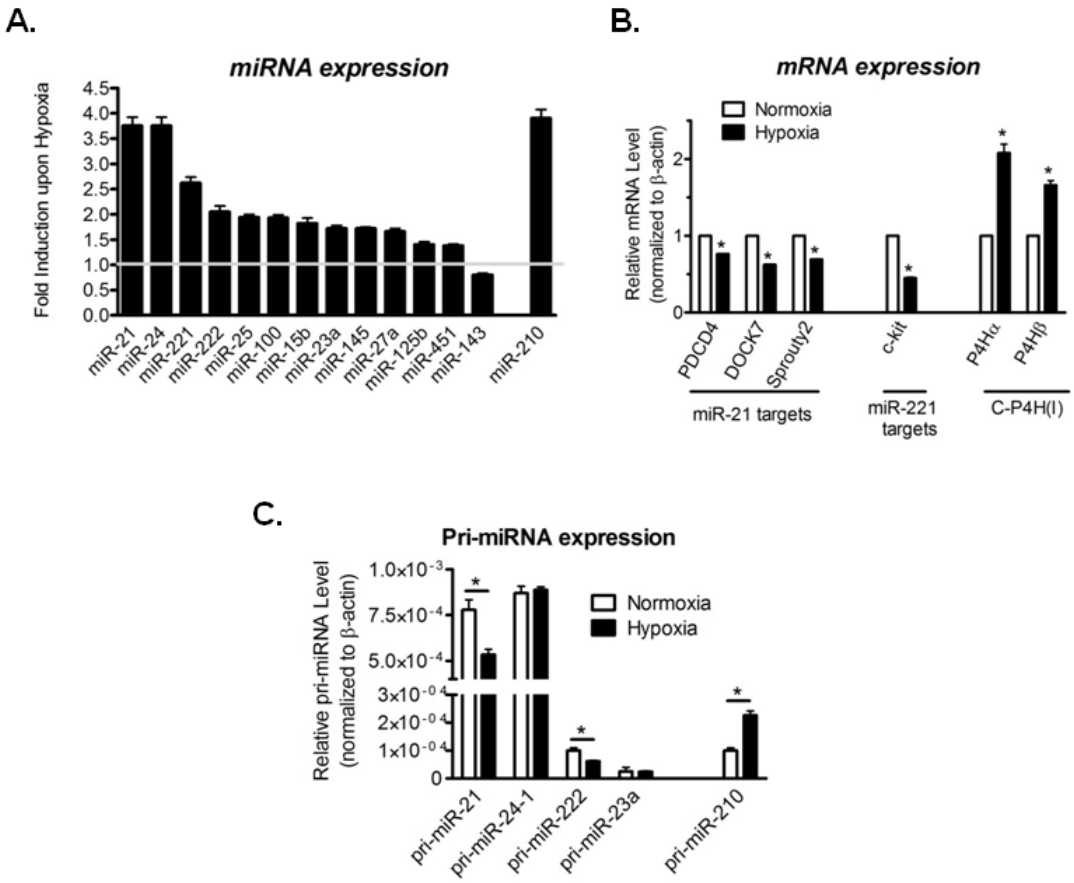

Figure. 3.11 Hypoxia post-transcriptionally upregulates the levels of miRNAs. Total RNAs were prepared from PASMCs exposed to normoxia or hypoxia for 24 h and were subjected to qRT-PCR analysis. **A.** Relative levels of miRNA expression normalized to U6 snRNA were quantitated, and fold induction (hypoxia/normoxia) is presented. **B.** Relative levels of miR-21 target gene (PDCD4, DOCK7, and Sprouty2) transcripts and miR-221/miR-222 target gene (c-kit) transcripts normalized to β-actin were quantitated and are presented by setting the expression levels of normoxia to 1. As a control for hypoxia treatment, C-P4Hα(I) and C-P4Hβ mRNAs were examined. *p<0.05. **C.** Relative levels of pri-miRNA expression normalized to β-actin were quantitated and are presented. *p<0.05.

protein levels of Ago2 increased after 24 h of hypoxia in the si-Control cells coincident with increases in the protein levels of C-P4H-α(I) (**Fig 3.12 B**). Knocking down Ago2 had no effect on the hypoxia-mediated increase in the protein levels of C-P4H-α(I) (**Fig 3.12 B**), which is consistent with our hypothesis that Ago2 lies downstream of C-P4H(I). In terms of the miRNA levels, 24 h of hypoxia increased the levels of mature miR-210, miR-21, miR-24, miR-222, and miR-23a in the si-Control cells compared to normoxia, as expected (**Fig 3.12 C**). Knockdown of Ago2 completely abolished or suppressed the hypoxia-mediated increase in the miRNAs (**Fig 3.12 C**), thus indicating that Ago2 plays an important role in the upregulation of miRNAs under hypoxia. The observation that the hypoxia-mediated induction of miR-210 was less affected by the Ago2 knockdown compared to the other miRNAs (**Fig 3.12 C**) could be due to the fact that miR-210 is transcriptionally activated by HIF-1 under hypoxia [128, 166].

Since the levels of Ago proteins have been implicated to be important in regulating miRNA levels [261, 307] and I have found that hypoxia increases the protein levels of Ago2, we wondered whether the hypoxia-mediated induction of miRNAs is solely due to the increase in Ago2 protein levels under hypoxia. Thus, to determine whether hypoxia-mediated upregulation of Ago2 would be sufficient for the elevation of miRNAs, WT Ago2 was overexpressed in U2OS cells to the level equivalent to that of cells treated with hypoxia. We found that while Ago2 was expressed in WT Ago2-transfected cells at levels similar to that observed in mock-transfected cells under hypoxia (**Fig 3.13 A**), the levels of mature miRNAs were not significantly affected (**Fig 3.13 B**). Thus, these results suggest that hypoxia-mediated induction of Ago2 protein levels is not

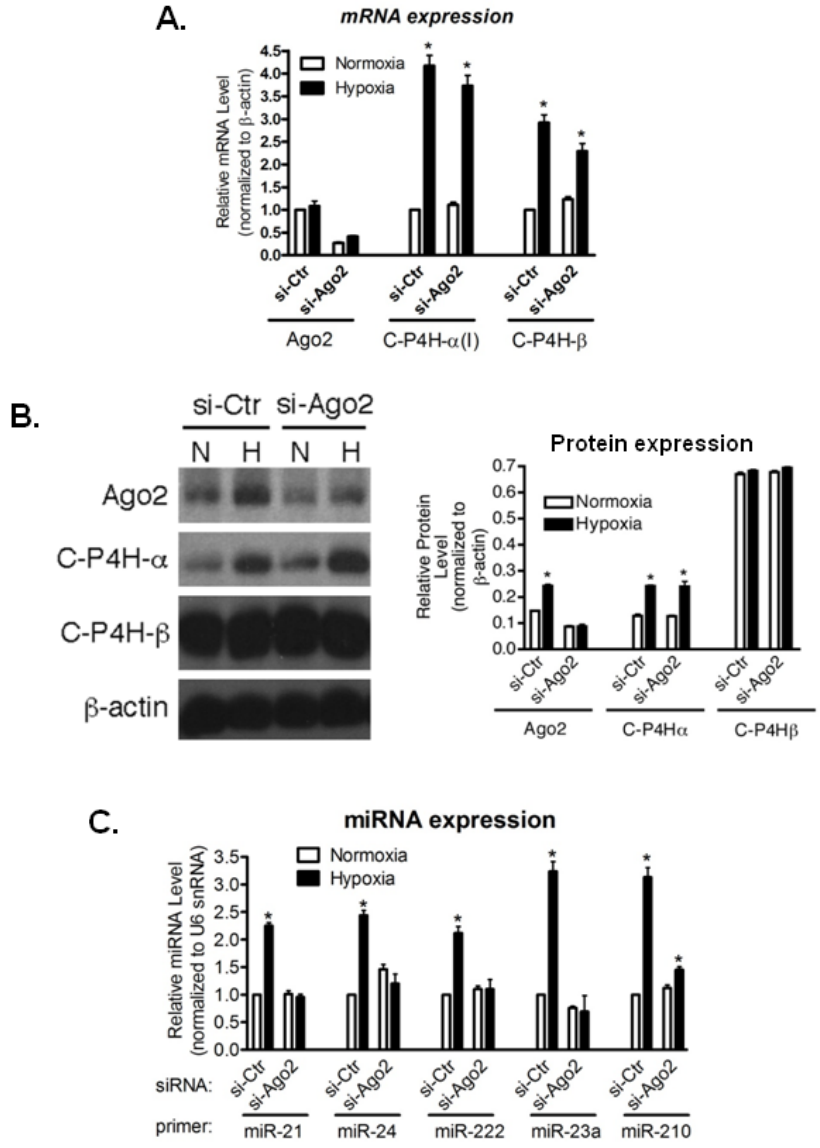

Figure. 3.12 Knockdown of Ago2 suppresses the hypoxia-mediated induction of miRNAs. PASMCs were transfected with siRNA against Ago2 (si-Ago2) or non-targeting control (si-Ctr) for 48 h, followed by exposure to normoxia (N) or hypoxia (H) for 24 h. qRT-PCR analysis (**A.**) and immunoblot analysis (**B.**) were performed to confirm downregulation of Ago2 by siRNA. Relative amounts of proteins normalized to β-actin were quantitated by densitometry, and the results presented are the average of three independent experiments (n=3). miRNA analysis was also conducted (**C.**), and relative levels of miRNA expression normalized to U6 snRNA were quantitated and are presented by setting the miRNA expression levels of the si-Ctr under normoxia to 1. *p<0.05.

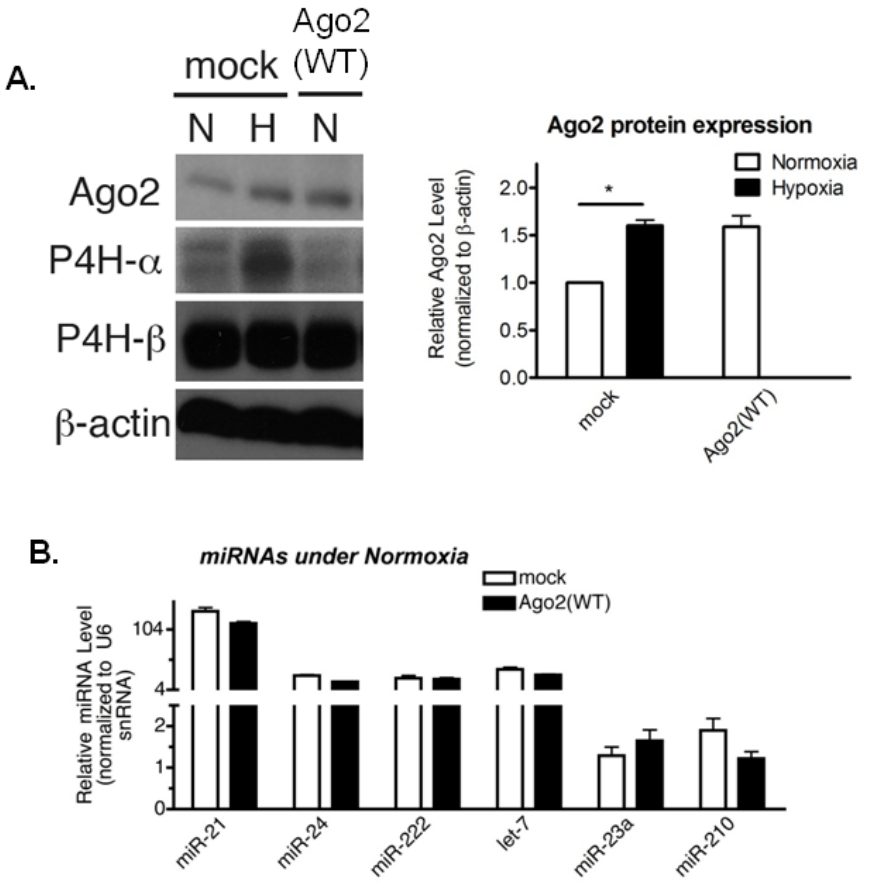

Figure. 3.13 Hypoxia-mediated upregulation of Ago2 protein levels is not sufficient for the increase in miRNA levels under hypoxia. **A.** U2OS cells were transfected with vector (mock) or Ago2 (WT) cDNA construct prior to exposure to normoxia (N) or hypoxia (H) for 24 h. Total cell lysates were prepared from the cells and were subjected to immunoblot analysis using anti-Ago2, anti-C-P4Hα, anti-C-P4Hβ, or anti-β-actin (loading control) antibodies (left panel). Relative amounts of Ago2 protein normalized to β-actin were quantitated by densitometry, and the results presented are the average of three independent experiments (n=3) (right panel). *p<0.05. **B.** Total RNAs were extracted from the cells used in **A.** and were subjected to qRT-PCR analysis. Relative levels of miRNA expression normalized to U6 snRNA were quantitated and are presented.

sufficient for the increase in miRNA levels under hypoxia; other factors, such as hypoxia-induced Ago2 hydroxylation by C-P4H(I), may be required as well.

To examine the potential role of C-P4H(I)-mediated hydroxylation in the increase in miRNA levels under hypoxia, the endogenous expression of C-P4H-α(I), the catalytic subunit of C-P4H(I), in human PASMCs was knocked down by using siRNA (si-P4Hα) prior to treating the cells with normoxia or hypoxia for 24 h. Total RNAs were prepared and subjected to qRT-PCR. As expected, hypoxia upregulated the levels of mature miR-210, miR-21, miR-24, miR-222, and miR-23a in the si-Control cells compared to normoxia (**Fig 3.14**). Knockdown of C-P4H-α(I) completely abolished or suppressed the hypoxia-mediated increase in the miRNAs (**Fig 3.14**), thus indicating that the prolyl hydroxylation activity of C-P4H(I) is crucial for the elevation of miRNAs under hypoxia, presumably through its effects on Ago2. Similar to before, the hypoxia-mediated induction of miR-210 was less affected by the C-P4H-α(I) knockdown compared to the other miRNAs (**Fig 3.14**), which could be due to the transcriptional upregulation of miR-210 by HIF-1 under hypoxia.

Given that C-P4H(I) activity is necessary for the increase in miRNAs under hypoxia, we wondered whether hypoxia-mediated upregulation of C-P4H-α(I) would be sufficient for the elevation of miRNAs. U2OS cells were transfected with an empty vector (mock) or C-P4H-α(I) expression construct and were exposed to 24 h of normoxia or hypoxia. Interestingly, preliminary results show that although C-P4H-α(I) was expressed in C-P4H-α(I)-transfected cells at levels similar to that observed in mock-transfected cells under hypoxia (**Fig 3.15 A**), neither the Ago2 protein levels (**Fig 3.15 A**)

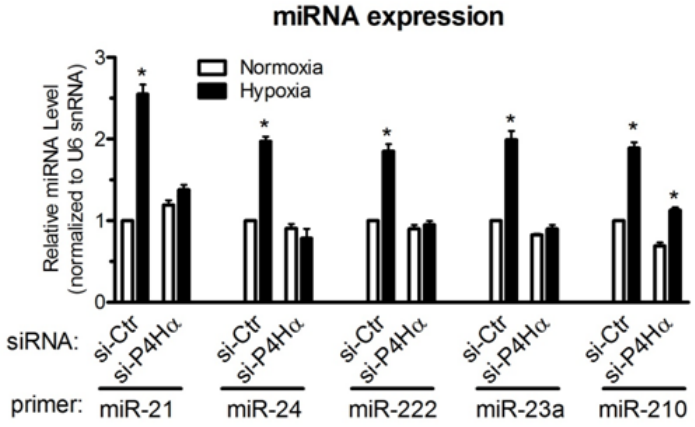

Figure. 3.14 Knockdown of C-P4H-α(I) suppresses the hypoxia-mediated induction of miRNAs. PASMCs were transfected with siRNA against C-P4Hα(I) (si-P4Hα) or non-targeting control (si-Ctr) for 48 h, followed by exposure to normoxia or hypoxia for 24 h. Total RNAs were prepared from the cells and were subjected to qRT-PCR analysis. Relative levels of miRNA expression normalized to U6 snRNA were quantitated and are presented by setting the miRNA expression levels of the si-Ctr under normoxia to 1. *p<0.05.

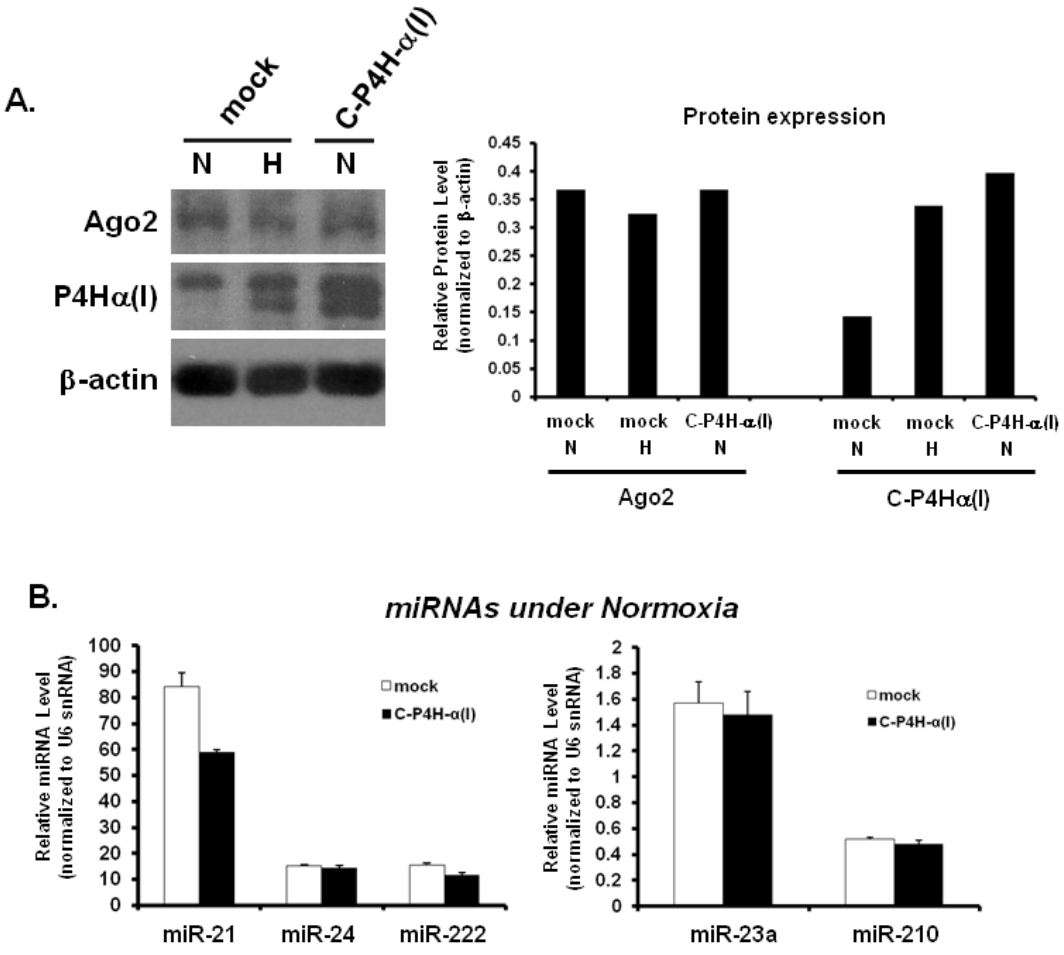

Figure. 3.15 Hypoxia-mediated upregulation of C-P4H-α(I) protein levels is not sufficient for the increase in Ago2 protein or miRNA levels under hypoxia. A. U2OS cells were transfected with vector (mock) or C-P4H-α(I) cDNA construct prior to exposure to normoxia (N) or hypoxia (H) for 24 h. Total cell lysates were prepared from the cells and were subjected to immunoblot analysis using anti-Ago2, anti-C-P4Hα(I), or anti-β-actin (loading control) antibodies (left panel). Relative amounts of C-P4Hα(I) protein normalized to β-actin were quantitated by densitometry and are presented (right panel). Note that these are preliminary results and have not been repeated. **B.** Total RNAs were extracted from the cells used in **A.** and were subjected to qRT-PCR analysis. Relative levels of miRNA expression normalized to U6 snRNA were quantitated and are presented. Note that these are preliminary results and have not been repeated.

nor mature miRNA levels (**Fig 3.15 B**) were significantly affected. These results suggest that increasing the protein levels of C-P4H-α(I) to the level similar to that of cells treated with hypoxia is not sufficient to lead to the accumulation of Ago2 or miRNAs under hypoxia.

3.11 Hsp90 activity is important for hypoxia-mediated induction of miRNAs and Ago2 activities.

As hypoxia promotes the interaction of Hsp90 with Ago2 through C-P4H(I)-mediated hydroxylation of Ago2, we speculated that Hsp90 activity may contribute to the hypoxia-mediated induction of miRNAs. To test this hypothesis, we utilized the well-known inhibitor GA, which specifically inhibits the ATPase activity of Hsp90 by binding to the ATP-binding site of Hsp90, thus preventing ATP from binding and inhibiting ATP hydrolysis [325, 329]. Since hydrolysis of ATP is essential for Hsp90 function, GA treatment results in the inactivation of Hsp90 [325, 329]. Human PASMCs were treated with mock (DMSO) or GA and then exposed to normoxia or hypoxia for 24 h. As a positive control to confirm Hsp90 inhibition by GA, we examined the Hsp70 mRNA levels, which were increased in the presence of GA (**Fig 3.16 A**), consistent with previous reports [330]. Total cell lysates were also prepared from the cells and subjected to Western blot analysis. As expected, the protein levels of Ago2 increased after 24 h of hypoxia in the mock-treated cells coincident with increases in the protein levels of C-P4H-α(I) (**Fig 3.16 B**). GA treatment did not significantly suppress the hypoxia-mediated accumulation of Ago2 (**Fig 3.16 B**), thus suggesting that the ATPase activity of Hsp90 is not essential for the increase in Ago2 protein levels under hypoxia. As for

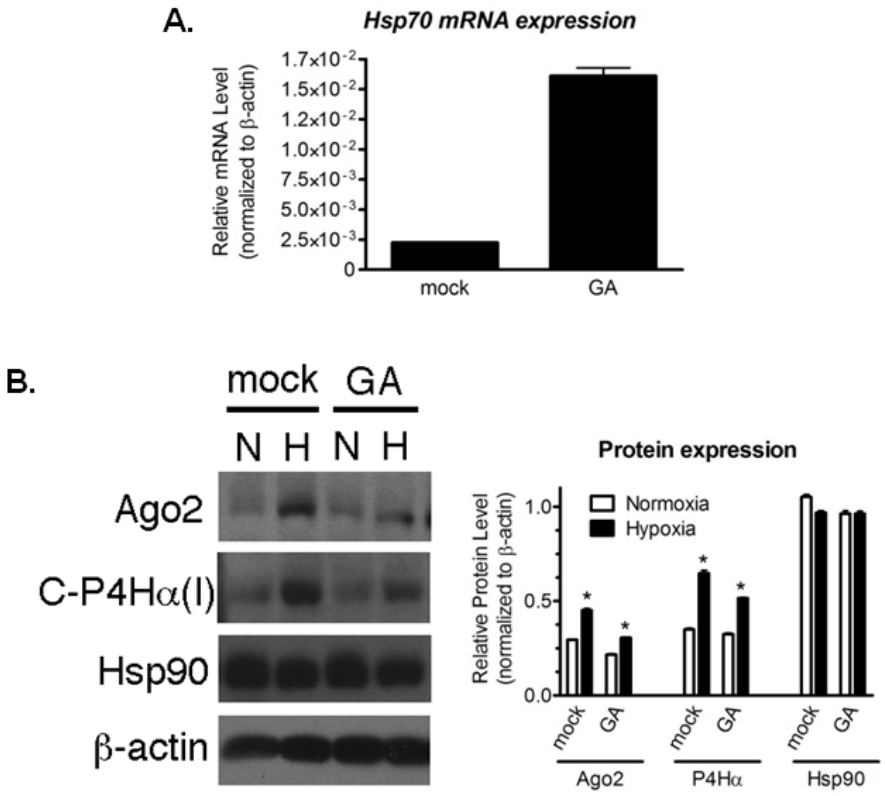

Figure. 3.16 ATPase activity of Hsp90 is not essential for the increase in Ago2 protein levels under hypoxia. PASMCs were treated with mock (DMSO) or 0.1 mM geldanamycin (GA) for 1.5 h, followed by exposure to normoxia (N) or hypoxia (H) for 24 h. **A.** Total RNAs were extracted from the cells and were subjected to qRT-PCR analysis of Hsp70 mRNA as a control to confirm Hsp90 activity inhibition by GA. Relative levels of mRNA expression normalized to β-actin were quantitated and are presented. **B.** Total cell lysates were also prepared from the cells and were subjected to immunoblot analysis using anti-Ago2, anti-C-P4Hα(I), anti-Hsp90, or anti-β-actin (loading control) antibodies (left panel). By densitometry, relative amounts of proteins normalized to β-actin were quantitated, and the results presented are the average of three independent experiments (n=3) (right panel). *p<0.05.

miRNA expression, hypoxia elevated the levels of mature miR-210, miR-21, miR-24, miR-222, and miR-23a in the mock-treated cells; however, the hypoxia-mediated increase in miRNA levels was abolished in the presence of GA (**Fig 3.17 A**). These results indicate that the increase in the miRNA levels under hypoxia is dependent on Hsp90 ATPase activity. The complete inhibition of the hypoxia-mediated induction of miR-210 by GA (**Fig 3.17 A**) could be due to the fact that Hsp90 ATPase activity is required for the activity of HIF-1 [331]; thus, by inhibiting the ATPase activity of Hsp90, HIF-1 can no longer stimulate the transcription of miR-210 under hypoxia.

We also investigate the role of Hsp90 in hypoxia-mediated induction of RISC activity. U2OS stable cell lines expressing the GFP-let-7 sensor were treated with mock (DMSO) or GA and then exposed to 24 h of normoxia or hypoxia. Total RNAs were prepared and subjected to qRT-PCR analysis. As expected, hypoxia reduced the GFP-let-7 mRNA levels in mock-treated cells; however, the hypoxia-mediated decrease in the mRNA levels of GFP-let-7 was blocked in the presence of GA (**Fig 3.17 B**). These results suggest that Hsp90 activity is crucial for hypoxia-mediated induction of the RISC activity, presumably because miRNA duplex loading into the RISC is inhibited by GA. We also examined whether Hsp90 plays a role in hypoxia-mediated induction of the miR-451 processing activity of Ago2. Following transfection of the miR-144/451 expression construct, U2OS cells were treated with mock (DMSO) or GA and then exposed to 24 h of normoxia or hypoxia. As expected, hypoxia increased the levels of miR-451 in mock-treated cells; however, this hypoxia-mediated increase was abolished in the presence of GA (**Fig 3.17 C**), suggesting that Hsp90 activity is also critical for the Dicer-like

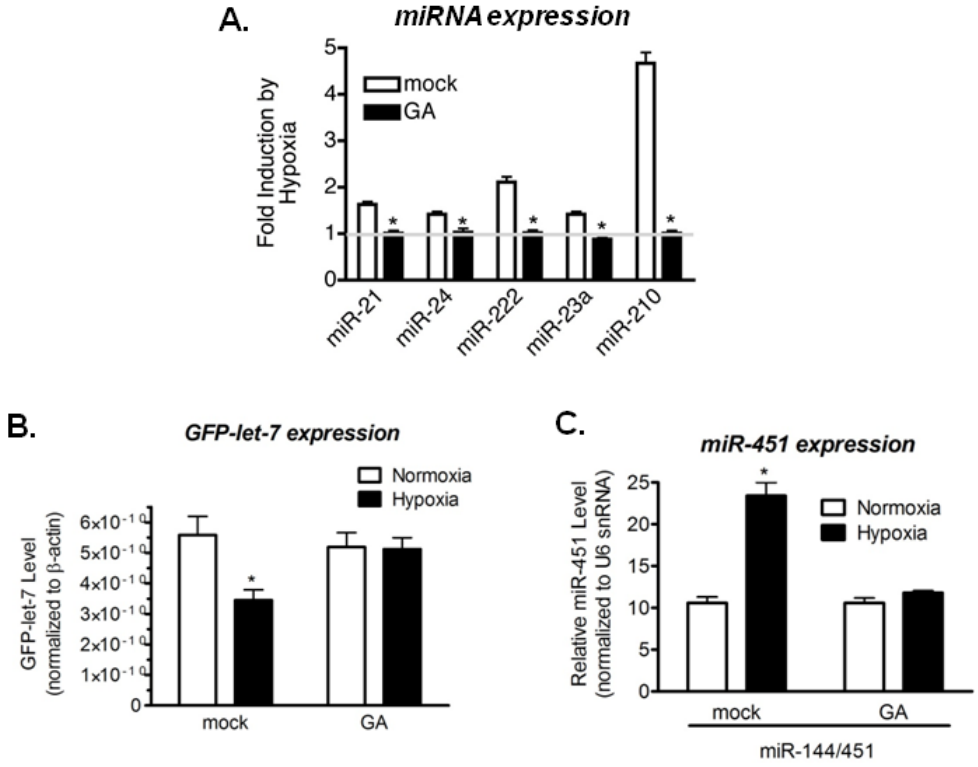

Figure. 3.17 ATPase activity of Hsp90 is important for the increase in miRNA levels and Ago2 RISC and miR-451 processing activities under hypoxia. A. PASMCs were treated with mock (DMSO) or 0.1 mM geldanamycin (GA) for 1.5 h, followed by exposure to normoxia or hypoxia for 24 h. Total RNAs were prepared from the cells and were subjected to qRT-PCR analysis. Relative levels of miRNA expression normalized to U6 snRNA were quantitated, and fold induction (hypoxia/normoxia) is presented. *p<0.05. **B.** U2OS cell line stably expressing GFP-let-7 was treated with mock (DMSO) or 1 mM GA for 1.5 h, followed by exposure to normoxia or hypoxia for 24 h. Relative expression of the GFP-let-7 mRNA normalized to β-actin was quantitated by qRT-PCR and is presented. *p<0.05. **C.** U2OS cells transfected with the miR-144/451 expression construct were treated with mock (DMSO) or 1 mM GA for 1.5 h, followed by exposure to normoxia or hypoxia for 24 h. Relative levels of miRNA expression normalized to U6 snRNA were quantitated by qRT-PCR and is presented. *p<0.05.

processing activity of Ago2. Together, these findings suggest that in addition to upregulation of Ago2 protein levels, hypoxia-mediated hydroxylation of Ago2 promotes its association with Hsp90 to elevate miRNA levels and enhance Ago2 RISC and miR-451 processing activities under hypoxia.

DISCUSSION

3.12 Hypoxia induces the formation of stress granules in PASMCs.

Although formation of stress granules has been documented in response to various stress stimuli, including hypoxia [177, 194], no studies have specifically looked at hypoxia-induced formation of stress granules in vascular SMCs. In this chapter, I showed that hypoxia treatment of human PASMCs rapidly stimulates the formation of stress granules, with stress granule formation detected as early as 30 min after hypoxia. Intriguingly, not all of the cells form stress granules upon hypoxia treatment; the percentage of stress granule-positive cells was observed to be at most ~10–15%. On the other hand, treatment of human PASMCs with arsenite resulted in stress granule formation in nearly all of the cells (**Fig 3.18**). This difference in the percentage of stress granule-positive cells could imply that stress granules formed in response to hypoxia have a quick turnover or that the formation of stress granules under hypoxia is dependent on other factors, such as the phase of the cell cycle. Indeed, studies on the formation of stress granules upon UV-damage revealed that only cells in the G1- and G2-phase of the cell cycle form stress granules; stress granules were not observed in cells in the S-phase [332]. In addition, we noticed that the size of the stress granules formed by hypoxia is

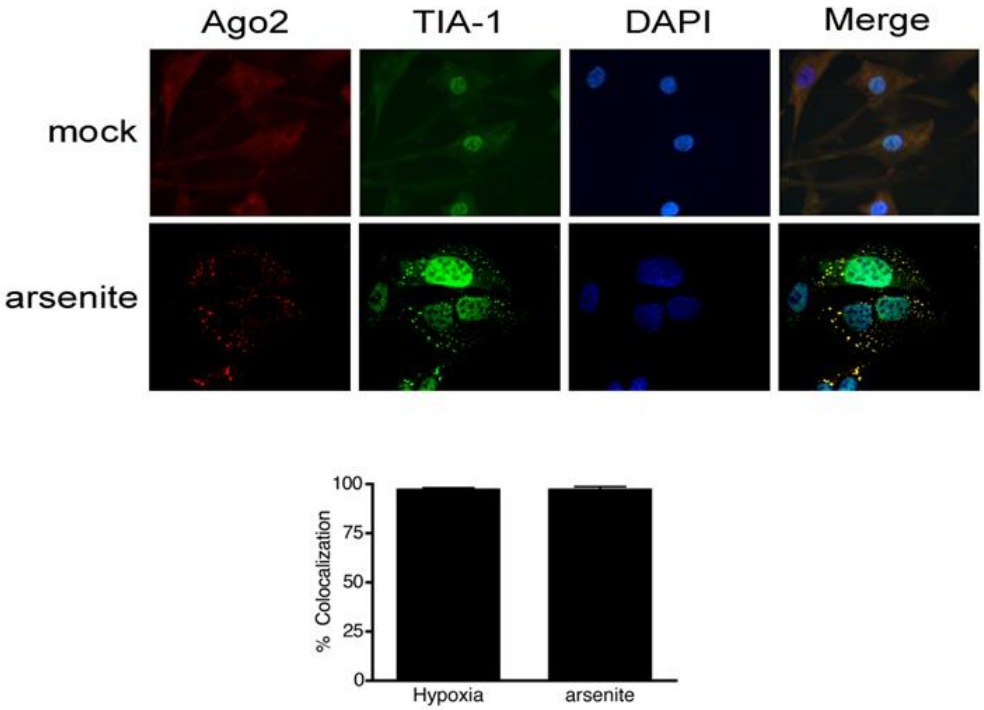

Figure. 3.18 Arsenite induces stress granule formation and promotes the localization of Ago2 to stress granules. PASMCs were treated with mock or arsenite for 45 min and were subjected to immunofluorescence staining with rhodamin-Ago2 antibodies (red) and FITC-TIA-1 antibodies (green) (upper panel). Quantification of the percentage of Ago2 colocalized with stress granules (SGs) for cells treated with 3 h hypoxia compared to cells treated with 45 min arsenite is presented (lower panel). Approximately 70 SGs in at least three cells have been examined for each condition.

different from that formed by arsenite. Hypoxia-induced stress granules were consistently found to be much larger than those formed in response to arsenite treatment (**Fig 3.1 B and Fig 3.18**). Moreover, while ~15 stress granules per cell were detected on average when cells were treated with hypoxia, arsenite-treated cells formed an average of ~60 stress granules per cell (**Fig 3.1 B and Fig 3.18**). Together, these findings suggest that different stress stimuli have distinct effects on stress granule assembly and that the stress granules formed in response to different stresses may not be entirely identical with each other.

3.13 Hypoxia-induced localization of Ago2 to stress granules involves Pro700 hydroxylation.

Similar to previous studies reporting the localization of Ago2 to stress granules upon arsenite or hippuristanol treatment [199], I found that hypoxia also induces Ago2 to translocate to stress granules. Thus, the localization of Ago2 to stress granules seems to be a general phenomenon observed in response to various types of stress stimuli. However, the functional significance of Ago2 in stress granules is still currently unclear. Interestingly, we found that unlike hypoxia, treatment of human PASMCs with arsenite did not significantly affect the protein or mRNA levels of Ago2, C-P4H-α(I), and C-P4Hβ (**Fig 3.19 A and B**). In addition, arsenite treatment generally decreased, rather than increased, the levels of mature miRNAs, RISC activity, and the miR-451 processing activity of Ago2 (**Fig 3.20 A–C**). Since arsenite treatment results in stress granule formation in nearly all of the cells and in the stress granule localization of nearly all of the Ago2 protein (**Fig 3.18**), the results of these arsenite treatment experiments suggest

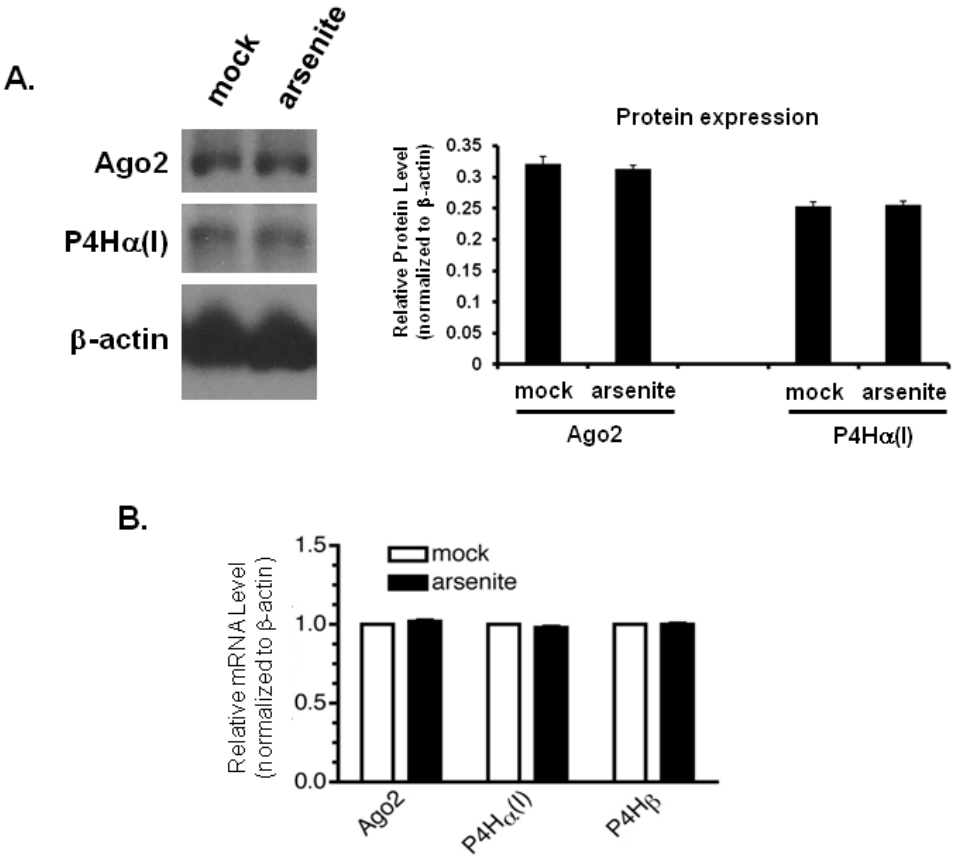

Figure. 3.19 Arsenite does not affect the protein or mRNA levels of Ago2 and C-P4H(I). **A.** Total cell lysates were prepared from PASMCs treated with mock or arsenite for 45 min and were subjected to immunoblot analysis using anti-Ago2, anti-P4Hα(I), or anti-β-actin (loading control) antibodies (left panel). By densitometry, relative amounts of proteins normalized to β-actin were quantitated, and the results presented are the average of three independent experiments (n=3) (right panel). **B.** Total RNAs were prepared from the cells used in **A.** and were subjected to qRT-PCR analysis of Ago2, P4Hα(I), and P4Hβ mRNAs. Relative levels of mRNA expression normalized to β-actin were quantitated and are presented by setting the expression levels of mock to 1.

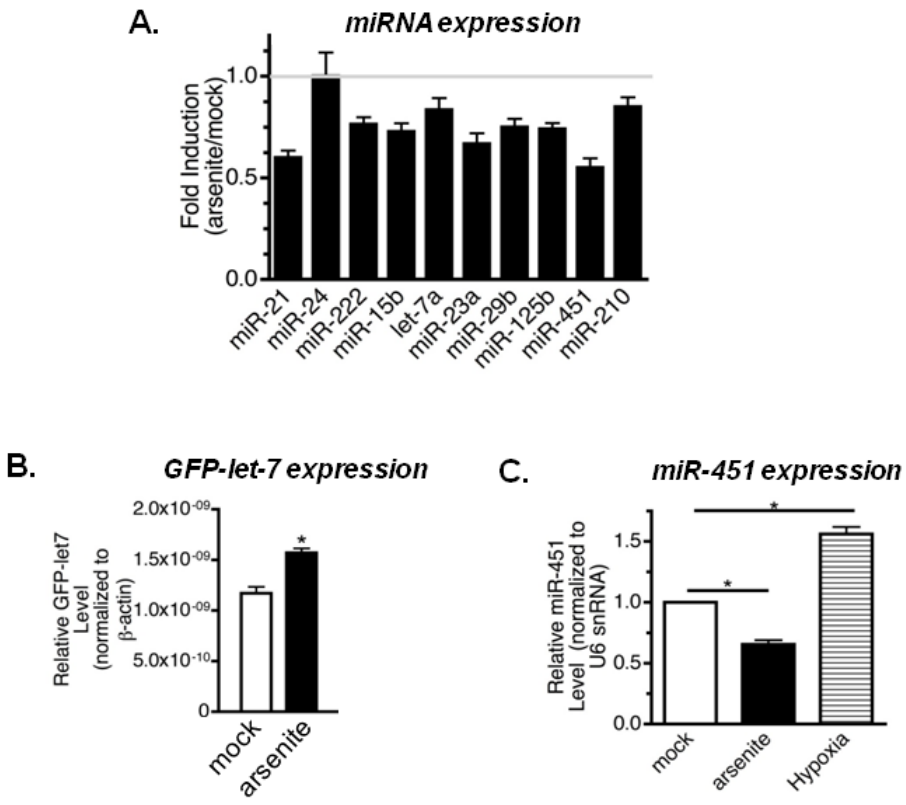

Figure. 3.20 Arsenite decreases miRNA levels, RISC activity, and the miR-451 processing activity of Ago2. A. Total RNAs were prepared from PASMCs treated with mock or arsenite for 45 min and were subjected to qRT-PCR analysis. Levels of expression of the indicated miRNAs normalized to U6 snRNA were quantitated, and fold induction (arsenite/mock) is presented. **B.** U2OS cell line stably expressing GFP-let-7 was treated with mock or arsenite for 45 min. Relative expression of the GFP-let-7 mRNA was quantitated by qRT-PCR and is presented after normalization to β-actin. *, $p<0.05$. **C.** U2OS cells transfected with the miR-144/451 expression construct were treated with mock, arsenite for 45 min, or hypoxia for 24 h. Levels of miR-451 normalized to U6 snRNA were quantitated by qRT-PCR and are presented by setting the expression levels of mock to 1. *, $p<0.05$.

that Ago2 localization to stress granules is not sufficient for the upregulation of Ago2 protein levels, miRNA levels, or Ago2 activities.

Although several core components, such as eIF3, eIF4E, eIF4G, and PABP, have been identified to be present in most stress granules [177], many studies have demonstrated that the composition and assembly rules of stress granules differ depending on the stress stimulus used to induce their formation. For instance, Hsp27 is present in stress granules formed upon heat shock, but it is not found in stress granules induced by arsenite treatment [333]. While eIF2α phosphorylation is required for the assembly of stress granules in response to hypoxia or arsenite treatment [334, 335], hippuristanol can induce stress granule formation even in the absence of eIF2α phosphorylation [336, 337]. Moreover, as mentioned above, Ago2 localization to hippuristanol-induced stress granules is shown to be dependent on the presence of miRNAs [199]. Thus, the results from our arsenite treatment experiments could also suggest that the Ago2 localized in stress granules formed upon arsenite treatment may be missing certain factors, such as miRNAs, target mRNAs, or other proteins, that are important for the activity of the RISC.

The studies by Qi *et al*. had noted that knocking down either C-P4H-α(I) or C-P4H-β using shRNA had no significant effect on the localization of Ago2 to stress granules induced by arsenite, hippuristanol, or heat shock [119], thus suggesting that hydroxylation does not affect Ago2 localization to stress granules. However, in this chapter, I found that Pro700 hydroxylation of Ago2 by C-P4H(I) promotes hypoxia-induced Ago2 localization to stress granules. This difference in the importance of hydroxylation for the localization of Ago2 to stress granules again highlights the fact that

properties of stress granules vary depending on the stress stimulus that elicits their formation. It is intriguing to speculate whether the localization of other proteins to hypoxia-induced stress granules could also be regulated by hydroxylation or other types of post-translational modifications.

Given the previous report by Pare *et al*. indicating that Hsp90 activity is important for the localization of Ago2 to hippuristanol-induced stress granules [324], we wondered whether Ago2 localization to stress granules formed in response to hypoxia also depended on Hsp90 activity. Human PASMCs were treated with DMSO or GA and then exposed to normoxia or hypoxia for 30 min or 3 h. The cells were then subjected to immunofluorescence staining with antibodies against Ago2 and TIA-1. As expected, DMSO-treated cells showed strong colocalization between Ago2 and stress granules, marked by TIA-1, after 30 min or 3 h of hypoxia (data not shown). GA treatment resulted in some decrease in the colocalization between Ago2 and stress granules for both hypoxia treatment time points; however, the decrease was modest and was not statistically significant (data not shown). It is possible that rather than regulating the translocation of Ago2 to stress granules, Hsp90 activity may be important for maintaining stable localization of Ago2 in stress granules. If this is the case, then Ago2 would still be able to localize to stress granules in the presence of GA; however, its association with stress granules would be less stable compared to DMSO-treated cells. Thus, it will be informative to perform the experiment again using live-cell imaging. At the current stage, we cannot exclude the possibility that Hsp90 activity may play a role in regulating Ago2 stress granule association.

3.14 Hypoxia promotes Hsp90-Ago2 interaction through Pro700 hydroxylation and induces Ago2 activities.

Ago2 is known to interact with Hsp90, a constitutively expressed protein that is part of the heat shock response [322]; however, it has been unclear whether this interaction can be subjected to regulation by stress or other physiological stimuli. In this chapter, I showed that hypoxia increases the association of Ago2 with Hsp90 through C-P4H(I)-mediated hydroxylation of Ago2, thus demonstrating for the first time that the interaction between Ago2 and Hsp90 can be modulated in response to stress. We propose that hypoxia promotes the association of Ago2 with Hsp90 by enhancing the Pro700 hydroxylation of Ago2. Our finding that Pro700 hydroxylation is important for the interaction of Ago2 with Hsp90 raises the possibility that this hydroxylation site may also play a role in the interaction between Ago2 and other known Ago2-interacting proteins. Interestingly, Dicer has been demonstrated to interact directly with the PIWI domain of Ago2 [338]. Since the Pro700 residue is located in the PIWI domain of Ago2, we wondered whether Pro700 hydroxylation could be involved in the interaction between Ago2 and Dicer. By performing co-IP experiments under normoxic conditions, I found that the association of Dicer with the P700A mut Ago2 was much weaker compared to WT Ago2 (**Fig 3.21**), therefore suggesting that C-P4H(I)-mediated Pro700 hydroxylation is important for the interaction between Ago2 and Dicer. Given our previous finding that the protein levels of Dicer were decreased after hypoxia treatment (**Fig 2.1 A**), it is intriguing to speculate that the affinity of Ago2 for Dicer might be increased under hypoxia through Pro700 hydroxylation as a way to compensate for the reduced amount of Dicer in the cell.

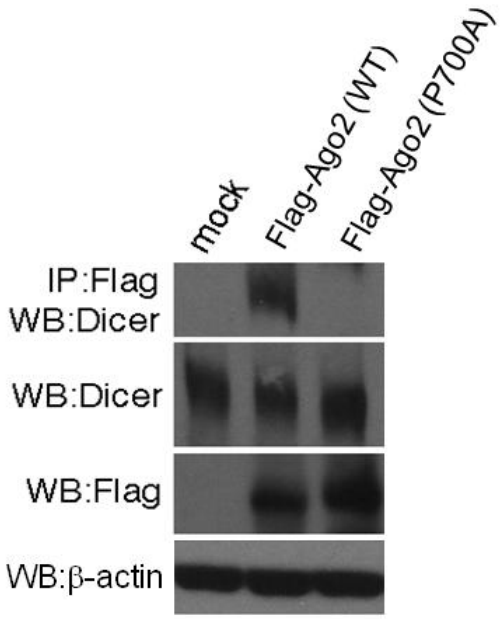

Figure. 3.21 Pro700 hydroxylation of Ago2 is important for the interaction between Ago2 and Dicer. U2OS cells were transfected with vector (mock), Flag-tagged Ago2 (WT), or Flag-tagged Pro700A mutant Ago (P700A) cDNA construct. Total cell lysates were prepared and were subjected to immunoprecipitation with anti-Flag antibody, followed by immunoblot with anti-Dicer antibody. Total cell lysates were also immunoblotted with anti-Dicer, anti-Flag (for Ago2), or anti-β-actin (loading control) antibodies.

Given that hypoxia increases the association of Ago2 with Hsp90 and the studies by Tahbaz *et al*. indicate that Hsp90 ATPase activity is important for the stability of Ago2 under normoxia [322], we had speculated that the activity of Hsp90 may play a role in the increase in Ago2 protein levels under hypoxia. However, my results in this chapter suggest that the ATPase activity of Hsp90 is not essential for the hypoxia-mediated accumulation of Ago2 and thus hint at the possibility that the mechanisms regulating Ago2 protein levels may be different between normoxic and hypoxic conditions. While Hsp90 activity may be important for Ago2 stability under normoxia, other mechanisms may be involved in regulating Ago2 protein levels under hypoxia. Although my results suggest that Hsp90 activity is not required for the upregulation of Ago2 under hypoxia, they do not exclude the possibility that interaction between Ago2 and Hsp90 may be necessary for hypoxia-mediated induction of Ago2. I have found that hypoxia upregulates Ago2 through Pro700 hydroxylation and that Pro700 hydroxylation is important for the association of Ago2 with Hsp90, thus suggesting that Ago2-Hsp90 interaction may play a role. It will be interesting to elucidate the exact mechanism by which protein levels of Ago2 are increased under hypoxia.

Even though the ATPase activity of Hsp90 is not crucial for hypoxia-mediated increase in Ago2 protein levels, I found that Hsp90 activity is important for the increase in miRNA levels and RISC activity under hypoxia, presumably because the activity of Hsp90 is required for the loading of miRNA/miRNA* duplexes into Ago2/RISC [252]. The loading of miRNA duplexes into Ago2/RISC and the subsequent unwinding of the duplexes to form mature miRNAs are key steps in miRNA biogenesis [200] as well as in the formation of mature RISC [252]; therefore, it would be reasonable that inhibition of

Hsp90 activity by GA treatment would suppress the hypoxia-mediated increase in miRNA levels and RISC activity. The finding that hypoxia-mediated induction of the miR-451 processing activity of Ago2 is also dependent on the ATPase activity of Hsp90 is particularly interesting, for it implies that Hsp90 activity is not only involved in the loading of miRNA duplexes into Ago proteins, but it also plays a role in the loading of pre-miRNAs, specifically pre-miR-451, into Ago2, thus extending on the findings of Iwasaki *et al*. [252]. The observation that GA treatment did not significantly suppress the hypoxia-mediated accumulation of Ago2, but still inhibited the hypoxia-mediated induction of miRNA levels and the RISC and miR-451 processing activities, suggests that an increase in Ago2 protein levels is not sufficient and emphasizes the importance of Hsp90 activity in the upregulation of miRNA levels and Ago2 activities under hypoxia. Given that miR-451 was one of the few miRNAs whose expression was strongly upregulated in the lungs of chronic hypoxia-treated rats during PAH development [93], the finding that Hsp90 activity is crucial for the increase in miR-451 levels under hypoxia may have interesting implications for the role of Hsp90 in the development of PAH.

3.15 Upregulation of miRNA levels under hypoxia is mediated by Ago2 and C-P4H(I).

In this chapter, I have demonstrated that knocking down either Ago2 or C-P4H-α(I) suppresses the increase in mature miRNA levels under hypoxia. However, interestingly, the levels of miRNAs under normoxia were generally not significantly affected by either of the knockdowns (**Fig 3.12 C and 3.14**). The finding that miRNA levels were affected by si-Ago2 or si-C-P4H-α(I) only under hypoxia suggests that Ago2

and C-P4H(I) play an especially important role in regulating miRNA expression in response to stress.

As discussed previously, miRNAs are important components of the hypoxic response [128]. Besides participating in the hypoxic response, miRNAs have also been implicated in the responses to other types of stress, such as nutrient deprivation, DNA damage, oncogenic stress, oxidative stress, and cardiac pressure overload [168, 192, 199, 287, 339-345]. The particular importance of miRNAs under stress conditions is also evident in studies involving the genetic knockout of miRNAs. For example, in the absence of stress, miR-208 knockout mice are viable and have no obvious phenotype; it is only when the mice are subjected to stress that a phenotype becomes visible [345]. In particular, when miR-208 knockout mice were subjected to thoracic aortic banding, a known inducer of cardiac hypertrophy, van Rooij *et al*. observed that the hypertrophic and fibrotic response in the knockout mice was blunted compared to the WT mice [345]. Thus, these results indicate that while loss of a miRNA gene may have subtle effects at baseline, the effects can become more obvious in response to stress, for miRNAs may play crucial roles in allowing cells to adapt to and tolerate stress conditions [346]. In a similar manner, it is possible that given the important functions of miRNAs in the hypoxic response, Ago2 and C-P4Hα(I) may play indispensable roles in regulating miRNA levels in the presence of hypoxia, thus leading to a significant effect on miRNA levels under hypoxia when their expression is downregulated.

Although I focused mainly on miRNAs that were upregulated by hypoxia, it is important to note that a significant fraction of miRNAs was also downregulated in

response to hypoxia, as indicated by my miRNA microarray analysis on human PASMCs treated with 24 h of normoxia or hypoxia. Hypoxia-mediated decrease in miRNA levels has also been reported in other studies. By examining the expression levels of lung miRNAs during the development of PAH induced by chronic hypoxia in rats, Caruso *et al.* noted that the expression of miRNAs, such as miR-30c and miR-22, decreased over time in the hypoxic samples compared to the normoxic controls [93]. In addition, the levels of various miRNAs, such miR-19a, miR-101, miR-141, miR-186, miR-195, miR-197, and miR-320 were found to be reduced in cancer cell lines exposed to hypoxia compared to normoxia [347]. Moreover, hypoxic treatment of primary human fibroblasts downregulated the levels of miR-449a and miR-449b, which in turn led to increased target gene expression [348]. The decrease in miRNA levels under hypoxia is most probably regulated by mechanisms distinct from the C-P4H(I)-Ago2 mechanism that we propose for the hypoxia-mediated post-transcriptional upregulation of miRNAs. Compared to the hypoxia-mediated increase in miRNAs, not much is known about the mechanisms underlying the decrease in miRNAs in response to hypoxia. Given that HIF-1 has also been shown to negatively regulate gene expression, it is reasonable to speculate that HIF-1-mediated transcriptional repression may play a role, at least in part, in the downregulation of certain miRNAs under hypoxia.

In summary, the results presented in this chapter demonstrate that in addition to regulating Ago2 protein levels, hypoxia regulates several other aspects of Ago2 as well: i) hypoxia induces the localization of Ago2 to stress granules, ii) hypoxia promotes the interaction between Ago2 and Hsp90, and iii) hypoxia enhances miRNA levels and the Ago2 RISC and Dicer-like processing activities.

3.16 Acknowledgments and publication status.

All experiments described in this chapter were planned and analyzed by C. Wu and A. Hata. J. So performed all stress granule experiments. The miRNA microarray analysis was done with the assistance of B. Davis-Dusenbery and Gordon Huggins. All other experiments were performed by C. Wu. Figures 3.2, 3.8 miR-144 expression, 3.10, 3.15, 3.18, 3.19, and 3.21 are unpublished. All other results are published in Wu C, So J, Davis-Dusenbery BN, Qi HH, Bloch DB, Shi Y, Lagna G, Hata A. *Hypoxia potentiates microRNA-mediated gene silencing through post-translational modification of Argonaute2*. Mol Cell Biol 2011 Dec;31(23):4760-74. See the attached appendix.

CHAPTER IV. ROLE OF TGF-β AND BMP IN THE REGULATION OF AGO2 IN PASMCS.

INTRODUCTION

4.1 TGF-β-mediated upregulation of C-P4H-α(I).

The catalytic α-subunit of the C-P4H(I) enzyme is known to be regulated by several factors. As described in chapter II, hypoxia exposure increases the expression of C-P4H-α(I) [104, 121]. Besides hypoxia, another modulator of C-P4H-α(I) is the growth factor TGF-β1 [122]. The TGF-β family regulates various cellular processes, one of which is the production of the extracellular matrix [24, 25]. Treatment of fibroblasts with TGF-β has been shown to strongly upregulate the synthesis of extracellular matrix components, such as collagens, proteoglycans, and glycoproteins [349-351]. In particular, activation of the TGF-β signaling pathway has been demonstrated to upregulate the expression of the type I collagen genes *proα1(I)* and *proα2(I)*, thus leading to an increase in type I collagen [349, 352, 353]. In addition to the direct activation of collagen gene expression, studies by Chen *et al*. reveal that TGF-β treatment may also induce collagen synthesis by stimulating the expression of the α-subunit of C-P4H(I), the enzyme which plays a critical role in the maturation and secretion of collagen [99, 122].

Chen *et al*. found that TGF-β1 treatment upregulated the activity of the C-P4H-α(I) promoter and increased the mRNA levels of C-P4H-α(I) [122]. Interestingly,

siRNA-mediated knockdown of the transcription factor upstream stimulatory factor (USF1 or USF2) inhibited the TGF-β1-mediated induction of C-P4H-α(I) promoter activity and mRNA levels [122]. USF1 and USF2 are ubiquitously expressed transcription factors that are part of the basic-Helix-Loop-Helix-Leucine Zipper transcription factor family [354]. These transcription factors form dimers, either heterodimers or homodimers, through the helix-loop-helix and leucine zipper domains and bind to DNA via the basic regions [355-357]. The USF dimers regulate gene transcription by binding to the E-box motif (CANNTG, where N can be any nucleotide) in the promoters of various genes, such as steroidogenic factor 1, carboxyl ester lipase, and surfactant protein A [357-361]. By performing ChIP experiments, Chen *et al*. demonstrated that TGF-β1 treatment enhanced the binding of USF1/USF2 to the E-box in the C-P4H-α(I) promoter [122]. Together, these results suggest that TGF-β1 upregulates C-P4H-α(I) transcription by promoting the interaction between USF1/USF2 and the E-box in the C-P4H-α(I) promoter. However, the exact molecular mechanism by which TGF-β1 enhances the USF1/USF2-E-box interaction has yet to be elucidated. Consistent with its stimulatory effects on C-P4H-α(I) expression, TGF-β treatment of lung fibroblasts was shown to increase the activity of the C-P4H enzyme by ~6-fold [362]. Thus, TGF-β not only increases the transcription of C-P4H-α(I), but it also induces C-P4H activity.

Given the stimulatory effects of TGF-β1 on C-P4H(I) and the importance of C-P4H(I) in regulating the stability of Ago2, as previously mentioned, we hypothesize that treatment of PASMCs with TGF-β1, and possibly also other members of the TGF-β

superfamily such as BMP, will lead to increases in Ago2 protein levels by upregulating C-P4H(I) and that the C-P4H(I) Pro700 hydroxylation site of Ago2 will be important to the TGF-β/BMP-mediated increase in Ago2. Thus, the results in this chapter address our **third specific aim, to examine the role of TGF-β and BMP in the regulation of Ago2 in PASMCs.**

RESULTS

4.2 TGF-β1 and BMP4 treatment increases the protein levels of Ago2.

To examine whether TGF-β1 and BMP4 regulate the protein expression of Ago2, human PASMCs were treated with or without TGF-β1 or BMP4 for 48 h, and total cell lysates were prepared and subjected to Western blot analysis. Treatment with either TGF-β1 or BMP4 increased the protein levels of Ago2 by ~2.6-fold and ~1.8-fold, respectively, compared to no growth factor treatment (**Fig 4.1**). A time course experiment was also performed, in which human PASMCs were treated with TGF-β1 or BMP4 for 24 h or 48 h, and total cell lysates were prepared and subjected to Western blot analysis. The protein levels of Ago2 were already upregulated after 24 h of TGF-β1 or BMP4 treatment, and this increase in Ago2 levels was further enhanced after 48 h of TGF-β1 or BMP4 treatment (**Fig 4.2 A**). In this time course experiment, we additionally examined the effect of two other growth factors, PDGF and stem cell factor (SCF), on Ago2 protein expression to investigate whether the increase in Ago2 protein levels is specific to the TGF-β superfamily of growth factors. Interestingly, we found that similar

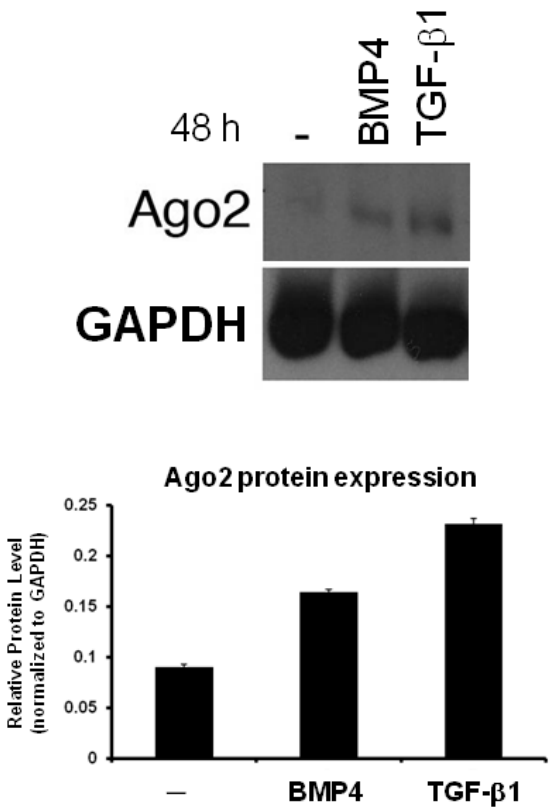

Figure. 4.1 BMP4 and TGF-β1 increase the protein levels of Ago2. PASMCs were treated with BMP4 or TGF-β1 for 48 h. Total cell lysates were prepared from the cells and were subjected to immunoblot analysis using anti-Ago2 or anti-GAPDH (loading control) antibodies (upper panel). By densitometry, relative amounts of proteins normalized to GAPDH were quantitated, and the results presented are the average of three independent experiments (n=3) (lower panel).

to TGF-β1 or BMP4, treating cells with PDGF for 24 h also upregulated the protein levels of Ago2, and the Ago2 protein levels were further induced after 48 h of PDGF treatment (**Fig 4.2 A**). These results suggest that the increase in Ago2 protein levels is not limited to the TGF-β superfamily of growth factors. However, unlike TGF-β1, BMP4, or PDGF, SCF treatment did not significantly increase the protein levels of Ago2 compared to no growth factor treatment (**Fig 4.2 A**), suggesting that the upregulation of Ago2 is somewhat growth factor specific.

Total RNAs were also prepared from the time course experiment and were subjected to qRT-PCR analysis. As a positive control for TGF-β1, BMP4, and PDGF treatment, we examined the mRNA levels of the SMC markers SMA and CNN, which were increased by TGF-β1 or BMP4 treatment and were decreased by PDGF treatment **(Fig 4.2 B**), consistent with previous reports [36, 38, 63-65]. Despite the increase in Ago2 protein levels after 24 h of TGF-β1 or BMP4 treatment, both of these growth factors decreased the mRNA levels of Ago2 during this time point **(Fig 4.2 B**), thus indicating that Ago2 is most likely upregulated through a post-transcriptional mechanism at this early time point. While Ago2 mRNA levels were also reduced after 48 h of BMP4 treatment compared to no growth factor treatment, 48 h of TGF-β1 treatment resulted in some increase in the mRNA levels of Ago2 **(Fig 4.2 B**). These results indicate that unlike BMP4, 48 h of TGF-β1 treatment may upregulate Ago2 at the transcriptional level.

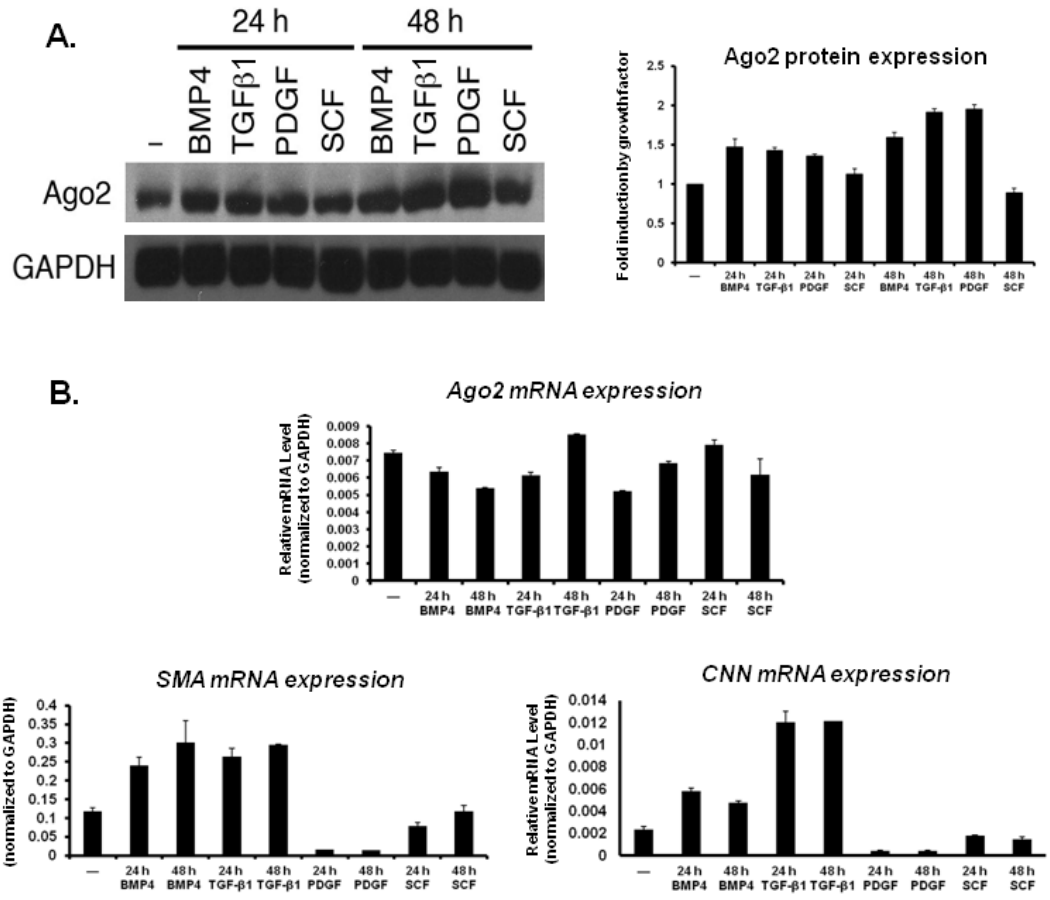

Figure. 4.2 Effect of TGF-β related and non-related growth factors on Ago2 expression. A. PASMCs were treated with BMP4, TGFβ1, PDGF, or SCF for 24 h or 48 h. Total cell lysates were prepared from the cells and were subjected to immunoblot analysis using anti-Ago2 or anti-GAPDH (loading control) antibodies (left panel). Relative amounts of proteins normalized to GAPDH were quantitated by densitometry, and the results presented are the average of three independent experiments (n=3). Fold induction (growth factor treatment/no treatment) is presented (right panel). **B.** Total RNAs were prepared from the cells used in **A.** and were subjected to qRT-PCR analysis. Relative levels of mRNA expression normalized to GAPDH were quantitated and are presented.

4.3 Upregulation of Ago2 protein levels upon BMP4 treatment involves the C-P4H(I)-mediated Pro700 hydroxylation of Ago2.

Given that previous studies have found that hydroxylation of Ago2 at Pro700 by the C-P4H(I) enzyme enhances the stability of Ago2 [119], we investigated whether C-P4H(I) may play a role in the increase in Ago2 protein levels by 24 h of TGF-β1 or BMP4 treatment. The mRNA and protein expression of C-P4H-α(I) and C-P4H-β were examined in human PASMCs treated with or without TGF-β1 or BMP4 for 24 h. Only TGF-β1 upregulated the mRNA levels of C-P4H-α(I) compared to no gowth factor treatment (**Fig 4.3 A**), which is consistent with the previous study by Chen *et al*. demonstrating that TGF-β1 treatment stimulates the transcription of C-P4H-α(I) [122]. Interestingly, both TGF-β1 and BMP4 increased the protein levels of C-P4H-α(I) and C-P4H-β compared to no growth factor treatment (**Fig 4.3 B**). These results indicate that TGF-β1 enhances not only the mRNA levels of C-P4H-α(I), but also the protein levels of C-P4H-α(I). Additionally, these results show that besides TGF-β1, BMP4 and potentially other growth factors can regulate the protein and/or mRNA levels of C-P4H-α(I) as well.

To investigate the importance of C-P4H(I)-mediated prolyl hydroxylation in the TGF-β1/BMP4-mediated upregulation of Ago2, Cos7 cells were transfected with an empty vector (mock), a WT Ago2, or a P700A mut Ago2 expression construct and then treated with TGF-β1 or BMP4 for 24 h. As mentioned previously, the mutant Ago2 contains a Pro700-to-alanine mutation and thus can no longer be hydroxylated by C-

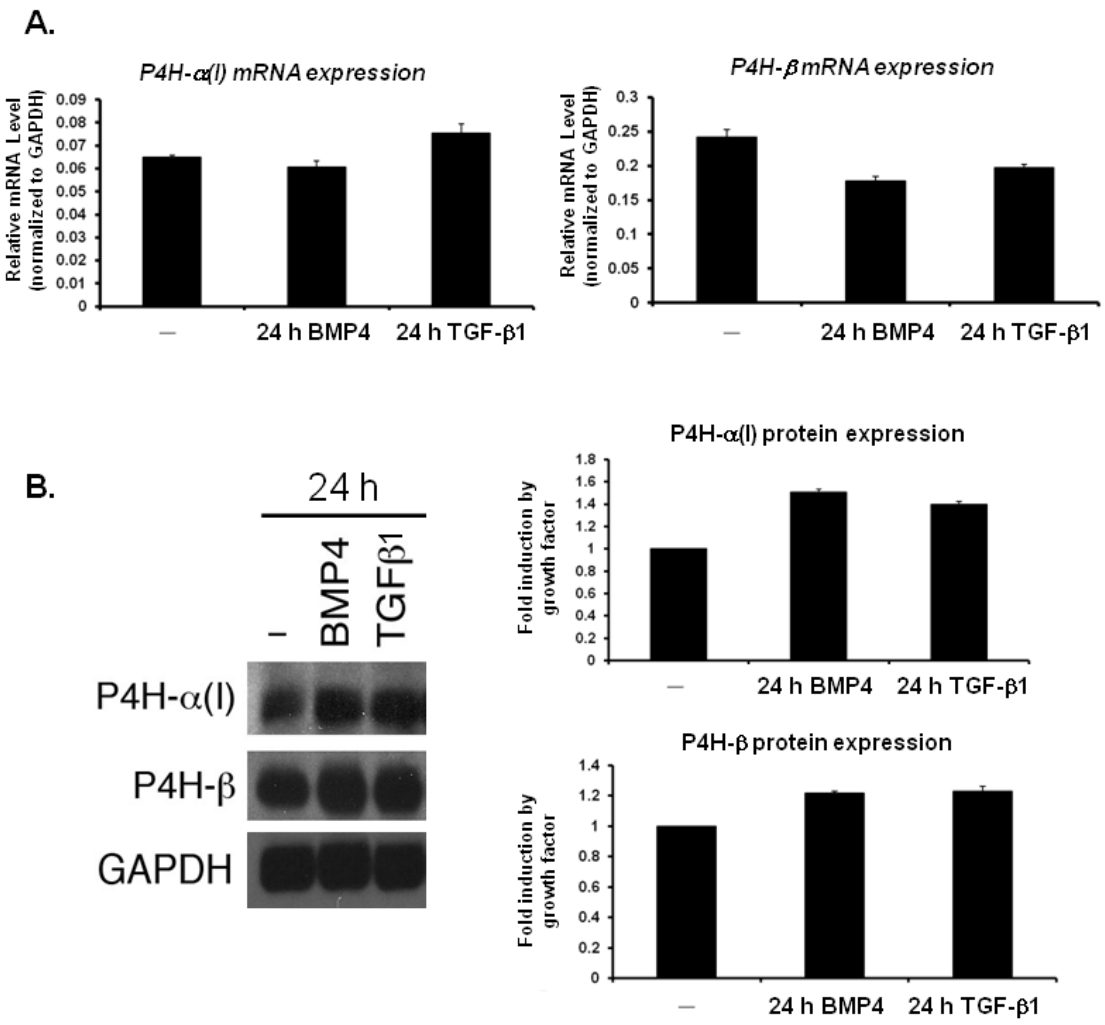

Figure. 4.3 BMP4 and TGF-β1 upregulate the protein levels of C-P4H(I). **A.** PASMCs were treated with BMP4 or TGFβ1 for 24 h. Total RNAs were prepared from the cells and were subjected to qRT-PCR analysis. Relative levels of mRNA expression normalized to GAPDH were quantitated and are presented. **B.** Total cell lysates were prepared from the cells used in **A.** and were subjected to immunoblot analysis using anti-P4H-α(I), anti-P4H-β, or anti-GAPDH (loading control) antibodies (left panel). Relative amounts of proteins normalized to GAPDH were quantitated by densitometry, and the results presented are the average of three independent experiments (n=3). Fold induction (growth factor treatment/no treatment) is presented (right panel).

P4H(I) at this position [119]. Cos7 cells were utilized in this experiment because PASMCs are not readily transfectable. Although Cos7 cells were used, the protein levels of endogenous Ago2 still increased after 24 h of TGF-β1 or BMP4 treatment in the mock-transfected cells coincident with increases in the protein levels of C-P4H-α(I) and C-P4H-β (data not shown), similar to the results obtained with human PASMCs. These findings suggest that the TGF-β1 or BMP4 effect on Ago2 is not a cell-type-specific phenomenon. Interestingly, I found that 24 h of BMP4 treatment increased the protein levels of exogenous WT Ago2, but not the P700A mut Ago2 (**Fig 4.4**), thus supporting our hypothesis that the C-P4H(I) Pro700 hydroxylation site of Ago2 plays an important role in the BMP4-mediated accumulation of Ago2. On the other hand, contrary to our expectations, TGF-β1 treatment upregulated the protein levels of exogenous WT Ago2 as well as that of the P700A mut Ago2 (data not shown). This result suggests that unlike BMP4, Pro700 hydroxylation of Ago2 may not be crucial for the increase in Ago2 protein levels upon TGF-β1 treatment; another mechanism may underlie the TGF-β1-mediated accumulation of Ago2.

4.4 Effect of TGF-β1 or BMP4 treatment on the subcellular localization of Ago2.

Since the subcellular localization of Ago2 can be subjected to regulation by various stimuli [199], we wondered whether TGF-β1 or BMP4 treatment has any effect on the localization of Ago2 in the cell. Human PASMCs were treated with or without TGF-β1 or BMP4 for 24 h or 48 h and then subjected to immunofluorescence staining with antibodies against Ago2 and C-P4H-β. In the absence of growth factor treatment,

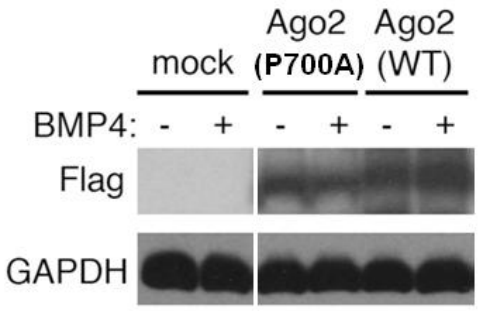

Figure. 4.4 BMP4 increases protein levels of exogenous WT Ago2, but not P700A mutant Ago2. Cos7 cells were transfected with vector (mock), Pro700A mutant (P700A) Ago2, or wild type (WT) Ago2 cDNA construct, followed by treatment with BMP4 for 24 h. Total cell lysates were prepared from the cells and were subjected to immunoblot analysis with anti-Flag or anti-GAPDH antibodies.

both Ago2 and C-P4H-β were mainly localized to the cytoplasm and showed a diffuse pattern of staining that is characteristic for ER staining (**Fig 4.5**). Consistent with previous findings by Qi *et al*. [119], strong colocalization between Ago2 and C-P4H-β was seen in the cytoplasm (**Fig 4.5**). Ago2 was also detected in bright cytoplasmic foci, presumably P-bodies, and interestingly, no colocalization with C-P4H-β was observed in these foci (**Fig 4.5**), thus suggesting that these foci contain Ago2, but not the C-P4H enzyme. Treatment with either TGF-β1 or BMP4 for 24 h did not have any obvious effect on the subcellular localization of Ago2 or C-P4H-β compared to no growth factor treatment (**Fig 4.5**). Ago2 and C-P4H-β still exhibited strong colocalization with each other in the presence of the growth factors (**Fig 4.5**). In addition, there were no apparent differences in the subcellular localization of Ago2 or C-P4H-β between the different growth factor treatments (**Fig 4.5**). Similar results were obtained for the 48 h growth factor treatment time point (data not shown). Together, these results indicate that unlike hypoxia, TGF-β1 and BMP4 do not have much effect on the subcellular localization of Ago2.

DISCUSSION

4.5 TGF-β1 and BMP4 regulate the protein levels of Ago2.

Previous studies from our lab have shown that treatment of human PASMCs with TGF-β1 or BMP4 regulates the expression of miRNAs [42, 363]. In particular, we have reported that upon TGF-β1 or BMP4 stimulation, the Smad signal transducer

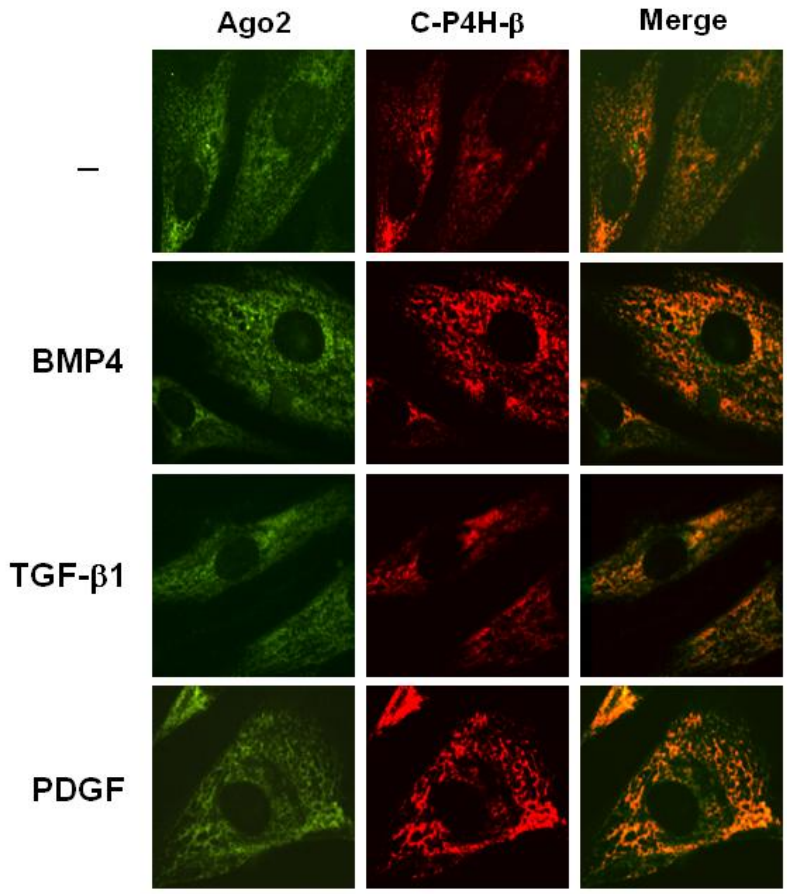

Figure. 4.5 BMP4, TGF-β1, and PDGF do not have a significant effect on the subcellular localization of Ago2 and C-P4H-β. PASMCs were treated with BMP4, TGFβ1, or PDGF for 24 h and were subjected to immunofluorescence staining with FITC-Ago2 antibodies (green) and rhodamin-C-P4H-β antibodies (red).

proteins are recruited to the Drosha/DGCR8/p68 "Microprocessor complex" to enhance the Drosha-mediated processing of certain pri-miRNAs to pre-miRNAs [42]. We found that the Smad proteins bind directly to a consensus sequence, which is similar to the Smad binding element (SBE) of TGF-β/BMP target gene promoters [32], located in the stem region of the pri-miRNAs [363]. The presence of this consensus sequence is important for the increase in the synthesis of the pre-miRNAs upon TGF-β1/BMP4 treatment and for the interaction of Smads, Drosha, and DGCR8 with the pri-miRNAs [363]. Thus, upon TGF-β1 or BMP4 treatment, the Smads bind to a SBE-like sequence present in a set of pri-miRNAs to facilitate Drosha-mediated pri-miRNA to pre-miRNA processing [363]. Additionally, our lab has recently shown that TGF-β1 and BMP4 can transcriptionally increase the expression of miR-143 and miR-145 [43]. These findings provide a couple of mechanisms by which the TGF-β/BMP signaling pathway regulates miRNA biogenesis.

In this chapter, I showed that TGF-β1 or BMP4 treatment of human PASMCs can also upregulate the protein levels of Ago2. Since the total levels of Ago proteins within the cell are important in regulating miRNA levels and Ago is the main component of the RISC [258-262, 268, 273, 307], my results suggest a novel regulation of miRNA biogenesis/activity by the TGF-β signaling pathway via increasing the stability of Ago2 and modulating RISC activity. We speculate that similar to hypoxia, TGF-β1/BMP4-mediated accumulation of Ago2 plays an important role in the upregulation of miRNA levels upon TGF-β1 or BMP4 treatment. Thus, the TGF-β signaling pathway may utilize multiple mechanisms to precisely modulate miRNA expression levels in the cell. It will

be interesting to investigate whether the expression of other protein components of the miRNA pathway, such as Drosha or Dicer, is also regulated by TGF-β and BMP.

4.6 Ago2 protein levels are also regulated by PDGF.

The finding that TGF-β1 and BMP4 regulate Ago2 protein levels suggests that other growth factors may also play a role in modulating Ago2. Indeed, Adams *et al*. demonstrated that treating MDA-MB-231 cells with epidermal growth factor (EGF) increased the stability of the Ago2 protein through the EGF receptor (EGFR)/MAPK pathway [364]. Moreover, in this chapter, I found that other than TGF-β1 and BMP4, the growth factor PDGF upregulated the protein levels of Ago2 in human PASMCs as well. Similar to 24 h of TGF-β1 or BMP4 treatment, Ago2 upregulation by PDGF appears to occur post-transcriptionally, for PDGF treatment decreased the mRNA levels of Ago2 **(Fig 4.2 B**). Interestingly, PDGF also induced the protein levels of C-P4H-α(I) and C-P4H-β compared to no growth factor treatment **(Fig 4.6 A**), thus suggesting that the increase in Ago2 protein levels upon PDGF treatment may be mediated by the C-P4H(I) enzyme. In fact, PDGF treatment of lung fibroblasts has been reported to enhance the enzymatic activity of C-P4H by ~2-fold [362]; as a result, it is plausible that PDGF treatment may likewise induce the activity of C-P4H(I) in PASMCs, leading to an increase in the hydroxylation and stability of Ago2.

It is particularly intriguing that TGF-β1, BMP4, and PDGF treatment all upregulated Ago2 protein levels because TGF-β1/BMP4 and PDGF generally exert opposite effects in PASMCs. For example, as described before, TGF-β1 or BMP4

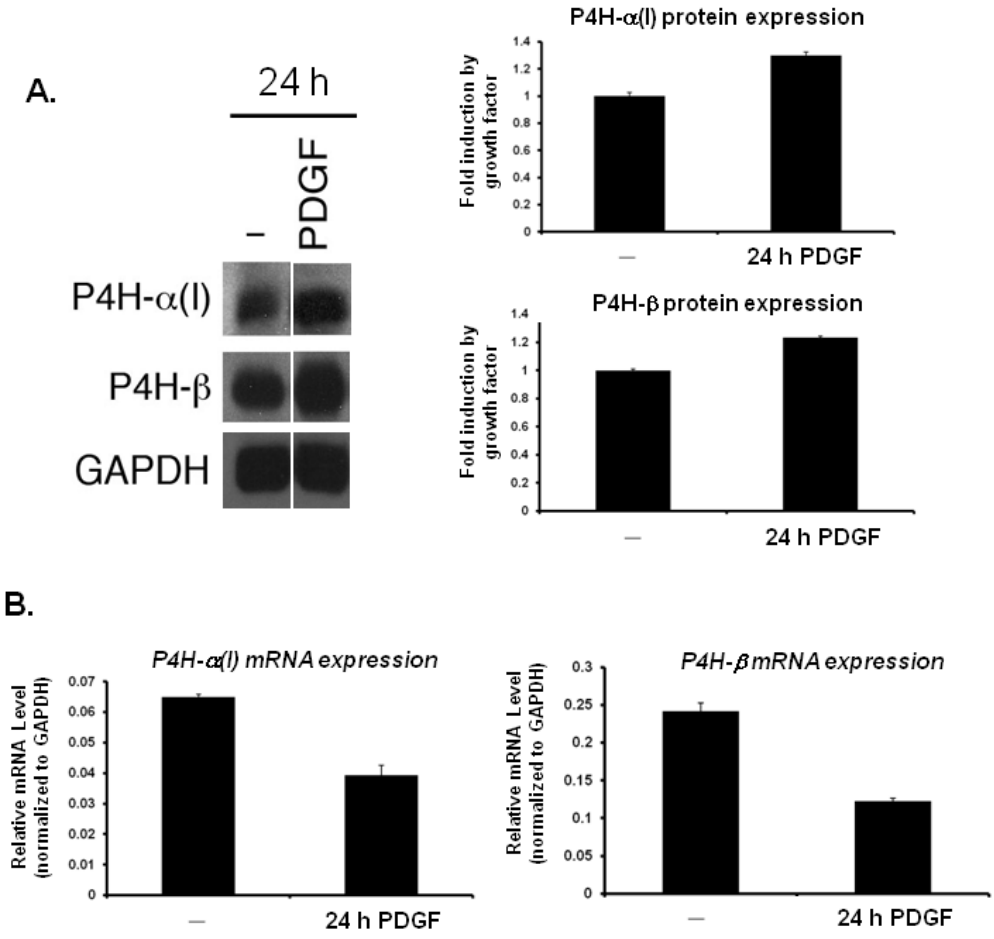

Figure. 4.6 PDGF upregulates the protein levels of C-P4H(I). **A.** PASMCs were treated with PDGF for 24 h. Total cell lysates were prepared from the cells and were subjected to immunoblot analysis using anti-P4H-α(I), anti-P4H-β, or anti-GAPDH (loading control) antibodies (left panel). Relative amounts of proteins normalized to GAPDH were quantitated by densitometry, and the results presented are the average of three independent experiments (n=3). Fold induction (growth factor treatment/no treatment) is presented (right panel). **B.** Total RNAs were prepared from the cells used in **A.** and were subjected to qRT-PCR analysis. Relative levels of mRNA expression normalized to GAPDH were quantitated and are presented.

treatment reduces proliferation and stimulates the expression of the contractile proteins SMA, CNN, and SM22α, thus promoting the differentiation of PASMCs [36, 38]. Conversely, PDGF is known to promote PASMC dediferentiation, increasing proliferation and migration and decreasing the expression of SMC differentiation markers, such as CNN, SMA, SM-MHC, and SM22α [60-65]. However, one aspect shared by TGF-β1, BMP4, and PDGF is that all of these growth factors have been shown to upregulate miRNA levels in PASMCs [42, 66]. Thus, it is interesting to speculate that accumulation of Ago2 may be important for the growth factor-mediated increase in miRNA levels. It is possible that there may be a limited amount of Ago2 protein in the cell, and so elevated levels of Ago2 may be needed for the stabilization and efficient function of the growth factor-induced miRNAs.

4.7 Increase in Ago2 protein levels upon BMP4 treatment, but not TGF-β1, is dependent on Pro700 hydroxylation of Ago2 by C-P4H(I).

My results in this chapter suggest that the Pro700 hydroxylation site is not only critical for the induction of Ago2 protein levels under hypoxia, but it is also important for the BMP4-mediated upregulation of Ago2. This finding suggests that hydroxylation of Ago2 may be a common mechanism employed by various physiological stimuli to regulate Ago2 levels in the cell. Although Pro700 hydroxylation of Ago2 does not appear to be crucial for the increase in Ago2 protein levels upon TGF-β1 treatment, this result does not exclude the possibility that C-P4H(I)-mediated hydroxylation may be involved in the TGF-β1-mediated upregulation of Ago2. Since I have not investigated whether the accumulation of Ago2 upon TGF-β1 treatment would be prevented by the

knockdown of C-P4H-α(I) using siRNA, it is still possible that hydroxylation of Ago2 by the C-P4H(I) enzyme may play role. Interestingly, I found that treating human PASMCs with TGF-β1 or BMP4 in the presence of ascorbic acid enhanced the TGF-β1/BMP4-mediated induction of Ago2 protein levels **(Fig 4.7**). In the absence of ascorbic acid, TGF-β1 and BMP4 increased the protein levels of Ago2 by ~2.6-fold and ~1.8-fold, respectively, compared to untreated cells **(Fig 4.7**). The addition of ascorbic acid resulted in a ~3.9-fold and 2.4-fold induction of Ago2 by TGF-β1 and BMP4, respectively, compared to untreated cells (**Fig 4.7**). As discussed previously, ascorbic acid is one of the cofactors for the C-P4H(I) enzymatic reaction, and it helps to enhance the catalytic hydroxylation reaction [103, 104]. Thus, the observation that TGF-β1-mediated induction of Ago2 can be further increased in the presence of ascorbic acid suggests that the hydroxylation activity of C-P4H(I) may be important for the upregulation of Ago2 by TGF-β1. However, this is by no means direct evidence for the role of C-P4H(I) in the TGF-β1-mediated accumulation of Ago2, for ascorbic acid is also known to be a cofactor for other enzymatic reactions [365-367]. Nevertheless, given that Qi *et al*. identified three -X-Pro-Gly triplets (119–121, 522–524, 699–701) in Ago2 that are predicted to be hydroxylated by C-P4H(I) [119], there is a possibility that the other Pro residues may be important for the increase in Ago2 protein levels upon TGF-β1 treatment. Instead of Pro700, TGF-β1 treatment may lead to the hydroxylation of Pro120 or Pro523; thus, it may be informative to look at the effect of TGF-β1 on the protein levels of Ago2 mutants containing either a Pro120-to-alanine mutation or a Pro523-to-alanine mutation. It is

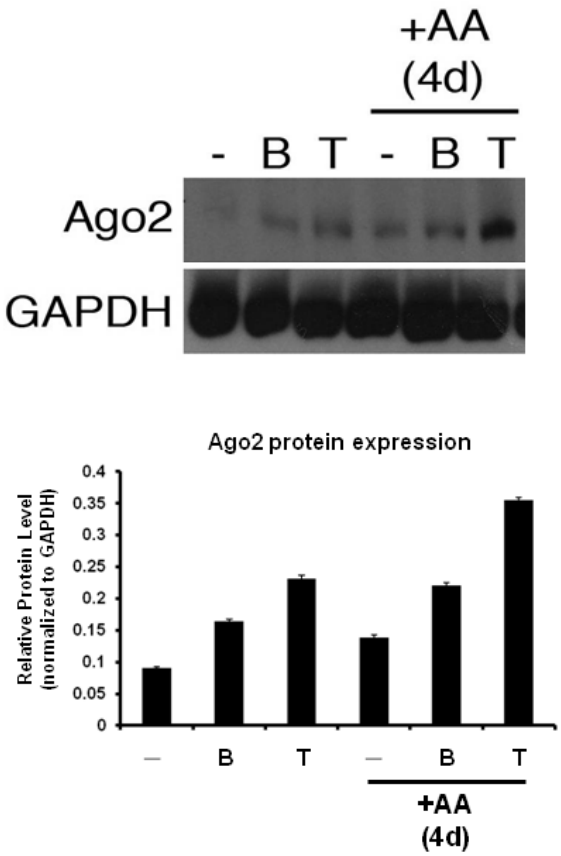

Figure. 4.7 Ascorbic acid upregulates Ago2 protein levels and enhances BMP4/TGF-β1-mediated induction of Ago2. PASMCs were cultured for a total of 4 days (4d) in the presence of ascorbic acid (AA) and were treated with BMP4 (B) or TGF-β1 (T) for 48 h. Total cell lysates were prepared from the cells and were subjected to immunoblot analysis with anti-Ago2 or anti-GAPDH (loading control) antibodies (upper panel). Relative amounts of proteins normalized to GAPDH were quantitated by densitometry, and the results presented are the average of three independent experiments (n=3) (lower panel).

intriguing to contemplate the idea that different growth factor stimuli may target different hydroxylation sites of Ago2.

4.8 Subcellular localization of Ago2 is not significantly affected by 24 h or 48 h of TGF-β1, BMP4, or PDGF treatment.

Previous studies by Qi *et al*. had noted that knocking down either C-P4H-α(I) or C-P4H-β using shRNA and mutating the Pro700 residue of Ago2 to alanine reduced the localization of Ago2 to P-bodies [119], thus suggesting that C-P4H(I)-mediated hydroxylation of Ago2 may play a role in Ago2 localization to P-bodies. Since I found that both TGF-β1 and BMP4 increased the protein levels of C-P4H(I) and TGF-β1 has been reported to increase C-P4H(I) activity [362], we had speculated that TGF-β1 or BMP4 treatment may induce the localization of Ago2 to P-bodies. However, my results in this chapter show that treatment with either TGF-β1 or BMP4 for 24 h or 48 h did not have any obvious effect on the subcellular localization of Ago2 compared to untreated cells. Treatment with PDGF for 24 h or 48 h also had no apparent effect on the subcellular localization of Ago2 (**Fig 4.5**). Given that I have only examined two growth factor treatment time points, I cannot rule out the possibility that treating the cells with the growth factors for a shorter amount of time may have an effect on the subcellular localization of Ago2. It is possible that growth factor-induced changes in Ago2 localization are transient and occur quickly after the growth factor treatment. As presented in chapter III, hypoxia rapidly induces the formation of stress granules and promotes Ago2 localization to stress granules within 3 h of hypoxia treatment. Thus, it

would be informative to examine the effect of TGF-β1, BMP4, or PDGF treatment on Ago2 subcellular localization at earlier time points.

4.9 Acknowledgments and publication status.

All experiments described in this chapter were planned and analyzed by C. Wu and A. Hata. B. Davis-Dusenbery performed the experiment in Figure 4.4. Experiments in Figures 4.2, 4.3, and 4.6 were performed in collaboration with B. Davis-Dusenbery. All other experiments were performed by C. Wu. All results are unpublished.

CHAPTER V. DISCUSSION AND FUTURE DIRECTIONS.

5.1 Summary and Significance.

PAH is a devastating disease characterized by obstructive remodeling of the small PAs, leading to a progressive increase in pulmonary arterial pressure and ultimately right ventricular heart failure and death [2, 3, 368]. Hypoxia plays a major role in the pathobiology of PAH [1, 75]. Acute hypoxia results in the selective constriction of PAs and elevation of pulmonary arterial pressure, while chronic exposure to hypoxia induces structural and functional changes to the pulmonary vasculature [368, 369]. Studies have found that the expression levels of various miRNAs are altered during the development of PAH induced by chronic hypoxia in rats [93], thus suggesting that changes in miRNA expression in response to hypoxia may play a role in PAH development. However, the mechanisms by which hypoxia regulates miRNAs and the miRNA pathway have not been fully understood. Elucidation of the mechanisms underlying hypoxia-mediated miRNA regulation will provide additional insights into the molecular basis of hypoxia-induced vascular remodeling and the pathobiology of PAH. Given the recent report on C-P4H(I)-mediated prolyl hydroxylation of Ago2, a key regulator of miRNA biogenesis and activity [119], we hypothesized that hypoxia may modulate Ago2, and thus the miRNA pathway, through its induction of C-P4H(I).

In this thesis, I showed that hypoxia upregulated the protein levels of Ago2 both *in vitro* in mammalian cell culture and *in vivo* in the chronic hypoxia rat model of PAH. The upregulation of Ago2 was found to be accompanied by increases in the

protein and mRNA levels of the α- and β-subunits of C-P4H(I), thus suggesting that the increase in Ago2 protein levels under hypoxia could be mediated by the hydroxylation activity of the C-P4H(I) enzyme. Indeed, hypoxia did not increase the mRNA levels of Ago2, indicating that Ago2 is upregulated at the post-transcriptional level under hypoxia. Also, downregulating the catalytic subunit C-P4H-α(I) and mutating Pro700 of Ago2 to alanine both prevented the hypoxia-mediated induction of Ago2 protein levels. Together, these results indicate that hypoxia post-transcriptionally upregulates Ago2 through C-P4H(I)-mediated Pro700 hydroxylation. Thus, the work presented here reveals that hypoxia can modulate the expression of core protein components of the miRNA pathway and, more importantly, provides a novel mechanism of miRNA regulation by hypoxia through hydroxylation of Ago2.

Of the four Ago subfamily proteins (Ago1–4) present in humans, I found that Ago2 was the most prominently upregulated by hypoxia in human PASMCs, thus underscoring the importance of Ago2 in the hypoxic response. Qi *et al*. had noted in their co-IP experiments that compared to Ago2, Ago1 and Ago3 associated less readily with C-P4H-α(I) [119]. Also, Ago1 and Ago3 were found to be hydroxylated by C-P4H(I) to a lesser extent compared to Ago2 in their *in vitro* hydroxylation assays [119]. Thus, if hypoxia promotes hydroxylation and the stability of Ago1 and Ago3 are similarly enhanced by hydroxylation, the weaker association of Ago1 and Ago3 with C-P4H-α(I) and their lower degree of hydroxylation could in part account for their smaller degree of upregulation by hypoxia. On the other hand, it is also possible that the different Ago proteins may be differentially affected by the hydroxylation modification. While

hydroxylation may play an important role for the stability of Ago2, it may not be as crucial for the stability of the other Ago proteins. For instance, Qi *et al*. had noticed that although the half-life of Ago2 was reduced when the Pro700 hydroxylation site was mutated to alanine, the half-lives of Ago1 and Ago3 were not affected by the Pro700-to-alanine mutation [119]. Further experiments involving the knockdown of C-P4H-α(I) or C-P4H-β would provide more insights into the role of hydroxylation in regulating the protein levels of the other Ago proteins.

To investigate the biological significance of hypoxia-induced hydroxylation of Ago2, we examined the subcellular localization, protein-protein interaction, and activities of Ago2 under hypoxia. We found that hypoxia induces stress granule formation and promotes the localization of Ago2 to stress granules. Ago2 stress granule localization was greatly reduced when Pro700 was mutated to alanine, indicating that C-P4H(I)-mediated Pro700 hydroxylation of Ago2 is important for the localization of Ago2 with stress granules in response to hypoxia. We also observed that hypoxia increased the association of Ago2 with Hsp90 and that this increase in association was prevented when C-P4H-α(I) was downregulated. Mutating Pro700 of Ago2 to alanine reduced the interaction between Ago2 and Hsp90 as well. Thus, these results suggest that hypoxia promotes Ago2-Hsp90 interaction through C-P4H(I)-mediated Pro700 hydroxylation of Ago2. These studies are the first to report that hydroxylation of Ago2 plays a role not only in the subcellular localization of Ago2, but also in the interaction of Ago2 with other proteins in the cell.

Moreover, we found that hypoxia decreased the mRNA levels of a GFP-let-7-sensor construct without altering the endogenous levels of let-7a, suggesting that Ago2 RISC activity is increased under hypoxia. Mutation of Pro700 of Ago2 to alanine abolished the hypoxia-mediated decrease in GFP-let-7 mRNA expression, thus implying that Pro700 hydroxylation of Ago2 is critical for the increase in RISC activity under hypoxia. Besides inducing RISC activity, hypoxia also enhanced the miR-451 processing activity of Ago2 and decreased the expression of several target genes of hypoxia-induced miRNAs. These findings demonstrate that hypoxia promotes various miRNA-related functions of Ago2. Additionally, we identified several miRNAs that were post-transcriptionally upregulated by hypoxia. Knockdown of either Ago2 or C-P4H-α(I) suppressed the hypoxia-mediated increase in these miRNAs, thus implying that both Ago2 and C-P4H(I) hydroxylation activity are involved in the upregulation of these miRNAs under hypoxia. Interestingly, the ATPase activity of Hsp90 is required for hypoxia-mediated induction of the miRNAs as well as for the increase in Ago2 RISC and miR-451 processing activities upon hypoxia treatment.

Altogether, the results presented here reveal that a series of non-transcriptional events occur in response to hypoxia: i) hydroxylation of Ago2 by the C-P4H(I) enzyme and increased Ago2 protein levels, ii) stress granule formation and Ago2 localization to stress granules, iii) enhanced association of Ago2 with Hsp90, and (iv) induction of Ago2 activities and miRNA levels, all of which contribute to efficient miRNA-mediated gene regulation under conditions of low oxygen. Studies on hypoxic regulation of gene expression have mainly focused on the role of the transcription factor HIF-1. In this

thesis, we present a novel mechanism for modulating gene expression under hypoxia by specific post-translational modification of Ago2. Furthermore, we have extended the original observations of the importance of hydroxylation of Ago2 from regulating Ago2 stability [119] to modulating the subcellular localization, protein-protein interaction, and activities of Ago2.

It is intriguing to note that the increase in Ago2 protein levels under hypoxia was accompanied by decreases in the protein levels of another core protein of the miRNA pathway, Dicer. Reduced expression of Dicer in response to hypoxia has been reported in other independent studies as well. The mRNA levels of Dicer were found to be downregulated in the lungs of chronic hypoxia-treated rats and in hypoxia-treated rat pulmonary artery fibroblasts [93], thus suggesting that hypoxia-mediated reduction of Dicer is not cell-type specific and may be a general phenomenon in hypoxic cells. As my results show that hypoxia induces both the protein levels and activities of Ago2, we speculate that the induction of Ago2 and modulation of Ago2 subcellular localization under hypoxia may serve as a complementary mechanism to augment miRNA-mediated regulation of gene expression when the amount of Dicer is limiting in the cell. In addition, given the hypoxia-mediated increase in the Dicer-like processing activity of Ago2, it is tempting to speculate that miR-451 and potentially other Dicer-independent miRNAs processed by Ago2 may play critical roles during the pathogenesis of PAH and other hypoxia-related diseases, such as cancer [130]. Interestingly, Caruso *et al*. observed that miR-451 was one of the few miRNAs that was significantly upregulated in the lungs of chronic hypoxia-treated rats during PAH development [93].

Finally, in this thesis, I presented evidence that upregulation of Ago2 protein levels is not limited to hypoxia. I found that TGF-β1, BMP4, and PDGF can also post-transcriptionally increase the protein levels of Ago2. Our lab has previously demonstrated that these growth factors can regulate miRNA expression [42, 66, 363]. TGF-β1 and BMP4 activate the transcription [43] or facilitate the pri-miRNA to pre-miRNA processing by Drosha of a subset of miRNAs [42, 363], while PDGF increases the levels of miR-221 at the transcriptional level [66]. Given that Ago2 is an important regulator of miRNA biogenesis and activity [258-262, 268, 273, 307], my results here suggest a novel mechanism by which TGF-β, BMP, and PDGF can regulate miRNA biogenesis/function through modulation of Ago2 protein levels and activity.

Similar to hypoxia, growth factor-mediated accumulation of Ago2 was accompanied by increases in the protein levels of C-P4H-α(I) and C-P4H-β, suggesting that Ago2 hydroxylation by C-P4H(I) may mediate the induction of Ago2 protein levels upon growth factor treatment. Indeed, mutating Pro700 of Ago2 to alanine prevented the BMP4-mediated upregulation of Ago2, thus implying that Pro700 hydroxylation of Ago2 is important for the increase in Ago2 protein levels upon BMP4 treatment. Although the C-P4H(I) Pro700 hydroxylation site does not seem to be critical for the TGF-β1-mediated induction of Ago2, we currently cannot rule out the possibility that hydroxylation by C-P4H(I) may still be involved. C-P4H-α(I) knockdown studies will need to be performed in the future to further investigate the role of C-P4H(I)-mediated hydroxylation in the increase in Ago2 protein levels by TGF-β1 treatment. Studies involving the effect of

TGF-β1 on the protein levels of other C-P4H(I) hydroxylation site mutants of Ago2 will be informative as well.

It is particularly interesting that TGF-β, BMP, PDGF, and hypoxia all have similar effects on Ago2. Given that these stimuli have been reported to be involved in the initiation and/or progression of PAH through their effects on PASMCs [4], the work presented in this thesis suggests that alterations in Ago2 protein expression may play a role in the pathobiology of PAH by deregulating miRNA regulation, thus enhancing our understanding of the molecular basis of PAH. The elucidation of the significance of C-P4H(I)-mediated hydroxylation in regulating Ago2 protein levels under hypoxia and upon BMP4 treatment in PASMCs may provide new molecular targets for PAH therapy. As I have demonstrated in this thesis that Pro700 hydroxylation of Ago2 plays an important role in regulating Ago2 protein levels, subcellular localization, protein-protein interaction, and RISC activity under hypoxia, it may be interesting to explore the possibility of developing drugs that target the Pro700 hydroxylation site of Ago2.

Future Directions

5.2 Mechanism by which hydroxylation mediates the upregulation of Ago2 protein levels under hypoxia.

In this thesis, I have shown that the Pro700 hydroxylation site of Ago2 is critical for the upregulation of Ago2 protein levels under hypoxia. However, the exact mechanism by which Pro700 hydroxylation mediates the increase in Ago2 remains to be

studied in the future. Since I found that hypoxia promotes the association of Ago2 with Hsp90 and previous studies have reported that the ATPase activity of Hsp90 is important for the stability of Ago2 under normoxia [322], we examined whether Hsp90 activity may play a role in the increase in Ago2 protein levels under hypoxia. Treatment of human PASMCs with GA, a specific inhibitor of Hsp90 ATPase activity [325, 329], did not significantly suppress the hypoxia-mediated accumulation of Ago2. This result suggests that the ATPase activity of Hsp90 is not essential for the increase in Ago2 under hypoxia and that other mechanisms may be involved in regulating the protein levels of Ago2 under hypoxia.

Besides prolyl 4-hydroxylation, ubiquitination has also been identified as a post-translational modification that regulates the stability of Ago2. As mentioned previously, the mLin41 protein was shown to interact with Ago2 and ubiquitinate Ago2 both *in vitro* and *in vivo* in mouse embryonic carcinoma cells [297]. Knockdown of the endogenous expression of mLin41 using siRNA decreased the amount of ubiquitinated Ago2 and increased the steady-state Ago2 protein levels, whereas overexpression of mLin41 reduced the protein levels of Ago2 [297]. These results suggest that mLin41 regulates Ago2 stability by mediating the ubiquitination and subsequent degradation of Ago2 [297]. Interestingly, Qi *et al*. had noted that while shRNA-mediated knockdown of C-P4H-α(I) decreased the protein levels of Ago2, the Ago2 levels were restored to that of the control upon treatment with the proteasome inhibitor MG132 [119], thus suggesting that hydroxylation of Ago2 may inhibit its degradation by the proteasome.

Although my results suggest that Hsp90 activity is not required for the upregulation of Ago2 under hypoxia, they do not exclude the possibility that interaction between Ago2 and Hsp90 is necessary for the hypoxia-mediated induction of Ago2. Given that Pro700 hydroxylation of Ago2 is important for its association with Hsp90 and that hypoxia promotes Ago2-Hsp90 interaction, it is conceivable that hypoxia-induced Hsp90 interaction may prevent Ago2 from being targeted by the proteasome, possibly by inhibiting the ubiquitination of Ago2. A recent study has demonstrated that Hsp90 can compete with receptor of activated C-kinase (RACK1) for binding to HIF-1α, thereby regulating the stability of HIF-1α [370]. Both RACK1 and Hsp90 were shown to bind to the PAS-A domain of HIF-1α; increased RACK1 expression reduced the association of Hsp90 with HIF-1α and vice versa [370]. Binding of Hsp90 enhances HIF-1α stability [371, 372], while RACK1 promotes HIF-1α ubiquitination through recruitment of the Elongin-C/B ubiquitin ligase complex and subsequent degradation of HIF-1α in a proteasome-dependent manner [370]. RACK1 was initially characterized as protein that stimulates translation by binding to both activated protein kinase C (PKC) and eIF6, thus facilitating the phosphorylation of eIF6 by PKC and subsequent ribosomal subunit association [373]. However, further studies reveal that RACK1 is multifunctional and participates in many other biological processes as well, such as cell spreading and establishment of cell-cell contacts and focal adhesions [374, 375]. RACK1 has multiple protein-binding sites and is considered to be a scaffold protein that can simultaneously bind to various proteins and signaling molecules [376-378]. Interestingly, RACK1 was recently reported to interact with Ago2 and regulate miRNA-mediated gene repression [379]. Thus, based on these findings, it is reasonable to hypothesize that hypoxia-

induced Hsp90 interaction with Ago2 may reduce ubiquitination and subsequent degradation of Ago2 by inhibiting the binding of RACK1 to Ago2, thereby leading to increased Ago2 protein levels under hypoxia.

To investigate the potential role of RACK1, the interaction between RACK1 and Ago2 will first be confirmed in human PASMCs and U2OS cells by performing co-IP experiments. RACK1 is expected to associate with Ago2 under normoxia, and this association is predicted to be decreased under hypoxia. The effect of RACK1 on Ago2 protein levels will then be examined by overexpression and knockdown experiments. Overexpression of RACK1 is expected to reduce the protein levels of Ago2, while knockdown of RACK1 using siRNA is expected to upregulate Ago2 protein levels under both normoxia and hypoxia. To confirm that RACK1-induced downregulation of Ago2 is mediated through the proteasome, cells will be transfected with a RACK1 expression construct and treated with MG132. The addition of MG132 is expected to inhibit RACK1-mediated decrease in Ago2 protein levels.

Moreover, the ability of Hsp90 to compete with RACK1 for binding to Ago2 will be investigated. GST-Ago2 will be co-transfected with various amounts of GST-Hsp90, the GST fusion proteins will be isolated, and Western blot analysis will be performed to detect bound RACK1, GST-Ago2, and GST-Hsp90. If competition between Hsp90 and RACK1 for Ago2 binding exists, GST-Hsp90 is expected to dose-dependently inhibit the binding of RACK1 to GST-Ago2. The reciprocal experiment could also be performed, in which case GST-RACK1 is predicted to dose-dependently inhibit the binding of Hsp90 to GST-Ago2. To further delineate the mechanism by which

RACK1 mediates the downregulation of Ago2, the interaction between RACK1 and Elongin-C will be examined in human PASMCs and U2OS cells by co-IP experiments. RACK1 is expected to associate with Elongin-C under both normoxia and hypoxia. Also, addition of GST-RACK1 to cell lysates is expected to increase the co-immunoprecipitation of Ago2 and Elongin-C. In addition, overexpression of RACK1 is expected to increase the ubiquitination of Ago2 in the presence of MG132. Together, these results would suggest that RACK1 recruits Ago2 to the Elongin-C/B ubiquitin ligase complex, which ubiquitinates Ago2 and promotes its subsequent proteasomal degradation. Thus, the hypoxia-mediated increase in Hsp90 interaction with Ago2 through Pro700 hydroxylation is thought to compete with RACK1 for Ago2 binding, thereby inhibiting the ubiquitination and degradation of Ago2, and this could, at least in part, lead to the accumulation of Ago2 under hypoxia.

Elucidation of the mechanism by which hydroxylation mediates the induction of Ago2 protein levels under hypoxia would provide additional insights into the regulation of Ago proteins by hypoxia and advance the understanding of regulation of the miRNA pathway in general. Since hypoxia plays a key role in PAH pathobiology [1, 75], further delineation of the mechanism underlying hypoxia-mediated upregulation of Ago2 would enhance our understanding of the molecular basis of PAH and enable the development of more effective therapies for PAH.

5.3 Mechanism regulating Ago2 localization in stress granules under hypoxia.

The results presented in this thesis demonstrate that the Pro700 hydroxylation site of Ago2 is important for the hypoxia-induced localization of Ago2 in stress granules.

However, the precise mechanism by which Pro700 hydroxylation promotes Ago2 localization in stress granules under hypoxia has yet to be elucidated. In fact, not much is currently known about how Ago2 is recruited to stress granules or the significance of Ago2 localization to stress granules. A recent study by Pare *et al*. reported that Ago2 mutants containing mutations in the PAZ or MID domain which affect its binding of small RNAs showed reduced localization to stress granules induced by arsenite treatment [380]. This decreased stress granule localization was not due to reduced expression or instability of the mutant Ago2 proteins, for Pare *et al*. showed that the expression level and stabilities of all the Ago2 mutants were similar to that of a WT Ago2 construct [380]. Thus, these findings suggest that Ago2 binding to small RNAs is critical for its localization to stress granules [380]. In their studies, Qi *et al*. had observed that the P700A mut Ago2, containing the Pro700-to-alanine mutation, was able to rescue RISC activity when overexpressed in cells in which the endogenous expression of Ago2 was downregulated by shRNA [119], suggesting that P700A mut Ago2 is capable of binding small RNAs. However, since I found that P700A mut Ago2 still exhibited reduced localization to stress granules under hypoxia compared to WT Ago2, this suggests that additional mechanisms, besides binding to small RNAs, could regulate Ago2 localization to stress granules induced by hypoxia.

Given that Pro700 hydroxylation of Ago2 is important for its association with Hsp90 and my results do not exclude the possibility that Hsp90 activity may play a role in maintaining stable localization of Ago2 in hypoxia-induced stress granules, it is plausible that Pro700 hydroxylation may stabilize the association of Ago2 with stress granules under hypoxia by facilitating its interaction with Hsp90, which in turn associates

with stress granule components. Indeed, Pare *et al*. noticed in HeLa cells that a fraction of Hsp90 localized to stress granules induced by hippuristanol treatment and colocalized with Ago2 in these stress granules [324]. Interestingly, studies have found that the stress granule component, polysomal ribonuclease 1 (PMR1), is one of the client proteins of Hsp90 [381]. PMR1 is a mRNA endonuclease that binds to specific mRNA targets and promotes their decay [382]. Through co-IP experiments in Cos-1 cells, Peng *et al*. showed that PMR1 associates with Hsp90 [381]. RNase A treatment had no effect on the association between PMR1 and Hsp90, thus implying that the interaction is most likely direct and not RNA-mediated [381]. In addition, GA treatment decreased the interaction between PMR1 and Hsp90 and reduced the protein levels of PMR1, most likely through a proteasome-dependent pathway [381]. These results suggest that Hsp90 activity is important for its interaction with PMR1 and for the stability of PMR1. Moreover, Yang *et al*. found that PMR1 colocalized with TIA-1 in stress granules induced by arsenite treatment [383]. Co-IP experiments revealed that the N-terminus of PMR1 is important for its association with TIA-1 in the presence of arsenite treatment [383]. Based on these findings, it is plausible that Pro700 hydroxylation may promote Ago2 association with stress granules under hypoxia by facilitating its interaction with Hsp90, which associates with PMR1, a TIA-1 interacting stress granule component.

To test this hypothesis, the subcellular localization of Hsp90 and PMR1 will be examined by immunofluorescence in human PASMCs and U2OS cells exposed to normoxia or hypoxia to see whether hypoxia has a similar effect on the subcellular localization of these proteins as the other stress stimuli reported in the studies mentioned above. Under normoxia, Hsp90 and PMR1 are expected to show a diffuse pattern of

staining in the cytoplasm; however, hypoxia is predicted to induce the localization of Hsp90 and PMR1 to TIA-1-positive stress granules. Co-staining with anti-Ago2 is also expected to show colocalization between Ago2 and Hsp90 or PMR1 in hypoxia-induced stress granules. In addition, the interactions between Hsp90 and PMR1 and between PMR1 and TIA-1 will be confirmed in human PASMCs and U2OS cells through co-IP experiments. Hsp90 is predicted to associate with PMR1 under both normoxia and hypoxia, while the interaction between PMR1 and TIA-1 is expected to be detected only in the presence of hypoxia. Additionally, total cell lysates from cells exposed to normoxia or hypoxia will be subjected to immunoprecipitation with anti-Ago2 antibody, followed by Western blot analysis with anti-Hsp90, anti-PMR1, and anti-TIA-1 antibodies. Ago2 association with Hsp90, PMR1, and TIA-1 is predicted to be increased under hypoxia compared to normoxia. If Pro700 hydroxylation of Ago2 is involved in its interaction with these proteins, the association of these proteins with the P700A mut Ago2 is expected to be reduced compared to their association with WT Ago2. Moreover, to investigate the potential significance of Hsp90 in mediating the interaction of Ago2 with PMR1 and TIA-1, knockdown experiments will be performed in which the endogenous expression of Hsp90 will be downregulated using siRNA. Knockdown of Hsp90 is expected to reduce the association of Ago2 with PMR1 and TIA-1 compared to the control. The localization of Ago2 in TIA-1-positive stress granules under hypoxia, as observed by live-cell microscopy, is also predicted to be less stable when the expression of Hsp90 is knocked down. Taken together, these results would suggest that Hsp90 plays an important role in mediating the interaction between Ago2 and the stress granule components, PMR1 and TIA-1. Hence, the hypoxia-mediated increase in Hsp90

interaction with Ago2 through Pro700 hydroxylation is speculated to promote the association of Ago2 with PMR1 and TIA-1, which could in part contribute to maintaining stable localization of Ago2 in stress granules under hypoxia.

Delineating the mechanism by which Pro700 hydroxylation mediates the association of Ago2 with stress granules formed in response to hypoxia will be an important step towards the general understanding of how Ago proteins are localized to stress granules. Further insights into the mechanisms underlying the targeting of Ago proteins to stress granules will provide novel opportunities to disrupt or prevent their localization to these cytoplasmic structures and thus enable us to better understand the role of stress granule localization in regulating the activities of Ago proteins.

5.4 Mechanism underlying hypoxia-mediated downregulation of Dicer or Drosha protein levels.

One of the more intriguing aspects of the work presented in this thesis is the finding that the protein levels of Dicer and Drosha are decreased upon hypoxia treatment of human PASMCs and U2OS cells. As mentioned previously, hypoxia-mediated reduction of Dicer has also been observed in hypoxia-treated rat pulmonary artery fibroblasts and *in vivo* in the lungs of chronic hypoxia-treated rats [93], thus implying that hypoxia-mediated downregulation of Dicer is not cell-type specific and may be a general phenomenon in hypoxic cells. Hypoxia-mediated reduction of Drosha has been reported in the lungs of chronic hypoxia-treated rats as well [93]. However, the mechanism underlying the decrease in Dicer or Drosha expression under hypoxia remains an outstanding question in the field.

To investigate whether the reduction in Dicer or Drosha protein levels under hypoxia is due to transcriptional or post-transcriptional effects, total RNAs will be prepared from human PASMCs exposed to normoxia or hypoxia and will be subjected to qRT-PCR analysis of Dicer or Drosha. If hypoxia decreases the mRNA levels of Dicer or Drosha compared to normoxia, then this would suggest that hypoxia-mediated reduction of Dicer or Drosha occurs transcriptionally. Since the transcription factor HIF-1 is a major player orchestrating the expression of various genes in response to hypoxia and has been reported to mediate transcriptional repression as well as induction [161, 384, 385], it would be interesting to examine whether HIF-1 could be involved in the transcriptional downregulation of Dicer or Drosha. If HIF-1 plays a role, knockdown of HIF-1 should prevent or suppress the hypoxia-mediated reduction of Dicer or Drosha mRNA levels; conversely, overexpression of HIF-1 is expected to reduce the mRNA levels of Dicer or Drosha under normoxia and further repress the Dicer or Drosha mRNA levels under hypoxia. The Dicer or Drosha gene promoter could also be inspected for the presence of potential HIF-1 consensus binding sites. If present, luciferase promoter constructs containing these HIF-1 binding sites could be created to examine whether these sites could confer hypoxia repression of Dicer or Drosha. In addition, ChIP experiments could be performed to determine whether these sites could indeed bind HIF-1 *in vivo*.

However, if the mRNA levels of Dicer or Drosha are not significantly altered under hypoxia compared to normoxia, then this would suggest that hypoxia-mediated decrease in Dicer or Drosha protein levels occurs post-transcriptionally. In this case, cells will be treated with hypoxia and cycloheximide, an inhibitor of *de novo* protein

biosynthesis. If cycloheximide treatment blocks the hypoxia-mediated reduction of Dicer or Drosha protein levels, then this would suggest that the decrease in Dicer or Drosha protein levels under hypoxia is mediated by newly synthesized proteins. On the other hand, if cycloheximide treatment has no significant effect on the hypoxia-mediated reduction of Dicer or Drosha, then this would imply that hypoxia regulates Dicer or Drosha post-translationally, such as by modulating protein stability and the rate of protein degradation.

A recent study found that Dicer is a target of the miR-103/107 miRNA family [386]. By using Pictar and TargetScan, Martello *et al*. detected eight evolutionarily conserved miR-103/107-binding sites in the 3'UTR of the Dicer mRNA [386]. Luciferase reporter experiments confirmed that miR-103/107 targets the 3'UTR of Dicer [386]. Overexpression of miR-103 or miR-107 reduced the protein levels of Dicer, while knockdown of miR-103/107 using an antagomiR increased Dicer protein levels [386]. These findings indicate that Dicer protein expression is regulated by the miR-103/107 family of miRNAs. Interestingly, the results from my miRNA microarray analysis of human PASMCs exposed to normoxia or hypoxia reveal that miR-103 is one of the miRNAs whose expression is induced by hypoxia. Likewise, hypoxia-mediated induction of the levels of miR-103 has also been reported in several different human cancer cell lines [168]. In addition, the putative promoter region of miR-103 was found to contain a HIF consensus binding site, and the levels of miR-103 were shown to be increased in cells overexpressing HIF-1 [168]. These results suggest that miR-103 may be a HIF-1-target gene and that HIF-1 may be involved in the increase in miR-103 levels under hypoxia.

Based on these findings, it is reasonable to hypothesize that hypoxia-mediated upregulation of miR-103 through HIF-1 may play a role, at least in part, in the downregulation of Dicer protein levels under hypoxia. To test this hypothesis, the endogenous expression of miR-103 in human PASMCs will be downregulated using an antagomiR, and the cells will be exposed to normoxia or hypoxia. Knockdown of miR-103 is expected to suppress the hypoxia-mediated reduction of Dicer protein levels. Additionally, the role of HIF-1 in regulating the expression of miR-103 will be examined by luciferase reporter experiments and ChIP. HIF-1 is predicted to bind to the HIF consensus binding site in the miR-103 promoter and induce the expression of miR-103. Downregulation of HIF-1 is also expected to suppress the hypoxia-mediated decrease in Dicer protein levels. Hence, instead of directly modulating the gene expression of Dicer, HIF-1 may indirectly regulate Dicer expression by enhancing the levels of miR-103 under hypoxia. In a similar manner, it is also plausible that Drosha is a target of one of the miRNAs induced by HIF-1 under hypoxia, and thus HIF-1 may indirectly downregulate the expression of Drosha under hypoxia as well.

5.5 Potential therapeutic targets for PAH.

As mentioned above, it may be interesting to explore the possibility of developing drugs for PAH that target the Pro700 hydroxylation site of Ago2, given its importance in regulating various aspects of Ago2 under hypoxia. The work presented in this thesis suggests that alterations in Ago2 protein expression, subcellular localization, and activity may contribute to changes in miRNA levels under hypoxia, which have been implicated in the development of PAH [1, 4, 93]. Designing drugs that specifically

recognize and bind to Pro700 of Ago2, thus preventing this residue from being hydroxylated by C-P4H(I), would inhibit the increase in Ago2 protein levels, RISC activity, and the levels of certain miRNAs under hypoxia. This may help reverse some of the miRNA-related changes observed in hypoxia. Although inhibitors of C-P4H(I) hydroxylation activity exist [387], which would decrease the hydroxylation of Ago2 and have a similar effect in suppressing the increase in Ago2 protein levels, activity, and miRNAs under hypoxia, the effect of C-P4H(I) inhibition would not be limited to Ago2 and thus unwanted side-effects are likely. C-P4H(I) has many other substrates besides Ago2, most notably procollagens [99]. Since C-P4H(I) is a key enzyme in collagen biosynthesis [99], inhibition of C-P4H(I) would prevent collagen formation as well. Given that hypoxia is known to induce the production of collagen [94, 95] and collagen deposits are greatly increased in the small PAs of PAH patients [388], inhibiting collagen formation might be beneficial in PAH treatment in the short-term, but long-term treatment with a C-P4H(I) inhibitor runs the risk of developing scurvy [105]. Thus, therapies that provide a targeted approach and can specifically target C-P4H(I)-mediated regulation of Ago2 would be more desired and more effective for PAH treatment.

5.6 Conclusions.

In conclusion, the work presented in this thesis uncovers a novel mechanism of miRNA regulation by hypoxia through post-translational modification of a core protein component of the miRNA pathway, Ago2. Previous studies on hypoxia-mediated regulation of miRNAs have focused heavily on the role of the transcription factor HIF-1 in modulating miRNAs at the transcriptional level. Here, we provide evidence that

hypoxia can upregulate miRNAs at the post-transcriptional level through hypoxia-induced hydroxylation of Ago2 by the C-P4H(I) enzyme. In addition, we show that hypoxia promotes the localization of Ago2 to stress granules, enhances Ago2 association with Hsp90, and upregulates Ago2 RISC and Dicer-like processing activities, contributing to efficient miRNA-mediated gene regulation under low oxygen conditions. Thus, this work reveals that non-transcriptional events can also play crucial roles in the regulation of miRNAs and gene expression under hypoxia. This study also advances our general knowledge about the regulation of miRNA biogenesis and activity, a currently poorly understood area of the field. More importantly, our findings provide further insights into the molecular basis of hypoxia-induced vascular remodeling and the pathobiology of PAH. Having a more thorough understanding of the molecular mechanisms underlying PAH will allow for the development of more targeted therapeutics for this disease.

CHAPTER VI. MATERIALS AND METHODS.

Cell culture

Human PASMCs were purchased from Lonza (#CC-2581) and maintained in Smooth Muscle Growth Medium-2 (Sm-GM2, Lonza) containing 5% fetal bovine serum (FBS, Sigma). PASMCs between passages 4 and 8 were used for all studies. Cos7 (American Type Culture Collection), U2OS (a kind gift from Dr. J. Kyriakis), and U2OS stable cell lines expressing the GFP-let-7 sensor construct (a kind gift from Dr. H. Qi [119]) were maintained in Dulbecco's Modified Eagle media (DMEM) supplemented with 10% FBS (Sigma). Growth factor treatments were performed under starvation conditions (0.2% FBS). Recombinant growth factors were purchased from R&D Systems. TGF-β1 was used at 400pM, BMP4 at 3nM, PDGF at 20ng/ml, and SCF at 5ng/ml. Sodium L-ascorbate was purchased from Sigma and was used at 25μM.

Normoxia/Hypoxia Treatment

Hypoxic conditions were generated by first replacing culture media with fresh media equilibrated with a hypoxic gas mixture and then incubating cells in a sealed, humidified, modular incubator chamber (Billups-Rothenberg) at 37°C after flushing with a mixture of 5% CO_2 and 95% N_2 for 5 min. Normoxic controls were cultured in a humidified incubator at 37°C in the presence of 5% CO_2.

Animal Study and Immunohistochemistry

All experiments were performed in accordance with the guidelines and regulations of the Institutional Animal Care and Use Committee at Tufts Medical Center. Adult male Sprague-Dawley were randomized to 17-days of normoxia or hypobaric hypoxia as described previously [82]. At the end of the exposure period, rats were sacrificed and the lungs were processed for paraffin embedding. Sections of 5-μm paraffin-embedded tissue sections were immunostained as described previously [92].

Plasmid DNA transfection and expression constructs

Cells were transfected using linear polyethylenimine (PEI), MW 25,000 (Polysciences, Inc.) according to the manufacturer's protocol. C-P4H-α(I) and amino-terminal Flag-tagged Ago1, Ago2, mutant Ago2 (Pro700A), Ago3, and Ago4 were kind gifts from Dr. H. Qi [119]. The miR-144/451 expression construct was a kind gift from Dr. E. Lai [242].

RNA Interference

Synthetic siRNAs targeting human *Ago2* or *C-P4H-α(I)* were obtained from Applied Biosystems (*Silencer*® Select Pre-designed) and transfected into cells using RNAiMAX (Invitrogen) according to the manufacturer's instructions. A siRNA with a non-targeting sequence (Negative Control siRNA, Qiagen) was used as a negative control. All siRNA

transfections were performed using 30nM siRNA; no toxicity was observed at the concentration used. The siRNA sequence targeting human *Ago2* is 5'-GGUCUAAAGGUGGAGAUAATT-3' and 5'-UUAUCUCCACCUUUAGACCTT-3'. The siRNA sequence targeting human *C-P4H-α(I)* is 5'-CUAGUACAGCGACAAAAGATT-3' and 5'-UCUUUUGUCGCUGUACUAGTT-3'

Antibodies and chemical inhibitors

Antibodies used in this study include anti-Ago1 (04-083, Millipore), anti-Ago2 (015-22031, Wako Chemicals), anti-Ago3 (SAB4200112, Sigma), anti-Ago4 (05-967, Millipore), anti-Drosha (A301-886A, Bethyl), anti-Dicer (ab14601, Abcam), anti-C-P4Hα(I) (PAB7221, Abnova), anti-C-P4Hβ (sc-20132, Santa Cruz), anti-Flag epitope tag (M2, Sigma), anti-Hsp90 (MAB3286, R&D Systems), anti-TIA-1 (sc-1751, Santa Cruz), anti-β-actin (A5441, Sigma), and anti-GAPDH (2E3-2E10, Abnova). The secondary antibodies used for immunofluorescence staining were purchased from Jackson Immunoresearch Laboratory Inc. Arsenite (S-7400) and geldanamycin (G3381) were purchased from Sigma. Concentrations of geldanamycin were optimized in each cell type to achieve maximal Hsp90 inhibition while minimizing cellular toxicity: 1 μM in U2OS cells and 0.1 μM in PASMCs.

Immunoprecipitation and western blot assays

Cells were lysed in TNE buffer (1% Nonidet P-40, 10mM Tris-HCl (pH 7.5), 1 mM EDTA, 150 mM NaCl). Total cell lysates or proteins immunoprecipitated with antibodies were separated on SDS-PAGE, transferred to PVDF membranes (Millipore), immunoblotted with antibodies, and visualized using an enhanced chemiluminescence detection system (Amersham Biosciences). ImageJ gel analysis software (rsbweb.nih.gov/ij/) was used to quantitate protein bands by densitometry.

RNA preparation and quantitative Reverse Transcriptase-Polymerase Chain Reaction (qRT-PCR)

Total RNA was extracted from cells by TRIzol (Invitrogen). For mRNA detection, 1μg of RNA was subjected to RT reaction using first-strand cDNA synthesis kit (Invitrogen) according to the manufacturer's instructions. The quantitative analysis of the change in expression levels was calculated by real-time PCR machine (iQ5, Bio-Rad). PCR cycling conditions were 94°C for 3min and 40 cycles of (94°C for 15s, 60°C for 20s and 72°C for 40s). For mature miRNA detection, TaqMan MicroRNA assay kit (Applied Biosystems) was used according to the manufacturer's instructions. Data analysis was performed by using comparative C_T method in BioRad software. Average of three experiments each performed in triplicate with standard errors is presented. The sequences of RT-PCR primers used in this study are published in [389] and [42].

MiRNA microarray analysis

Applied Biosystems human microRNA array A v2.0 was used to quantitate the miRNA levels of 377 human miRNAs according to the manufacturer's protocol. Total RNA was isolated from PASMCs exposed to normoxia or hypoxia for 24 h. Megaplex reverse transcriptase reaction was utilized to generate cDNA, which was added to Taqman universal PCR master mix and then applied to the array. The Applied Biosystems 7900HT TaqMan low density array (TLDA) real time PCR system was used to monitor the reactions. Arrays were analyzed using the comparative C_T method in Applied Biosystems' RQ manager.

Immunofluorescence staining, fluorescence imaging, and image analysis

PASMCs or U2OS cells, plated on coverslips, were fixed with 2% paraformaldehyde/phosphate-buffered saline solution and permeabilized using methanol. Cells were then incubated for at least 1 h at room temperature sequentially with primary and secondary antibodies to detect the proteins of interest. After washing, cells were mounted on microscope slides using VECTASHIELD® Mounting Medium with 4'-6-diamidino-2-phenylindole (DAPI) (Vector Laboratories). Images were taken on a Nikon Eclipse E800 microscope with a CF160 Infinity optical system and a Hamamatsu C4742-95 digital camera. Images were quantitated using ImageJ software (rsbweb.nih.gov/ij/). Intensity profiles generated using the ImageJ Color Profiler plugin were used to determine colocalization between Ago2 and stress granules.

Statistical Analysis

The results presented are average of at least three experiments each performed in triplicate with standard errors. Statistical analyses were performed by analysis of variance, followed by Tukey's multiple comparison test or by Student's t test as appropriate, using Prism 4 (GraphPAD Software Inc.). P values of <0.05 were considered significant and are indicated with asterisks.

CHAPTER VII. REFERENCES.

1. Paulin, R., et al., *From oncoproteins/tumor suppressors to microRNAs, the newest therapeutic targets for pulmonary arterial hypertension.* J Mol Med (Berl), 2011.
2. Rich, S., et al., *Primary pulmonary hypertension. A national prospective study.* Ann Intern Med, 1987. **107**(2): p. 216-23.
3. Rubin, L.J. and S. Rich, *Primary Pulmonary Hypertension*. 1997, New York, NY: Marcel Dekker, Inc.
4. Tajsic, T. and N.W. Morrell, *Smooth muscle cell hypertrophy, proliferation, migration and apoptosis in pulmonary hypertension.* Comprehensive physiology, 2011. **1**: p. 295-317.
5. Yeager, M.E., et al., *Microsatellite instability of endothelial cell growth and apoptosis genes within plexiform lesions in primary pulmonary hypertension.* Circ Res, 2001. **88**(1): p. E2-E11.
6. Peacock, A.J., et al., *An epidemiological study of pulmonary arterial hypertension.* Eur Respir J, 2007. **30**(1): p. 104-9.
7. Junqueira, L.C. and J. Carneiro, *Basic Histology: Text & Atlas*. 11th ed. 2005, New York: McGraw-Hill.
8. Cines, D.B., et al., *Endothelial cells in physiology and in the pathophysiology of vascular disorders.* Blood, 1998. **91**(10): p. 3527-61.
9. Owens, G.K., M.S. Kumar, and B.R. Wamhoff, *Molecular regulation of vascular smooth muscle cell differentiation in development and disease.* Physiol Rev, 2004. **84**(3): p. 767-801.
10. Gabbiani, G., et al., *Vascular smooth muscle cells differ from other smooth muscle cells: predominance of vimentin filaments and a specific alpha-type actin.* Proc Natl Acad Sci U S A, 1981. **78**(1): p. 298-302.
11. Hungerford, J.E., et al., *Development of the aortic vessel wall as defined by vascular smooth muscle and extracellular matrix markers.* Dev Biol, 1996. **178**(2): p. 375-92.
12. Mack, C.P. and G.K. Owens, *Regulation of smooth muscle alpha-actin expression in vivo is dependent on CArG elements within the 5' and first intron promoter regions.* Circ Res, 1999. **84**(7): p. 852-61.
13. Babij, P., C. Kelly, and M. Periasamy, *Characterization of a mammalian smooth muscle myosin heavy-chain gene: complete nucleotide and protein coding sequence and analysis of the 5' end of the gene.* Proc Natl Acad Sci U S A, 1991. **88**(23): p. 10676-80.
14. Madsen, C.S., et al., *Smooth muscle-specific expression of the smooth muscle myosin heavy chain gene in transgenic mice requires 5'-flanking and first intronic DNA sequence.* Circ Res, 1998. **82**(8): p. 908-17.
15. Miano, J.M., et al., *Smooth muscle myosin heavy chain exclusively marks the smooth muscle lineage during mouse embryogenesis.* Circ Res, 1994. **75**(5): p. 803-12.
16. Miano, J.M., et al., *Serum response factor-dependent regulation of the smooth muscle calponin gene.* J Biol Chem, 2000. **275**(13): p. 9814-22.

17. Duband, J.L., et al., *Calponin and SM 22 as differentiation markers of smooth muscle: spatiotemporal distribution during avian embryonic development.* Differentiation, 1993. **55**(1): p. 1-11.
18. Strasser, P., et al., *Mammalian calponin. Identification and expression of genetic variants.* FEBS Lett, 1993. **330**(1): p. 13-8.
19. Li, L., et al., *SM22 alpha, a marker of adult smooth muscle, is expressed in multiple myogenic lineages during embryogenesis.* Circ Res, 1996. **78**(2): p. 188-95.
20. Owens, G., *Regulation of differentiation of vascular smooth muscle cells.* Physiol. Rev., 1995. **75**(3): p. 487-517.
21. Woodcock-Mitchell, J., et al., *Alpha-smooth muscle actin is transiently expressed in embryonic rat cardiac and skeletal muscles.* Differentiation, 1988. **39**(3): p. 161-6.
22. Arciniegas, E., et al., *Transforming growth factor beta 1 promotes the differentiation of endothelial cells into smooth muscle-like cells in vitro.* J Cell Sci, 1992. **103 (Pt 2)**: p. 521-9.
23. Basson, C.T., et al., *Differential modulation of vascular cell integrin and extracellular matrix expression in vitro by TGF-beta 1 correlates with reciprocal effects on cell migration.* J Cell Physiol, 1992. **153**(1): p. 118-28.
24. Massagué, J., *TGFb signal transduction.* Annu. Rev. Biochem., 1998. **67**: p. 753-791.
25. Goumans, M.J., Z. Liu, and P. ten Dijke, *TGF-beta signaling in vascular biology and dysfunction.* Cell Res, 2009. **19**(1): p. 116-27.
26. Schmierer, B. and C.S. Hill, *TGFbeta-SMAD signal transduction: molecular specificity and functional flexibility.* Nat Rev Mol Cell Biol, 2007. **8**(12): p. 970-82.
27. Chen, D., M. Zhao, and G.R. Mundy, *Bone morphogenetic proteins.* Growth Factors, 2004. **22**(4): p. 233-41.
28. Lories, R.J., *Role of Transforming Growth Factor β and Bone Morphogenetic Protein Signaling in Fibroblast Activation in Chronic Rheumatic Diseases.* Adv Rheumatol, 2011. **9**(2): p. 39-44.
29. Massague, J., *TGFbeta in Cancer.* Cell, 2008. **134**(2): p. 215-30.
30. Massague, J. and Y.G. Chen, *Controlling TGF-beta signaling.* Genes Dev, 2000. **14**(6): p. 627-44.
31. Shi, Y. and J. Massague, *Mechanisms of TGF-beta signaling from cell membrane to the nucleus.* Cell, 2003. **113**(6): p. 685-700.
32. Massague, J., J. Seoane, and D. Wotton, *Smad transcription factors.* Genes Dev, 2005. **19**(23): p. 2783-810.
33. Feng, X.H. and R. Derynck, *Specificity and versatility in tgf-beta signaling through Smads.* Annu Rev Cell Dev Biol, 2005. **21**: p. 659-93.
34. Hata, A., et al., *OAZ uses distinct DNA- and protein-binding zinc fingers in separate BMP-Smad and Olf signaling pathways.* Cell, 2000. **100**(2): p. 229-40.
35. Ross, S. and C.S. Hill, *How the Smads regulate transcription.* Int J Biochem Cell Biol, 2008. **40**(3): p. 383-408.

36. Hautmann, M.B., C.S. Madsen, and G.K. Owens, *A transforming growth factor beta (TGFbeta) control element drives TGFbeta-induced stimulation of smooth muscle alpha-actin gene expression in concert with two CArG elements.* J Biol Chem, 1997. **272**(16): p. 10948-56.
37. Blobe, G.C., W.P. Schiemann, and H.F. Lodish, *Role of transforming growth factor beta in human disease.* N Engl J Med, 2000. **342**(18): p. 1350-8.
38. Lagna, G., et al., *Control of phenotypic plasticity of smooth muscle cells by bone morphogenetic protein signaling through the myocardin-related transcription factors.* J Biol Chem, 2007. **282**(51): p. 37244-55.
39. Adam, P.J., et al., *Positive- and negative-acting Kruppel-like transcription factors bind a transforming growth factor beta control element required for expression of the smooth muscle cell differentiation marker SM22alpha in vivo.* J Biol Chem, 2000. **275**(48): p. 37798-806.
40. Kawai-Kowase, K., et al., *PIAS1 mediates TGFbeta-induced SM alpha-actin gene expression through inhibition of KLF4 function-expression by protein sumoylation.* Arterioscler Thromb Vasc Biol, 2009. **29**(1): p. 99-106.
41. Parmacek, M.S., *Myocardin-related transcription factors: critical coactivators regulating cardiovascular development and adaptation.* Circ Res, 2007. **100**(5): p. 633-44.
42. Davis, B.N., et al., *SMAD proteins control DROSHA-mediated microRNA maturation.* Nature, 2008. **454**(7200): p. 56-61.
43. Davis-Dusenbery, B.N., et al., *down-regulation of Kruppel-like factor-4 (KLF4) by microRNA-143/145 is critical for modulation of vascular smooth muscle cell phenotype by transforming growth factor-beta and bone morphogenetic protein 4.* J Biol Chem, 2011. **286**(32): p. 28097-110.
44. Cordes, K.R., et al., *miR-145 and miR-143 regulate smooth muscle cell fate and plasticity.* Nature, 2009. **460**(7256): p. 705-10.
45. Deng, Z., et al., *Familial primary pulmonary hypertension (gene PPH1) is caused by mutations in the bone morphogenetic protein receptor-II gene.* Am J Hum Genet, 2000. **67**(3): p. 737-44.
46. Lane, K.B., et al., *Heterozygous germline mutations in BMPR2, encoding a TGF-beta receptor, cause familial primary pulmonary hypertension.* Nat Genet, 2000. **26**(1): p. 81-4.
47. Thomson, J.R., et al., *Sporadic primary pulmonary hypertension is associated with germline mutations of the gene encoding BMPR-II, a receptor member of the TGF-beta family.* J Med Genet, 2000. **37**(10): p. 741-5.
48. Morrell, N.W., et al., *Cellular and molecular basis of pulmonary arterial hypertension.* J Am Coll Cardiol, 2009. **54**(1 Suppl): p. S20-31.
49. Beppu, H., et al., *BMPR-II heterozygous mice have mild pulmonary hypertension and an impaired pulmonary vascular remodeling response to prolonged hypoxia.* Am J Physiol Lung Cell Mol Physiol, 2004. **287**(6): p. L1241-7.
50. Takahashi, H., et al., *Down-regulation of type II bone morphogenetic protein receptor in hypoxic pulmonary hypertension.* Am J Physiol Lung Cell Mol Physiol, 2005.

51. Morty, R.E., et al., *Dysregulated bone morphogenetic protein signaling in monocrotaline-induced pulmonary arterial hypertension.* Arterioscler Thromb Vasc Biol, 2007. **27**(5): p. 1072-8.
52. Pak, O., et al., *The effects of hypoxia on the cells of the pulmonary vasculature.* Eur Respir J, 2007. **30**(2): p. 364-72.
53. Rajkumar, R., et al., *Genomewide RNA expression profiling in lung identifies distinct signatures in idiopathic pulmonary arterial hypertension and secondary pulmonary hypertension.* Am J Physiol Heart Circ Physiol. **298**(4): p. H1235-48.
54. Tallquist, M. and A. Kazlauskas, *PDGF signaling in cells and mice.* Cytokine Growth Factor Rev, 2004. **15**(4): p. 205-13.
55. Matsui, T., et al., *Isolation of a novel receptor cDNA establishes the existence of two PDGF receptor genes.* Science, 1989. **243**(4892): p. 800-4.
56. Heldin, C.H. and A. Ostman, *Ligand-induced dimerization of growth factor receptors: variations on the theme.* Cytokine Growth Factor Rev, 1996. **7**(1): p. 3-10.
57. Andrae, J., R. Gallini, and C. Betsholtz, *Role of platelet-derived growth factors in physiology and medicine.* Genes Dev, 2008. **22**(10): p. 1276-312.
58. Lemmon, M.A. and J. Schlessinger, *Cell signaling by receptor tyrosine kinases.* Cell. **141**(7): p. 1117-34.
59. Madhani, H.D., *Accounting for specificity in receptor tyrosine kinase signaling.* Cell, 2001. **106**(1): p. 9-11.
60. Perros, F., et al., *Platelet-derived growth factor expression and function in idiopathic pulmonary arterial hypertension.* Am J Respir Crit Care Med, 2008. **178**(1): p. 81-8.
61. Schermuly, R.T., et al., *Reversal of experimental pulmonary hypertension by PDGF inhibition.* J Clin Invest, 2005. **115**(10): p. 2811-21.
62. Yu, Y., et al., *PDGF stimulates pulmonary vascular smooth muscle cell proliferation by upregulating TRPC6 expression.* Am J Physiol Cell Physiol, 2003. **284**(2): p. C316-30.
63. Holycross, B.J., et al., *Platelet-derived growth factor-BB-induced suppression of smooth muscle cell differentiation.* Circ Res, 1992. **71**(6): p. 1525-32.
64. Blank, R.S. and G.K. Owens, *Platelet-derived growth factor regulates actin isoform expression and growth state in cultured rat aortic smooth muscle cells.* J Cell Physiol, 1990. **142**(3): p. 635-42.
65. Kawai-Kowase, K. and G.K. Owens, *Multiple repressor pathways contribute to phenotypic switching of vascular smooth muscle cells.* Am J Physiol Cell Physiol, 2007. **292**(1): p. C59-69.
66. Davis, B.N., et al., *Induction of microRNA-221 by platelet-derived growth factor signaling is critical for modulation of vascular smooth muscle phenotype.* J Biol Chem, 2009. **284**(6): p. 3728-38.
67. Yu, K., et al., *ATRA activates and PDGF-BB represses the SM22alpha promoter through KLF4 binding to, or dissociating from, its cis-DNA elements.* Cardiovasc Res, 2011. **90**(3): p. 464-74.

68. Wamhoff, B.R., et al., *A G/C element mediates repression of the SM22alpha promoter within phenotypically modulated smooth muscle cells in experimental atherosclerosis.* Circ Res, 2004. **95**(10): p. 981-8.
69. Wang, D.Z., et al., *Potentiation of serum response factor activity by a family of myocardin-related transcription factors.* Proc Natl Acad Sci U S A, 2002. **99**(23): p. 14855-60.
70. Zhou, J., G. Hu, and B.P. Herring, *Smooth muscle-specific genes are differentially sensitive to inhibition by Elk-1.* Mol Cell Biol, 2005. **25**(22): p. 9874-85.
71. Yoshida, T., et al., *Platelet-derived growth factor-BB represses smooth muscle cell marker genes via changes in binding of MKL factors and histone deacetylases to their promoters.* Am J Physiol Cell Physiol, 2007. **292**(2): p. C886-95.
72. Doi, H., et al., *HERP1 inhibits myocardin-induced vascular smooth muscle cell differentiation by interfering with SRF binding to CArG box.* Arterioscler Thromb Vasc Biol, 2005. **25**(11): p. 2328-34.
73. Corjay, M.H., R.S. Blank, and G.K. Owens, *Platelet-derived growth factor-induced destabilization of smooth muscle alpha-actin mRNA.* J Cell Physiol, 1990. **145**(3): p. 391-7.
74. Grinnan, D.C., P. Fairman, and J. Pinson, *Recurrence of severe pulmonary hypertension following the removal of a lung allograft.* Chest, 2007. **132**(6): p. 2057-8; author reply 2058.
75. Humbert, M., O. Sitbon, and G. Simonneau, *Treatment of pulmonary arterial hypertension.* N Engl J Med, 2004. **351**(14): p. 1425-36.
76. Xu, X.Q. and Z.C. Jing, *High-altitude pulmonary hypertension.* Eur Respir Rev, 2009. **18**(111): p. 13-7.
77. Stenmark, K.R., et al., *Animal models of pulmonary arterial hypertension: the hope for etiological discovery and pharmacological cure.* Am J Physiol Lung Cell Mol Physiol, 2009. **297**(6): p. L1013-32.
78. Cooper, A.L. and D. Beasley, *Hypoxia stimulates proliferation and interleukin-1alpha production in human vascular smooth muscle cells.* Am J Physiol, 1999. **277**(4 Pt 2): p. H1326-37.
79. Ambalavanan, N., et al., *Role of nitric oxide in regulating neonatal porcine pulmonary artery smooth muscle cell proliferation.* Biol Neonate, 1999. **76**(5): p. 291-300.
80. Stotz, W.H., D. Li, and R.A. Johns, *Exogenous nitric oxide upregulates p21(waf1/cip1) in pulmonary microvascular smooth muscle cells.* J Vasc Res, 2004. **41**(3): p. 211-9.
81. Lu, S.Y., et al., *Inhibition of hypoxia-induced proliferation and collagen synthesis by vasonatrin peptide in cultured rat pulmonary artery smooth muscle cells.* Life Sci, 2005. **77**(1): p. 28-38.
82. Preston, I.R., et al., *Role of 12-lipoxygenase in hypoxia-induced rat pulmonary artery smooth muscle cell proliferation.* Am J Physiol Lung Cell Mol Physiol, 2006. **290**(2): p. L367-74.
83. Benitz, W.E., et al., *Hypoxia inhibits proliferation of fetal pulmonary arterial smooth muscle cells in vitro.* Pediatr Res, 1986. **20**(10): p. 966-72.

84. Eddahibi, S., et al., *Induction of serotonin transporter by hypoxia in pulmonary vascular smooth muscle cells. Relationship with the mitogenic action of serotonin.* Circ Res, 1999. **84**(3): p. 329-36.
85. Stiebellehner, L., et al., *Bovine distal pulmonary arterial media is composed of a uniform population of well-differentiated smooth muscle cells with low proliferative capabilities.* Am J Physiol Lung Cell Mol Physiol, 2003. **285**(4): p. L819-28.
86. Hassoun, P.M., et al., *Hypoxia stimulates the release by bovine pulmonary artery endothelial cells of an inhibitor of pulmonary artery smooth muscle cell growth.* Am J Respir Cell Mol Biol, 1989. **1**(5): p. 377-84.
87. Moudgil, R., E.D. Michelakis, and S.L. Archer, *Hypoxic pulmonary vasoconstriction.* J Appl Physiol, 2005. **98**(1): p. 390-403.
88. Platoshyn, O., et al., *Sustained membrane depolarization and pulmonary artery smooth muscle cell proliferation.* Am J Physiol Cell Physiol, 2000. **279**(5): p. C1540-9.
89. Remillard, C.V. and J.X. Yuan, *High altitude pulmonary hypertension: role of K+ and Ca2+ channels.* High Alt Med Biol, 2005. **6**(2): p. 133-46.
90. Kourembanas, S. and M. Bernfield, *Hypoxia and endothelial-smooth muscle cell interactions in the lung.* Am J Respir Cell Mol Biol, 1994. **11**(4): p. 373-4.
91. Sarkar, J., et al., *MicroRNA-21 plays a role in hypoxia-mediated pulmonary artery smooth muscle cell proliferation and migration.* Am J Physiol Lung Cell Mol Physiol, 2010. **299**(6): p. L861-71.
92. Chan, M.C., et al., *Molecular basis for antagonism between PDGF and the TGFbeta family of signalling pathways by control of miR-24 expression.* EMBO J, 2010. **29**(3): p. 559-73.
93. Caruso, P., et al., *Dynamic changes in lung microRNA profiles during the development of pulmonary hypertension due to chronic hypoxia and monocrotaline.* Arterioscler Thromb Vasc Biol, 2010. **30**(4): p. 716-23.
94. Parks, W.C., et al., *Response of lobar vessels to hypoxic pulmonary hypertension.* Am Rev Respir Dis, 1989. **140**(5): p. 1455-7.
95. Stenmark, K.R., K.A. Fagan, and M.G. Frid, *Hypoxia-induced pulmonary vascular remodeling: cellular and molecular mechanisms.* Circ Res, 2006. **99**(7): p. 675-91.
96. Koyama, H., et al., *Fibrillar collagen inhibits arterial smooth muscle proliferation through regulation of Cdk2 inhibitors.* Cell, 1996. **87**(6): p. 1069-78.
97. Hedin, U., et al., *Diverse effects of fibronectin and laminin on phenotypic properties of cultured arterial smooth muscle cells.* J Cell Biol, 1988. **107**(1): p. 307-19.
98. Newby, A.C. and S.J. George, *Proliferation, migration, matrix turnover, and death of smooth muscle cells in native coronary and vein graft atherosclerosis.* Curr Opin Cardiol, 1996. **11**(6): p. 574-82.
99. Myllyharju, J. and K.I. Kivirikko, *Collagens, modifying enzymes and their mutations in humans, flies and worms.* Trends Genet, 2004. **20**(1): p. 33-43.
100. Kivirikko, K.I. and J. Myllyharju, *Prolyl 4-hydroxylases and their protein disulfide isomerase subunit.* Matrix Biol, 1998. **16**(7): p. 357-68.

101. Siddiq, A., L.R. Aminova, and R.R. Ratan, *Hypoxia inducible factor prolyl 4-hydroxylase enzymes: center stage in the battle against hypoxia, metabolic compromise and oxidative stress.* Neurochem Res, 2007. **32**(4-5): p. 931-46.
102. Gunzler, V., et al., *Syncatalytic inactivation of prolyl 4-hydroxylase by synthetic peptides containing the unphysiologic amino acid 5-oxaproline.* J Biol Chem, 1988. **263**(36): p. 19498-504.
103. Clifton, I.J., et al., *Structural studies on 2-oxoglutarate oxygenases and related double-stranded beta-helix fold proteins.* J Inorg Biochem, 2006. **100**(4): p. 644-69.
104. Takahashi, Y., et al., *Hypoxic induction of prolyl 4-hydroxylase alpha (I) in cultured cells.* J Biol Chem, 2000. **275**(19): p. 14139-46.
105. Myllyharju, J., *Prolyl 4-hydroxylases, key enzymes in the synthesis of collagens and regulation of the response to hypoxia, and their roles as treatment targets.* Ann Med, 2008. **40**(6): p. 402-17.
106. Koivu, J., et al., *A single polypeptide acts both as the beta subunit of prolyl 4-hydroxylase and as a protein disulfide-isomerase.* J Biol Chem, 1987. **262**(14): p. 6447-9.
107. Pihlajaniemi, T., et al., *Molecular cloning of the beta-subunit of human prolyl 4-hydroxylase. This subunit and protein disulphide isomerase are products of the same gene.* Embo J, 1987. **6**(3): p. 643-9.
108. Bottomley, M.J., et al., *Quality control in the endoplasmic reticulum: PDI mediates the ER retention of unassembled procollagen C-propeptides.* Curr Biol, 2001. **11**(14): p. 1114-8.
109. Freedman, R.B., T.R. Hirst, and M.F. Tuite, *Protein disulphide isomerase: building bridges in protein folding.* Trends Biochem Sci, 1994. **19**(8): p. 331-6.
110. Helaakoski, T., et al., *Cloning, baculovirus expression, and characterization of a second mouse prolyl 4-hydroxylase alpha-subunit isoform: formation of an alpha 2 beta 2 tetramer with the protein disulfide-isomerase/beta subunit.* Proc Natl Acad Sci U S A, 1995. **92**(10): p. 4427-31.
111. Annunen, P., et al., *Cloning of the human prolyl 4-hydroxylase alpha subunit isoform alpha(II) and characterization of the type II enzyme tetramer. The alpha(I) and alpha(II) subunits do not form a mixed alpha(I)alpha(II)beta2 tetramer.* J Biol Chem, 1997. **272**(28): p. 17342-8.
112. Van Den Diepstraten, C., et al., *Cloning of a novel prolyl 4-hydroxylase subunit expressed in the fibrous cap of human atherosclerotic plaque.* Circulation, 2003. **108**(5): p. 508-11.
113. Kukkola, L., et al., *Identification and characterization of a third human, rat, and mouse collagen prolyl 4-hydroxylase isoenzyme.* J Biol Chem, 2003. **278**(48): p. 47685-93.
114. Annunen, P., H. Autio-Harmainen, and K.I. Kivirikko, *The novel type II prolyl 4-hydroxylase is the main enzyme form in chondrocytes and capillary endothelial cells, whereas the type I enzyme predominates in most cells.* J Biol Chem, 1998. **273**(11): p. 5989-92.

115. Nissi, R., et al., *Prolyl 4-hydroxylase isoenzymes I and II have different expression patterns in several human tissues.* J Histochem Cytochem, 2001. **49**(9): p. 1143-53.
116. Pelham, H.R., *The retention signal for soluble proteins of the endoplasmic reticulum.* Trends Biochem Sci, 1990. **15**(12): p. 483-6.
117. Vuori, K., et al., *Characterization of the human prolyl 4-hydroxylase tetramer and its multifunctional protein disulfide-isomerase subunit synthesized in a baculovirus expression system.* Proc Natl Acad Sci U S A, 1992. **89**(16): p. 7467-70.
118. John, D.C., M.E. Grant, and N.J. Bulleid, *Cell-free synthesis and assembly of prolyl 4-hydroxylase: the role of the beta-subunit (PDI) in preventing misfolding and aggregation of the alpha-subunit.* Embo J, 1993. **12**(4): p. 1587-95.
119. Qi, H.H., et al., *Prolyl 4-hydroxylation regulates Argonaute 2 stability.* Nature, 2008. **455**(7211): p. 421-4.
120. Hofbauer, K.H., et al., *Oxygen tension regulates the expression of a group of procollagen hydroxylases.* Eur J Biochem, 2003. **270**(22): p. 4515-22.
121. Fahling, M., et al., *Translational control of collagen prolyl 4-hydroxylase-alpha(I) gene expression under hypoxia.* J Biol Chem, 2006. **281**(36): p. 26089-101.
122. Chen, L., et al., *Human prolyl-4-hydroxylase alpha(I) transcription is mediated by upstream stimulatory factors.* J Biol Chem, 2006. **281**(16): p. 10849-55.
123. Levene, C.I. and C.J. Bates, *The effect of hypoxia on collagen synthesis in cultured 3T6 fibroblasts and its relationship to the mode of action of ascorbate.* Biochimica et Biophysica Acta (BBA) - General Subjects, 1976. **444**(2): p. 446-452.
124. Perhonen, M., et al., *Skeletal muscle collagen type I and III mRNA, [corrected] prolyl 4-hydroxylase, and collagen in hypobaric trained rats.* J Appl Physiol, 1996. **80**(6): p. 2226-33.
125. Kivirikko, K.I. and T. Pihlajaniemi, *Collagen hydroxylases and the protein disulfide isomerase subunit of prolyl 4-hydroxylases.* Adv Enzymol Relat Areas Mol Biol, 1998. **72**: p. 325-98.
126. Rocnik, E.F., B.M. Chan, and J.G. Pickering, *Evidence for a role of collagen synthesis in arterial smooth muscle cell migration.* J Clin Invest, 1998. **101**(9): p. 1889-98.
127. John, D.C., et al., *Expression of an engineered form of recombinant procollagen in mouse milk.* Nat Biotechnol, 1999. **17**(4): p. 385-9.
128. Gorospe, M., et al., *Post-Transcriptional Control of the Hypoxic Response by RNA-Binding Proteins and MicroRNAs.* Front Mol Neurosci, 2011. **4**: p. 7.
129. Lendahl, U., et al., *Generating specificity and diversity in the transcriptional response to hypoxia.* Nat Rev Genet, 2009. **10**(12): p. 821-32.
130. Harris, A.L., *Hypoxia--a key regulatory factor in tumour growth.* Nat Rev Cancer, 2002. **2**(1): p. 38-47.
131. Ema, M., et al., *A novel bHLH-PAS factor with close sequence similarity to hypoxia-inducible factor 1alpha regulates the VEGF expression and is potentially*

involved in lung and vascular development. Proc Natl Acad Sci U S A, 1997. **94**(9): p. 4273-8.
132. Gu, Y.Z., et al., *Molecular characterization and chromosomal localization of a third alpha-class hypoxia inducible factor subunit, HIF3alpha.* Gene Expr, 1998. **7**(3): p. 205-13.
133. Wang, G.L., et al., *Hypoxia-inducible factor 1 is a basic-helix-loop-helix-PAS heterodimer regulated by cellular O2 tension.* Proc Natl Acad Sci U S A, 1995. **92**(12): p. 5510-4.
134. Semenza, G.L., *Regulation of mammalian O2 homeostasis by hypoxia-inducible factor 1.* Annu Rev Cell Dev Biol, 1999. **15**: p. 551-78.
135. Kaelin, W.G., Jr., *The von Hippel-Lindau protein, HIF hydroxylation, and oxygen sensing.* Biochem Biophys Res Commun, 2005. **338**(1): p. 627-38.
136. Loboda, A., A. Jozkowicz, and J. Dulak, *HIF-1 and HIF-2 transcription factors--similar but not identical.* Mol Cells, 2010. **29**(5): p. 435-42.
137. Gordan, J.D., et al., *HIF-2alpha promotes hypoxic cell proliferation by enhancing c-myc transcriptional activity.* Cancer Cell, 2007. **11**(4): p. 335-47.
138. Weidemann, A. and R.S. Johnson, *Biology of HIF-1alpha.* Cell Death Differ, 2008. **15**(4): p. 621-7.
139. Bruick, R.K. and S.L. McKnight, *A conserved family of prolyl-4-hydroxylases that modify HIF.* Science, 2001. **294**(5545): p. 1337-40.
140. Epstein, A.C., et al., *C. elegans EGL-9 and mammalian homologs define a family of dioxygenases that regulate HIF by prolyl hydroxylation.* Cell, 2001. **107**(1): p. 43-54.
141. Appelhoff, R.J., et al., *Differential function of the prolyl hydroxylases PHD1, PHD2, and PHD3 in the regulation of hypoxia-inducible factor.* J Biol Chem, 2004. **279**(37): p. 38458-65.
142. Huang, J., et al., *Sequence determinants in hypoxia-inducible factor-1alpha for hydroxylation by the prolyl hydroxylases PHD1, PHD2, and PHD3.* J Biol Chem, 2002. **277**(42): p. 39792-800.
143. Tanimoto, K., et al., *Mechanism of regulation of the hypoxia-inducible factor-1 alpha by the von Hippel-Lindau tumor suppressor protein.* Embo J, 2000. **19**(16): p. 4298-309.
144. Ohh, M., et al., *Ubiquitination of hypoxia-inducible factor requires direct binding to the beta-domain of the von Hippel-Lindau protein.* Nat Cell Biol, 2000. **2**(7): p. 423-7.
145. Cockman, M.E., et al., *Hypoxia inducible factor-alpha binding and ubiquitylation by the von Hippel-Lindau tumor suppressor protein.* J Biol Chem, 2000. **275**(33): p. 25733-41.
146. Ivan, M., et al., *HIFalpha targeted for VHL-mediated destruction by proline hydroxylation: implications for O2 sensing.* Science, 2001. **292**(5516): p. 464-8.
147. Jaakkola, P., et al., *Targeting of HIF-alpha to the von Hippel-Lindau ubiquitylation complex by O2-regulated prolyl hydroxylation.* Science, 2001. **292**(5516): p. 468-72.
148. Loenarz, C., et al., *Evidence for a stereoelectronic effect in human oxygen sensing.* Angew Chem Int Ed Engl, 2009. **48**(10): p. 1784-7.

149. Hon, W.C., et al., *Structural basis for the recognition of hydroxyproline in HIF-1 alpha by pVHL.* Nature, 2002. **417**(6892): p. 975-8.
150. Min, J.H., et al., *Structure of an HIF-1alpha -pVHL complex: hydroxyproline recognition in signaling.* Science, 2002. **296**(5574): p. 1886-9.
151. Huang, L.E., et al., *Regulation of hypoxia-inducible factor 1alpha is mediated by an O2-dependent degradation domain via the ubiquitin-proteasome pathway.* Proc Natl Acad Sci U S A, 1998. **95**(14): p. 7987-92.
152. Kallio, P.J., et al., *Signal transduction in hypoxic cells: inducible nuclear translocation and recruitment of the CBP/p300 coactivator by the hypoxia-inducible factor-1alpha.* Embo J, 1998. **17**(22): p. 6573-86.
153. Hirsila, M., et al., *Characterization of the human prolyl 4-hydroxylases that modify the hypoxia-inducible factor.* J Biol Chem, 2003. **278**(33): p. 30772-80.
154. Wenger, R.H., D.P. Stiehl, and G. Camenisch, *Integration of oxygen signaling at the consensus HRE.* Sci STKE, 2005. **2005**(306): p. re12.
155. Huang, X., Q.T. Le, and A.J. Giaccia, *MiR-210--micromanager of the hypoxia pathway.* Trends Mol Med, 2010. **16**(5): p. 230-7.
156. Ruas, J.L., L. Poellinger, and T. Pereira, *Role of CBP in regulating HIF-1-mediated activation of transcription.* J Cell Sci, 2005. **118**(Pt 2): p. 301-11.
157. Carrero, P., et al., *Redox-regulated recruitment of the transcriptional coactivators CREB-binding protein and SRC-1 to hypoxia-inducible factor 1alpha.* Mol Cell Biol, 2000. **20**(1): p. 402-15.
158. Huang, L.E., et al., *Activation of hypoxia-inducible transcription factor depends primarily upon redox-sensitive stabilization of its alpha subunit.* J Biol Chem, 1996. **271**(50): p. 32253-9.
159. Ziel, K.A., et al., *Ref-1/Ape is critical for formation of the hypoxia-inducible transcriptional complex on the hypoxic response element of the rat pulmonary artery endothelial cell VEGF gene.* Faseb J, 2004. **18**(9): p. 986-8.
160. Chen, K.F., et al., *Transcriptional repression of human cad gene by hypoxia inducible factor-1alpha.* Nucleic Acids Res, 2005. **33**(16): p. 5190-8.
161. Mazure, N.M., et al., *Repression of alpha-fetoprotein gene expression under hypoxic conditions in human hepatoma cells: characterization of a negative hypoxia response element that mediates opposite effects of hypoxia inducible factor-1 and c-Myc.* Cancer Res, 2002. **62**(4): p. 1158-65.
162. Jiang, B.H., et al., *Dimerization, DNA binding, and transactivation properties of hypoxia-inducible factor 1.* J Biol Chem, 1996. **271**(30): p. 17771-8.
163. Ryan, H.E., J. Lo, and R.S. Johnson, *HIF-1 alpha is required for solid tumor formation and embryonic vascularization.* Embo J, 1998. **17**(11): p. 3005-15.
164. Carmeliet, P., et al., *Role of HIF-1alpha in hypoxia-mediated apoptosis, cell proliferation and tumour angiogenesis.* Nature, 1998. **394**(6692): p. 485-90.
165. Wood, S.M., et al., *Selection and analysis of a mutant cell line defective in the hypoxia-inducible factor-1 alpha-subunit (HIF-1alpha). Characterization of hif-1alpha-dependent and -independent hypoxia-inducible gene expression.* J Biol Chem, 1998. **273**(14): p. 8360-8.
166. Huang, X., et al., *Hypoxia-inducible mir-210 regulates normoxic gene expression involved in tumor initiation.* Mol Cell, 2009. **35**(6): p. 856-67.

167. Hua, Z., et al., *MiRNA-directed regulation of VEGF and other angiogenic factors under hypoxia.* PLoS One, 2006. **1**: p. e116.
168. Kulshreshtha, R., et al., *A microRNA signature of hypoxia.* Mol Cell Biol, 2007. **27**(5): p. 1859-67.
169. Camps, C., et al., *hsa-miR-210 Is induced by hypoxia and is an independent prognostic factor in breast cancer.* Clin Cancer Res, 2008. **14**(5): p. 1340-8.
170. Fasanaro, P., et al., *MicroRNA-210 modulates endothelial cell response to hypoxia and inhibits the receptor tyrosine kinase ligand Ephrin-A3.* J Biol Chem, 2008. **283**(23): p. 15878-83.
171. Giannakakis, A., et al., *miR-210 links hypoxia with cell cycle regulation and is deleted in human epithelial ovarian cancer.* Cancer Biol Ther, 2008. **7**(2): p. 255-64.
172. Pulkkinen, K., et al., *Hypoxia induces microRNA miR-210 in vitro and in vivo ephrin-A3 and neuronal pentraxin 1 are potentially regulated by miR-210.* FEBS Lett, 2008. **582**(16): p. 2397-401.
173. Zhang, Z., et al., *MicroRNA miR-210 modulates cellular response to hypoxia through the MYC antagonist MNT.* Cell Cycle, 2009. **8**(17): p. 2756-68.
174. Marx, J., *Cell biology. How cells endure low oxygen.* Science, 2004. **303**(5663): p. 1454-6.
175. Johnson, A.B. and M.C. Barton, *Hypoxia-induced and stress-specific changes in chromatin structure and function.* Mutat Res, 2007. **618**(1-2): p. 149-62.
176. Johnson, A.B., N. Denko, and M.C. Barton, *Hypoxia induces a novel signature of chromatin modifications and global repression of transcription.* Mutat Res, 2008. **640**(1-2): p. 174-9.
177. Kedersha, N. and P. Anderson, *Mammalian stress granules and processing bodies.* Methods Enzymol, 2007. **431**: p. 61-81.
178. Kedersha, N., et al., *Stress granules and processing bodies are dynamically linked sites of mRNP remodeling.* J Cell Biol, 2005. **169**(6): p. 871-84.
179. Anderson, P. and N. Kedersha, *Stress granules: the Tao of RNA triage.* Trends Biochem Sci, 2008. **33**(3): p. 141-50.
180. Moser, J.J. and M.J. Fritzler, *Cytoplasmic ribonucleoprotein (RNP) bodies and their relationship to GW/P bodies.* Int J Biochem Cell Biol. **42**(6): p. 828-43.
181. Parker, R. and U. Sheth, *P bodies and the control of mRNA translation and degradation.* Mol Cell, 2007. **25**(5): p. 635-46.
182. Liu, J., et al., *MicroRNA-dependent localization of targeted mRNAs to mammalian P-bodies.* Nat Cell Biol, 2005. **7**(7): p. 719-23.
183. Sen, G.L. and H.M. Blau, *Argonaute 2/RISC resides in sites of mammalian mRNA decay known as cytoplasmic bodies.* Nat Cell Biol, 2005. **7**(6): p. 633-6.
184. Sawicka, K., et al., *Polypyrimidine-tract-binding protein: a multifunctional RNA-binding protein.* Biochem Soc Trans, 2008. **36**(Pt 4): p. 641-7.
185. Guhaniyogi, J. and G. Brewer, *Regulation of mRNA stability in mammalian cells.* Gene, 2001. **265**(1-2): p. 11-23.
186. Wouters, B.G., et al., *Control of the hypoxic response through regulation of mRNA translation.* Semin Cell Dev Biol, 2005. **16**(4-5): p. 487-501.

187. Srivastava, S.P., K.U. Kumar, and R.J. Kaufman, *Phosphorylation of eukaryotic translation initiation factor 2 mediates apoptosis in response to activation of the double-stranded RNA-dependent protein kinase.* J Biol Chem, 1998. **273**(4): p. 2416-23.
188. Pillai, R.S., et al., *Inhibition of translational initiation by Let-7 MicroRNA in human cells.* Science, 2005. **309**(5740): p. 1573-6.
189. Humphreys, D.T., et al., *MicroRNAs control translation initiation by inhibiting eukaryotic initiation factor 4E/cap and poly(A) tail function.* Proc Natl Acad Sci U S A, 2005. **102**(47): p. 16961-6.
190. Petersen, C.P., et al., *Short RNAs repress translation after initiation in mammalian cells.* Mol Cell, 2006. **21**(4): p. 533-42.
191. Nottrott, S., M.J. Simard, and J.D. Richter, *Human let-7a miRNA blocks protein production on actively translating polyribosomes.* Nat Struct Mol Biol, 2006. **13**(12): p. 1108-14.
192. Bhattacharyya, S.N., et al., *Relief of microRNA-mediated translational repression in human cells subjected to stress.* Cell, 2006. **125**(6): p. 1111-24.
193. Gottschald, O.R., et al., *TIAR and TIA-1 mRNA-binding proteins co-aggregate under conditions of rapid oxygen decline and extreme hypoxia and suppress the HIF-1alpha pathway.* J Mol Cell Biol, 2010. **2**(6): p. 345-56.
194. Anderson, P. and N. Kedersha, *Stress granules.* Curr Biol, 2009. **19**(10): p. R397-8.
195. Gilks, N., et al., *Stress granule assembly is mediated by prion-like aggregation of TIA-1.* Mol Biol Cell, 2004. **15**(12): p. 5383-98.
196. Stoecklin, G., et al., *MK2-induced tristetraprolin:14-3-3 complexes prevent stress granule association and ARE-mRNA decay.* Embo J, 2004. **23**(6): p. 1313-24.
197. Tourriere, H., et al., *The RasGAP-associated endoribonuclease G3BP assembles stress granules.* J Cell Biol, 2003. **160**(6): p. 823-31.
198. Kedersha, N., et al., *Dynamic shuttling of TIA-1 accompanies the recruitment of mRNA to mammalian stress granules.* J Cell Biol, 2000. **151**(6): p. 1257-68.
199. Leung, A.K., J.M. Calabrese, and P.A. Sharp, *Quantitative analysis of Argonaute protein reveals microRNA-dependent localization to stress granules.* Proc Natl Acad Sci U S A, 2006. **103**(48): p. 18125-30.
200. Kim, V.N., J. Han, and M.C. Siomi, *Biogenesis of small RNAs in animals.* Nat Rev Mol Cell Biol, 2009. **10**(2): p. 126-39.
201. Lee, R.C., R.L. Feinbaum, and V. Ambros, *The C. elegans heterochronic gene lin-4 encodes small RNAs with antisense complementarity to lin-14.* Cell, 1993. **75**(5): p. 843-54.
202. Lee, Y.S. and A. Dutta, *MicroRNAs in cancer.* Annu Rev Pathol, 2009. **4**: p. 199-227.
203. Sempere, L.F., et al., *Expression profiling of mammalian microRNAs uncovers a subset of brain-expressed microRNAs with possible roles in murine and human neuronal differentiation.* Genome Biol, 2004. **5**(3): p. R13.
204. Shah, P.P., L.E. Hutchinson, and S.S. Kakar, *Emerging role of microRNAs in diagnosis and treatment of various diseases including ovarian cancer.* J Ovarian Res, 2009. **2**(1): p. 11.

205. Davis, B.N. and A. Hata, *Regulation of MicroRNA Biogenesis: A miRiad of mechanisms.* Cell Commun Signal, 2009. **7**: p. 18.
206. Rodriguez, A., et al., *Identification of mammalian microRNA host genes and transcription units.* Genome Res, 2004. **14**(10A): p. 1902-10.
207. Chhabra, R., et al., *Upregulation of miR-23a-27a-24-2 cluster induces caspase-dependent and -independent apoptosis in human embryonic kidney cells.* PLoS One, 2009. **4**(6): p. e5848.
208. Altuvia, Y., et al., *Clustering and conservation patterns of human microRNAs.* Nucleic Acids Res, 2005. **33**(8): p. 2697-706.
209. Baskerville, S. and D.P. Bartel, *Microarray profiling of microRNAs reveals frequent coexpression with neighboring miRNAs and host genes.* Rna, 2005. **11**(3): p. 241-7.
210. Borchert, G.M., W. Lanier, and B.L. Davidson, *RNA polymerase III transcribes human microRNAs.* Nat Struct Mol Biol, 2006. **13**(12): p. 1097-101.
211. Ozsolak, F., et al., *Chromatin structure analyses identify miRNA promoters.* Genes Dev, 2008. **22**(22): p. 3172-83.
212. Lee, Y., et al., *MicroRNA maturation: stepwise processing and subcellular localization.* EMBO J, 2002. **21**(17): p. 4663-70.
213. Cai, X., C.H. Hagedorn, and B.R. Cullen, *Human microRNAs are processed from capped, polyadenylated transcripts that can also function as mRNAs.* Rna, 2004. **10**(12): p. 1957-66.
214. O'Donnell, K.A., et al., *c-Myc-regulated microRNAs modulate E2F1 expression.* Nature, 2005. **435**(7043): p. 839-43.
215. Iliopoulos, D., H.A. Hirsch, and K. Struhl, *An epigenetic switch involving NF-kappaB, Lin28, Let-7 MicroRNA, and IL6 links inflammation to cell transformation.* Cell, 2009. **139**(4): p. 693-706.
216. Chang, T.C., et al., *Widespread microRNA repression by Myc contributes to tumorigenesis.* Nat Genet, 2008. **40**(1): p. 43-50.
217. Corcoran, D.L., et al., *Features of mammalian microRNA promoters emerge from polymerase II chromatin immunoprecipitation data.* PLoS One, 2009. **4**(4): p. e5279.
218. Krol, J., I. Loedige, and W. Filipowicz, *The widespread regulation of microRNA biogenesis, function and decay.* Nat Rev Genet, 2010. **11**(9): p. 597-610.
219. Winter, J., et al., *Many roads to maturity: microRNA biogenesis pathways and their regulation.* Nat Cell Biol, 2009. **11**(3): p. 228-34.
220. Han, J., et al., *The Drosha-DGCR8 complex in primary microRNA processing.* Genes Dev, 2004. **18**(24): p. 3016-27.
221. Wang, Y., et al., *DGCR8 is essential for microRNA biogenesis and silencing of embryonic stem cell self-renewal.* Nat Genet, 2007. **39**(3): p. 380-5.
222. Han, J., et al., *Molecular basis for the recognition of primary microRNAs by the Drosha-DGCR8 complex.* Cell, 2006. **125**(5): p. 887-901.
223. Zeng, Y., R. Yi, and B.R. Cullen, *Recognition and cleavage of primary microRNA precursors by the nuclear processing enzyme Drosha.* Embo J, 2005. **24**(1): p. 138-48.

224. Lee, Y., et al., *The nuclear RNase III Drosha initiates microRNA processing.* Nature, 2003. **425**(6956): p. 415-9.
225. Gregory, R.I., et al., *The Microprocessor complex mediates the genesis of microRNAs.* Nature, 2004. **432**(7014): p. 235-40.
226. Newman, M.A. and S.M. Hammond, *Emerging paradigms of regulated microRNA processing.* Genes Dev, 2010. **24**(11): p. 1086-92.
227. Yi, R., et al., *Exportin-5 mediates the nuclear export of pre-microRNAs and short hairpin RNAs.* Genes Dev, 2003. **17**(24): p. 3011-6.
228. Lund, E., et al., *Nuclear export of microRNA precursors.* Science, 2004. **303**(5654): p. 95-8.
229. Bohnsack, M.T., K. Czaplinski, and D. Gorlich, *Exportin 5 is a RanGTP-dependent dsRNA-binding protein that mediates nuclear export of pre-miRNAs.* RNA, 2004. **10**(2): p. 185-91.
230. Wang, X., et al., *Dynamic mechanisms for pre-miRNA binding and export by Exportin-5.* Rna, 2011. **17**(8): p. 1511-28.
231. Zeng, Y. and B.R. Cullen, *Structural requirements for pre-microRNA binding and nuclear export by Exportin 5.* Nucleic Acids Res, 2004. **32**(16): p. 4776-85.
232. Grishok, A., et al., *Genes and mechanisms related to RNA interference regulate expression of the small temporal RNAs that control C. elegans developmental timing.* Cell, 2001. **106**(1): p. 23-34.
233. Hutvagner, G., et al., *A cellular function for the RNA-interference enzyme Dicer in the maturation of the let-7 small temporal RNA.* Science, 2001. **293**(5531): p. 834-8.
234. Filippov, V., et al., *A novel type of RNase III family proteins in eukaryotes.* Gene, 2000. **245**(1): p. 213-21.
235. Wu, H., et al., *Human RNase III is a 160-kDa protein involved in preribosomal RNA processing.* J Biol Chem, 2000. **275**(47): p. 36957-65.
236. Fortin, K.R., R.H. Nicholson, and A.W. Nicholson, *Mouse ribonuclease III. cDNA structure, expression analysis, and chromosomal location.* BMC Genomics, 2002. **3**(1): p. 26.
237. MacRae, I.J. and J.A. Doudna, *Ribonuclease revisited: structural insights into ribonuclease III family enzymes.* Curr Opin Struct Biol, 2007. **17**(1): p. 138-45.
238. MacRae, I.J., K. Zhou, and J.A. Doudna, *Structural determinants of RNA recognition and cleavage by Dicer.* Nat Struct Mol Biol, 2007. **14**(10): p. 934-40.
239. Park, J.E., et al., *Dicer recognizes the 5' end of RNA for efficient and accurate processing.* Nature, 2011. **475**(7355): p. 201-5.
240. Cifuentes, D., et al., *A novel miRNA processing pathway independent of Dicer requires Argonaute2 catalytic activity.* Science, 2010. **328**(5986): p. 1694-8.
241. Cheloufi, S., et al., *A dicer-independent miRNA biogenesis pathway that requires Ago catalysis.* Nature, 2010. **465**(7298): p. 584-9.
242. Yang, J.S., et al., *Conserved vertebrate mir-451 provides a platform for Dicer-independent, Ago2-mediated microRNA biogenesis.* Proc Natl Acad Sci U S A, 2010. **107**(34): p. 15163-8.
243. Siolas, D., et al., *Synthetic shRNAs as potent RNAi triggers.* Nat Biotechnol, 2005. **23**(2): p. 227-31.

244. Haase, A.D., et al., *TRBP, a regulator of cellular PKR and HIV-1 virus expression, interacts with Dicer and functions in RNA silencing.* EMBO Rep, 2005. **6**(10): p. 961-7.
245. Chendrimada, T.P., et al., *TRBP recruits the Dicer complex to Ago2 for microRNA processing and gene silencing.* Nature, 2005. **436**(7051): p. 740-4.
246. Gregory, R.I., et al., *Human RISC couples microRNA biogenesis and posttranscriptional gene silencing.* Cell, 2005. **123**(4): p. 631-40.
247. Zhang, H., et al., *Single processing center models for human Dicer and bacterial RNase III.* Cell, 2004. **118**(1): p. 57-68.
248. Lee, Y., et al., *The role of PACT in the RNA silencing pathway.* Embo J, 2006. **25**(3): p. 522-32.
249. Maniataki, E. and Z. Mourelatos, *A human, ATP-independent, RISC assembly machine fueled by pre-miRNA.* Genes Dev, 2005. **19**(24): p. 2979-90.
250. MacRae, I.J., et al., *In vitro reconstitution of the human RISC-loading complex.* Proc Natl Acad Sci U S A, 2008. **105**(2): p. 512-7.
251. Preall, J.B. and E.J. Sontheimer, *RNAi: RISC gets loaded.* Cell, 2005. **123**(4): p. 543-5.
252. Iwasaki, S., et al., *Hsc70/Hsp90 chaperone machinery mediates ATP-dependent RISC loading of small RNA duplexes.* Mol Cell, 2010. **39**(2): p. 292-9.
253. Ma, J.B., et al., *Structural basis for 5'-end-specific recognition of guide RNA by the A. fulgidus Piwi protein.* Nature, 2005. **434**(7033): p. 666-70.
254. Parker, J.S., S.M. Roe, and D. Barford, *Structural insights into mRNA recognition from a PIWI domain-siRNA guide complex.* Nature, 2005. **434**(7033): p. 663-6.
255. Wang, Y., et al., *Structure of the guide-strand-containing argonaute silencing complex.* Nature, 2008. **456**(7219): p. 209-13.
256. Wang, Y., et al., *Structure of an argonaute silencing complex with a seed-containing guide DNA and target RNA duplex.* Nature, 2008. **456**(7224): p. 921-6.
257. Wang, Y., et al., *Nucleation, propagation and cleavage of target RNAs in Ago silencing complexes.* Nature, 2009. **461**(7265): p. 754-61.
258. Matranga, C., et al., *Passenger-strand cleavage facilitates assembly of siRNA into Ago2-containing RNAi enzyme complexes.* Cell, 2005. **123**(4): p. 607-20.
259. Miyoshi, K., et al., *Slicer function of Drosophila Argonautes and its involvement in RISC formation.* Genes Dev, 2005. **19**(23): p. 2837-48.
260. Leuschner, P.J., et al., *Cleavage of the siRNA passenger strand during RISC assembly in human cells.* EMBO Rep, 2006. **7**(3): p. 314-20.
261. Diederichs, S. and D.A. Haber, *Dual role for argonautes in microRNA processing and posttranscriptional regulation of microRNA expression.* Cell, 2007. **131**(6): p. 1097-108.
262. Czech, B. and G.J. Hannon, *Small RNA sorting: matchmaking for Argonautes.* Nat Rev Genet. **12**(1): p. 19-31.
263. Yigit, E., et al., *Analysis of the C. elegans Argonaute family reveals that distinct Argonautes act sequentially during RNAi.* Cell, 2006. **127**(4): p. 747-57.
264. Tolia, N.H. and L. Joshua-Tor, *Slicer and the argonautes.* Nat Chem Biol, 2007. **3**(1): p. 36-43.

265. Hutvagner, G. and M.J. Simard, *Argonaute proteins: key players in RNA silencing.* Nat Rev Mol Cell Biol, 2008. **9**(1): p. 22-32.
266. Peters, L. and G. Meister, *Argonaute proteins: mediators of RNA silencing.* Mol Cell, 2007. **26**(5): p. 611-23.
267. Seto, A.G., R.E. Kingston, and N.C. Lau, *The coming of age for Piwi proteins.* Mol Cell, 2007. **26**(5): p. 603-9.
268. Ender, C. and G. Meister, *Argonaute proteins at a glance.* J Cell Sci, 2010. **123**(Pt 11): p. 1819-23.
269. Ma, J.B., K. Ye, and D.J. Patel, *Structural basis for overhang-specific small interfering RNA recognition by the PAZ domain.* Nature, 2004. **429**(6989): p. 318-22.
270. Lingel, A., et al., *Nucleic acid 3'-end recognition by the Argonaute2 PAZ domain.* Nat Struct Mol Biol, 2004. **11**(6): p. 576-7.
271. Song, J.J., et al., *Crystal structure of Argonaute and its implications for RISC slicer activity.* Science, 2004. **305**(5689): p. 1434-7.
272. Jinek, M. and J.A. Doudna, *A three-dimensional view of the molecular machinery of RNA interference.* Nature, 2009. **457**(7228): p. 405-12.
273. Liu, J., et al., *Argonaute2 is the catalytic engine of mammalian RNAi.* Science, 2004. **305**(5689): p. 1437-41.
274. Brodersen, P. and O. Voinnet, *Revisiting the principles of microRNA target recognition and mode of action.* Nat Rev Mol Cell Biol, 2009. **10**(2): p. 141-8.
275. Lytle, J.R., T.A. Yario, and J.A. Steitz, *Target mRNAs are repressed as efficiently by microRNA-binding sites in the 5' UTR as in the 3' UTR.* Proc Natl Acad Sci U S A, 2007. **104**(23): p. 9667-72.
276. Forman, J.J., A. Legesse-Miller, and H.A. Coller, *A search for conserved sequences in coding regions reveals that the let-7 microRNA targets Dicer within its coding sequence.* Proc Natl Acad Sci U S A, 2008. **105**(39): p. 14879-84.
277. Bartel, D.P., *MicroRNAs: target recognition and regulatory functions.* Cell, 2009. **136**(2): p. 215-33.
278. Selbach, M., et al., *Widespread changes in protein synthesis induced by microRNAs.* Nature, 2008. **455**(7209): p. 58-63.
279. Lim, L.P., et al., *Microarray analysis shows that some microRNAs downregulate large numbers of target mRNAs.* Nature, 2005. **433**(7027): p. 769-73.
280. Baek, D., et al., *The impact of microRNAs on protein output.* Nature, 2008. **455**(7209): p. 64-71.
281. Eulalio, A., E. Huntzinger, and E. Izaurralde, *Getting to the root of miRNA-mediated gene silencing.* Cell, 2008. **132**(1): p. 9-14.
282. Kiriakidou, M., et al., *An mRNA m7G cap binding-like motif within human Ago2 represses translation.* Cell, 2007. **129**(6): p. 1141-51.
283. Chendrimada, T.P., et al., *MicroRNA silencing through RISC recruitment of eIF6.* Nature, 2007. **447**(7146): p. 823-8.
284. Behm-Ansmant, I., et al., *mRNA degradation by miRNAs and GW182 requires both CCR4:NOT deadenylase and DCP1:DCP2 decapping complexes.* Genes Dev, 2006. **20**(14): p. 1885-98.

285. Eulalio, A., et al., *Target-specific requirements for enhancers of decapping in miRNA-mediated gene silencing.* Genes Dev, 2007. **21**(20): p. 2558-70.
286. Vasudevan, S., Y. Tong, and J.A. Steitz, *Switching from repression to activation: microRNAs can up-regulate translation.* Science, 2007. **318**(5858): p. 1931-4.
287. Vasudevan, S. and J.A. Steitz, *AU-rich-element-mediated upregulation of translation by FXR1 and Argonaute 2.* Cell, 2007. **128**(6): p. 1105-18.
288. Davis, N.B., et al., *Smad proteins bind a conserved RNA sequence to promote microRNA maturation by Drosha.* Mol Cell, 2010. **39**: p. 373-384.
289. Suzuki, H.I., et al., *Modulation of microRNA processing by p53.* Nature, 2009. **460**(7254): p. 529-33.
290. Yamagata, K., et al., *Maturation of MicroRNA Is Hormonally Regulated by a Nuclear Receptor.* Mol Cell, 2009. **36**(2): p. 340-7.
291. Heo, I. and V.N. Kim, *Regulating the regulators: posttranslational modifications of RNA silencing factors.* Cell, 2009. **139**(1): p. 28-31.
292. Paroo, Z., et al., *Phosphorylation of the human microRNA-generating complex mediates MAPK/Erk signaling.* Cell, 2009. **139**(1): p. 112-22.
293. Zeng, Y., et al., *Phosphorylation of Argonaute 2 at serine-387 facilitates its localization to processing bodies.* Biochem J, 2008. **413**(3): p. 429-36.
294. Mittelstadt, P.R., et al., *Activating p38 MAPK: new tricks for an old kinase.* Cell Cycle, 2005. **4**(9): p. 1189-92.
295. Keren, A., Y. Tamir, and E. Bengal, *The p38 MAPK signaling pathway: a major regulator of skeletal muscle development.* Mol Cell Endocrinol, 2006. **252**(1-2): p. 224-30.
296. Rudel, S., et al., *Phosphorylation of human Argonaute proteins affects small RNA binding.* Nucleic Acids Res, 2011. **39**(6): p. 2330-43.
297. Rybak, A., et al., *The let-7 target gene mouse lin-41 is a stem cell specific E3 ubiquitin ligase for the miRNA pathway protein Ago2.* Nat Cell Biol, 2009. **11**(12): p. 1411-20.
298. Slack, F.J., et al., *The lin-41 RBCC gene acts in the C. elegans heterochronic pathway between the let-7 regulatory RNA and the LIN-29 transcription factor.* Mol Cell, 2000. **5**(4): p. 659-69.
299. Meroni, G. and G. Diez-Roux, *TRIM/RBCC, a novel class of 'single protein RING finger' E3 ubiquitin ligases.* Bioessays, 2005. **27**(11): p. 1147-57.
300. Leung, A.K., et al., *Poly(ADP-ribose) regulates stress responses and microRNA activity in the cytoplasm.* Mol Cell, 2011. **42**(4): p. 489-99.
301. Devalaraja-Narashimha, K. and B.J. Padanilam, *PARP-1 inhibits glycolysis in ischemic kidneys.* J Am Soc Nephrol, 2009. **20**(1): p. 95-103.
302. van Rooij, E. and E.N. Olson, *MicroRNAs: powerful new regulators of heart disease and provocative therapeutic targets.* J Clin Invest, 2007. **117**(9): p. 2369-76.
303. Kloosterman, W.P. and R.H. Plasterk, *The diverse functions of microRNAs in animal development and disease.* Dev Cell, 2006. **11**(4): p. 441-50.
304. Preiss, T. and M.W. Hentze, *From factors to mechanisms: translation and translational control in eukaryotes.* Curr Opin Genet Dev, 1999. **9**(5): p. 515-21.

305. Tanaka, S., T. Uehara, and Y. Nomura, *Up-regulation of protein-disulfide isomerase in response to hypoxia/brain ischemia and its protective effect against apoptotic cell death.* J Biol Chem, 2000. **275**(14): p. 10388-93.
306. Kulshreshtha, R., et al., *A microRNA component of the hypoxic response.* Cell Death Differ, 2008. **15**(4): p. 667-71.
307. Winter, J. and S. Diederichs, *Argonaute proteins regulate microRNA stability: Increased microRNA abundance by Argonaute proteins is due to microRNA stabilization.* RNA Biol, 2011. **8**(6).
308. Donker, R.B., et al., *The expression of Argonaute2 and related microRNA biogenesis proteins in normal and hypoxic trophoblasts.* Mol Hum Reprod, 2007. **13**(4): p. 273-9.
309. Kallio, P.J., et al., *Activation of hypoxia-inducible factor 1alpha: posttranscriptional regulation and conformational change by recruitment of the Arnt transcription factor.* Proc Natl Acad Sci U S A, 1997. **94**(11): p. 5667-72.
310. Salceda, S. and J. Caro, *Hypoxia-inducible factor 1alpha (HIF-1alpha) protein is rapidly degraded by the ubiquitin-proteasome system under normoxic conditions. Its stabilization by hypoxia depends on redox-induced changes.* J Biol Chem, 1997. **272**(36): p. 22642-7.
311. Kallio, P.J., et al., *Regulation of the hypoxia-inducible transcription factor 1alpha by the ubiquitin-proteasome pathway.* J Biol Chem, 1999. **274**(10): p. 6519-25.
312. Doench, J.G., C.P. Petersen, and P.A. Sharp, *siRNAs can function as miRNAs.* Genes Dev, 2003. **17**(4): p. 438-42.
313. Taipale, M., D.F. Jarosz, and S. Lindquist, *HSP90 at the hub of protein homeostasis: emerging mechanistic insights.* Nat Rev Mol Cell Biol, 2010. **11**(7): p. 515-28.
314. Borkovich, K.A., et al., *hsp82 is an essential protein that is required in higher concentrations for growth of cells at higher temperatures.* Mol Cell Biol, 1989. **9**(9): p. 3919-30.
315. Hartl, F.U. and M. Hayer-Hartl, *Converging concepts of protein folding in vitro and in vivo.* Nat Struct Mol Biol, 2009. **16**(6): p. 574-81.
316. Schneider, C., et al., *Pharmacologic shifting of a balance between protein refolding and degradation mediated by Hsp90.* Proc Natl Acad Sci U S A, 1996. **93**(25): p. 14536-41.
317. McClellan, A.J., M.D. Scott, and J. Frydman, *Folding and quality control of the VHL tumor suppressor proceed through distinct chaperone pathways.* Cell, 2005. **121**(5): p. 739-48.
318. McClellan, A.J., et al., *Protein quality control: chaperones culling corrupt conformations.* Nat Cell Biol, 2005. **7**(8): p. 736-41.
319. Connell, P., et al., *The co-chaperone CHIP regulates protein triage decisions mediated by heat-shock proteins.* Nat Cell Biol, 2001. **3**(1): p. 93-6.
320. Xu, W., et al., *Chaperone-dependent E3 ubiquitin ligase CHIP mediates a degradative pathway for c-ErbB2/Neu.* Proc Natl Acad Sci U S A, 2002. **99**(20): p. 12847-52.

321. Young, J.C., N.J. Hoogenraad, and F.U. Hartl, *Molecular chaperones Hsp90 and Hsp70 deliver preproteins to the mitochondrial import receptor Tom70.* Cell, 2003. **112**(1): p. 41-50.
322. Tahbaz, N., J.B. Carmichael, and T.C. Hobman, *GERp95 belongs to a family of signal-transducing proteins and requires Hsp90 activity for stability and Golgi localization.* J Biol Chem, 2001. **276**(46): p. 43294-9.
323. Johnston, M., et al., *HSP90 protein stabilizes unloaded argonaute complexes and microscopic P-bodies in human cells.* Mol Biol Cell, 2010. **21**(9): p. 1462-9.
324. Pare, J.M., et al., *Hsp90 regulates the function of argonaute 2 and its recruitment to stress granules and P-bodies.* Mol Biol Cell, 2009. **20**(14): p. 3273-84.
325. McDonald, E., P. Workman, and K. Jones, *Inhibitors of the HSP90 molecular chaperone: attacking the master regulator in cancer.* Curr Top Med Chem, 2006. **6**(11): p. 1091-107.
326. Leu, J.I., et al., *A small molecule inhibitor of inducible heat shock protein 70.* Mol Cell, 2009. **36**(1): p. 15-27.
327. Kamal, A., et al., *A high-affinity conformation of Hsp90 confers tumour selectivity on Hsp90 inhibitors.* Nature, 2003. **425**(6956): p. 407-10.
328. Cheng, Y. and C. Zhang, *MicroRNA-21 in cardiovascular disease.* J Cardiovasc Transl Res, 2010. **3**(3): p. 251-5.
329. Panaretou, B., et al., *ATP binding and hydrolysis are essential to the function of the Hsp90 molecular chaperone in vivo.* Embo J, 1998. **17**(16): p. 4829-36.
330. Shu, C.W., et al., *Transactivation of hsp70-1/2 in geldanamycin-treated human non-small cell lung cancer H460 cells: involvement of intracellular calcium and protein kinase C.* J Cell Biochem, 2005. **94**(6): p. 1199-209.
331. Minet, E., et al., *Hypoxia-induced activation of HIF-1: role of HIF-1alpha-Hsp90 interaction.* FEBS Lett, 1999. **460**(2): p. 251-6.
332. Pothof, J., et al., *MicroRNA-mediated gene silencing modulates the UV-induced DNA-damage response.* EMBO J, 2009. **28**(14): p. 2090-9.
333. Kedersha, N.L., et al., *RNA-binding proteins TIA-1 and TIAR link the phosphorylation of eIF-2 alpha to the assembly of mammalian stress granules.* J Cell Biol, 1999. **147**(7): p. 1431-42.
334. Gardner, L.B., *Hypoxic inhibition of nonsense-mediated RNA decay regulates gene expression and the integrated stress response.* Mol Cell Biol, 2008. **28**(11): p. 3729-41.
335. McEwen, E., et al., *Heme-regulated inhibitor kinase-mediated phosphorylation of eukaryotic translation initiation factor 2 inhibits translation, induces stress granule formation, and mediates survival upon arsenite exposure.* J Biol Chem, 2005. **280**(17): p. 16925-33.
336. Mazroui, R., et al., *Inhibition of ribosome recruitment induces stress granule formation independently of eukaryotic initiation factor 2alpha phosphorylation.* Mol Biol Cell, 2006. **17**(10): p. 4212-9.
337. Bordeleau, M.E., et al., *Stimulation of mammalian translation initiation factor eIF4A activity by a small molecule inhibitor of eukaryotic translation.* Proc Natl Acad Sci U S A, 2005. **102**(30): p. 10460-5.

338. Tahbaz, N., et al., *Characterization of the interactions between mammalian PAZ PIWI domain proteins and Dicer.* EMBO Rep, 2004. **5**(2): p. 189-94.
339. Bommer, G.T., et al., *p53-mediated activation of miRNA34 candidate tumor-suppressor genes.* Curr Biol, 2007. **17**(15): p. 1298-307.
340. Chang, T.C., et al., *Transactivation of miR-34a by p53 broadly influences gene expression and promotes apoptosis.* Mol Cell, 2007. **26**(5): p. 745-52.
341. He, L., et al., *A microRNA component of the p53 tumour suppressor network.* Nature, 2007. **447**(7148): p. 1130-4.
342. Raver-Shapira, N., et al., *Transcriptional activation of miR-34a contributes to p53-mediated apoptosis.* Mol Cell, 2007. **26**(5): p. 731-43.
343. Tarasov, V., et al., *Differential regulation of microRNAs by p53 revealed by massively parallel sequencing: miR-34a is a p53 target that induces apoptosis and G1-arrest.* Cell Cycle, 2007. **6**(13): p. 1586-93.
344. Martin, D.W., Jr. and N.T. Owen, *Repression and derepression of purine biosynthesis in mammalian hepatoma cells in culture.* J Biol Chem, 1972. **247**(17): p. 5477-85.
345. van Rooij, E., et al., *Control of stress-dependent cardiac growth and gene expression by a microRNA.* Science, 2007. **316**(5824): p. 575-9.
346. Leung, A.K. and P.A. Sharp, *microRNAs: a safeguard against turmoil?* Cell, 2007. **130**(4): p. 581-5.
347. Hebert, C., et al., *High mobility group A2 is a target for miRNA-98 in head and neck squamous cell carcinoma.* Mol Cancer, 2007. **6**: p. 5.
348. Muth, M., et al., *"Hypoxia-induced down-regulation of microRNA-449a/b impairs control over targeted SERPINE1 (PAI-1) mRNA - a mechanism involved in SERPINE1 (PAI-1) overexpression".* J Transl Med, 2010. **8**: p. 33.
349. Cutroneo, K.R., *How is Type I procollagen synthesis regulated at the gene level during tissue fibrosis.* J Cell Biochem, 2003. **90**(1): p. 1-5.
350. Imai, Y., et al., *Analysis of proteoglycan synthesis by retro-ocular tissue fibroblasts under the influence of interleukin 1 beta and transforming growth factor-beta.* Eur J Endocrinol, 1994. **131**(6): p. 630-8.
351. Kuang, P.P., et al., *Fibulin-5 gene expression in human lung fibroblasts is regulated by TGF-beta and phosphatidylinositol 3-kinase activity.* Am J Physiol Cell Physiol, 2006. **291**(6): p. C1412-21.
352. King, S.L., et al., *Bleomycin stimulates pro-alpha 1 (I) collagen promoter through transforming growth factor beta response element by intracellular and extracellular signaling.* J Biol Chem, 1994. **269**(18): p. 13156-61.
353. Cutroneo, K.R., *Human SP1 but not human AP1 binding to the TGF-beta element in the 5' flanking region of the rat PROalpha1(I) collagen gene.* Mol Biol Rep, 2000. **27**(3): p. 191-4.
354. Atchley, W.R. and W.M. Fitch, *A natural classification of the basic helix-loop-helix class of transcription factors.* Proc Natl Acad Sci U S A, 1997. **94**(10): p. 5172-6.
355. Baxevanis, A.D. and C.R. Vinson, *Interactions of coiled coils in transcription factors: where is the specificity?* Curr Opin Genet Dev, 1993. **3**(2): p. 278-85.

356. Sha, M., et al., *Anti-cooperative biphasic equilibrium binding of transcription factor upstream stimulatory factor to its cognate DNA monitored by protein fluorescence changes.* J Biol Chem, 1995. **270**(33): p. 19325-9.
357. Corre, S. and M.D. Galibert, *Upstream stimulating factors: highly versatile stress-responsive transcription factors.* Pigment Cell Res, 2005. **18**(5): p. 337-48.
358. Harris, A.N. and P.L. Mellon, *The basic helix-loop-helix, leucine zipper transcription factor, USF (upstream stimulatory factor), is a key regulator of SF-1 (steroidogenic factor-1) gene expression in pituitary gonadotrope and steroidogenic cells.* Mol Endocrinol, 1998. **12**(5): p. 714-26.
359. Bengtsson, S.H., et al., *Transcriptional regulation of the human carboxyl ester lipase gene in THP-1 monocytes: an E-box required for activation binds upstream stimulatory factors 1 and 2.* Biochem J, 2002. **365**(Pt 2): p. 481-8.
360. Gao, E., et al., *The basic helix-loop-helix-zipper transcription factor USF1 regulates expression of the surfactant protein-A gene.* J Biol Chem, 1997. **272**(37): p. 23398-406.
361. Gao, E., et al., *Transcription factor USF2 is developmentally regulated in fetal lung and acts together with USF1 to induce SP-A gene expression.* Am J Physiol Lung Cell Mol Physiol, 2003. **284**(6): p. L1027-36.
362. Koslowski, R., et al., *Evidence for the involvement of TGF-beta and PDGF in the regulation of prolyl 4-hydroxylase and lysyloxidase in cultured rat lung fibroblasts.* Exp Toxicol Pathol, 2003. **55**(4): p. 257-64.
363. Davis, B.N., et al., *Smad proteins bind a conserved RNA sequence to promote microRNA maturation by Drosha.* Mol Cell, 2010. **39**(3): p. 373-84.
364. Adams, B.D., K.P. Claffey, and B.A. White, *Argonaute-2 expression is regulated by epidermal growth factor receptor and mitogen-activated protein kinase signaling and correlates with a transformed phenotype in breast cancer cells.* Endocrinology, 2009. **150**(1): p. 14-23.
365. Rebouche, C.J., *Ascorbic acid and carnitine biosynthesis.* Am J Clin Nutr, 1991. **54**(6 Suppl): p. 1147S-1152S.
366. Levine, M., et al., *Ascorbic acid and reaction kinetics in situ: a new approach to vitamin requirements.* J Nutr Sci Vitaminol (Tokyo), 1992. **Spec No**: p. 169-72.
367. Englard, S. and S. Seifter, *The biochemical functions of ascorbic acid.* Annu Rev Nutr, 1986. **6**: p. 365-406.
368. Farber, H.W. and J. Loscalzo, *Pulmonary arterial hypertension.* N Engl J Med, 2004. **351**(16): p. 1655-65.
369. Weissmann, N., et al., *Oxygen sensors in hypoxic pulmonary vasoconstriction.* Cardiovasc Res, 2006. **71**(4): p. 620-9.
370. Liu, Y.V., et al., *RACK1 competes with HSP90 for binding to HIF-1alpha and is required for O(2)-independent and HSP90 inhibitor-induced degradation of HIF-1alpha.* Mol Cell, 2007. **25**(2): p. 207-17.
371. Isaacs, J.S., et al., *Hsp90 regulates a von Hippel Lindau-independent hypoxia-inducible factor-1 alpha-degradative pathway.* J Biol Chem, 2002. **277**(33): p. 29936-44.

372. Mabjeesh, N.J., et al., *Geldanamycin induces degradation of hypoxia-inducible factor 1alpha protein via the proteosome pathway in prostate cancer cells.* Cancer Res, 2002. **62**(9): p. 2478-82.
373. Ceci, M., et al., *Release of eIF6 (p27BBP) from the 60S subunit allows 80S ribosome assembly.* Nature, 2003. **426**(6966): p. 579-84.
374. Hermanto, U., et al., *RACK1, an insulin-like growth factor I (IGF-I) receptor-interacting protein, modulates IGF-I-dependent integrin signaling and promotes cell spreading and contact with extracellular matrix.* Mol Cell Biol, 2002. **22**(7): p. 2345-65.
375. Cox, E.A., et al., *RACK1 regulates integrin-mediated adhesion, protrusion, and chemotactic cell migration via its Src-binding site.* Mol Biol Cell, 2003. **14**(2): p. 658-69.
376. Nilsson, J., et al., *Regulation of eukaryotic translation by the RACK1 protein: a platform for signalling molecules on the ribosome.* EMBO Rep, 2004. **5**(12): p. 1137-41.
377. Rodriguez, M.M., et al., *RACK1, a protein kinase C anchoring protein, coordinates the binding of activated protein kinase C and select pleckstrin homology domains in vitro.* Biochemistry, 1999. **38**(42): p. 13787-94.
378. McCahill, A., et al., *The RACK1 scaffold protein: a dynamic cog in cell response mechanisms.* Mol Pharmacol, 2002. **62**(6): p. 1261-73.
379. Jannot, G., et al., *The ribosomal protein RACK1 is required for microRNA function in both C. elegans and humans.* EMBO Rep, 2011. **12**(6): p. 581-6.
380. Pare, J.M., J. Lopez-Orozco, and T.C. Hobman, *MicroRNA-binding is required for recruitment of human Argonaute 2 to stress granules and P-bodies.* Biochem Biophys Res Commun, 2011.
381. Peng, Y., X. Liu, and D.R. Schoenberg, *The 90-kDa heat shock protein stabilizes the polysomal ribonuclease 1 mRNA endonuclease to degradation by the 26S proteasome.* Mol Biol Cell, 2008. **19**(2): p. 546-52.
382. Dompenciel, R.E., V.R. Garnepudi, and D.R. Schoenberg, *Purification and characterization of an estrogen-regulated Xenopus liver polysomal nuclease involved in the selective destabilization of albumin mRNA.* J Biol Chem, 1995. **270**(11): p. 6108-18.
383. Yang, F., et al., *Polysome-bound endonuclease PMR1 is targeted to stress granules via stress-specific binding to TIA-1.* Mol Cell Biol, 2006. **26**(23): p. 8803-13.
384. Semenza, G.L., *Regulation of oxygen homeostasis by hypoxia-inducible factor 1.* Physiology (Bethesda), 2009. **24**: p. 97-106.
385. Eltzschig, H.K., et al., *HIF-1-dependent repression of equilibrative nucleoside transporter (ENT) in hypoxia.* J Exp Med, 2005. **202**(11): p. 1493-505.
386. Martello, G., et al., *A MicroRNA targeting dicer for metastasis control.* Cell, 2010. **141**(7): p. 1195-207.
387. Rose, N.R., et al., *Inhibition of 2-oxoglutarate dependent oxygenases.* Chem Soc Rev, 2011. **40**(8): p. 4364-97.
388. Naeije, R. and B. Rondelet, *Pathobiology of pulmonary arterial hypertension.* Bull Mem Acad R Med Belg, 2004. **159**(Pt 2): p. 219-26.

389. Wu, C., et al., *Hypoxia potentiates microRNA-mediated gene silencing through post-translational modification of Argonaute2.* Mol Cell Biol, 2011.

MOLECULAR AND CELLULAR BIOLOGY, Dec. 2011, p. 4760–4774 Vol. 31, No. 23
0270-7306/11/$12.00 doi:10.1128/MCB.05776-11

Hypoxia Potentiates MicroRNA-Mediated Gene Silencing through Posttranslational Modification of Argonaute2▽

Connie Wu,[1] Jessica So,[2] Brandi N. Davis-Dusenbery,[2] Hank H. Qi,[3,4,5] Donald B. Bloch,[6] Yang Shi,[3,4] Giorgio Lagna,[2,7] and Akiko Hata[1,2,7]*

Graduate Program in Biochemistry, Sackler School of Graduate Biomedical Sciences, Boston, Department of Biochemistry, Tufts University School of Medicine, Boston, Massachusetts 02111[1]; Molecular Cardiology Research Institute, Tufts Medical Center, Boston, Massachusetts 02111[2]; Division of Newborn Medicine and Epigenetics Program, Department of Medicine, Children's Hospital Boston, Harvard Medical School, Boston, Massachusetts 02115[3]; Department of Cell Biology, Harvard Medical School, Boston, Massachusetts 02115[4]; Department of Anatomy and Cell Biology, Carver College of Medicine, University of Iowa, Iowa City, Iowa 52242[5]; Center for Immunology and Inflammatory Diseases, Massachusetts General Hospital, Boston, Massachusetts 02114[6]; and Cardiovascular Research Institute, University of California, San Francisco, San Francisco, California 94158[7]

Received 9 June 2011/Returned for modification 30 June 2011/Accepted 22 September 2011

Hypoxia contributes to the pathogenesis of various human diseases, including pulmonary artery hypertension (PAH), stroke, myocardial or cerebral infarction, and cancer. For example, acute hypoxia causes selective pulmonary artery (PA) constriction and elevation of pulmonary artery pressure. Chronic hypoxia induces structural and functional changes to the pulmonary vasculature, which resembles the phenotype of human PAH and is commonly used as an animal model of this disease. The mechanisms that lead to hypoxia-induced phenotypic changes have not been fully elucidated. Here, we show that hypoxia increases type I collagen prolyl-4-hydroxylase [C-P4H(I)], which leads to prolyl-hydroxylation and accumulation of Argonaute2 (Ago2), a critical component of the RNA-induced silencing complex (RISC). Hydroxylation of Ago2 is required for the association of Ago2 with heat shock protein 90 (Hsp90), which is necessary for the loading of microRNAs (miRNAs) into the RISC, and translocation to stress granules (SGs). We demonstrate that hydroxylation of Ago2 increases the level of miRNAs and increases the endonuclease activity of Ago2. In summary, this study identifies hypoxia as a mediator of the miRNA-dependent gene silencing pathway through posttranslational modification of Ago2, which might be responsible for cell survival or pathological responses under low oxygen stress.

Pulmonary artery hypertension (PAH) is a disease characterized by pulmonary vascular remodeling and right ventricular hypertrophy (43). Hypoxia is considered a major factor in the pathogenesis of PAH (43) as well as tumor growth (17). Acute hypoxia causes selective pulmonary artery (PA) constriction and an increase in pulmonary artery pressure. Exposure to chronic hypoxia induces structural and functional changes to the pulmonary vasculature, which resembles that of human PAH and is commonly used as an animal model of this disease (43). Chronic hypoxia treatment in animals induces pulmonary artery smooth muscle cells (PASMCs) to undergo dedifferentiation; the cells become less contractile and more proliferative and display increased motility (2). This phenotype switch is believed to be the underlying cause of hypoxia-induced vascular remodeling, characterized by thickening of the vascular smooth muscle cell (vSMC) layer and elevation of PA resistance (37). Various growth factor signaling pathways, including transforming growth factor β (TGFβ), bone morphogenetic proteins (BMPs), and platelet-derived growth factors (PDGFs), regulate the vSMC phenotypic switch to maintain PASMC homeostasis as well as promote repair following vascular injury (37). These growth factors modulate the vSMC phenotype through direct alterations in protein-coding gene expression as well as through modulation of the levels of small regulatory RNAs, such as microRNAs (miRNAs), which subsequently regulate the expression of a number of protein-coding genes (3, 9, 10).

Recent studies indicate a critical role of miRNAs in the hypoxia response in oxygen-deprived neoplastic tumors and pulmonary tissues (25). Hypoxia causes a change in gene expression through a transcription factor, hypoxia-inducible factor-1 (HIF-1), which orchestrates the transcriptional regulation of a variety of genes, including genes encoding miRNAs, such as miR-210 or miR-181b (25). However, an HIF-1-independent effect of hypoxia on miRNA expression or its effect on proteins required for miRNA biogenesis/function, such as Argonaute (Ago) proteins, has not been investigated. To elucidate the molecular basis for hypoxia-mediated vascular remodeling and the pathogenesis of PAH, it is critical to uncover the mechanism of hypoxia-induced regulation of miRNA levels and function.

miRNAs play a critical role in a wide range of physiological and pathological cellular processes (6–8, 11, 31). The important function of miRNAs is particularly evident when cells are exposed to stress, such as hypoxia, nutrient deprivation, oxida-

* Corresponding author. Mailing address: Cardiovascular Research Institute, University of California, San Francisco, 555 Mission Bay Blvd. South, Room 252T, San Francisco, CA 94158-9001. Phone: (415) 476-9758. Fax: (415) 514-1173. E-mail: akiko.hata@ucsf.edu.

▽ Published ahead of print on 3 October 2011.

tion, or DNA damage (24, 46). Small RNAs, such as miRNAs and small interfering RNAs (siRNAs), guide a ribonucleoprotein complex known as the RNA-induced silencing complex (RISC), containing a member of the conserved Ago protein family, to sites predominantly in the 3′ untranslated regions (UTRs) of their target mRNAs, resulting in the destabilization of the mRNAs and/or inhibition of translation (24, 46). In humans, there are four members of the Ago protein subfamily, Ago1 to -4. Only Ago2 is known to exhibit endonuclease activity (12). Ago1 to -4 are ubiquitously expressed and associate with both miRNAs and siRNAs (12). It has been elucidated that the ATP hydrolysis activity of the Hsc70/Hsp90 chaperone machinery is required for the loading of small RNA duplexes (siRNA and miRNA) into RISC (21). Small RNA duplexes then guide Ago proteins to their target mRNAs (12). Perfect complementarity between the small RNA sequence and the target sequence promotes Ago2-mediated endonuclease activity, whereas mismatches in the binding region of the miRNA lead to repression of gene expression at the level of translation or mRNA stability (12). More recently, it was demonstrated that the Dicer-independent cleavage of precursor miR-451 (pre-miR-451) to generate mature miR-451 requires Ago2, indicating a novel role of Ago2 in the second processing step of miRNA biogenesis (4, 51). However, the mechanism of action and the mechanism of regulation of Ago proteins are poorly understood.

It has been demonstrated that Ago proteins are posttranslationally modified and regulated at the level of protein stability and silencing function in mammals (12). Ago proteins associate with both the α and β subunits of type I collagen prolyl-4-hydroxylase [C-P4H(I); EC 1.14.11.2] and can be hydroxylated, which results in increased Ago stability and activity (42). In HeLa S3 cells, high levels of hydroxylation are observed in Ago2 at proline (Pro) 700 (42). However, it is unclear whether Ago2 hydroxylation is regulated by physiological stimuli and whether hydroxylation affects Ago2 function. C-P4H(I) was originally identified as a critical regulator of collagen synthesis. Hydroxylation of collagen by C-P4H(I) is essential for the formation of triple-helical collagen and is a rate-limiting step in collagen synthesis (34). Inactivation of C-P4H(I) leads to the formation of hypohydroxylated collagen, which is unstable, and leads to the classical symptoms of scurvy (34). Because collagen constitutes the major extracellular matrix protein, the quantity and activity of C-P4H(I) are tightly regulated (34). Posttranscriptional regulation of C-P4Hα(I) at the level of mRNA stability (13) and translational control (14) has been demonstrated to be a key regulatory mechanism of collagen synthesis in fibrosarcoma. Induction of collagen upon activation of the TGFβ signaling pathway is also associated with the induction of C-P4H(I) (50).

In this study, we demonstrate that hypoxia increases C-P4H(I) expression and induces accumulation of Ago2 through C-P4H(I)-mediated prolyl-hydroxylation at Pro700. We demonstrate that hypoxia-induced prolyl-hydroxylation of Ago2 by C-P4H(I) promotes the association of Ago2 with Hsp90, leads to the translocation of Ago2 to stress granules (SGs), and increases miRNA levels. A hydroxylation-resistant mutant of Ago2 fails to associate with Hsp90, translocate to stress granules, or increase the levels of miRNAs. Thus, we propose that hypoxia-induced posttranslational modification of Ago2 affects protein stability and subcellular localization and results in increased levels of miRNAs and enhanced silencing of target mRNAs.

MATERIALS AND METHODS

Cell culture. Human primary pulmonary artery smooth muscle cells (PASMCs) were purchased from Lonza (number CC-2581) and maintained in smooth muscle growth medium-2 (Sm-GM2) (Lonza) containing 5% fetal bovine serum (FBS) (Sigma). U2OS and U2OS stable cell lines expressing the green fluorescent protein (GFP)-let-7 sensor construct, described previously (42), were maintained in Dulbecco's modified Eagle medium (DMEM) supplemented with 10% FBS (Sigma). Cells were maintained at 37°C in the presence of 5% CO_2.

Animal study and immunohistochemistry. All experiments were performed in accordance with guidelines and regulations of the Institutional Animal Care and Use Committee at Tufts Medical Center. Adult male Sprague-Dawley rats were randomized to 17 days of normoxia or hypobaric hypoxia as described previously (41). At the end of the exposure period, rats were sacrificed and the lungs were processed for paraffin embedding. Portions (5 μm) of paraffin-embedded tissue sections were immunostained as described previously (3).

Normoxia/hypoxia treatment. Hypoxic conditions were generated by first replacing culture media with fresh media equilibrated with a hypoxic gas mixture and then incubating cells in a sealed modular incubator chamber (Billups-Rothenberg) after flushing with a mixture of 5% CO_2 and 95% N_2 for 5 min. Normoxic controls were cultured in a humidified incubator at 37°C in the presence of 5% CO_2.

Plasmid DNA transfection and expression constructs. Cells were transfected using linear polyethylenimine (PEI), with a molecular weight (MW) of 25,000 (Polysciences, Inc.) according to the manufacturer's protocol. Amino-terminal Flag-tagged Ago1, Ago2, mutant Ago2 (Pro700A), and Ago3 were reported previously (42). The miR-144/451 expression construct was described previously (51).

RNA interference. Synthetic small interfering RNAs (siRNAs) targeting human *Ago2* or *C-P4Hα(I)* were obtained from Applied Biosystems (Silencer Select Pre-designed) and transfected into cells by using RNAiMAX (Invitrogen) according to the manufacturer's instructions. An siRNA with a nontargeting sequence (Negative Control siRNA, Qiagen) was used as a negative control.

The following primers were used: for *Ago2*, 5′-GGUCUAAAGGUGGAGAUAATT-3′ and 5′-UUAUCUCCACCUUUAGACCTT-3′; for *C-P4Hα(I)*, 5′-CUAGUACAGCGACAAAAGATT-3′ and 5′-UCUUUUGUCGCUGUACUAGTT-3′.

Antibodies and chemical inhibitors. Antibodies used in this study include anti-Ago1 (04-083; Millipore), anti-Ago2 (015-22031; Wako Chemicals), anti-Ago3 (SAB4200112; Sigma), anti-Ago4 (05-967; Millipore), anti-Drosha (A301-886A; Bethyl), anti-Dicer (ab14601; Abcam), anti-C-P4Hα(I) (PAB7221; Abnova), anti-C-P4Hβ (sc-20132; Santa Cruz), anti-Flag epitope tag (M2; Sigma), anti-Hsp90 (MAB3286; R&D Systems), anti-TIA-1 (sc-1751; Santa Cruz), and anti-β-actin (A5441; Sigma). The secondary antibodies used for immunofluorescence staining were purchased from Jackson ImmunoResearch Laboratory Inc. Arsenite (S-7400) and geldanamycin (GA; G3381) were purchased from Sigma. Concentrations of geldanamycin were optimized in each cell type to achieve maximal Hsp90 inhibition while minimizing cellular toxicity: 1 μM in U2OS cells and 0.1 μM in PASMCs.

Immunoprecipitation and Western blot assays. Immunoprecipitation and Western blot assays were performed as described previously (9). Protein bands were quantitated by densitometry using ImageJ gel analysis software (rsbweb.nih.gov/ij/).

RNA preparation and quantitative reverse transcriptase PCR (qRT-PCR). Total RNA was extracted from cells by TRIzol (Invitrogen). For detection of mRNAs, 1 μg of RNA was subjected to RT reaction using a first-strand cDNA synthesis kit (Invitrogen) according to the manufacturer's instructions. The quantitative analysis of the change in expression levels was calculated by a real-time-PCR machine (iQ5; Bio-Rad). PCR cycle conditions were 94°C for 3 min and 40 cycles of 94°C for 15 s, 60°C for 20 s, and 72°C for 40 s. For detection of mature miRNAs, the TaqMan microRNA assay kit (Applied Biosystems) was used according to the manufacturer's instructions. Data analysis was performed by using the comparative threshold cycle (C_T) method in Bio-Rad software. The average of results of three experiments, each performed in triplicate with standard errors, is presented.

The sequences of RT-PCR primers were as follows: human *Ago1*, 5′-GGGAAACAGTTCTACAATGG-3′ and 5′-CCCTGAGTAGGTGTTCTTGA-3′; human *Ago2*, 5′-ATGTTTACAAGTCGGACAGG-3′ and 5′-TCATCTTTGACC

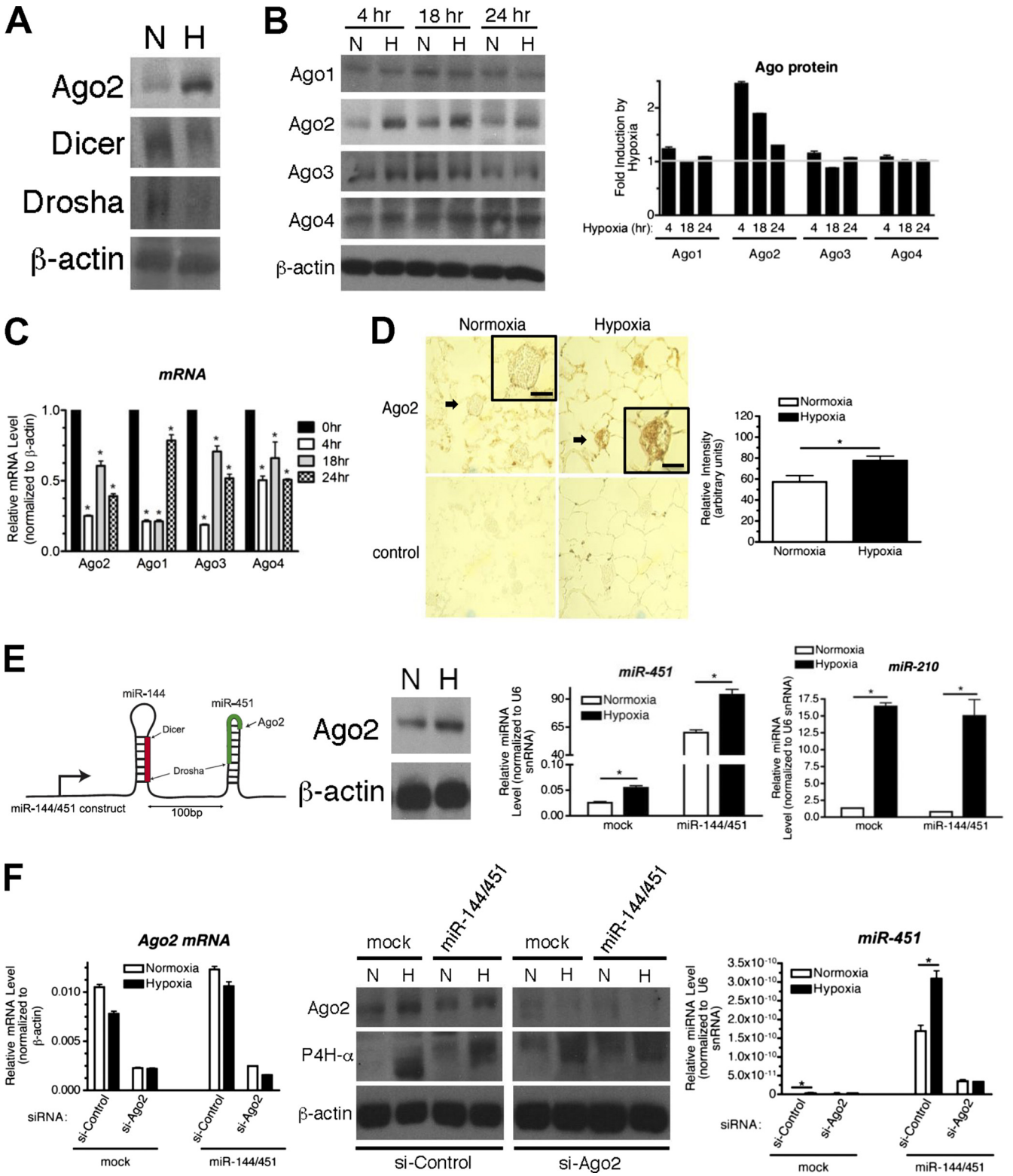

FIG. 1. Hypoxia mediates the posttranscriptional induction of Ago2. (A) Total cell lysates from PASMCs treated with normoxia (N) or hypoxia (H) for 24 h were subjected to immunoblot analysis with anti-Ago2, anti-Dicer, anti-Drosha, or anti-β-actin (loading control) antibodies. (B) Total cell lysates from PASMCs treated with normoxia (N) or hypoxia (H) for 4, 18, or 24 h were subjected to immunoblot analysis with anti-Ago1 to -4 or anti-β-actin (loading control) antibodies (left panel). By densitometry, relative amounts of Ago proteins normalized to β-actin were quantitated. Fold induction (hypoxia/normoxia) is presented (right panel). (C) PASMCs were treated with normoxia or hypoxia for 4, 18, or 24 h and subjected to qRT-PCR analysis of Ago1 to -4 mRNAs. Relative levels of mRNA expression normalized to β-actin were quantitated. *, $P < 0.05$. (D) Immunohistochemical examination of lung sections from rats after 17-day hypoxia or normoxia treatment with anti-Ago2 antibodies

ATGATTCC-3′; human *Ago3*, 5′-GGAACAATGAGACGGAAATA-3′ and 5′-CTTCTAGTGGCAGGTAGGTG-3′; human *Ago4*, 5′-ATGTGGGCCTACAG CTAATA-3′ and 5′-TATCTTCAGGCAAAGATTGG-3′; human *C-P4Hα(I)*, 5′-AAGGCGAGATTTCTACCATA-3′ and 5′-TTGGTCATCTGAAGCAGAC T-3′; human *C-P4Hβ*, 5′-CATACCATTTGGGATCACTT-3′ and 5′-GTCTTG ATTTCACCTCCAAA-3′; human Hsp70, 5′-CGGTCCGGATAACGGCTAGC CTGA-3′ and 5′-GTTGGAACACCCCCACGCAGG-3′; human PDCD4, 5′-A TTAATCTGGATGTCCCACA-3′ and 5′-TAAGACGACCTCCATCTCC-3′; human DOCK7, 5′-GCAGAACGGTGGCAGCCGAA-3′ and 5′-TCGGTAAG GGGCACTGTGGTGT-3′; human Sprouty2, 5′-TACAGGTGTGAGGACTGT GG-3′ and 5′-AAGAGACCTTTCACACAGCA-3′; human c-kit, 5′-CACCGA AGGAGGCACTTACAC-3′ and 5′-GGAATCCTGCTGCCACACA-3′; GFP-*let-7*, 5′-GAACGGCATCAAGGTGAACTT-3′ and 5′-GACGACCTCGAGTG AGGTAGTAGGTTGTATA-3′; human primary miR-21 transcript (pri-miR-21), 5′-TTTTGTTTTGCTTGGGAGGA-3′ and 5′-AGCAGACAGTCAGGCA GGAT-3′; human pri-miR-24-1, 5′-GCGGTGAACTCTCTCTTGTA-3′ and 5′-TTACAGACACGAAGGCTTTT-3′; human pri-miR-222, 5′-ACATTATCAG CTGGGGCTTG-3′ and 5′-ATGGATGGGTGGATGGATAA-3′; human pri-miR-210, 5′-GACCCACTGTGCGTGTGAC-3′ and 5′-CGAATGATTTCGCT TACCC-3′; human pri-miR-23a, 5′-TTTGCTTCCTGTCACAAATC-3′ and 5′-GGAACTTAGCCACTGTGAAC-3′.

Immunofluorescence staining, fluorescence imaging, and image analysis. PASMCs or U2OS cells were fixed with 2% paraformaldehyde/phosphate-buffered saline solution and permeabilized using methanol. Cells were then incubated for at least 1 h at room temperature sequentially with primary and secondary antibodies. After washing, cells were mounted on microscope slides using VECTASHIELD mounting medium with DAPI (4′,6-diamidino-2-phenylindole) (Vector Laboratories). Images were taken on a Nikon Eclipse E800 microscope with a CF160 infinity optical system and a Hamamatsu C4742-95 digital camera. Images were quantitated using ImageJ software (http://rsbweb.nih.gov/ij/). Intensity profiles generated using the ImageJ Color Profiler plug-in were used to determine colocalization between Ago2 and stress granules.

Statistical analysis. The results presented are average results of at least three experiments each performed in triplicate with standard errors. Statistical analyses were performed by analysis of variance, followed by Tukey's multiple comparison test or by Student's *t* test as appropriate, using Prism 4 (GraphPAD Software Inc.). *P* values of <0.05 were considered significant.

RESULTS

Hypoxia increases Ago2. To examine a potential effect of hypoxia on the protein expression of components of the miRNA biogenesis pathway, the miRNA processing enzymes (Dicer and Drosha) and Ago2 protein were examined by immunoblot analysis in PASMCs treated with normoxia or hypoxia (95% N_2, 5% CO_2) for 24 h. The Ago2 level was significantly increased, while Dicer and Drosha were reduced by hypoxia (Fig. 1A). Next, we examined other members of the Ago protein family (Ago1 to -4) after hypoxia treatment in PASMCs. Only Ago2 was significantly increased as early as 4 h after hypoxia treatment (Fig. 1B). Despite the increase in protein levels (Fig. 1B), mRNAs of Ago2, as well as other Ago family members, were reduced ~40 to 70% upon hypoxia treatment (Fig. 1C), indicating that the induction of Ago2 is likely to occur through a posttranscriptional mechanism. To examine whether induction of Ago2 can be observed under chronic hypoxia *in vivo*, lung sections prepared from rats treated with hypoxia for 17 days were stained with anti-Ago2 antibodies. Chronic hypoxia-treated lungs exhibited pulmonary artery remodeling, such as thickening of the medial wall (Fig. 1D). It was confirmed that the Ago2 protein was elevated in pulmonary arteries after hypoxia treatment (Fig. 1D, arrowheads).

It is reported that Ago2 exhibits Dicer-like processing activity and cleaves pre-miR-451 to generate mature miR-451 (4, 51). To demonstrate that hypoxia-mediated induction of Ago2 leads to an induction of Ago2 activity, we examined whether hypoxia increases the level of mature miR-451. Human osteosarcoma U2OS cells were transfected with an miR-144/451 expression construct (Fig. 1E, left panel), which encodes pre-miR-144 and pre-miR-451 (51). In U2OS cells, endogenous Ago2 (Fig. 1E, middle panel) and exogenously expressed Ago1 and Ago3 (data not shown) were elevated upon hypoxia. Hypoxia treatment also increased the level of endogenous miR-451 by ~2-fold (Fig. 1E, mock). When the miR-144/451 construct was transfected, the level of miR-451 under normoxia was >2,000-fold higher than that in the mock-treated cells as a result of the processing of exogenous pre-miR-451 to miR-451 by Ago2 (Fig. 1E, miR-451 and miR-144/451). Hypoxia treatment further increased the levels of miR-451 by ~1.5-fold similarly to the endogenous miR-451 (Fig. 1E, miR-451). Both the basal level and the hypoxia-induced level of miR-451 were reduced when endogenous Ago2 was downregulated, demonstrating that Ago2 is essential for the maturation of miR-451 from the miR-144/451 construct (Fig. 1F). These results confirm an increase in Ago2 activity as well as an increase in Ago2 protein after hypoxia treatment (Fig. 1E, middle panel). Altogether, these results indicate a rapid posttranscriptional mechanism of induction of Ago2 protein upon hypoxia treatment in both PASMCs and U2OS cells.

Hydroxylation of Ago2 by C-P4H(I) is mediated by hypoxia. It is reported that Ago2 is prolyl-hydroxylated by C-P4H(I) at Pro700, which inhibits Ago2 degradation and results in the induction of Ago2 (42). As hypoxia-mediated induction of C-P4H(I) has been reported previously (13, 14), we examined whether hypoxia induces C-P4H(I) in PASMCs, which then leads to the accumulation of Ago2. We found that both the mRNA (Fig. 2A) and protein (Fig. 2B) levels of both the α (C-P4Hα) and β (C-P4Hβ) subunits of C-P4H(I) were increased ~2- to 3-fold by hypoxia. Induction of C-P4Hα/β was observed as early as 1 h after hypoxia treatment and was more rapid than the induction of Ago2 (Fig. 2C), supporting the hypothesis that hydroxylation of Ago2 by C-P4H(I) mediates the induction of Ago2 upon hypoxia.

(brown, ×400). As a control, staining without the primary antibodies was performed. PAs are indicated with arrowheads. The insets in the panel are enlargements of the indicated PAs. Scale bars, 25 μm (left panel). Relative expression of Ago2 in the PAs was quantitated using ImageJ software (right panel). *, $P < 0.05$. (E) U2OS cells were transfected with vector (mock) or miR-144/451 construct, followed by normoxia (N) or hypoxia (H) treatment for 24 h. Schematic of the miR-144/451 construct is shown (left panel); mature miR-144 is highlighted in red, and mature miR-451 is highlighted in green. Levels of miR-451 or miR-210 normalized to U6 snRNA are presented (right panels). *, $P < 0.05$. Total cell lysates were prepared from U2OS cells treated with N or H for 24 h and were subjected to immunoblot analysis using anti-Ago2 or β-actin (loading control) antibodies (middle panel). (F) U2OS cells were transfected with control siRNA (si-Control) or siRNA against Ago2 (si-Ago2) and vector (mock) or miR-144/451 construct, followed by normoxia (N) or hypoxia (H) treatment for 24 h. Downregulation of Ago2 by siRNA was confirmed by qRT-PCR analysis (left panel) and immunoblot analysis (middle panel). The same membrane was blotted with anti-C-P4Hα and anti-β-actin (loading control) antibodies. Relative levels of miR-451 normalized to U6 snRNA are presented (right panel). *, $P < 0.05$.

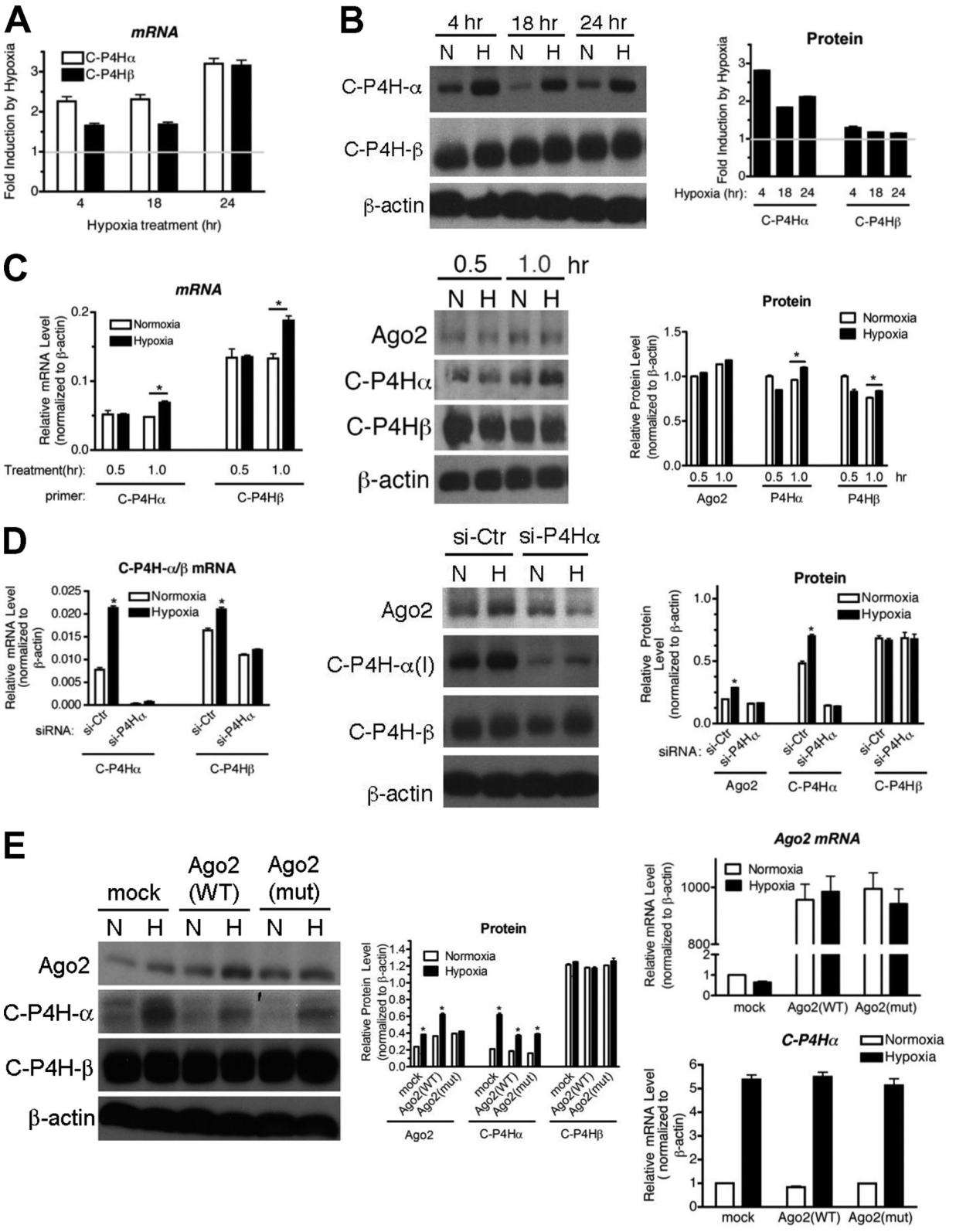

FIG. 2. Prolyl-hydroxylation of Ago2 by C-P4H(I) is critical for the hypoxia-mediated induction of Ago2. (A) PASMCs were exposed to normoxia or hypoxia for 4, 18, or 24 h and subjected to qRT-PCR analysis of C-P4Hα and C-P4Hβ mRNAs. The relative levels of mRNA expression normalized to β-actin were quantitated. Fold induction (hypoxia/normoxia) is presented. (B) Total cell lysates from PASMCs treated with normoxia (N) or hypoxia (H) for 4, 18, or 24 h were subjected to immunoblot analysis with anti-C-P4Hα, anti-C-P4Hβ, or anti-β-actin (loading control) antibodies (left panel). By densitometry, relative amounts of C-P4H(I) proteins normalized to β-actin were quantitated. Fold induction (hypoxia/normoxia) is presented (right panel). (C) Total cell lysates from PASMCs treated with normoxia (N) or hypoxia (H) for 0.5 or 1 h were

To investigate the role of C-P4H(I) in the induction of Ago2 by hypoxia, we used siRNA to knock down C-P4Hα, which is critical for the catalytic activity of C-P4H(I), prior to hypoxia treatment in PASMCs. siRNA downregulated 97% of endogenous C-P4Hα (Fig. 2D). Downregulation of C-P4Hα was associated with a weak reduction of C-P4Hβ (Fig. 2D). Under the condition of C-P4Hα knockdown, accumulation of Ago2 by hypoxia was abolished (Fig. 2D), suggesting an essential role of C-P4H(I) in hypoxia-mediated stabilization of Ago2. The significance of C-P4H(I)-mediated prolyl-hydroxylation was confirmed by examining a mutant of Ago2 [Ago2(mut)], which is mutated at Pro700 to Ala (42). The wild type [Ago2(WT)] or the Ago2 mutant [Ago2(mut)] was transfected into U2OS cells, followed by hypoxia treatment. Exogenous Ago2(WT) or Ago2(mut) showed no effect on the levels of the C-P4Hβ subunit (Fig. 2E). Unlike endogenous Ago2 (Fig. 2E, mock) or exogenously expressed Ago2(WT), Ago2(mut) did not accumulate upon hypoxia (Fig. 2E), supporting a critical role of the C-P4H(I) hydroxylation site in the hypoxia-induced accumulation of Ago2.

Hypoxia induces Ago2 translocation to stress granules. Previous studies suggest that upon various cellular stresses, Ago2 translocates to specific compartments of the cell, including SGs and processing bodies (P-bodies) (28, 38, 42). PASMCs were subjected to immunofluorescence staining with antibodies against Ago2 or C-P4Hβ (Fig. 3A). As previously reported (42), under normoxia, Ago2 was found to be colocalized with C-P4Hβ in the cytoplasm (Fig. 3A and B, Normoxia). Upon hypoxia treatment for 3 h, Ago2 accumulated at foci in the cytoplasm, which coincided with staining for TIA-1, a marker of SGs (42), suggesting hypoxia-induced translocation of Ago2 to SGs (Fig. 3B). No SGs were found in cells under normoxia (Fig. 3A and B). In both PASMCs and U2OS cells, ~5 to 10% of cells contained SGs at 30 min after hypoxia, with the percentage of SG-positive cells increasing to 10 to 15% after 3 h and then gradually declining by 24 h (Fig. 3B, right panel). Ago2 localized to SGs in more than 97% of SG-positive cells (Fig. 3C, Mock). These results suggest that hypoxia promotes (i) formation of SGs and (ii) translocation of Ago2 to SGs. Interestingly, we observed that translocation of the prolyl-hydroxylation site mutant [Ago(mut)] to SGs after hypoxia treatment was greatly reduced (~40%) compared with that of the wild-type Ago2 (>97%) (Fig. 3C), suggesting that prolyl-hydroxylation increases SG localization of Ago2 either by facilitating (i) the translocation of Ago2 to SGs or (ii) a stable localization of Ago2 in SGs.

Hypoxia induces association of Ago2 with Hsp90. A previous study indicated that the interaction of Ago with the chaperone protein complex, Hsc70/Hsp90, is critical for the loading of siRNA or miRNA into RISC (21). We examined whether hypoxia-induced prolyl-hydroxylation of Ago2 affects the association of Ago2 with Hsp90. Total cell lysates from PASMCs exposed to normoxia or hypoxia were subjected to immunoprecipitation with anti-Hsp90 antibody, followed by immunoblot analysis with anti-Ago2 antibody (Fig. 4A). Association of endogenous Ago2 with Hsp90 was observed under normoxia; however, the Ago2-Hsp90 interaction was greatly increased after hypoxia (Fig. 4A). Hypoxia-induced interaction between Ago2 and Hsp90 was inhibited when C-P4H(I) activity was downregulated by si-C-P4Hα (Fig. 4B), indicating an importance of prolyl-hydroxylation of Ago2. Consistently, association of Hsp90 with the prolyl-hydroxylation site Ago2 mutant [Ago(mut)] was significantly reduced in comparison with Ago2(WT) (Fig. 4C), indicating a critical role of Pro700 hydroxylation of Ago2 by C-P4H(I) in the association with Hsp90. As a previous report demonstrated that the amino (N)-terminal 323 amino acids of Ago2 are sufficient to interact with Hsp90 *in vitro* (48), we speculate that hydroxylated Pro700 cooperates with the N-terminal region of Ago2 to form an interface between Ago2 and Hsp90 *in vivo*.

Hypoxia increases Ago2 function. As hypoxia promotes the association of Ago2 with Hsp90, which is critical for the loading of small RNA duplexes into RISC (21), we speculated that hypoxia may increase RISC activity. A sequence perfectly complementary to let-7 was ligated to the 3′UTR of the GFP gene (GFP-let-7 sensor) and stably transfected into U2OS cells. Hypoxia treatment decreased the GFP-let-7 sensor mRNA expression to 40% of the normoxia level (Fig. 5A, lower left panel). Because endogenous let-7a levels were not altered by hypoxia (Fig. 5A, right panel), this result suggests that the let-7-RISC activity was elevated upon hypoxia presumably due to an effect on Ago2. As was observed with PASMCs, the mRNA levels of C-P4Hα and C-P4Hβ were increased by hypoxia in U2OS cells (Fig. 5A, lower left panel). In U2OS cells transfected with Ago2(WT), let-7-RISC activity was induced by hypoxia similar to that in mock-treated cells; however, when Ago2(mut) was expressed, hypoxia no longer induced let-7-RISC activity (Fig. 5B). These results confirm that hypoxia-mediated prolyl-hydroxylation of Ago2 augments RISC activity. Finally, to investigate the effect of hypoxia-mediated induction of miRNAs on target gene expression, levels of expression of validated targets of miR-21 (PDCD4, DOCK7, and

immunoblotted with anti-Ago2, anti-C-P4Hα, anti-C-P4Hβ, or β-actin (loading control) antibodies (middle panel). By densitometry, relative amounts of Ago2 and C-P4H(I) proteins normalized to β-actin were quantitated (right panel). *, $P < 0.05$. Levels of C-P4Hα/β mRNAs after N or H treatment (0.5 or 1 h) were quantitated by qRT-PCR normalized to β-actin (left panel). *, $P < 0.05$. (D) PASMCs were transfected with siRNA against C-P4Hα (si-P4Hα) or nontargeting control (si-Ctr) for 48 h prior to treatment with normoxia (N) or hypoxia (H) for 24 h. Total cell lysates were subjected to immunoblot analysis using anti-Ago2, anti-C-P4Hα(I), anti-C-P4Hβ, or anti-β-actin (loading control) antibodies (middle panel). By densitometry, relative amounts of Ago2 and C-P4H(I) proteins normalized to β-actin were quantitated and are presented (right panel). Total RNAs were extracted from the same cells and subjected to qRT-PCR analysis. Relative C-P4Hα/β mRNA levels normalized to β-actin are presented as mean ± standard deviation (SD) (left panel). *, $P < 0.05$. (E) U2OS cells were transfected with vector (mock), wild type (WT) Ago2, or Pro700A mutant (mut) Ago2 cDNA construct followed by treatment with normoxia (N) or hypoxia (H) for 24 h. Relative levels of Ago2 or C-P4H(I) proteins normalized to β-actin were examined by immunoblotting (left panel) and quantitated by densitometry (middle panel). Relative mRNA levels of Ago2 (upper right panel) and C-P4Hα (lower right panel) normalized to β-actin are presented as mean ± SD. *, $P < 0.05$.

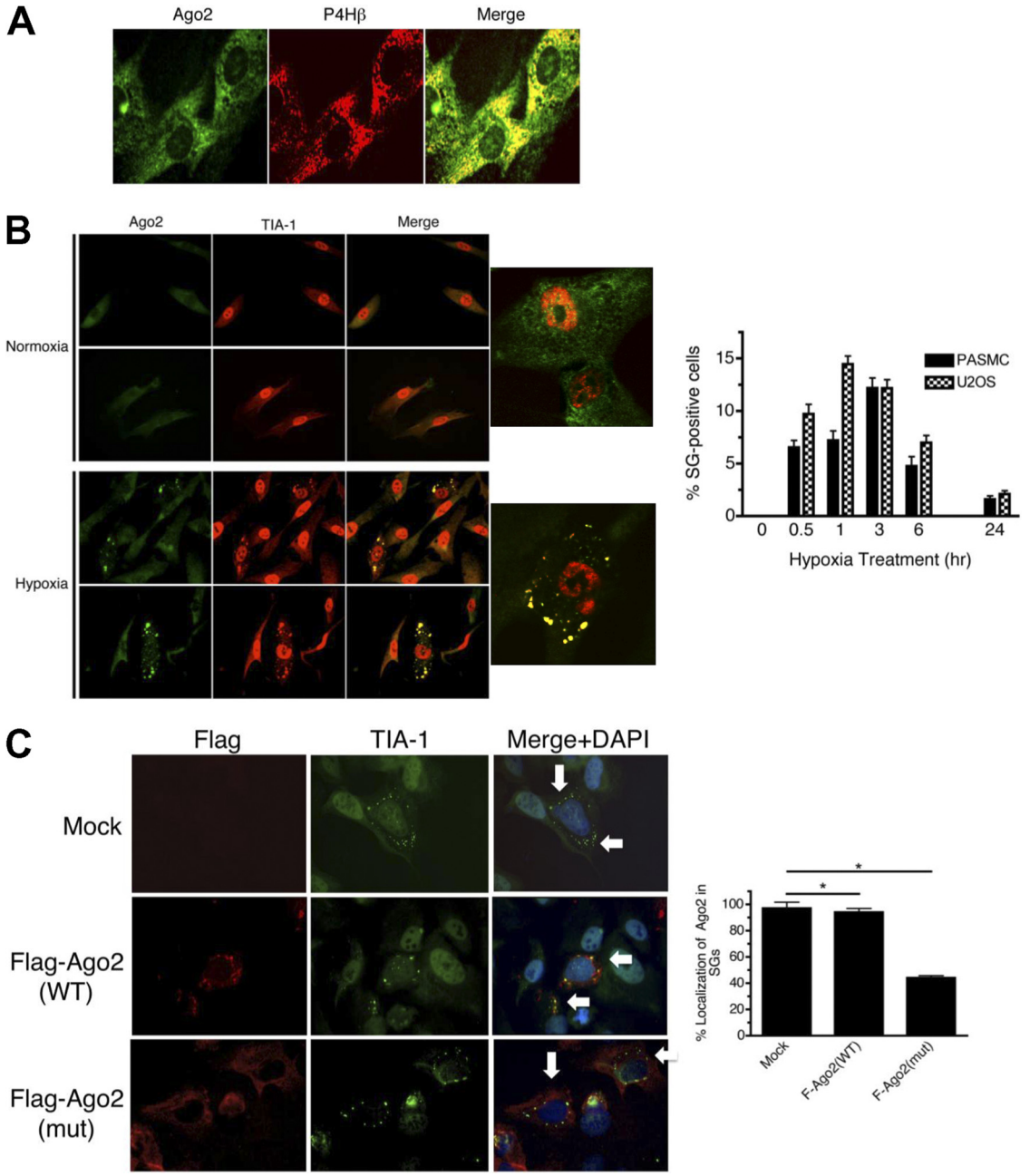

FIG. 3. Hypoxia induces the translocation of Ago2 to SGs. (A) Subcellular localization of Ago2 was examined by immunofluorescence analysis in PASMCs stained with FITC-Ago2 (green) and rhodamine-P4Hβ subunit (red) under normoxia. (B) PASMCs were treated with normoxia or hypoxia for 3 h and subjected to immunofluorescence staining with FITC-Ago2 antibodies (green) and rhodamine-TIA-1 antibodies (red). The accompanying graph shows quantification of cells containing SGs after treatment with hypoxia for the indicated periods of time. Approximately 200 cells from at least 10 independent fields have been counted for each time point, and SG-positive cells are presented as a percentage of the total population. (C) U2OS cells were transfected with vector (mock), Flag-tagged Ago2(WT), or Flag-tagged Ago2(mut) cDNA construct followed by treatment with hypoxia for 3 h. Immunofluorescence staining was performed using rhodamine-Flag antibodies (red) and FITC-TIA-1 antibodies (green). Arrows indicate the position of TIA-1-positive stress granules. The accompanying graph shows quantification of the percentage of Ago2 localized in SGs for each condition. Mock refers to the localization of endogenous Ago2. Approximately 70 SGs in at least three cells have been examined for each condition. *, $P < 0.05$.

Sprouty2) (5) and miR-221 (c-kit) (10) were examined. Consistent with the hypoxia-mediated increase in the levels of miR-21 and miR-221 (Fig. 6A, left panel), the levels of the targets of these miRNAs were significantly downregulated by hypoxia (Fig. 5C). In summary, these results demonstrate that hypoxia-mediated induction of Ago2 results in the elevation of various Ago2 functions, including RISC activity and Dicer-like processing activity (Fig. 1E).

Since Hsp90 is an ATPase and is required for the loading of miRNA or siRNA into RISC (21), we examined the effect of

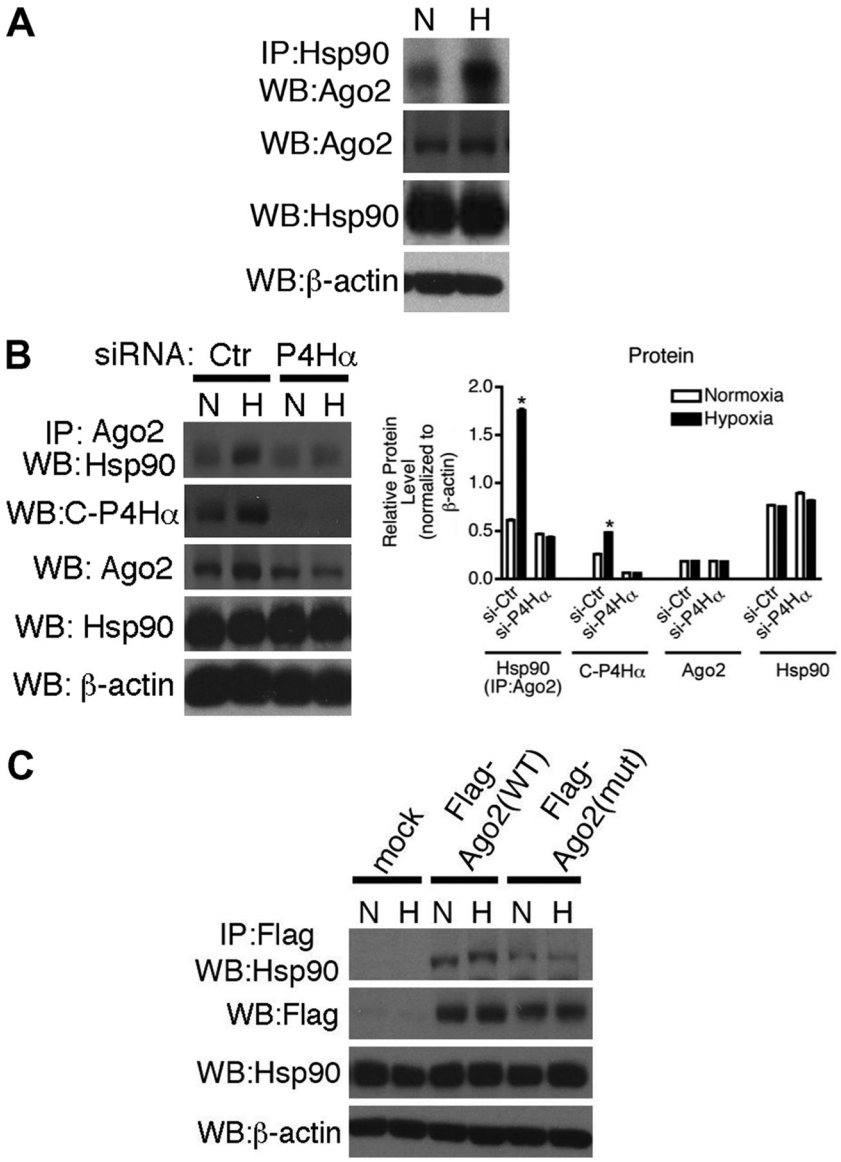

FIG. 4. C-P4H(I)-mediated prolyl-hydroxylation of Ago2 promotes the interaction between Ago2 and Hsp90. (A) Total cell lysates from PASMCs treated with normoxia (N) or hypoxia (H) for 24 h were subjected to immunoprecipitation with anti-Hsp90 antibody and immunoblotted with anti-Ago2 antibody. Total cell lysates were also subjected to immunoblot analysis with anti-Ago2, anti-Hsp90, or anti-β-actin (loading control) antibodies. (B) Total cell lysates from PASMCs transfected with siRNA against C-P4Hα(I) (si-P4Hα) or nontargeting control (si-Ctr) siRNA for 48 h prior to treatment with normoxia (N) or hypoxia (H) for 24 h were subjected to immunoprecipitation with anti-Ago2 antibody and immunoblotted with anti-Hsp90 antibody. Total cell lysates were also subjected to immunoblot analysis with anti-C-P4Hα, anti-Ago2, anti-Hsp90, or anti-β-actin (loading control) antibodies (left panel). By densitometry, relative amounts of Hsp90, C-P4Hα, and Ago2 proteins normalized to β-actin were quantitated and are presented (right panel). (C) U2OS cells were transfected with vector (mock), Flag-tagged Ago22(WT), or Flag-tagged Ago2(mut) cDNA construct and treated with normoxia (N) or hypoxia (H) for 24 h. Total cell lysates were subjected to immunoprecipitation with anti-Flag antibody, followed by immunoblotting with anti-Hsp90 antibody. Total cell lysates were also subjected to immunoblot analysis with anti-Flag (for Ago2), anti-Hsp90, or anti-β-actin (loading control) antibodies.

inhibition of the ATPase activity of Hsp90 on hypoxia-induced Ago2 activities. Cells were treated with geldanamycin (GA), a specific inhibitor of the ATPase activity of Hsp90, prior to hypoxia treatment. GA treatment increased the Hsp70 mRNA level as previously reported (45), confirming inhibition of Hsp90 by GA (Fig. 5D, left panel). The hypoxia-induced increase in Ago2 protein level was not significantly inhibited by GA (Fig. 5D, middle and right panels), showing that ATP hydrolysis by Hsp90 is not required for hypoxia-mediated accumulation of Ago2. Next, hypoxia-mediated induction of the RISC activity (GFP-let-7) and miR-451 processing activity was examined after GA treatment. Downregulation of the GFP-let-7 sensor mRNA expression by hypoxia was abolished by GA treatment (Fig. 5E), indicating that the ATPase activity of Hsp90 is essential for the induction of the RISC activity upon hypoxia, presumably because GA blocks the loading of the miRNA duplex into RISC. Furthermore, hypoxia-mediated induction of the miR-451 processing activity of Ago2 was

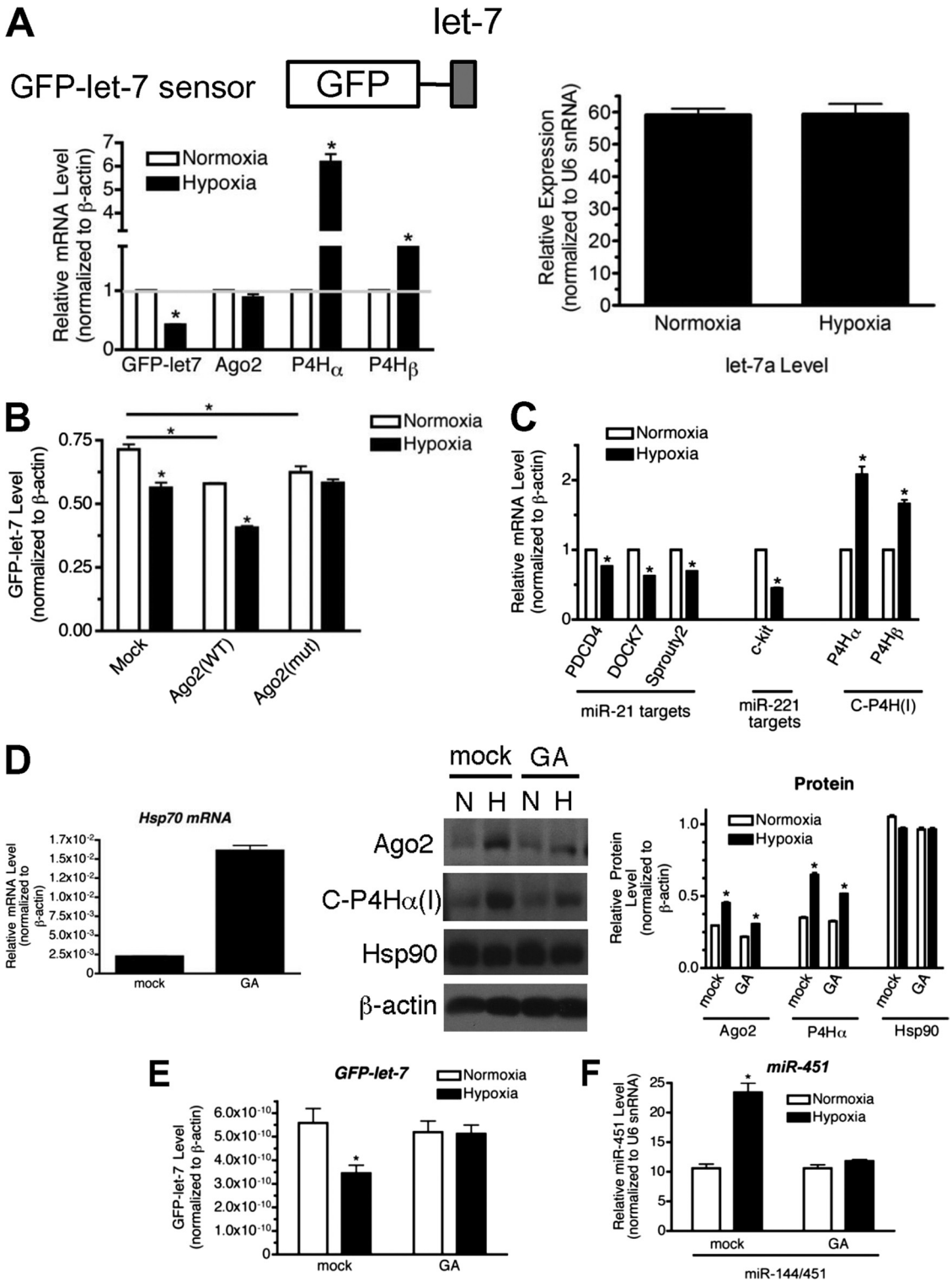

FIG. 5. Hypoxia increases Ago2 activity. (A) U2OS cell line stably expressing the GFP-let-7 sensor construct (upper left panel) was exposed to normoxia or hypoxia for 24 h and subjected to qRT-PCR analysis of GFP-let-7, Ago2, C-P4Hα, and C-P4Hβ mRNAs or let-7a miRNA. Relative levels of mRNA expression normalized to β-actin are presented by setting the expression levels of normoxia to 1 (lower left panel). Relative expression levels of let-7a normalized to U6 snRNA are presented (right panel). *, $P < 0.05$. (B) U2OS cell line stably expressing GFP-let-7 was transfected with vector (mock), wild-type (WT) Ago2, or Pro700A mutant (mut) Ago2 cDNA construct followed by treatment with normoxia or hypoxia for 24 h. Relative expression of the GFP-let-7 sensor was measured by qRT-PCR analysis and is presented after normalization to β-actin. *, $P < 0.05$. (C) PASMCs were exposed to normoxia or hypoxia for 24 h and subjected to qRT-PCR analysis of miR-21 target gene (PDCD4, DOCK7, and Sprouty2) transcripts and miR-221 target gene (c-kit) transcripts. Relative levels of mRNA expression normalized to β-actin are presented by setting the expression levels of normoxia to 1. C-P4Hα(I) and C-P4Hβ mRNAs were examined as controls for hypoxia treatment.

blocked by GA treatment (Fig. 5F), indicating that the ATPase activity of Hsp90 is also required for the Dicer-like processing activity of Ago2. These results demonstrate the functional importance of Ago2-Hsp90 interaction in various Ago2 functions regulated by hypoxia.

Ago2 and C-P4H(I) are essential for the hypoxia-mediated increase in miRNAs. To examine the potential effect of hypoxia on miRNA expression, miRNA microarray analysis was performed in PASMCs treated with hypoxia for 24 h. Thirty-seven percent of 292 miRNAs (107 miRNAs) detected in PASMCs were induced ≥1.5-fold upon hypoxia (Table 1). Furthermore, when C-P4Hα was knocked down by siRNA, 94% of the hypoxia-induced miRNAs (101 of 107 miRNAs) were either no longer induced by hypoxia or had reduced induction by hypoxia (Table 1). This result suggests a potential relationship between hydroxylation of Ago2 and elevation of miRNA expression. Induction of 14 miRNAs by hypoxia between ~1.3- and 4-fold was validated by qRT-PCR analysis (Fig. 6A, left panel). miR-210 gene transcription is known to be activated by HIF-1 (1, 25). Indeed, ~2-fold induction of the primary transcript of miR-210 (pri-miR-210) was observed upon hypoxia (Fig. 6A, right panel). However, primary transcripts of all other miRNAs examined were not induced and were rather repressed under hypoxia (Fig. 6A, right panel). These results suggest that hypoxia elevates the miRNAs through a posttranscriptional mechanism.

To investigate a potential link between Ago2 and the hypoxia-mediated induction of miRNAs, Ago2 was knocked down by siRNA (si-Ago2) in PASMCs. Transfection of si-Ago2 reduced ~70% of the endogenous Ago2 mRNA and ~50% of the Ago2 protein level (Fig. 6B). Knockdown of Ago2 had no effect on the hypoxia-mediated induction of C-P4Hα (Fig. 6B). Hypoxia-mediated increase in the miRNAs examined was either abolished or reduced when Ago2 was knocked down (Fig. 6C), suggesting that Ago2 plays an essential role in the accumulation of miRNAs in response to hypoxia. However, compared to the miRNAs whose hypoxia-mediated induction was completely abolished by si-Ago2, miR-210, which is transcriptionally regulated by HIF-1, was less affected by the knockdown of Ago2 and exhibited a weak increase upon hypoxia (Fig. 6C).

If the hypoxia-mediated increase in Ago2 protein were sufficient for the induction of miRNAs, then overexpression of Ago2(WT) to the level equivalent to that of hypoxia treated cells might be sufficient to induce miRNAs. To test this possibility, U2OS cells were transfected with an empty vector (mock) or Ago2(WT) expression construct, followed by exposure to hypoxia. Although Ago2(WT)-transfected cells expressed Ago2 at levels similar to that of mock-transfected cells under hypoxia (Fig. 6D, left and middle panels), mature miRNA levels were unchanged (Fig. 6D, right panel), suggesting that hypoxia-induced prolyl-hydroxylation of Ago2 is required for the induction of miRNAs. Furthermore, downregulation of C-P4H(I) activity by si-P4Hα, which downregulated ~97% of endogenous C-P4Hα (Fig. 2D), either abolished or reduced the hypoxia-mediated induction of all miRNAs examined (Fig. 6E). These results indicate that prolyl-hydroxylation of Ago2 is critical for the elevation of miRNAs in response to hypoxia. Again, compared to the miRNAs whose hypoxia-mediated induction was completely abolished by si-P4Hα, HIF-1-regulated miR-210 was less affected by the knockdown of C-P4Hα and exhibited a modest increase upon hypoxia (Fig. 6E). As prolyl-hydroxylation of Ago2 by C-P4H(I) promotes the association of Ago2 with Hsp90, we hypothesized that induction of the miRNAs by hypoxia is dependent on the ATPase activity of Hsp90. Cells were treated with GA, followed by hypoxia treatment and miRNA analysis. All miRNAs examined failed to accumulate upon hypoxia under GA treatment (Fig. 6F). Because HIF-1 activity also requires the ATPase activity of Hsp90 (33), induction of HIF-1-dependent miR-210 was also abolished by GA treatment (Fig. 6F). Altogether, these results demonstrate that hypoxic stress mediates a series of nontranscriptional events: (i) prolyl-hydroxylation of Ago2 by C-P4H(I), (ii) formation of SGs and translocation of Ago2 to SGs, (iii) association of Ago2 with Hsp90, and (iv) an increase in Ago2 activity and miRNAs, all of which contribute to efficient gene silencing by miRNAs under low oxygen stress.

DISCUSSION

Chronic exposure of animals to hypoxia induces pulmonary artery remodeling and elevation of pulmonary artery pressure, similar to that seen in PAH patients (47). The small pulmonary arteries of animals treated with chronic hypoxia and those of PAH patients exhibit a significant increase in extracellular matrix proteins, including collagen deposits (36). A hypoxic environment is known to facilitate the formation of collagen deposits during the process of wound healing in skin or the remodeling of small pulmonary arteries by inducing procollagen, as well as C-P4H(I), which generates covalent cross-bridging between collagen fibers (35). Although molecular oxygen (O_2) is required for the activity of C-P4H(I) (16), several studies have in fact shown that the activity of collagen prolyl 4-hydroxylase is induced, rather than inhibited, under low oxygen tension (30, 39, 49). Exposure of fibroblasts to 24 h of hypoxia increased the activity of collagen prolyl 4-hydroxylase by about 4-fold compared to normoxia and enhanced the de-

*, $P < 0.05$. (D) PASMCs were treated with mock (DMSO) or 0.1 μM geldanamycin (GA) for 1.5 h prior to exposure to normoxia (N) or hypoxia (H) for 24 h. Total RNAs extracted from the cells were subjected to qRT-PCR analysis of Hsp70 mRNA as a control. Relative levels of mRNA expression normalized to β-actin are presented (left panel). Total cell lysates from the same cells were subjected to immunoblot analysis of Ago2, C-P4Hα(I), Hsp90, or β-actin (loading control) antibodies (middle panel). Relative amounts of proteins normalized to β-actin were quantitated by densitometry and are presented (right panel). *, $P < 0.05$. (E) U2OS cell line stably expressing GFP-let-7 was treated with mock (dimethyl sulfoxide [DMSO]) or 1 μM geldanamycin (GA) for 1.5 h prior to exposure to normoxia or hypoxia for 24 h. Relative expression of the GFP-let-7 sensor was measured by qRT-PCR analysis and is presented after normalization to β-actin. *, $P < 0.05$. (F) U2OS cells transfected with miR-144/451 expression construct were treated with mock (DMSO) or 1 μM geldanamycin (GA) for 1.5 h prior to exposure to normoxia or hypoxia for 24 h. Levels of miR-451 normalized to U6 snRNA are presented. *, $P < 0.05$.

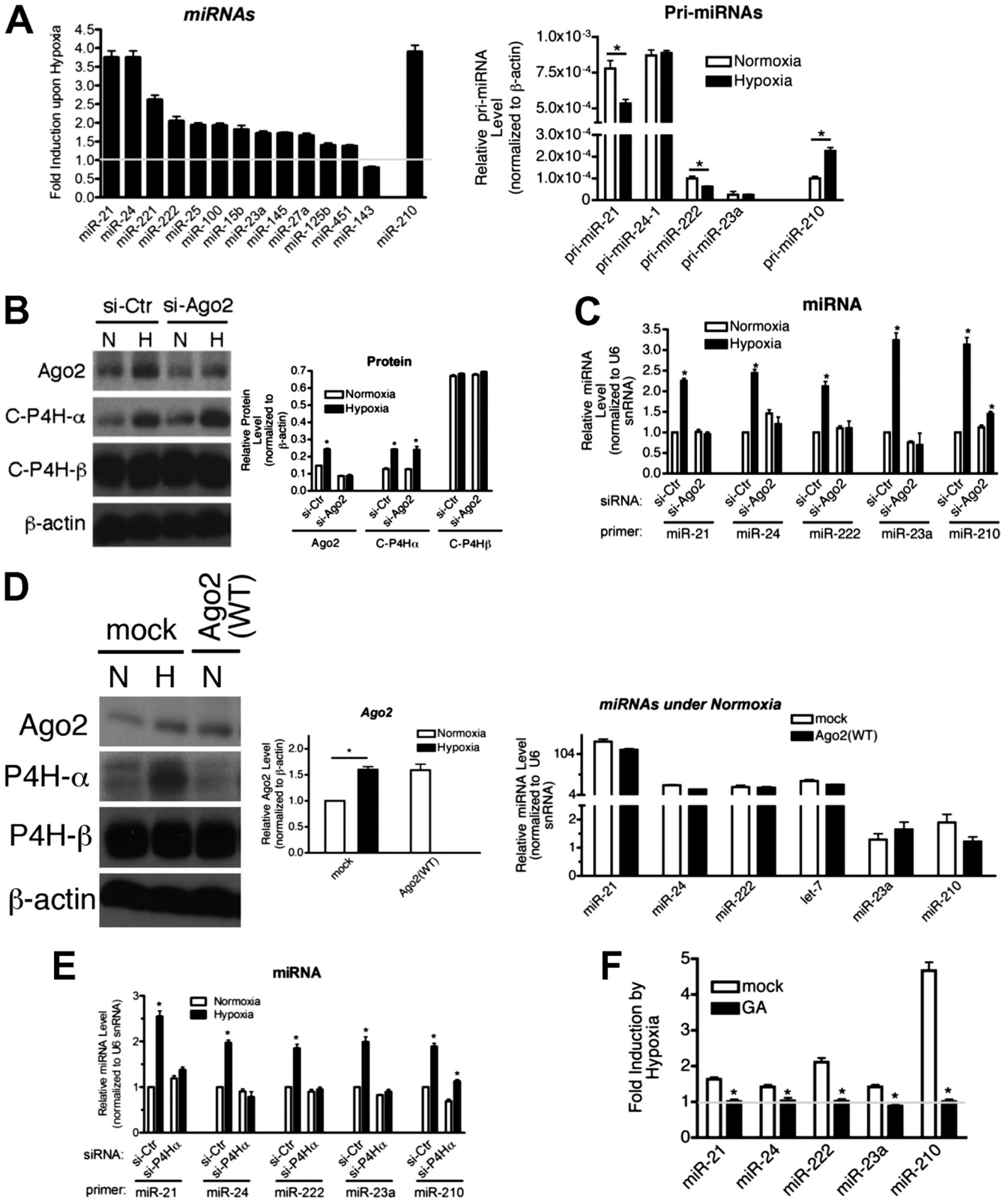

FIG. 6. C-P4H(I)-mediated prolyl-hydroxylation of Ago2 is required for the induction of miRNAs upon hypoxia. (A) Levels of expression of miRNAs normalized to U6 snRNA were examined by qRT-PCR in PASMCs exposed to normoxia or hypoxia for 24 h. Fold induction (hypoxia/normoxia) is presented (left panel). Relative expression levels of pri-miRNAs normalized to β-actin were examined by qRT-PCR in PASMCs exposed to normoxia or hypoxia for 24 h (right panel). (B) PASMCs were transfected with siRNA against Ago2 (si-Ago2) or nontargeting control (si-Ctr) for 48 h prior to treatment with normoxia (N) or hypoxia (H) for 24 h. Protein levels of Ago2, C-P4Hα, and C-P4Hβ were measured by immunoblotting (left panel), and relative amounts of proteins normalized to β-actin were quantitated by densitometry (right panel). *, $P < 0.05$.

gree of proline hydroxylation in newly synthesized collagen (30). Hypoxic exposure of fibroblasts also increased the levels of hydroxyproline residue secreted from the cells into the culture medium (49). These results demonstrate that the hydroxylation activity of collagen prolyl 4-hydroxylase is regulated differently compared to that of the related prolyl hydroxylase domain protein (PHD), whose activity is known to be inhibited by hypoxia (16).

The PHDs are well-known regulators of the HIF-1α transcription factor (16). Under normoxia, PHDs hydroxylate HIF-1α, and this hydroxylation leads to the proteasomal degradation of HIF-1α (16). The activity of PHDs is inhibited under hypoxia; as a result, HIF-1α is no longer hydroxylated and accumulates in the cell to regulate the transcription of a variety of genes that are critical for conferring hypoxia tolerance (16). Like collagen prolyl 4-hydroxylase, O_2 is required for PHD activity (16); thus, it is not surprising that the activity of PHDs would be inhibited under conditions of low oxygen tension. While it may seem paradoxical that hypoxia induces the hydroxylation activity of collagen prolyl 4-hydroxylase, an important difference between collagen prolyl 4-hydroxylase and the PHDs is that the PHDs have a much higher K_m value for O_2, and thus a lower affinity for O_2, compared to collagen prolyl 4-hydroxylase (18). The K_m values of the PHDs range from 230 μM to 250 μM, slightly above the concentration of dissolved O_2 in the atmosphere, while the K_m of type I collagen prolyl 4-hydroxylase is only 40 μM (18). This significant difference between their K_m values for O_2 could contribute to the differential regulation of their hydroxylation activities under low oxygen tension. Even though the concentration of O_2 is reduced under hypoxia, the hydroxylation activity of C-P4H(I) would still be maintained because of its relatively high oxygen affinity. This maintenance of activity would correlate with the important role that C-P4H(I) plays in the formation of collagen deposits under hypoxic conditions. Moreover, hypoxia has been shown to upregulate C-P4Hα(I), the subunit which is critical for the catalytic activity of C-P4H(I), at both the transcriptional and posttranscriptional levels (13, 14, 19). Thus, the relatively high oxygen affinity of C-P4H(I) along with the hypoxia-mediated increase in C-P4Hα(I) expression could lead to increased prolyl-hydroxylation of its substrates under hypoxia.

In this study, we characterized a role of Ago2 downstream of the hypoxia-mediated induction of C-P4H(I) activity and downstream effects of the miRNA pathway as an alternative mechanism of regulation of gene expression in cells under hypoxia. As Ago proteins are the key components of the RISC, regulation of Ago protein stability and/or activities has a significant impact on the silencing activities of siRNAs and miRNAs. It is increasingly evident that posttranslational modifications of Ago proteins, including phosphorylation and ubiquitination, modulate Ago protein stability and function, which subsequently alter gene expression (12). It is unclear, however, how such modifications are induced and how such modifications affect Ago protein functions. In this study, we demonstrate a functional significance of prolyl-hydroxylation of Ago2 which is mediated by hypoxia treatment. We are able to extend the significance of hydroxylation of Ago2 from modulation of Ago2 protein stability to modulation of the localization of Ago2 and its activities. Recently, induction of poly(ADP-ribosylation) of Ago proteins by poly(ADP-ribose) polymerase 13 (PARP-13) upon oxidative stress or translation initiation inhibition has been reported (29). Unlike hydroxylation, poly(ADP-ribosylation) of Ago relieves miRNA-mediated gene silencing, presumably due to disruption of electrostatic interaction or steric hindrance between the miRNA/Ago complex and target mRNA (29). It is plausible that different cellular stresses might mediate distinct posttranslational modifications of Ago to modulate miRNA-mediated gene silencing activity.

The molecular pathways in response to hypoxia are complex, but the transcription factor HIF-1 is known to play a key role by orchestrating the expression of a wide variety of genes that are critical for hypoxic tolerance (44). Our result that hypoxia mediates the accumulation of Ago2 in a C-P4H(I)-dependent manner is interesting because this is a second mechanism, in addition to HIF-1-mediated transcriptional regulation, that cells under low oxygen stress can use to modulate gene expression. It is particularly intriguing that a critical enzyme in the miRNA biogenesis pathway, Dicer, is strongly suppressed under hypoxia not only in cultured PASMCs or U2OS cells but also in the lungs of rats treated with chronic hypoxia (2). Furthermore, a reduction of Dicer mRNA was observed in rat pulmonary artery fibroblasts after chronic hypoxia treatment (2), suggesting that downregulation of Dicer upon hypoxia treatment is not limited to a specific cell type. Thus, we speculate that the modulation of localization and activities of Ago2 serves as an alternative mechanism to augment miRNA-mediated gene regulation under a condition of limited amount of Dicer in the cell.

Consistent with our observation in PASMCs, miR-451 was reported as one of the few miRNAs significantly induced in lungs from rats treated with chronic hypoxia (2). Interestingly, similar to our result in PASMCs, lungs from rats exposed to

(C) miRNA analysis was conducted in the same cells used in panel B. Relative levels of miRNA expression normalized to U6 snRNA are presented by setting the miRNA expression levels of the si-Ctr under normoxia to 1. *, $P < 0.05$. (D) U2OS cells were transfected with vector (mock) or Ago2(WT) cDNA construct followed by treatment with normoxia (N) or hypoxia (H) for 24 h. Total cell lysates were subjected to immunoblot analysis using anti-Ago2, anti-C-P4Hα, anti-C-P4Hβ, or anti-β-actin (loading control) antibodies (left panel). By densitometry, relative amounts of Ago2 protein normalized to β-actin were quantitated and are presented (middle panel). Total RNAs were extracted from the same cells and subjected to qRT-PCR analysis of the indicated miRNAs. Relative levels of miRNA expression normalized to U6 snRNA are presented (right panel). (E) PASMCs were transfected with siRNA against C-P4Hα(I) (si-P4Hα) or nontargeting control (si-Ctr) for 48 h prior to treatment with normoxia or hypoxia for 24 h. Total RNAs were subjected to qRT-PCR analysis of the indicated miRNAs. Relative levels of miRNA expression normalized to U6 snRNA are presented by setting the miRNA expression levels of the si-Ctrl under normoxia to 1. *, $P < 0.05$. (F) miRNA analysis was conducted in PASMCs treated with mock (DMSO) or 0.1 μM geldanamycin (GA) for 1.5 h prior to exposure to normoxia or hypoxia for 24 h. Levels of expression of the indicated miRNAs normalized to U6 snRNA were measured, and fold induction (hypoxia/normoxia) is presented.

TABLE 1. List of miRNAs induced by hypoxia ≥1.5-fold compared to normoxia[a]

miRNA	Fold induction (hypoxia vs. normoxia)	miRNA	Fold induction (hypoxia vs. normoxia)
hsa-miR-576-3p	53.2234814	**hsa-miR-19a**	1.954962558
hsa-miR-383	21.13556796	**hsa-miR-493**	1.949407874
hsa-miR-199b-5p	16.46910188	hsa-miR-137	1.946221586
hsa-miR-425*	16.27652682	**hsa-miR-579**	1.933023232
hsa-miR-376a*	13.27867211	**hsa-miR-335**	1.930097833
hsa-miR-192	12.5246812	hsa-miR-340	1.92955742
hsa-miR-454*	12.12761518	hsa-miR-409-5p	1.909437868
hsa-miR-361-5p	6.138609836	**hsa-miR-494**	1.890645626
hsa-miR-500	5.780731148	**hsa-miR-204**	1.880614278
hsa-miR-181c	5.69543477	hsa-miR-20a	1.87133387
hsa-miR-431	5.500615181	**hsa-miR-128**	1.869917962
hsa-miR-363	4.348633054	**hsa-miR-106b**	1.854641029
hsa-miR-139-5p	4.243406757	**hsa-miR-495**	1.852372156
hsa-miR-589	4.029413817	hsa-miR-17	1.835091471
hsa-miR-301b	3.491318505	**hsa-miR-27a**	1.828833805
hsa-miR-135b	3.366347188	hsa-miR-886-5p	1.824078701
hsa-miR-198	3.304449565	**hsa-miR-126**	1.821881312
hsa-miR-369-5p	3.219712737	hsa-miR-125a-5p	1.799267857
hsa-miR-337-5p	3.187788638	hsa-miR-134	1.790975965
hsa-miR-221*	3.153091369	hsa-miR-132	1.780357512
hsa-miR-199a-5p	3.096923995	**hsa-miR-195**	1.760950037
hsa-miR-628-5p	3.033938784	hsa-miR-29c	1.760299579
hsa-miR-433	2.70462575	**hsa-miR-7-1***	1.756692865
hsa-miR-29a*	2.660408852	**hsa-miR-19b**	1.755060759
hsa-miR-302b	2.64615391	**hsa-miR-26a**	1.755036429
hsa-let-7d	2.531088542	hsa-miR-339-3p	1.741028689
hsa-miR-770-5p	2.485398137	hsa-miR-539	1.737625255
hsa-miR-212	2.478599159	hsa-miR-365	1.720979577
hsa-miR-660	2.449000344	**hsa-let-7e**	1.709293305
hsa-miR-138	2.442341563	**hsa-miR-130a**	1.708838405
hsa-miR-140-3p	2.402935588	**hsa-miR-27b**	1.696146726
hsa-miR-15b	2.399289054	**hsa-let-7c**	1.681050397
hsa-miR-125a-3p	2.38119204	**hsa-miR-18a**	1.662118194
hsa-miR-642	2.373083684	hsa-miR-140-5p	1.657469102
hsa-miR-29b	2.315532452	hsa-miR-34a	1.651985446
hsa-miR-221	2.313788469	**hsa-miR-15a***	1.649646582
hsa-miR-20b	2.272368763	hsa-miR-296-5p	1.643090536
hsa-miR-493*	2.239604488	hsa-miR-146b-5p	1.623858559
hsa-miR-26b	2.236613507	**hsa-miR-143**	1.6151498
hsa-miR-382	2.236390275	**hsa-miR-10a**	1.611821493
hsa-miR-130b*	2.210460534	**hsa-let-7b**	1.610126431
hsa-miR-16	2.20144069	**hsa-miR-7**	1.594098721
hsa-miR-597	2.141108605	hsa-miR-618	1.586598375
hsa-let-7g	2.101226925	hsa-miR-24	1.583246595
hsa-miR-93	2.092896513	**hsa-miR-376c**	1.573787742
hsa-miR-21	2.070173919	**hsa-miR-374b**	1.564888619
hsa-miR-455-3p	2.05066663	**hsa-miR-101**	1.550530577
hsa-miR-342-3p	2.031254454	**hsa-miR-106a**	1.549648461
hsa-miR-103	2.028426428	**hsa-miR-223**	1.520878577
hsa-miR-186	2.020715164	**hsa-miR-301a**	1.512485149
hsa-miR-362-3p	1.992525208	**hsa-miR-454**	1.504819007
hsa-miR-632	1.968282059	**hsa-miR-487b**	1.498771009
hsa-miR-20a*	1.966616942	hsa-miR-210	1.46457084
hsa-miR-455-5p	1.958946472		

[a] miRNAs whose induction was abolished (shaded and bolded) or reduced (shaded) when C-P4Hα was knocked down are indicated. Nonshaded miRNAs are those whose induction was not affected by C-P4Hα knockdown.

hypoxia also show a ~40% decrease in Dicer expression compared to normoxia-treated samples (2). These *in vivo* hypoxia results are consistent with our observation that under the condition when Dicer is repressed, miR-451 can be induced through activation of Ago2 because the maturation of miR-451, unlike those of other miRNAs, does not require Dicer. Decreased expression of Dicer is also observed in various pathological conditions, such as cancer (26, 27) and severe respiratory syncytial virus disease (20). It is intriguing to speculate that miR-451 and potentially other miRNAs that are processed by Ago2 might play a critical role during the pathogenesis of these disorders.

SGs are known to be sites where nontranslating mRNAs accumulate when cells experience various stresses, such as oxidative stress (e.g., arsenite), translational inhibition (e.g., hippuristanol), UV damage, osmotic stress, or heat shock (22).

More recently, Ago proteins were also found to localize to SGs in an miRNA-dependent manner (28). Therefore, the SG has been suggested to be a site where Ago2 and miRNAs actively silence target mRNAs (22). In this study, we demonstrated that hypoxia mediates the formation of SGs and translocation of Ago2 to SGs. Hypoxia-mediated SG formation is rapid and reaches a maximum level after 3 h and then gradually decreases by 24 h. Interestingly, the percentage of SG-positive cells after hypoxia, even at the time point of maximal SG formation, is ~10 to 15%, unlike after arsenite treatment, where nearly all cells form SGs (data not shown). This might suggest that (i) hypoxia-induced SGs have a quick turnover or (ii) hypoxia-induced SG formation is dependent on other conditions, such as cell cycle phase. Consistent with the latter possibility, SG formation mediated by UV damage was reported to occur only in G_1- and G_2-phase cells (40). Furthermore, we observed that cells exposed to arsenite formed SGs with an average of ~60 SGs/cell (data not shown), unlike those exposed to hypoxic stress, which formed an average of ~15 SGs/cell in less than 15% of cells (Fig. 3B, left panel). It was also evident that the SGs induced by hypoxia are substantially larger than the arsenite-induced SGs, suggesting that the components of SGs mediated by these two different stresses might be distinct. Despite differences in the number and size of SGs, nearly all of the Ago2 translocated to SGs upon either arsenite (data not shown) or hypoxia (Fig. 3C) treatment. However, localization of Ago2 to SGs alone is not sufficient for the increase in Ago2, Ago2 activities, or the accumulation of miRNAs, as arsenite treatment did not alter the mRNA or protein levels of Ago2 or C-P4H(I) and miRNA expression was reduced upon arsenite treatment (data not shown), rather than increased, as was observed for hypoxia treatment. Furthermore, both the miR-451 processing activity of Ago2 and RISC activity (data not shown) were decreased after arsenite treatment. Although SGs induced by different stresses mostly contain TIA-1, a number of studies have indicated that SGs are not all identical in terms of their protein contents. For example, heat shock-induced SGs contain Hsp27, while arsenite-induced SGs do not (23). Both arsenite-induced SGs and hypoxia-induced SGs are dependent on the phosphorylation of eIF2α (15, 32). In addition, colocalization of Ago2 with SGs induced by hippuristanol, an inhibitor of eIF4A, is miRNA dependent (28). Our observation that Ago2 colocalizes with arsenite-induced SGs but has no significant effect on Ago2 activities and accumulation of miRNAs may suggest that the Ago2 localized in arsenite-induced SGs lacks critical factors, such as miRNAs, target mRNAs, or proteins other than Ago2, that are required for RISC activity.

Ago proteins can also be found in the nucleus (12). Although the exact mechanism of Ago function in the nucleus is unclear, it is suggested that it might play a role in transcriptional gene silencing by guiding DNA or histone H3 lysine methylation (12). It is interesting to speculate that hypoxia-mediated prolyl-hydroxylation might also affect the nuclear functions of Ago proteins.

ACKNOWLEDGMENTS

We thank Eric Lai for the miR-144/451 expression construct. We also thank Tomoya Uchimura for technical support.

This work was supported by grants from the NHLBI (HL093154), LeDucq Foundation, and American Heart Association (to A.H.).

REFERENCES

1. **Camps, C., et al.** 2008. hsa-miR-210 is induced by hypoxia and is an independent prognostic factor in breast cancer. Clin. Cancer Res. **14:**1340–1348.
2. **Caruso, P., et al.** 2010. Dynamic changes in lung microRNA profiles during the development of pulmonary hypertension due to chronic hypoxia and monocrotaline. Arterioscler. Thromb. Vasc. Biol. **30:**716–723.
3. **Chan, M. C., et al.** 2010. Molecular basis for antagonism between PDGF and the TGFbeta family of signalling pathways by control of miR-24 expression. EMBO J. **29:**559–573.
4. **Cheloufi, S., C. O. Dos Santos, M. M. Chong, and G. J. Hannon.** 2010. A dicer-independent miRNA biogenesis pathway that requires Ago catalysis. Nature **465:**584–589.
5. **Cheng, Y., and C. Zhang.** 2010. MicroRNA-21 in cardiovascular disease. J. Cardiovasc. Transl. Res. **3:**251–255.
6. **Cowland, J. B., C. Hother, and K. Gronbaek.** 2007. MicroRNAs and cancer. APMIS **115:**1090–1106.
7. **Croce, C. M., and G. A. Calin.** 2005. miRNAs, cancer, and stem cell division. Cell **122:**6–7.
8. **Cullen, B. R.** 2006. Viruses and microRNAs. Nat. Genet. **38**(Suppl.)**:**S25–S30.
9. **Davis, B. N., A. C. Hilyard, G. Lagna, and A. Hata.** 2008. SMAD proteins control DROSHA-mediated microRNA maturation. Nature **454:**56–61.
10. **Davis, B. N., A. C. Hilyard, P. H. Nguyen, G. Lagna, and A. Hata.** 2009. Induction of microRNA-221 by platelet-derived growth factor signaling is critical for modulation of vascular smooth muscle phenotype. J. Biol. Chem. **284:**3728–3738.
11. **Eisenberg, I., M. S. Alexander, and L. M. Kunkel.** 2009. miRNAS in normal and diseased skeletal muscle. J. Cell Mol. Med. **13:**2–11.
12. **Ender, C., and G. Meister.** 2010. Argonaute proteins at a glance. J. Cell Sci. **123:**1819–1823.
13. **Fahling, M., et al.** 2006. Heterogeneous nuclear ribonucleoprotein-A2/B1 modulate collagen prolyl 4-hydroxylase, alpha (I) mRNA stability. J. Biol. Chem. **281:**9279–9286.
14. **Fahling, M., et al.** 2006. Translational control of collagen prolyl 4-hydroxylase-alpha(I) gene expression under hypoxia. J. Biol. Chem. **281:**26089–26101.
15. **Gardner, L. B.** 2008. Hypoxic inhibition of nonsense-mediated RNA decay regulates gene expression and the integrated stress response. Mol. Cell. Biol. **28:**3729–3741.
16. **Gorres, K. L., and R. T. Raines.** 2010. Prolyl 4-hydroxylase. Crit. Rev. Biochem. Mol. Biol. **45:**106–124.
17. **Harris, A. L.** 2002. Hypoxia—a key regulatory factor in tumour growth. Nat. Rev. Cancer **2:**38–47.
18. **Hirsila, M., P. Koivunen, V. Gunzler, K. I. Kivirikko, and J. Myllyharju.** 2003. Characterization of the human prolyl 4-hydroxylases that modify the hypoxia-inducible factor. J. Biol. Chem. **278:**30772–30780.
19. **Hofbauer, K. H., et al.** 2003. Oxygen tension regulates the expression of a group of procollagen hydroxylases. Eur. J. Biochem. **270:**4515–4522.
20. **Inchley, C. S., T. Sonerud, H. O. Fjaerli, and B. Nakstad.** 2011. Reduced Dicer expression in the cord blood of infants admitted with severe respiratory syncytial virus disease. BMC Infect. Dis. **11:**59.
21. **Iwasaki, S., et al.** 2010. Hsc70/Hsp90 chaperone machinery mediates ATP-dependent RISC loading of small RNA duplexes. Mol. Cell **39:**292–299.
22. **Kedersha, N., and P. Anderson.** 2007. Mammalian stress granules and processing bodies. Methods Enzymol. **431:**61–81.
23. **Kedersha, N. L., M. Gupta, W. Li, I. Miller, and P. Anderson.** 1999. RNA-binding proteins TIA-1 and TIAR link the phosphorylation of eIF-2 alpha to the assembly of mammalian stress granules. J. Cell Biol. **147:**1431–1442.
24. **Kim, V. N.** 2005. MicroRNA biogenesis: coordinated cropping and dicing. Nat. Rev. Mol. Cell Biol. **6:**376–385.
25. **Kulshreshtha, R., et al.** 2007. A microRNA signature of hypoxia. Mol. Cell. Biol. **27:**1859–1867.
26. **Kumar, M. S., J. Lu, K. L. Mercer, T. R. Golub, and T. Jacks.** 2007. Impaired microRNA processing enhances cellular transformation and tumorigenesis. Nat. Genet. **39:**673–677.
27. **Kumar, M. S., et al.** 2009. Dicer1 functions as a haploinsufficient tumor suppressor. Genes Dev. **23:**2700–2704.
28. **Leung, A. K., J. M. Calabrese, and P. A. Sharp.** 2006. Quantitative analysis of Argonaute protein reveals microRNA-dependent localization to stress granules. Proc. Natl. Acad. Sci. U. S. A. **103:**18125–18130.
29. **Leung, A. K., et al.** 2011. Poly(ADP-ribose) regulates stress responses and microRNA activity in the cytoplasm. Mol. Cell **42:**489–499.
30. **Levene, C. I., and C. J. Bates.** 1976. The effect of hypoxia on collagen synthesis in cultured 3T6 fibroblasts and its relationship to the mode of action of ascorbate. Biochim. Biophys. Acta **444:**446–452.
31. **Liu, C. J.** 2009. MicroRNAs in skeletogenesis. Front. Biosci. **14:**2757–2764.
32. **McEwen, E., et al.** 2005. Heme-regulated inhibitor kinase-mediated phosphorylation of eukaryotic translation initiation factor 2 inhibits translation,

induces stress granule formation, and mediates survival upon arsenite exposure. J. Biol. Chem. **280:**16925–16933.
33. **Minet, E., et al.** 1999. Hypoxia-induced activation of HIF-1: role of HIF-1alpha-Hsp90 interaction. FEBS Lett. **460:**251–256.
34. **Myllyharju, J.** 2008. Prolyl 4-hydroxylases, key enzymes in the synthesis of collagens and regulation of the response to hypoxia, and their roles as treatment targets. Ann. Med. **40:**402–417.
35. **Myllyharju, J., and K. I. Kivirikko.** 2004. Collagens, modifying enzymes and their mutations in humans, flies and worms. Trends Genet. **20:**33–43.
36. **Naeije, R., and B. Rondelet.** 2004. Pathobiology of pulmonary arterial hypertension. Bull. Mem. Acad. R. Med. Belg. **159:**219–226.
37. **Owens, G. K., M. S. Kumar, and B. R. Wamhoff.** 2004. Molecular regulation of vascular smooth muscle cell differentiation in development and disease. Physiol. Rev. **84:**767–801.
38. **Pare, J. M., et al.** 2009. Hsp90 regulates the function of argonaute 2 and its recruitment to stress granules and P-bodies. Mol. Biol. Cell **20:**3273–3284.
39. **Perhonen, M., X. Han, W. Wang, J. Karpakka, and T. E. Takala.** 1996. Skeletal muscle collagen type I and III mRNA, [corrected] prolyl 4-hydroxylase, and collagen in hypobaric trained rats. J. Appl. Physiol. **80:**2226–2233.
40. **Pothof, J., N. S. Verkaik, I. W. van IJcken, et al.** 2009. MicroRNA-mediated gene silencing modulates the UV-induced DNA-damage response. EMBO J. **28:**2090–2099.
41. **Preston, I. R., N. S. Hill, R. R. Warburton, and B. L. Fanburg.** 2006. Role of 12-lipoxygenase in hypoxia-induced rat pulmonary artery smooth muscle cell proliferation. Am. J. Physiol. Lung Cell. Mol. Physiol. **290:**L367–L374.
42. **Qi, H. H., et al.** 2008. Prolyl 4-hydroxylation regulates Argonaute 2 stability. Nature **455:**421–424.
43. **Rich, S., et al.** 1987. Primary pulmonary hypertension. A national prospective study. Ann. Intern. Med. **107:**216–223.
44. **Semenza, G. L.** 2009. Regulation of oxygen homeostasis by hypoxia-inducible factor 1. Physiology (Bethesda) **24:**97–106.
45. **Shu, C. W., N. L. Cheng, W. M. Chang, T. L. Tseng, and Y. K. Lai.** 2005. Transactivation of hsp70-1/2 in geldanamycin-treated human non-small cell lung cancer H460 cells: involvement of intracellular calcium and protein kinase C. J. Cell. Biochem. **94:**1199–1209.
46. **Siomi, H., and M. C. Siomi.** 2010. Posttranscriptional regulation of microRNA biogenesis in animals. Mol. Cell **38:**323–332.
47. **Stenmark, K. R., B. Meyrick, N. Galie, W. J. Mooi, and I. F. McMurtry.** 2009. Animal models of pulmonary arterial hypertension: the hope for etiological discovery and pharmacological cure. Am. J. Physiol. Lung Cell. Mol. Physiol. **297:**L1013–L1032.
48. **Tahbaz, N., J. B. Carmichael, and T. C. Hobman.** 2001. GERp95 belongs to a family of signal-transducing proteins and requires Hsp90 activity for stability and Golgi localization. J. Biol. Chem. **276:**43294–43299.
49. **Takahashi, Y., S. Takahashi, Y. Shiga, T. Yoshimi, and T. Miura.** 2000. Hypoxic induction of prolyl 4-hydroxylase alpha (I) in cultured cells. J. Biol. Chem. **275:**14139–14146.
50. **Tsuji-Naito, K., S. Ishikura, M. Akagawa, and H. Saeki.** 2010. α-Lipoic acid induces collagen biosynthesis involving prolyl hydroxylase expression via activation of TGF-β-Smad signaling in human dermal fibroblasts. Connect. Tissue Res. **51:**378–387.
51. **Yang, J. S., et al.** 2010. Conserved vertebrate mir-451 provides a platform for Dicer-independent, Ago2-mediated microRNA biogenesis. Proc. Natl. Acad. Sci. U. S. A. **107:**15163–15168.

The EMBO Journal (2010) 29, 559–573 | © 2010 European Molecular Biology Organization | All Rights Reserved 0261-4189/10
www.embojournal.org

THE EMBO JOURNAL

Molecular basis for antagonism between PDGF and the TGFβ family of signalling pathways by control of miR-24 expression

Mun Chun Chan[1], Aaron C Hilyard[1], Connie Wu[2], Brandi N Davis[2], Nicholas S Hill[3], Ashish Lal[4], Judy Lieberman[4], Giorgio Lagna[1] and Akiko Hata[1,2,*]

[1]Molecular Cardiology Research Institute, Tufts Medical Center, Boston, MA, USA, [2]Department of Biochemistry, Tufts University School of Medicine, Boston, MA, USA, [3]Pulmonary, Critical Care, and Sleep Division, Tufts Medical Center, Boston, MA, USA and [4]Immune Disease Institute and Program in Cellular and Molecular Medicine, Children's Hospital Boston, Harvard Medical School, Boston, MA, USA

Modulation of the vascular smooth-muscle-cell (vSMC) phenotype from a quiescent 'contractile' phenotype to a proliferative 'synthetic' phenotype has been implicated in vascular injury repair, as well as pathogenesis of vascular proliferative diseases. Both bone morphogenetic protein (BMP) and transforming growth factor-β (TGFβ)-signalling pathways promote a contractile phenotype, while the platelet-derived growth factor-BB (PDGF-BB)-signalling pathway promotes a switch to the synthetic phenotype. Here we show that PDGF-BB induces microRNA-24 (miR-24), which in turn leads to downregulation of Tribbles-like protein-3 (Trb3). Repression of Trb3 coincides with reduced expression of Smad proteins and decrease in BMP and TGFβ signalling, promoting a synthetic phenotype in vSMCs. Inhibition of miR-24 by antisense oligonuclotides abrogates the downregulation of Trb3 as well as pro-synthetic activity of the PDGF-signalling pathway. Thus, this study provides a molecular basis for the antagonism between the PDGF and TGFβ pathways, and its effect on the control of the vSMC phenotype.
The EMBO Journal (2010) **29,** 559–573. doi:10.1038/emboj.2009.370; Published online 17 December 2009
Subject Categories: signal transduction; differentiation & death
Keywords: BMP; microRNA; PDGF; TGFβ; vascular smooth-muscle cell

Introduction

During embryonic development, the transforming growth factor-β (TGFβ) and BMP pathways play multiple essential roles in the induction of ventral mesoderm (Davidson and Zon, 2000), cardiac myogenesis (Monzen *et al*, 2002; Schneider *et al*, 2003), vasculogenesis (Moser and Patterson, 2005), and angiogenesis. Targeted inactivation of BMP-signal transducers Smad1 and Smad5 produces a severe vascular phenotype (Moser and Patterson, 2005). TGFβ1- or TGFβ2-null mice die prematurely due to vascular defects. Proliferative and obliterative vascular diseases such as atherosclerosis, post-angioplasty restenosis, lymphangioleiomyomatosis (LAM), and pulmonary arterial hypertension (PAH) share common pathological characteristics, including abnormal proliferation and migration of vascular smooth-muscle-cells (vSMCs), and decrease in their ability to contract. In response to vascular injury, vSMCs undergo a unique process known as 'phenotype modulation': transition from a quiescent, 'contractile' phenotype to a proliferative, 'synthetic' state (Owens, 1995; Owens *et al*, 2004). Phenotypic plasticity is essential for vascular development and vascular remodelling after injury. However, an aberrant switch from a contractile to synthetic phenotype, characterized by proliferation and transformation into myofibroblasts, is a mechanism underlying the formation of plexiform lesions as well as various proliferative vascular disorders (Smith *et al*, 1990; Yi *et al*, 2000). It was shown that TGFβs and BMPs are able to inhibit vSMC proliferation and migration, and stimulate the expression of contractile vSMC markers, such as smooth-muscle α-actin (SMA), calponin-1 (CNN), and SM22α (SM22) (Misiakos *et al*, 2001; Guo *et al*, 2004; Lagna *et al*, 2007). Loss-of-function mutations of genes encoding receptors of TGFβs and BMPs have been linked to vascular disorders such as idiopathic PAH (IPAH) and hereditary hemorrhagic telangiectasia (ten Dijke and Arthur, 2007). Altogether, these results support the hypothesis that inhibition of TGFβ or BMP signalling plays an important role in the pathogenesis of proliferative and obliterative vascular diseases.

Unlike TGFβs and BMPs, platelet-derived growth factors (PDGFs) potently mediate a switch from a contractile to synthetic phenotype characterized by downregulation of vSMC marker gene expression as well as increased proliferation and migration (Owens *et al*, 2004; Lagna *et al*, 2007). Platelet-derived growth factor-BB (PDGF-BB) is able to counteract the contractile activity of TGFβ and BMP signalling, and inhibit contractile gene expression in vSMCs (Lagna *et al*, 2007). Elevated expression of proteins in the PDGF-signalling pathway is found in various cardiovascular disorders and vascular injuries, including atherosclerosis and restenosis (Andrae *et al*, 2008). PDGF released from platelets and endothelial cells at sites of vascular injury is thought to be a contributing factor to atherosclerosis (McNamara *et al*, 1996). Inhibition of PDGF signalling by the PDGF receptor (PDGFR) kinase inhibitor, imatinib mesylate (Gleevec) reduced atherosclerosis development, suggesting critical involvement of the PDGF pathway in vascular proliferative disorders (Andrae *et al*, 2008). However, the exact mechanism by which the PDGF pathway contributes to vascular disease remains unclear.

*Corresponding author. Molecular Cardiology Research Institute, Tufts Medical Center, 800 Washington Street, Box 8486, Boston, MA 02111, USA. Tel.: +1 617 636 0614; Fax: +1 617 636 5649;
E-mail: akiko.hata@tufts.edu

Received: 26 May 2009; accepted: 6 November 2009; published online: 17 December 2009

We recently reported that both TGFβ and BMP signals induce several small non-coding RNAs of the microRNA (miRNA) family, including miR-21, in vSMCs. miR-21 binds to the 3′-untranslated region (UTR) of programmed cell death-4 (PDCD4) mRNA, promoting degradation of PDCD4 mRNA and induction of vSMC contractile genes (Davis *et al*, 2008). The BMP pathway also activates the transcription of contractile genes by promoting nuclear translocation of two members of the myocardin (Myocd) family of transcription factors, MRTF-A and MRTF-B (Lagna *et al*, 2007), both potent transcription activators of vSMC-specific contractile genes containing CArG box (CC $(A/T)_6GG$) sequences in their promoter regions (Li *et al*, 2006; Kuwahara *et al*, 2007; Medjkane *et al*, 2009). In contrast, PDGF-BB suppresses the expression of Myocd or inhibits Myocd binding to the CArG box and abolishes vSMC gene transcription (Yoshida *et al*, 2007). Our study indicates that PDGF-BB also induces the expression of miR-221 (miR-221) in vSMCs (Davis *et al*, 2009). miR-221 targets the 3′-UTR of c-Kit and p27Kip1 mRNAs, and downregulates the expression of these proteins. Downregulation of c-Kit decreases Myocd protein and vSMC-specific genes, while downreguation of p27Kip1 promotes proliferation (Davis *et al*, 2009). Although TGFβ/BMP and the PDGF pathways have opposing effects on various aspects of vSMC phenotype modulation, direct crosstalk between these pathways has not been investigated. In this study, we demonstrate that PDGF-BB induces miR-24 (miR-24) in vSMCs. We show that miR-24 targets Tribbles-like protein-3 (Trb3) mRNA and downregulates its expression. Trb3 was previously identified as a protein that interacts with type-II BMP receptor (BMPRII) through a domain that is frequently mutated in familial IPAH patients (Chan *et al*, 2007). Trb3 promotes degradation of Smad ubiquitin-regulatory factor-1 (Smurf1), a negative regulator of BMP and TGFβ Smad-dependent signalling (Chan *et al*, 2007). In concurrence with our previous result, we find that PDGF-miR-24-mediated downregulation of Trb3 in vSMCs results in decreased Smad protein levels and vSMC contractile gene expression. Inhibition of miR-24 function in vSMCs prevents cells from switching to a synthetic phenotype upon PDGF-BB treatment. Thus, we propose that miR-24 is a key regulator of the crosstalk between the pro-contractile TGFβ/BMP signal and the pro-synthetic PDGF signal.

Results

PDGF-BB inhibits the BMP-mediated contractile phenotype

Human primary pulmonary smooth-muscle cells (PASMCs) were treated with BMP4 alone, PDGF-BB alone, or both BMP4 and PDGF-BB. The change in vSMC phenotype was evaluated by measuring the level of expression of vSMC-specific contractile gene markers, such as SMA, CNN and SM22; cell proliferation; and collagen lattice contraction.

As reported previously (Lagna *et al*, 2007), BMP4 induces SMA, CNN, and SM22, and PDGF-BB reduces their expression both at the mRNA (Figure 1A, top panel) and protein level (Figure 1A, bottom panel). When cells were treated with both BMP4 and PDGF-BB, no vSMC marker induction was observed, indicating an antagonism between BMP4 and PDGF-BB (Figure 1A, SMA, CNN, or SM22). Induction of a direct BMP target gene, *Id3*, whose expression was elevated ~4-fold after 6 h treatment with BMP4, was significantly reduced by co-stimulation with BMP4 and PDGF (Figure 1A, Id3).

The level of deformation (contraction) of collagen lattices can be affected by reorganization of actin or in response to contractile stimuli such as BMP4 in vSMCs (Neuman *et al*, 2009). To examine whether the change in vSMC markers shown in Figure 1A affects the contractility of the cells, PASMCs were treated with BMP4, PDGF-BB, or both for 24 h and the size of the collagen gel was measured 24 h after it was released from the culture plate wall. BMP4 treatment reduced the size of collagen lattice to 73%, indicating that BMP4 elevates collagen contraction, presumably through increased expression of contractile gene markers (Figure 1B). PDGF-BB treatment did not affect the gel size at a detectable level (Figure 1B). However, when PDGF-BB was added with BMP4, no significant contraction was observed (Figure 1B). Similarly, BMP4-induced cell growth inhibition (about 50%) was reversed by co-treatment with PDGF-BB (Figure 1C). Altogether, these results indicate that PDGF-BB exerts an antagonizing effect on the BMP pathway, potentially by affecting its basic signalling machinery.

Downregulation of Trb3 upon PDGF-BB stimulation

Trb3 can act as an important modulator of the BMP-signalling pathway by regulating the expression level of Smad signal-transducing proteins (Chan *et al*, 2007). Furthermore, changes in the level of Trb3 in vSMCs affects the vSMC phenotype (Chan *et al*, 2007). Therefore, we examined potential modulation of Trb3 upon PDGF-BB stimulation. In a time-course experiment, we monitored the change in Trb3 mRNA by semi-quantitative RT–PCR (qRT–PCR) upon PDGF-BB or BMP4 treatment in PASMCs (Figure 2A). Trb3 mRNA decreased after 8 h and stayed low up to 72 h after PDGF-BB treatment (Figure 2A, and data not shown). BMP4 treatment alone had no effect on Trb3 mRNA expression (Figure 2A). In agreement with the mRNA level, Trb3 protein was reduced by PDGF-BB treatment after 4 h and further reduced after 24 h in PASMCs (Figure 2B). Immunofluorescence staining of PASMCs indicated that PDGF-BB reduces the expression of Trb3 and of the contractile marker SMA (Figure 2C). Downregulation of Trb3 protein and mRNA by PDGF was also confirmed in the rat PASMC line PAC1 (Supplementary Figure S1). We previously reported that downregulation of Trb3 results in reduction of Smad signal transducers for both the BMP- and TGFβ-signalling pathway (Chan *et al*, 2007). We examined whether PDGF-BB treatment reduces BMP-specific Smad1 (Figure 2D, left panel) or TGFβ-specific Smad2 and Smad3 (Figure 2D, right panel) by immunoblot analysis. BMP4 or TGFβ treatment did not significantly affect Trb3 or Smad levels (Figure 2D). PDGF-BB stimulation, however, dramatically reduced both Trb3 and Smad protein (Figure 2D). Anti-phospho-Smad1/5 or anti-phospho-Smad2 antibody immunoblots indicate robust induction of phosphorylation of Smads upon BMP4 or TGFβ treatment (Figure 2D). Co-treatment with PDGF-BB and BMP4 or TGFβ resulted in significant reduction in phospho-Smad levels, due to decreased total Smad protein (Figure 2D). These results suggest that PDGF-BB may in part antagonize the BMP or TGFβ pathways by decreasing Trb3 expression, which leads to downregulation of Smad signal transducers.

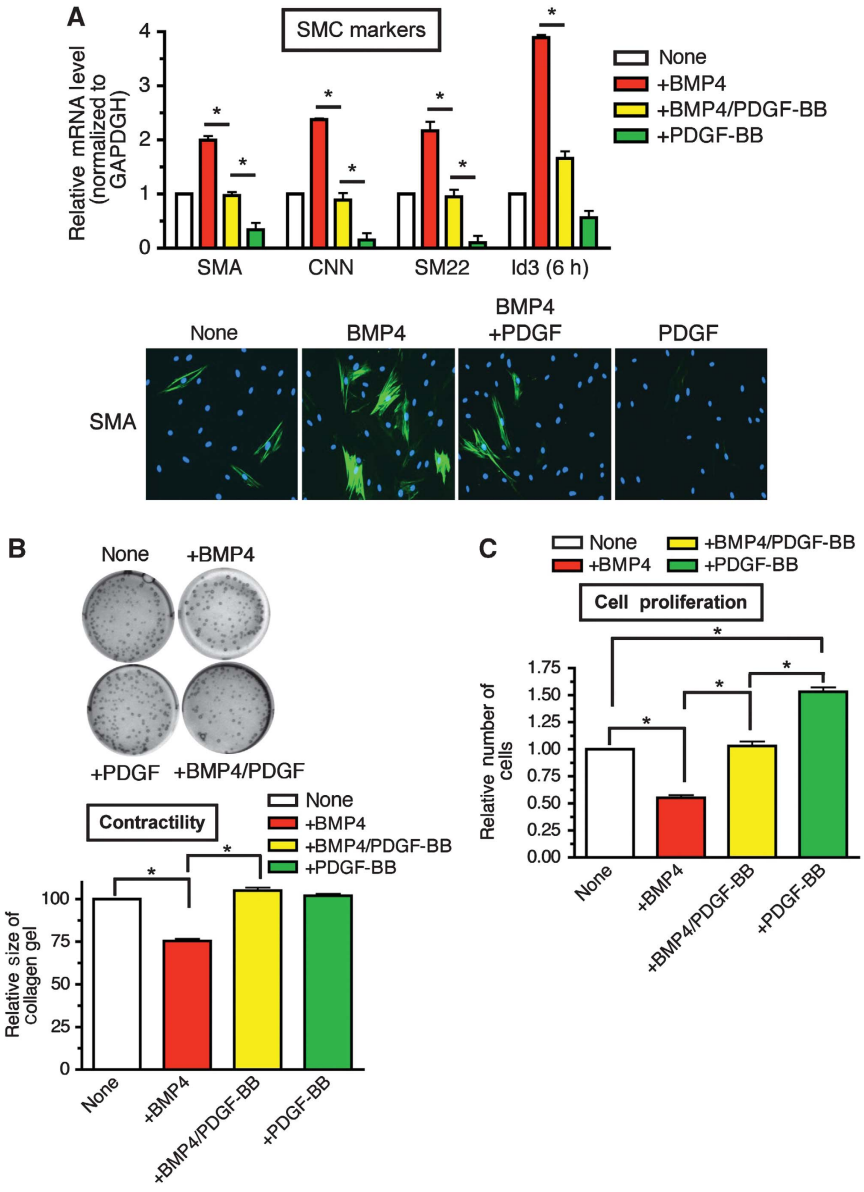

Figure 1 PDGF-BB inhibits BMP-mediated contractile phenotype in PASMCs. (**A**) Human PASMCs were treated with 3 nM BMP-4 alone (+BMP4), both 3 nM BMP4 and 20 ng/ml PDGF-BB (+BMP4/PDGF-BB), or 20 ng/ml PDGF-BB alone (+PDGF-BB) for 24 h (for vSMC markers) or 6 h (for Id3), followed by qRT–PCR (top panel) and immunofluorescence staining (bottom panel). The relative mRNA levels of vSMC markers SMA, CNN, or SM22, as well as the BMP-target gene Id3, were examined by qRT–PCR. Results were normalized to GAPDH expression, and the relative mRNA levels are presented as means ± s.e.m., with each experiment conducted in triplicate ($n=3$) (top panel). The difference between two results indicated by asterisks is statistically significant; $^*P<0.001$. Immunofluorescence staining was performed with FITC-conjugated anti-SMA antibody (green) and by DAPI staining (blue) (bottom panel). (**B**) PASMCs were treated with 3 nM BMP4, 20 ng/ml PDGF-BB, or both for 24 h prior to being embedded to collagen gel lattices. Twenty-four hours after the collagen lattices were dissociated from the dish, gel contraction was photographed by using a digital camera (top panel). The area of the gel lattices was determined with the ImageJ software, and the relative lattice area was obtained by dividing the area at each time point by the initial area of the well (bottom panel). Experiments were performed three times. Data represent the means ± s.e.m.; $^*P<0.01$. (**C**) PASMCs were starved for 24 h, followed by treatment with BMP4, PDGF-BB, or both for 48 h. Cells were tryspinized and counted using a haemocytometer. The relative number of cells compared with untreated cells was plotted as means ± s.e.m. ($n=3$); $^*P<0.01$.

Trb3 is a novel target of miR-24

Next we investigated the mechanism by which PDGF-BB downregulates Trb3. The activity of a *Trb3* promoter–luciferase-reporter construct, which contains a ~1.9-kb region of the human Trb3 gene promoter (Ohoka *et al*, 2005), was not affected by PDGF-BB treatment (Supplementary Figure S2A). Furthermore, the transcription rate of Trb3 gene was not altered by PDGF treatment (Supplementary Figure S2B). It is likely that PDGF-BB controls Trb3 mRNA level through a mechanism other than transcriptional regulation. As an alternative mechanism, we examined miRNA-mediated downregulation of *Trb3*. Computational analysis by TargetScan5.1 predicted that the 3′-UTR of the *Trb3* transcript contains an 8-mer miR-24 seed sequence at a position 78–84 nucleotides after the stop codon, which is phylogenetically conserved among mammals (Figure 3A, upper panel). To examine whether miR-24 can downregulate Trb3 mRNA expression in vSMCs, three different doses of chemically

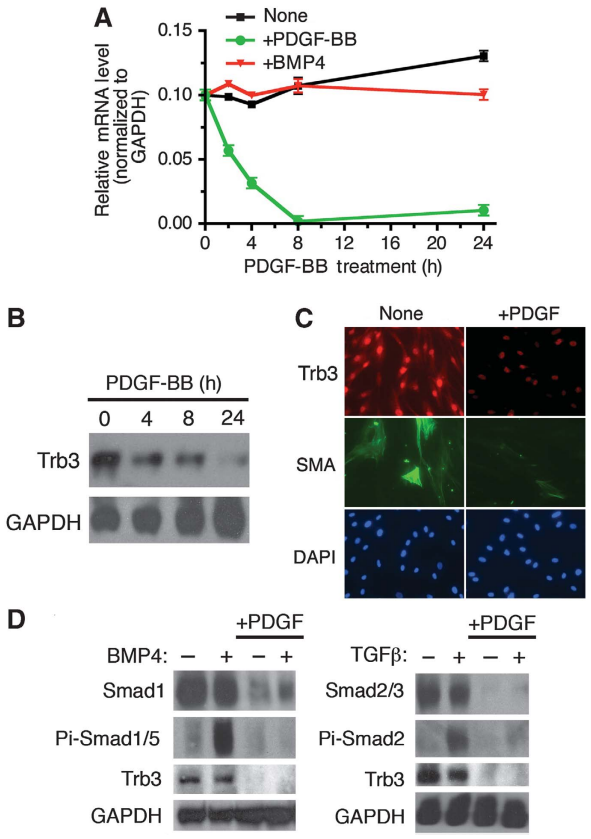

Figure 2 PDGF-BB stimulation decreases Trb3 expression. (**A**) PASMCs were stimulated with 3 nM BMP-4 or 20 ng/ml PDGF-BB for 2, 4, 8, or 24 h and subjected to qRT–PCR analysis. Relative expression of Trb3 mRNA normalized to GAPDH is plotted. (**B**) PASMCs were treated with 20 ng/ml PDGF-BB for 4, 8, or 24 h. Cells were harvested and subjected to immunoblot analysis using anti-human Trb3 antibody and anti-GAPDH antibody used as loading control. The results are representative of three independent experiments. (**C**) PASMCs were treated with 20 ng/ml PDGF-BB for 24 h and then subjected to immunofluorescence staining using anti-hTrb3 antibody conjugated to Cy3 (red), anti-SMA antibody conjugated to FITC (green), and by DAPI staining (blue). (**D**) Whole-cell lysates from PASMCs treated with 3 nM BMP4 or 100 pM TGFβ1 for 0.5 h, 20 ng/ml PDGF-BB for 4 h, or stimulated with PDGF-BB for 4 h followed by BMP4 or TGFβ1 for 0.5 h were subjected to immunoblot analysis using anti-Smad1, anti-Smad2/3, anti-phospho-Smad-1/5 (Pi-Smad1/5), or anti-phospho-Smad2 (Pi-Smad2) antibody; anti-hTrb3 antibody; or anti-GAPDH antibody (loading control). The experiment was repeated twice, with similar results.

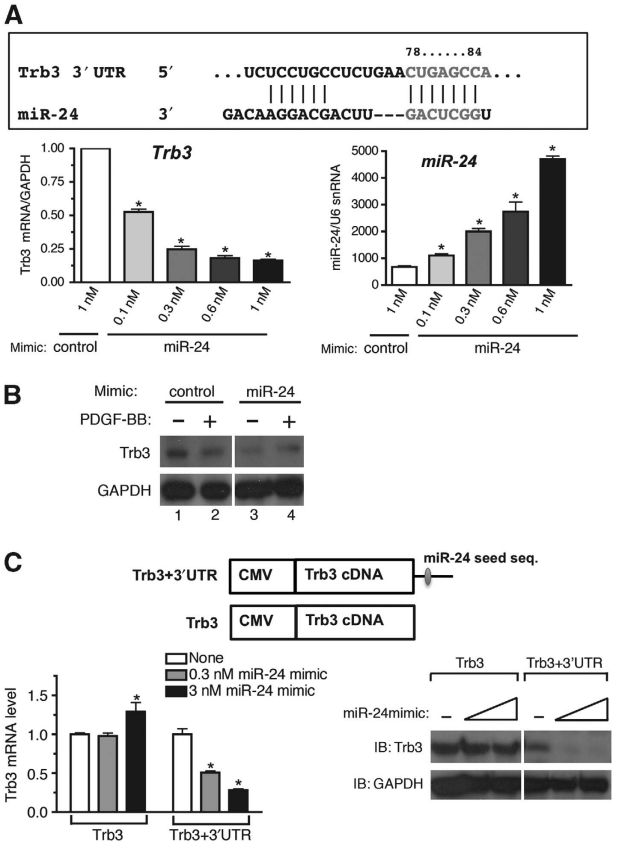

Figure 3 miR-24 leads to downregulation of Trb3. (**A**) A schematic representation of the miR-24-targeting site in the 3′-UTR Trb3 transcripts (top panel). The conserved 8-mer seed sequence is shown in grey. PASMCs were transfected with 1 nM non-specific (GFP) mimic (control) or increasing amounts (0.1, 0.3, 0.6, or 1 nM) of chemically modified, synthetic miR-24 oligonucleotides (miR-24 mimic). Twenty-four hours after transfection of mimic, cells were harvested and subjected to qRT–PCR analysis. Relative Trb3 mRNA level normalized to GAPDH (bottom left), as well as levels of mature miR-24 normalized to U6 snRNA (bottom right), is plotted as means ± s.e.m. ($n=3$); $^*P<0.001$ (versus the expression levels of control-transfected PASMCs). (**B**) PASMCs were transfected with 0.3 nM control mimic or 0.3 nM miR-24 mimic. Twenty-four hours after transfection of mimic, cells were stimulated with 20 ng/ml PDGF-BB for 6 h and subjected to immunoblot analysis with anti-hTrb3 antibody or anti-GAPDH antibody (loading control). The experiment was repeated three times, with similar results. (**C**) Cos7 cells were transfected with a construct carrying the human Trb3 cDNA construct with the 3′-UTR, which includes the miR-24 seed sequence (Trb3 + 3′-UTR) or deleted in the 3′-UTR (Trb3), with increasing amounts of miR-24 mimic (0.3 or 3 nM). Cells were harvested and subjected to qRT–PCR analysis (left panel) and immunoblot analysis (right panel). Relative Trb3 mRNA expression normalized to GAPDH is plotted ($n=3$); $^*P<0.001$ (compared with no miR-24 mimic transfection (white bar) of each set). Immunoblot analysis was performed using anti-hTrb3 antibody and anti-GAPDH antibody used as loading control. The immunoblot presented is representative of three independent experiments. A full-colour version of this figure is available at *The EMBO Journal* Online.

modified, synthetic miR-24 oligonucleotides (miR-24 mimic) were transfected into PASMCs, followed by qRT–PCR analysis of Trb3 mRNA. Increasing amounts of miR-24 mimic (about 1.6, 3.0, 4.0, and 7.0 times the endogenous miR-24 level) were expressed in PASMCs (Figure 3A, right panel). Under these conditions, Trb3 mRNA level was reduced to an average of 52, 24, 18, and 16% of the basal level, respectively (Figure 3A, left panel), suggesting that miR-24 targets Trb3 mRNA and leads to its degradation. Next, miR-24 mimic or control mimic were transfected into PASMCs, followed by 24-h PDGF-BB treatment and Trb3 protein immunoblot analysis. The miR-24 mimic alone significantly reduced Trb3 protein to a level lower than that in PDGF-BB-treated cells with the control mimic (Figure 3B, lanes 2 and 3). In the presence of miR-24 mimic, PDGF-BB did not further reduce Trb3 (Figure 3B, lanes 3 and 4). To examine whether miR-24 targets the predicted miR-24 seed sequence in the 3′-UTR of Trb mRNA, a Trb3 cDNA expression construct with or without the 3′-UTR sequence was generated (Figure 3C, top panel) and transfected into Cos7 cells. The effect of miR-24 mimic on the expression of the two different constructs was examined by qRT–PCR and immunoblot analyses. As shown in Figure 3C, miR-24 mimic dose dependently suppressed both mRNA (Figure 3C, left panel) and protein (Figure 3C, right

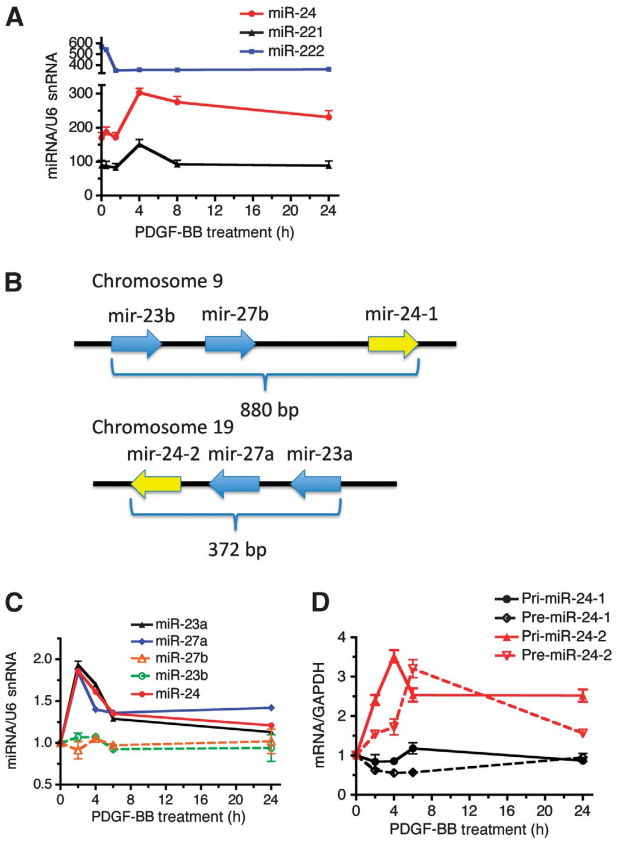

Figure 4 PDGF-BB induces miR-24 expression. (**A**) PASMCs were stimulated with 20 ng/ml of PDGF-BB for 1, 2, 4, 8, or 24 h, followed by qRT–PCR to determine the expression of miR-24, miR-221, and miR-222. The expression of individual miRNA normalized to U6 snRNA is plotted (means ± s.e.m., $n = 3$). (**B**) A schematic representation of the miR-24-1 gene cluster on human chromosome-9, which includes miR-23b and miR-27b, and the miR-24-2 gene cluster on human chromosome-19, which includes miR-27a and miR-23a. (**C**) PASMCs were treated with PDGF-BB for 2, 4, 6, or 24 h, followed by qRT–PCR analysis using primers for miR-23a, miR-27a, miR-27b, miR-23b, or miR-24. The time-course change in the expression of miRNA normalized to U6 snRNA after PDGF-BB stimulation is plotted (means ± s.e.m., $n = 3$). (**D**) PASMCs were treated with PDGF-BB for 2, 4, 6, or 24 h, followed by qRT–PCR analysis of primary transcripts of miR-24-1 (Pri-miR-24-1), primary transcripts of miR-24-2 (Pri-miR-24-2), intermediate products of miR-24-1 (Pre-miR 24-1), and intermediate products of miR-24-2 (Pre-miR-24-2). The time-course change in the expression of RNAs was normalized to GAPDH and plotted (means ± s.e.m., $n = 3$).

panel) expression from the construct containing the 3′-UTR (Figure 3C, Trb3 + 3′-UTR). No change in Trb3 mRNA or protein was observed when the 3′-UTR was missing (Figure 3C, Trb3), indicating that the 3′-UTR, and presumably the miR-24 seed sequence contained in it, is essential for downregulation of Trb3 by miR-24.

PDGF-BB induces miR-24-2 transcription

We speculated that PDGF-BB might downregulate Trb3 by inducing the expression of miR-24 in PASMCs. We recorded a time-course profile of the expression of miR-24 as well as miR-221, which was previously found to be induced by PDGF-BB (Davis *et al*, 2009), in PASMCs after PDGF-BB treatment (Figure 4A, black line). miR-222 serves as a negative control as its expression is not regulated by PDGF-BB (Davis *et al*, 2009) (Figure 4A, blue line). miR-24 was induced about 1.5-fold 4 h after PDGF-BB treatment and remained above the basal level up to 24 h, similar to miR-221 (Figure 4A, red line). This is consistent with the result that Trb3 mRNA level decreases to approximately 25% of the basal level within 4 h after PDGF-BB treatment (Figure 2A). The miR-24 gene is encoded in a gene cluster comprising miR-27 and miR-23 within a genomic region of less than 900 bp. There are two copies of the miR-24 gene cluster; one located on chromosome-9 (miR-24-1 gene cluster, encoding miR-24-1, miR-23b, and miR-27b) and the other on chromosome-19 (miR-24-2 gene cluster, coding for miR-24-2, miR-23a, and miR-27a) (Figure 4B). The sequences of miR-24-1 and miR-24-2 are identical and indistinguishable by qRT–PCR analysis, while sequences of miR-23a and miR-23b, or miR-27a and miR-27b are different. To determine whether both miR-24-1 and miR-24-2 are similarly regulated by PDGF-BB, the levels of the two variants of miR-23 and miR-27 were examined individually by qRT–PCR (Figure 4C). The miRNAs in the miR-24-2 gene cluster (miR-23a and miR-27a) were induced ~2-fold by PDGF-BB, similar to miR-24 (Figure 4C). By contrast, miR-23b (Figure 4C, green dotted line) and miR-27b (Figure 4C, orange dotted line) were not altered by PDGF-BB treatment. These results indicate that the miR-24-2 cluster, but not miR-24-1 cluster, is regulated by PDGF-BB. To examine which step of miR-24-2 biogenesis is regulated by PDGF-BB, we examined the level of miR-24 primary transcripts (Pri-miR-24-2) and the first processing product (Pre-miR-24-2) after PDGF-BB treatment. These precursor RNAs are sufficiently distinct for miR-24-1 and miR-24-2 to be distinguishable by RT–PCR. Induction of both Pri-miR-24-2 (~3.5 fold) and Pre-miR-24-2 (~3.2-fold) was observed within 2–4 h after PDGF treatment, suggesting that the miR-24-2 gene cluster is regulated by the PDGF pathway at the transcriptional level (Figure 4D, red solid and dotted lines). The expression of neither Pri-miR-24-1 nor Pre-miR-24-1 was altered by PDGF-BB treatment (Figure 4D, black solid and dotted lines), confirming that PDGF-BB does not modulate the expression of the miR-24-1 gene cluster.

miR-24 is a critical mediator of the pro-synthetic activity of PDGF-BB

To investigate the potential role of miR-24 in the PDGF-mediated downregulation of Trb3, 2′-*O*-methyl-modified RNA oligonucleotides complementary to the miR-24 sequence (anti-miR-24) were transfected into PASMCs to inhibit endogenous miR-24, and the levels of Trb3 and the vSMC marker SMA were examined. Transfection of 50 nM anti-miR-24 decreased endogenous miR-24 level by approximately 60% (Figure 5A, right panel). Induction of miR-24 by PDGF-BB was significantly reduced by anti-miR-24 transfection in comparison with cells transfected with control oligonucleotides (anti-GFP) (Figure 5A, right panel). In control cells, PDGF-BB treatment decreased Trb3 mRNA expression by approximately 50% (Figure 5A, left panel). In anti-miR-24-transfected cells, however, the level of Trb3 was slightly increased (~10%) as compared with the basal level and not significantly decreased by PDGF-BB, suggesting that PDGF-BB is unable to downregulate Trb3 when expression of endogenous miR-24 is impaired (Figure 5A, left panel). Similarly, the ability of PDGF-BB to reduce SMA expression was decreased in the presence of anti-miR-24 (Figure 5A, left panel). These results indicate that miR-24 plays a critical

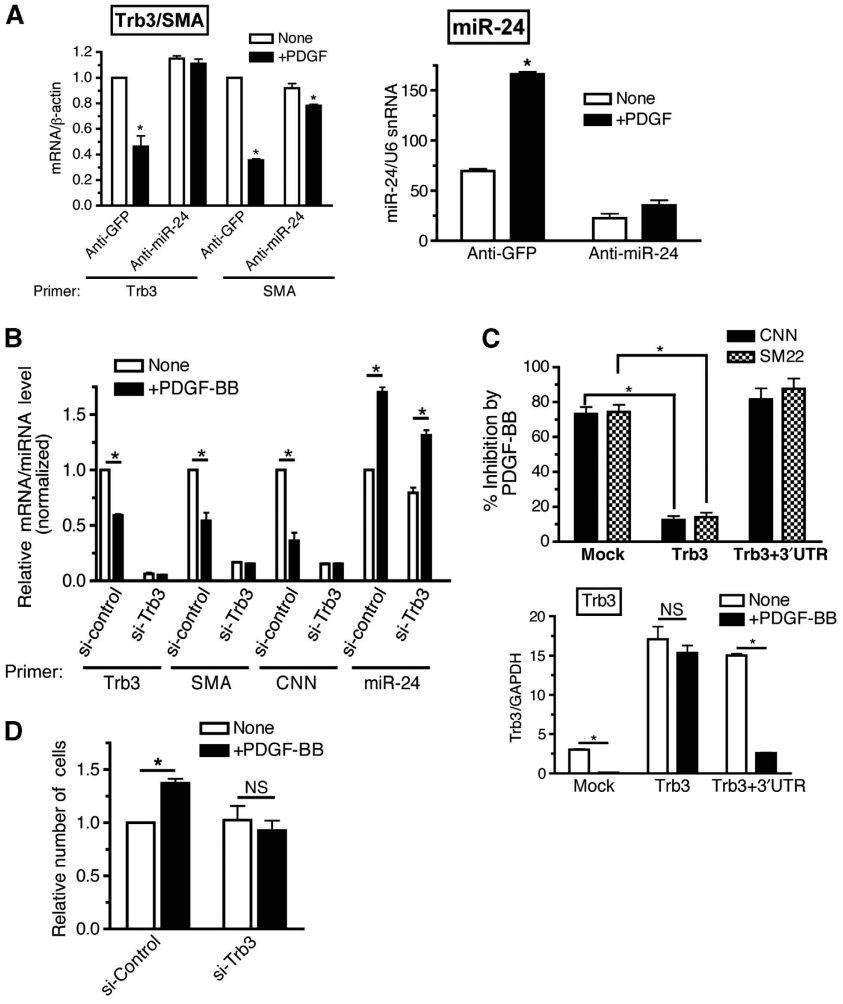

Figure 5 miR-24 expression is crucial for PDGF-BB downregulation of Trb3. (**A**) PASMCs were transfected with 50 nM control antisense (anti-GFP) or anti-miR-24 (anti-miR-24), followed by stimulation with or without 20 ng/ml of PDGF-BB (+PDGF) for 24 h. qRT–PCR analysis was performed and relative expression of Trb3 or SMA mRNA normalized to β-actin (left panel) and miR-24 expression normalized to U6 snRNA expression (right panel) was also examined and plotted as means ± s.e.m. ($n=3$); $^*P<0.001$ (compared with unstimulated sample transfected with the same anti-miR). (**B**) PASMCs were transfected with 50 nM non-targeting control siRNA (si-Control) or siRNA against human Trb3 (si-Trb3) for 24 h, followed by stimulation with 20 ng/ml PDGF-BB (+PDGF-BB) for 24 h. Relative expression of Trb3, SMA, or CNN normalized to GAPDH and miR-24 expression normalized to U6 snRNA is plotted (means ± s.e.m., $n=3$; $^*P<0.001$). (**C**) Rat PAC1 cells were transfected with a construct carrying the human Trb3 cDNA construct with the 3′-UTR (Trb3 + 3′-UTR) or deleted in 3′UTR (Trb3), followed by stimulation with 20 ng/ml PDGF-BB (+PDGF-BB) for 24 h. Percent inhibition of CNN or SM22 mRNA level upon PDGF treatment is plotted (top panel). Relative expression of both endogenous rat Trb3 and exogenous human Trb3 mRNA normalized to GAPDH is plotted (bottom panel) as means ± s.e.m. ($n=3$); $^*P<0.001$. (**D**) PASMCs were transfected with 50 nM si-Control or si-Trb3 for 24 h, followed by treatment with PDGF-BB for 48 h. Cells were tryspinized and counted using a haemocytometer. The relative number of cells compared with untreated cells is plotted as means ± s.e.m. ($n=3$); $^*P<0.01$.

role in the regulation of Trb3 and vSMC genes by PDGF-BB. To investigate whether other targets of miR-24, besides Trb3, are involved in PDGF-BB-mediated downregulation of vSMC genes, Trb3 was silenced by small interfering RNA (siRNA) (si-Trb3) in PASMCs (Figure 5B). Transfection of si-Trb3 reduced endogenous Trb3 mRNA expression to 5% of that of the control (Figure 5B). miR-24 was induced similarly by PDGF-BB treatment both in si-Trb3 cells and si-Control cells (Figure 5B). PDGF-BB-mediated downregulation of SMA and CNN was observed in si-Control cells but not in si-Trb3 cells (Figure 5B, left panel), suggesting that Trb3 is required for the PDGF-BB-mediated decrease in contractile gene expression. To further confirm a critical role of the PDGF–miR-24–Trb3 axis, Trb3 expression constructs with or without the 3′-UTR (see Figure 3C, top panel) were transfected prior to PDGF treatment and the effect of PDGF on contractile markers *CNN* and *SM22* was examined in PAC1 cells (Figure 5C). If PDGF suppresses *SM22* through miR-24-mediated downregulation of Trb3, it is expected that only the Trb3 construct missing the 3′-UTR (Trb3), which is resistant to miR-24, is able to rescue *SM22* and *CNN* expression. Similar levels of expression of Trb3 from the construct with or without 3′-UTR (~5-fold over the endogenous level) were observed at the basal state (Figure 5C, bottom panel). Both Trb3 constructs elevated the basal expression of both *CNN* and *SM22* about two- three-fold (Supplementary Figure S5). Unlike the Trb3 construct with the 3′-UTR (Trb3 + 3′-UTR), the Trb3 construct deleted in 3′-UTR (Trb3) was able to reduce the level of inhibition of *CNN* and *SM22* by PDGF (Figure 5C, top panel), confirming that the PDGF-mediated miR-24–Trb3-regulatory pathway plays a critical role in the pro-synthetic effect of PDGF-BB. Next a potential role of miR-24-mediated downregulation of

Trb3 in PDGF-mediated cell growth regulation was examined. In control cells (si-Control), PDGF-BB treatment promoted proliferation of PASMCs (Figure 5D). When endogenous Trb3 level was downregulated by si-Trb3, the proliferative effect of PDGF-BB treatment was attenuated, suggesting that Trb3 is required not only for PDGF-mediated contractile gene regulation, but also for its cell-proliferative effect (Figure 5D). Altogether, these results support that the miR-24¡Trb3 axis is essential for the pro-synthetic activity of PDGF-BB.

miR-24 antagonizes BMP4 signals

We previously proposed that Trb3 stabilizes Smad1/5 proteins by promoting proteasome-dependent degradation of Smurf1, which is an E3 ubiquitin ligase for Smads (Chan *et al*, 2007). Therefore, we hypothesized that miR-24 inhibits the BMP–Smad pathway through downregulation of Trb3 and Smads. Overexpression of miR-24 in PASMCs decreased both Trb3 and Smad1 protein levels and abolished BMP4-mediated phosphorylation of Smad1/5 proteins (Figure 6A), similar to the effect of PDGF-BB treatment (see Figure 2D), suggesting that miR-24 is able to inhibit the BMP–Smad pathway in PASMCs. Next the inhibitory effect of miR-24 on the BMP–Smad pathway was further demonstrated by examining the expression of various transcriptional and post-transcriptional targets of BMP–Smads after transfection of miR-24 mimic or control (GFP) mimic. Transfection of 0.3 nM miR-24 mimic into PASMCs elevated the miR-24 level ~2-fold over the endogenous level (Figure 6B, miR-24) and reduced Trb3 mRNA to 30% of the endogenous level (Figure 6B, Trb3). In the presence of miR-24 mimic, induction of both vSMC-specific BMP targets SMA and CNN, and the non-vSMC-specific BMP target Id3 was significantly reduced as compared with that in control mimic-transfected cells, although not completely abolished (Figure 6B). To confirm that the miR-24-mediated inhibition of BMP activity on SMA and Id3 is due to downregulation of Trb3 and its function, PASMCs transfected with miR-24 mimic were infected with adenovirus carrying either wild-type Trb3 (Trb3 (WT)) cDNA or a Trb3 mutant cDNA deleted in amino acids 239–266 (Trb3 (ΔK)), which is unable to promote degradation of Smurf1, and therefore unable to positively modulate BMP signalling (Chan *et al*, 2007). Both Trb3 constructs are deleted in the 3′-UTR and therefore resistant to the miR-24 mimic (Figure 6C, bottom left panel). Both Trb3 (WT) and Trb3 (ΔK) were expressed at similar levels (Figure 6C, bottom left panel), and expression of Trb3 had no effect on miR-24 mimic expression (Figure 6C, bottom right panel). Similar to the result in Figure 6B, transfection of miR-24 mimic inhibited the induction of SMA and Id3 by BMP4 (Figure 6C, top panel). Exogenous Trb3 (WT) abolished the inhibitory effect of miR-24 mimic and rescued the BMP4-mediated induction of SMA and Id3, confirming the essential role of the miR-24–Trb3 axis in the regulation of the BMP pathway (Figure 6C, top panel). In contrast Trb3 (ΔK) was not able to inhibit the effect of miR-24 mimic (Figure 6C, top panel). Thus, these results support our hypothesis that miR-24 inhibits the BMP–Smad-signalling pathway through downregulation of Trb3.

Our previous study demonstrated that Smad proteins control miR-21 biosynthesis at the first processing step by Drosha microprocessor complex, which results in miR-21 (Davis *et al*, 2008) induction of about two-fold by BMP4 or TGFβ. Therefore, we speculated that miR-24-mediated downregulation of Trb3 and Smad may affect the regulation of miR-21 synthesis by BMP4. Overexpression of miR-24 abolished the BMP4-mediated induction of miR-21 (Figure 6D). Downregulation of Trb3 by siRNA (si-Trb3) phenocopied the effect of miR-24 mimic and abolished miR-21 induction by BMP4 (Figure 6E). These results indicate that miR-24 negatively regulates both transcriptional and non-transcriptional functions of BMP–Smads through a mechanism involving predominantly downregulation of Trb3. In agreement with these results, we observed that PDGF-BB treatment reduces miR-21 expression, presumably as a result of induction of miR-24 (Supplementary Figure S3). We next examined whether miR-24 expression affects other BMP4 responses in vSMCs, such as cell growth suppression (Lagna *et al*, 2007) and induction of actin remodelling (Neuman *et al*, 2009). miR-24 mimic expression abolished the BMP4-mediated cell growth inhibition in PASMCs (Figure 6F). Similarly, contraction of PASMCs in a collagen lattice in response to BMP4-induced actin remodelling was inhibited by miR-24 mimic (Figure 6G). Altogether, these results suggest that miR-24 can interfere with different pro-contractile activities of the BMP4 pathway in vSMCs.

To examine whether inhibition of the BMP–Smad pathway by miR-24 is cell-type-specific, a clone of the mouse embryonal carcinoma P19 cell line stably transformed with the BMP target gene promoter–luciferase reporter (BRE-Luc) (Ku *et al*, 2005) was transfected with miR-24 mimic, control (GFP) mimic, or si-Trb3, and stimulated with BMP4 (Figure 6H). In comparison with control cells, increasing amounts of miR-24 mimic decreased the response of BRE-Luc to BMP4 (Figure 6H). At the highest dose of miR-24 mimic, the response of BRE-Luc was similar to that elicited in si-Trb3-transfected cells (Figure 6H). Finally, we measured the effect of miR-24 on BMP4/Smad-mediated osteoblastic differentiation of mouse myoblast C2C12 cells, which is characterized by induction of the osteoblast marker alkaline phosphatase (ALP). When miR-24 was overexpressed in C2C12 cells, BMP4-mediated ALP induction was reduced by half, suggesting that miR-24 antagonizes the ability of BMP4 to promote osteoblast differentiation (Figure 6I). Trb3 level was decreased to 35% and induction of the BMP target gene Id3 was decreased to half in miR-24 mimic-expressing cells, suggesting that the miR-24–Trb3–Smad axis blocks osteoblast differentiation. Thus, we conclude that miR-24 antagonizes the BMP–Smad-signalling pathway both in vSMCs and non-vSMCs.

Next, we addressed whether miR-24 plays an essential role in inhibition of pro-contractile BMP activity by PDGF-BB. PASMCs were transfected with anti-miR-24 or anti-GFP (control), followed by treatment with BMP4 alone or BMP4 and PDGF-BB. In control cells, PDGF-BB blocked the induction of vSMC markers by BMP4 (Figure 7A, anti-GFP). When miR-24 activity was inhibited by anti-miR-24, however, PDGF-BB was unable to inhibit the BMP4-mediated induction of contractile genes (Figure 7A, anti-miR-24). Similar results were obtained by examining the effect of PDGF-BB on other pro-contractile signals by BMP4, such as cell growth inhibition (Figure 7B) and induction of cell contraction (Figure 7C). Altogether, these results demonstrate that miR-24 induction is essential for the ability of PDGF-BB to antagonize the pro-contractile BMP4 signals.

Hypoxia induces miR-24 and downregulation of Trb3 and BMP signal

It has been shown that the Trb3 level is altered by various pathological or physiological conditions (Bowers *et al*, 2003; Qi *et al*, 2006). Therefore, we examined a possible change in Trb3 protein and miR-24 expression in lung and pulmonary artery (PA) samples using a rat hypoxia-induced PAH model. qRT–PCR analysis demonstrated that the levels of Trb3 and vSMC markers in hypoxia-treated lung samples were reduced to about 40–50% of that in normoxia-treated control lung samples (Figure 8A, top panel). Conversely, miR-24 level was elevated about two-fold in hypoxia-treated samples in

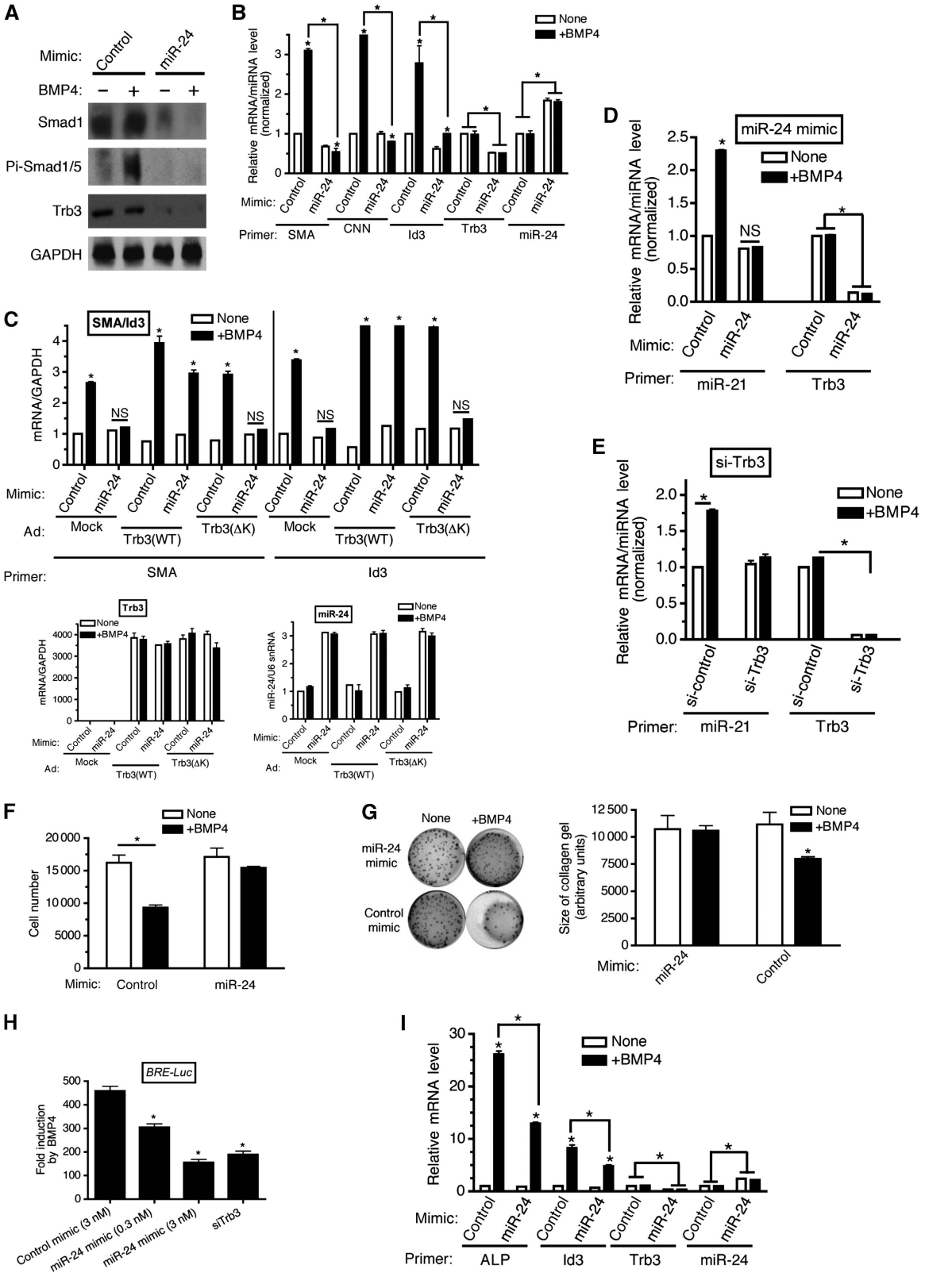

comparison with that in control samples (Figure 8A, bottom panel). miR-221, which was previously shown to be induced by the PDGF-signalling pathway, similar to miR-24 (Davis *et al*, 2009), was also increased about 1.5-fold after hypoxia treatment, while the level of an unrelated miRNA, miR-100, was unchanged (Figure 8A, bottom panel). Immunohistochemical analysis of SMA demonstrated that the medial layer of hypoxic rat PAs is thicker than that of a control (normoxic) rat due to overproliferation of vSMCs, which is characteristic of PAs of patients with PAH (Figure 8B). Phospho-Smad1/5/8 staining was detected in the medial layer of normoxic PAs (Figure 8B). At higher magnification, much of phospho-Smad1/5/8 staining had nuclear localization, suggesting that the BMP signal is active in those cells (Figure 8B). Consistent with a previous report (Yang *et al*, 2005), dramatically reduced staining of total Smad1 and phospho-Smad1/5/8 was observed in hypoxic rat PAs, suggesting a decrease in BMP signalling in these cells (Figure 8B). Reduced expression of Trb3 was also observed in the media layer of the PAs from rats subjected to hypoxia (Figure 8B). To examine whether the decrease in Trb3 protein level in hypoxic PAs is due to a change in miR-24 expression, the same samples were probed for miR-24 expression by a fluorescence *in situ* hybridization (FISH) using fluorescein isothiocyanate (FITC)-conjugated anti-miR-24 probes (Figure 8C, top two panels, green). Quantitative analysis of miR-24 staining indicates that the media of the hypoxia-treated sample expresses a twofold higher level of miR-24 as compared with the normoxic media, after normalization for the different medial areas in the two samples (Figure 8C, top two panels), indicating that miR-24 expression is modulated by vascular injury in the vSMC layer *in vivo*. The complementary patterns of expression of Trb3 and miR-24 in the media of PAs, as well as in lung samples from normoxia or hypoxia-treated rat, strongly support the hypothesis that elevated expression of miR-24 leads to downregulation of Trb3 *in vivo*.

miR-24 affects the TGFβ pathway

Trb3-dependent regulation of Smurf1 not only stabilizes BMP-specific Smads but also TGFβ-specific Smads, Smad2 and Smad3 (Chan *et al*, 2007). Indeed we observed that PDGF stimulation decreases the level of Trb3 and Smad1 (Figure 2D, left panel), as well as Smad2 and Smad3, in PASMCs (Figure 2D, right panel). Thus, we speculated that miR-24 might negatively regulate the TGFβ-signalling pathway. Overexpression of miR-24 decreased total Smad2 and Smad3, as well as Trb3 protein level and abolished the TGFβ-mediated phosphorylation of Smad2 (Figure 9A), similar to the observation with the BMP-specific Smad (see Figure 6A). This result suggests that miR-24 is able to inhibit the TGFβ−Smad-signalling pathway. The mink lung epithelial cell line Mv1Lu was transfected with a luciferase-reporter construct (SBE-Luc), which contained four copies of the Smad DNA-binding element (SBE). Induction of the SBE-Luc reporter by TGFβ treatment was dramatically reduced by miR-24 mimic (Figure 9B), suggesting that miR-24 inhibits the TGFβ–Smad-signalling pathway. To examine whether miR-24-mediated inhibition of SBE-Luc reporter activity is due to downregulation of Trb3, Trb3 expression constructs with or without the 3′-UTR (see Figure 3C, top panel) were co-transfected with miR-24 mimic. A similar level of Trb3 mRNA was expressed from both constructs in Mv1Lu cells (Figure 9C, right panel). The inhibitory effect of miR-24 mimic was absent when Trb3 construct lacking the 3′-UTR was co-transfected, presumably because Trb3 mRNA expressed from this construct is resistant to miR-24 (Figure 9C, left panel, Trb3). In contrast, the Trb3 construct with the 3′-UTR was unable to rescue the inhibitory activity of the miR-24 mimic (Figure 9C, left panel, Trb3 + 3′-UTR), suggesting that inhibition of the TGFβ–Smad pathway by miR-24 requires targeting of Trb3 by miR-24. The TGFβ–Smad-signalling pathway induces the expression of contractile genes in vSMCs in a Smad-dependent manner (Lagna *et al*, 2007). We examined the effect of Trb3 downregulation

Figure 6 miR-24 inhibits BMP signalling in vSMCs through downregulation of Trb3 (**A**). PASMCs were transfected with 0.3 nM Control mimic or 0.3 nM miR-24 mimic. Twenty-four hours after transfection of mimic, cells were stimulated with 3 nM BMP4 for 2 h and subjected to immunoblot analysis using anti-Trb3, anti-Smad1, anti-phospho-Smad1/5 (Pi-Smad1/5), or anti-GAPDH antibody (loading control). The experiment was repeated twice and produced similar results. (**B**) PASMCs were transfected with 0.1 nM miR-24 mimic or control mimic, followed by stimulation with 3 nM BMP4 (+BMP4) for 6 h (Id3) or for 24 h (all other markers). qRT–PCR was then performed. Relative expression of SMA, Id3, and Trb3 normalized to GAPDH and miR-24 expression normalized to U6 snRNA are plotted (means ± s.e.m., $n=3$; $^*P<0.001$). (**C**) PASMCs were transfected with 0.3 nM miR-24 mimic or control mimic, followed by adenoviral transduction of the Trb3 expression construct (Trb3 (WT) or Trb3 (ΔK)), or adenoviral transduction of GFP expression construct as control. Twenty-four hours later stimulation with 3 nM BMP4 was performed for 6 h for Id3 or 24 h for SMA. qRT–PCR was then performed and relative expression of SMA, Id3, and Trb3 normalized to GAPDH and miR-24 expression normalized to U6 snRNA are plotted (means ± s.e.m., $n=3$; $^*P<0.001$). (**D**) PASMCs were transfected with 0.3 nM control mimic or miR-24 mimic (left panel) for 24 h, followed by stimulation with 3 nM BMP4 (+BMP4) for 4 h. qRT–PCR was then performed to determine relative expression of miR-21 normalized to U6 snRNA and Trb3 expression normalized to GAPDH (means ± s.e.m., $n=3$; $^*P<0.001$). (**E**) PASMCs were transfected with 50 nM si-Control or si-Trb3 (right panel) for 24 h, followed by stimulation with 3 nM BMP4 (+BMP4) for 4 h. qRT–PCR was then performed to determine relative expression of miR-21 normalized to U6 snRNA and Trb3 expression normalized to GAPDH (means ± s.e.m., $n=3$; $^*P<0.001$). (**F**) PASMCs were transfected with 3 nM control mimic (control) or miR-24 mimic (miR-24 mimic) for 24 h, placed in starvation media for 24 h, followed by stimulation with BMP4 (+BMP4) for 48 h. Cells were trypsinized and counted using a haemocytometer. The relative number of cells is plotted means ± s.e.m. ($n=3$); $^*P<0.001$ (compared with unstimulated). (**G**) PASMCs were transfected with 3 nM control mimic (control) or miR-24 mimic (miR-24 mimic) for 24 h, followed by stimulation with BMP4 (+BMP4) for 24 h or left unstimulated (none). PASMCs were then embedded to collagen gel lattices with continued stimulation. Twenty-four hours after the collagen lattices were dissociated from the dish, gel contraction was photographed by using a digital camera (left panel). The relative size of collagen gel was quantitated using ImageJ and is plotted (means ± s.e.m., $n=3$; $^*P<0.001$, compared with unstimulated condition (right panel)). (**H**) A clone of P19 cells, stably transfected with the BMP reporter construct BRE-Luc, was transfected with 3 nM control mimic, 0.3 nM or 3 nM miR-24 mimic, or 50 nM si-Trb3, followed by 24-h BMP4 treatment. Luciferase activity was then measured and fold induction of the activity after BMP4 treatment is plotted (means ± s.e.m., $n=3$; $^*P<0.001$, compared with control mimic). (**I**) C2C12 cells were transfected with 0.003 nM control mimic (control) or 0.003 nM miR-24 mimic (miR-24) for 24 h followed by stimulation with BMP4 (+BMP4) for 2 h, or left unstimulated (none). qRT–PCR was then performed. Relative expression of ALP, Id3, and Trb3 normalized to GAPDH and miR-24 expression normalized to U6 snRNA are plotted (means ± s.e.m., $n=3$; $^*P<0.001$).

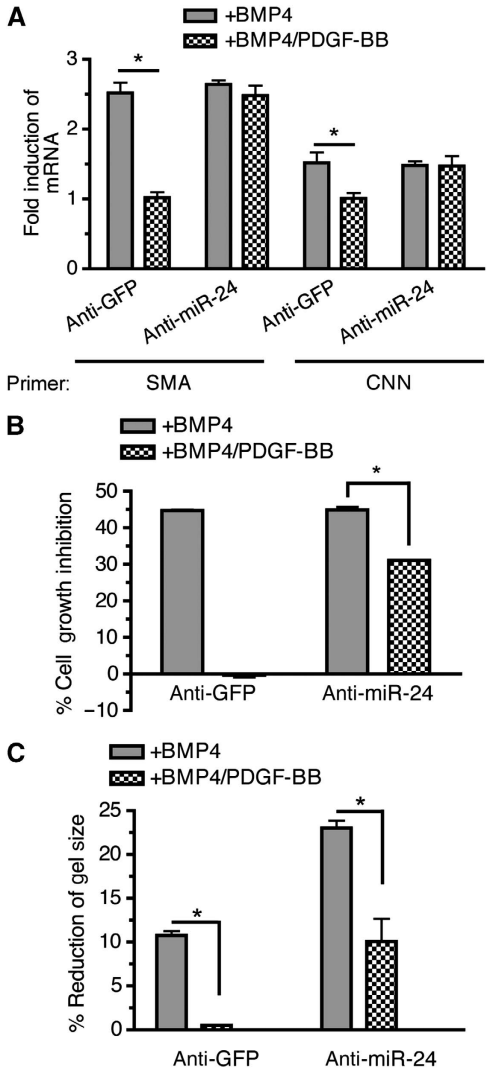

Figure 7 miR-24 expression is essential for PDGF-BB inhibition of the BMP-mediated contractile phenotype in PASMCs. PASMCs were transfected with 50 nM anti-GFP (control) or anti-miR-24 for 24 h prior to stimulation with 3 nM BMP4, 20 ng/ml PDGF-BB, or both, as indicated. (**A**) qRT–PCR anaylses of SMA and CNN were performed. The fold induction of SMA mRNA (compared with no stimulation) is plotted; error bars represent s.e.m. ($n=3$); $^*P<0.001$. (**B**) Cells were trypsinized and counted using a haemocytometer. The percentage of cell growth inhibition is plotted as means ± s.e.m. ($n=3$); $^*P<0.001$. (**C**) Cells were embedded in collagen gel lattices and treated with 3 nM BMP4 alone (+BMP4), or 3 nM BMP4 and 20 ng/ml PDGF-BB (+BMP4/PDGF-BB). Twenty-four hours after the collagen lattices were dissociated from the dish, percentage reduction of gel size as compared with the no stimulation condition was measured and is plotted (means ± s.e.m., $n=3$; $^*P<0.001$).

on contractile gene expression in vSMCs. Endogenous Trb3 was downregulated by siRNA (si-Trb3) in PASMCs and the levels of contractile markers (SMA, CNN, and SM22), as well as the well-characterized TGFβ–Smad-target gene, plasminogen activator inhibitor-1 (PAI-1), were examined after TGFβ treatment (Figure 9D). TGFβ treatment induced all three vSMC markers and PAI-1 expression (Figure 9D). However, in si-Trb3-transfected cells in which Trb3 level was reduced to ~30% of endogenous level, not only PAI-1 but also vSMC markers could not be augmented by TGFβ (Figure 9D). This result confirms that Trb3 is essential for induction of vSMC markers by TGFβ, presumably because Trb3 critically regulates the protein stability of TGFβ-specific Smads. Next the effect of miR-24 overexpression on TGFβ-mediated induction of vSMC genes and miR-21 was examined. The expression of exogenous miR-24 ~3-fold over the endogenous level (see Figure 9E, right panel, miR-24) reduced Trb3 mRNA to ~20% of the endogenous level (Figure 9E, left panel, Trb3). Similar to the result in Figure 9D using si-Trb3-transfected cells, both the basal and the TGFβ-induced level of contractile markers SMA and CNN were significantly reduced by elevation of miR-24 expression (Figure 9E, left panel). Induction of miR-21 upon TGFβ stimulation was also abolished in the presence of miR-24 mimic (Figure 9E, right panel, miR-21). These results suggest that miR-24 negatively regulates the TGFβ–Smad signal via silencing Trb3, followed by downregulation of Smad signal transducers. Finally, induction of vSMC-specific genes by TGFβ was inhibited by co-treatment with PDGF-BB (Figure 9F), as shown for the BMP4 pathway (Figure 7A). Trb3 mRNA was also decreased by TGFβ/PDGF-BB co-treatment. Inhibition of TGFβ-induced contractile genes, as well as Trb3, by PDGF-BB was blocked when miR-24 was inhibited by anti-miR-24 (Figure 9F), suggesting that PDGF-BB interferes with the pro-contractile TGFβ signal by modulating Trb3 and Smads level via induction of miR-24 (Figure 9F). Altogether, these results demonstrate that miR-24 plays a critical role in the regulation of the vSMC phenotype switch by antagonizing pro-contractile signals by members of the TGFβ superfamily of signalling pathways, as summarized in Figure 9G.

Discussion

In this study, we elucidated a novel mechanism by which PDGF-BB signal promotes the dedifferentiation of vSMCs. We demonstrated that PDGF-BB induces miR-24 and induces degradation of Trb3 mRNA, which in turn leads to downregulation of Smad signal transducers. The Smad proteins are essential mediators of the pro-contractile signal transmitted by BMP and TGFβ. miR-24 is clustered closely with miR-23 and miR-27 at two genomic loci known as the miR-24-1 gene cluster, an ~880-bp region encoding miR-23b, -27b, and -24-1, and the miR-24-2 gene cluster, a ~370-bp region encoding miR-23a, -27a, and -24-2. Our result indicates that all three miRNAs of the miR-24-2 cluster, but not the miR-24-1 cluster, are regulated to a similar extent by PDGF-BB at the level of primary transcripts, suggesting that the miR-24-2 gene cluster is transcribed into a single transcript, which will then be processed into three independent miRNAs. Differential expression and regulation of miR-24-1 and miR-24-2 have been observed previously. In mouse mesenchymal C3H10T1/2 cells, BMP2 induces miR-24-1 expression without affecting the expression of miR-24-2 (Sun *et al*, 2009). Interestingly, miR-24-1 but not miR-23b or miR-27b encoded in the same gene locus are regulated by BMP2, suggesting that three miRNAs in the miR-24-1 cluster might be differentially regulated during processing. In mouse myoblast C2C12 cells, TGFβ was shown to repress miR-24-2, as well as miR-23a and miR-27a (Sun *et al*, 2008). We did not observe significant changes in the expression of miR-24 upon TGFβ or BMP stimulation, suggesting that neither the miR-24-1 nor the miR-24-2 cluster is regulated by TGFβ or BMP at the level

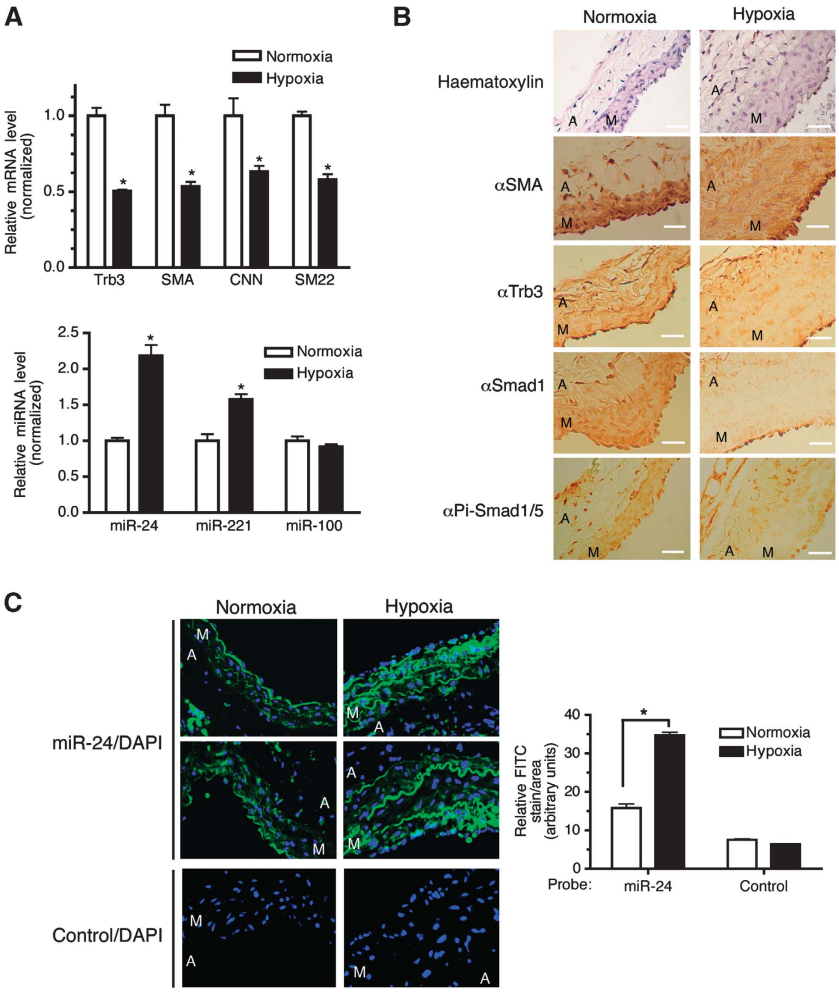

Figure 8 Modulation of Trb3 and miR-24 expression in a rat PAH model (**A**). qRT–PCR analysis of lung samples from rats after 17-day hypoxia or normoxia treatment. Relative expression of Trb3, SMA, CNN, and SM22 (top panel); or miR-24, miR-221, and miR-100 was plotted by normalizing the level of expression of normoxia samples as 1 (means ± s.e.m., $n=3$; $^*P<0.001$). (**B**) Histological examination of PAs from rats after 17-day hypoxia or normoxia treatment with anti-SMA, anti-Smad1, anti-phospho Smad1/5 (Pi-Smad1/5), or anti-Trb3 antibodies (brown, ×400) and by haematoxylin staining (blue, ×400). The media (M) and adventitia (A) of the PAs are indicated. (**C**) Sections of PAs were probed with either anti-miR-24 (top two panels) or control (bottom panel) conjugated to FITC (green). Cells were counterstained with DAPI (blue). The media (M) and adventitia (A) of the PAs are indicated. Relative expression of miR-24 was quantitated using the ImageJ software and imaged ($n=3$; $^*P<0.001$).

of transcription or processing in PASMCs. Thus, the mechanism of regulation of the miR-24 gene clusters by growth-factor-signalling pathways appears to be cell-type-specific. It will be interesting to investigate whether PDGF-BB-mediated transcriptional activation of the miR-24-2 cluster is limited to vSMCs.

Previously we showed that PDGF-BB signalling induces miR-221 in vSMCs and mediates downregulation of the c-Kit receptor and the cyclin-dependent kinase inhibitor p27Kip1 (Davis *et al*, 2009). Decreased expression of p27Kip1 promotes an increase in cell growth, while a decrease in c-Kit leads to inhibition of contractile gene markers by modulating the level of Myocd protein, a transcriptional activator critical for induction of contractile genes (Davis *et al*, 2009). We investigated a potential crosstalk between miR-221 and miR-24 activities by monitoring the effect of miR-221 overexpression on the level of Trb3 or miR-24, and found no evidence that miR-221 affects Trb3 or miR-24 expression (M Chun Chan and A Hata, unpublished observation). Conversely, overexpression of miR-24 did not affect the expression of miR-221 or the expression of its target genes (M Chun Chan and A Hata, unpublished observation). Furthermore, we observed that miR-24 does not play a role in regulating PDGF-BB-mediated migration (Supplementary Figure S4), an important characteristic of the synthetic phenotype. In comparison, we previously reported that the increase in miR-221 expression by PDGF-BB stimulation is required for vSMC migration (Davis *et al*, 2009). These observations suggest that miR-221 and miR-24 act independently to promote the synthetic phenotype in vSMCs despite their coordinated regulation by PDGF-BB.

We showed previously that BMP Smad-dependent signalling promotes nuclear translocation of MRTF-A and MRTF-B, members of the Myocd family with function similar to Myocd (Lagna *et al*, 2007). We speculate that nuclear accumulation of MRTF-A/B by BMP is inhibited by PDGF induction of miR-24 via Trb3-dependent downregulation of BMP–Smad signal transducers. Thus, it is intriguing to speculate that PDGF-BB might inhibit the expression of contractile markers by inhibiting the function of Myocd through induction of miR-221 and MRTF-A/B, through induction of miR-24.

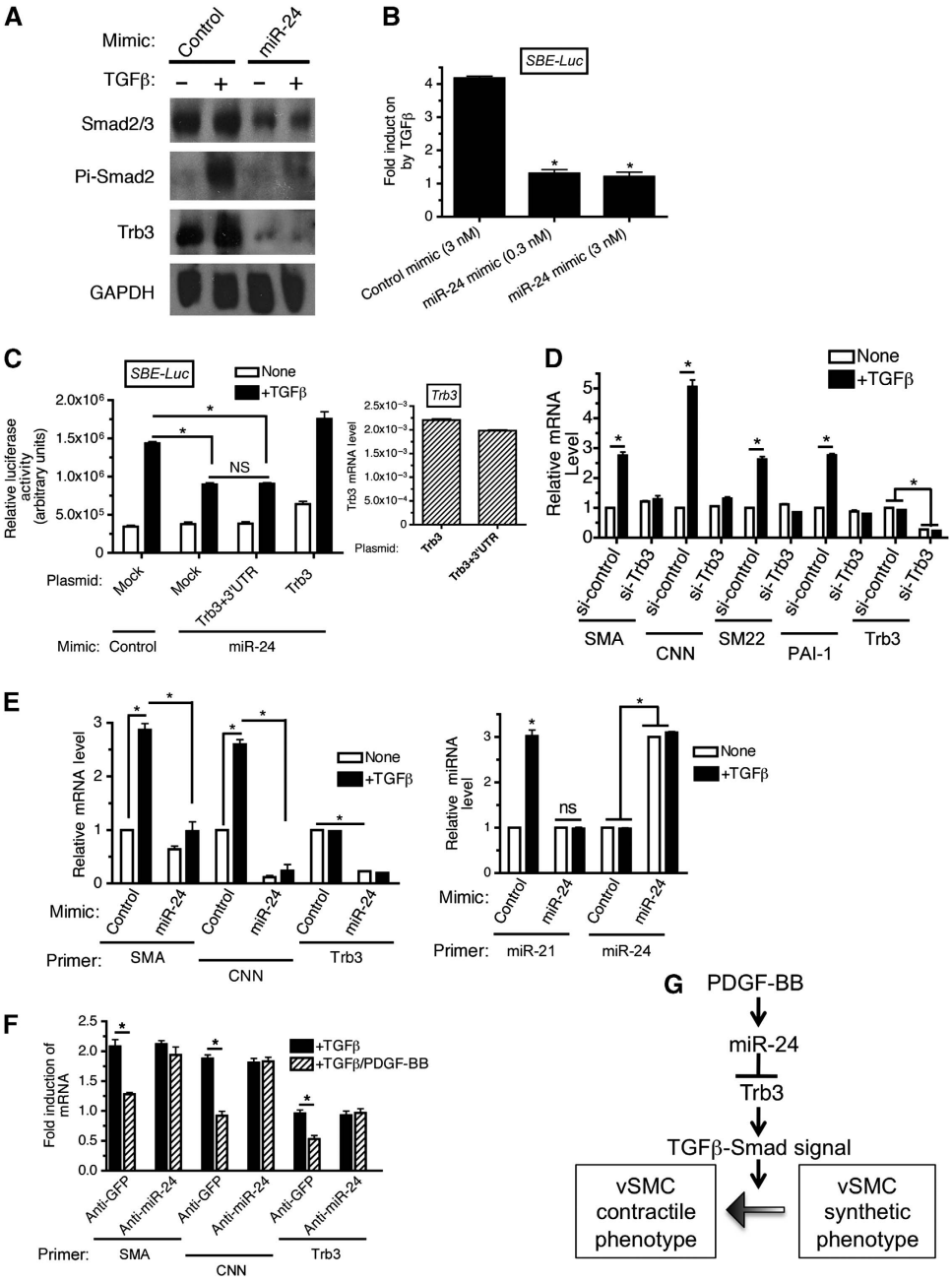

Figure 9 miR-24 antagonizes TGFβ signalling. (**A**) PASMCs were transfected with 0.3 nM Control mimic or 0.3 nM miR-24 mimic. Twenty-four hours after transfection of mimic, cells were stimulated with 100 pM TGFβ1 for 2 h and subjected to immunoblot analysis with anti-Trb3, anti-Smad2/3, anti-phospho-Smad2 (Pi-Smad2), or anti-GAPDH antibody (loading control). The experiment was repeated twice and produced similar results. (**B**) Mv1Lu cells were transfected with the TGFβ reporter construct SBE-Luc as well as with 3 nM control mimic, or 0.3 or 3 nM miR24 mimic. Cells were then stimulated with 100 pM TGFβ1 for 24 h and luciferase activities were measured. Results are plotted as fold induction upon TGFβ stimulation (means ± s.e.m., $n=3$; $^*P<0.001$), versus fold induction with control mimic). (**C**) Mv1Lu cells was transfected with SBE-Luc, 3 nM control mimic, or miR-24 mimic, as well as the Trb3 expression construct with the 3′-UTR containing the miR-24 seed sequence (Trb3 + 3′-UTR) or without the 3'UTR (Trb3). Cells were stimulated with 100 pM TGFβ1 for 24 h and luciferase activities were measured (means ± s.e.m., $n=3$). Relative exogenous Trb3 mRNA normalized to GAPDH in samples transfected with control mimic were monitored by qRT–PCR (right panel). (**D**) PASMCs were transfected with 50 nM si-Control or si-Trb3, followed by 100 pM TGFβ1 treatment for 24 h. qRT–PCR analysis of SMA, CNN, SM22, PAI-1, or Trb3 mRNA was performed. The relative mRNA levels normalized to GAPDH are plotted as means ± s.e.m. ($n=3$; $^*P<0.001$). (**E**) PASMCs were transfected with 3 nM control mimic (control), or miR-24 mimic, followed by 100 pM TGFβ1 treatment for 24 h. qRT–PCR analysis of SMA, CNN, or Trb3 mRNA, or miR-21 or miR-24 was performed. Relative mRNA levels normalized to GAPDH and miR-21 expression normalized to U6 snRNA were plotted as means ± s.e.m. ($n=3$; $^*P<0.001$). (**F**) PASMCs were transfected with 50 nM anti-GFP (control) or anti-miR-24 for 24 h. Cells were then treated with 100 pM TGFβ1 alone (+TGFβ) or both100 pM TGFβ1 and 20 ng/ml PDGF-BB (+TGFβ/PDGF-BB) for 24 h. qRT–PCR analysis for SMA, CNN, or Trb3 was performed and data of fold induction of mRNA as compared with unstimulated was plotted as means ± s.e.m. ($n=3$; $^*P<0.001$). (**G**) A schematic representation of the mechanism of antagonism between PDGF and the TGFβ-signalling pathway mediated by miR-24.

Our previous study demonstrates that miR-21 biosynthesis is facilitated by both the BMP- and TGFβ-signalling pathway (Davis *et al*, 2008). Upon translocation into the nucleus, Smads become part of a large Drosha microprocessor complex and facilitate cleavage and processing of Pri-miR-21 (Davis *et al*, 2008). Mature miR-21 downregulates PDCD4,

which in turn elevates contractile gene expression (Davis *et al*, 2008). In this study, we showed that modulation of miR-24 or Trb3 affects the induction of miR-21 by BMP4 (Figure 6D and E). Therefore, another mechanism by which miR-24 could mediate the inhibition of contractile genes is through increased levels of PDCD4 due to inhibition of miR-21 biogenesis.

We demonstrated antagonism between miR-24 and the TGFβ superfamily of signalling pathways in both vSMCs and non-vSMCs. In human hepatocellular carcinoma cells, consistent with our observation, increased expression of miR-24-2, miR-23a, and miR-27a has been suggested to change the TGFβ signal from being growth-inhibitory, proapoptotic to growth-stimulatory, antiapoptotic (Huang *et al*, 2008). Similarly, increased expression of miR-24 has been observed in various tumours, such as pancreatic adenocarcinomas, uterine leiomyomas, chromic lymphotic leukaemias, breast carcinomas, and cholangiocarcinomas (Mattie *et al*, 2006; Meng *et al*, 2006; Fulci *et al*, 2007; Lee *et al*, 2007; Wang *et al*, 2007). These results suggest that inhibition of TGFβ signalling by miR-24 might be a relatively common mechanism during tumorigenesis. Another example of the antagonistic activity of miR-24 on TGFβ-superfamily signalling is during erythropoiesis. miR-24 inhibits activin-dependent erythropoiesis by targeting the activin type-I receptor (also known as ALK4) gene (Wang *et al*, 2008). Furthermore, the antimyogenic activity of TGFβ is inhibited by elevated expression of miR-24 during skeletal muscle differentiation in myoblast C2C12 cells (Sun *et al*, 2008). In vSMCs, mRNA or protein levels of BMP or TGFβ receptors are not affected by miR-24 (data not shown). We identified Trb3 as a novel target of miR-24. We have shown previously that Trb3 mediates degradation of Smurf1 (Chan *et al*, 2007). Besides a role in degradation of Smads, Smurf1 is known to facilitate the antagonistic action of Smad7 by targeting Smad7 at the plasma membrane (Suzuki *et al*, 2002). Furthermore, Smurf1 promotes degradation of RhoA (Wang *et al*, 2006), which is a downstream signal transducer critical for mediating the pro-contractile signal from the BMP pathway in vSMCs (Chan *et al*, 2007; Lagna *et al*, 2007). Thus, we speculate that induction of miR-24 by PDGF-BB leads to inhibition of pro-contractile signals via multiple mechanisms through degradation of different effectors critical for the TGFβ- or BMP-signalling pathways.

Trb3 is known to interact and negatively regulate the transcription factor peroxisome proliferation-activated receptor-γ (PPARγ), a master regulator of adipogenesis (Takahashi *et al*, 2008). Concurrently, it has been shown that expression of Trb3, both at the mRNA and the protein level, is silenced during early adipogenesis (Bezy *et al*, 2007). Constitutive expression of Trb3 in preadipocytes blocks adipocyte differentiation, suggesting that downregulation of Trb3 is essential for adipogenesis (Bezy *et al*, 2007). Recently, it was reported that BMP2-mediated adipocyte differentiation in 10T1/2 cells is enhanced by overexpression of miR-24 (Sun *et al*, 2009). This observation is contradictory to our study as miR-24 inhibits BMP signalling in vSMCs. We do not know whether miR-24 causes downregulation of Smads in preadipocytes similar to vSMCs. However, we speculate that overexpression of miR-24 in 10T1/2 cells causes downregulation of Trb3, which in turn leads to activation of PPARγ and adipocyte differentiation.

Aberrant regulation of the vSMC phenotype, in particular the switch from a highly contractile to a less contractile, synthetic phenotype, is a critical phenomenon underlying the pathogenesis of a variety of vascular proliferative diseases, including PAH. In this study we confirm that PDGF signalling is a potent inducer of the synthetic phenotype and is able to oppose the contractile action of the BMP or TGFβ pathways, and propose that it acts via induction of miR-24. Increased expression of both PDGF ligands and receptors has been reported using PAH animal models, as well as for human patients (Andrae *et al*, 2008). The tyrosine-kinase inhibitor imatinib mesylate, which strongly antagonizes the PDGF-signalling pathway, is able to reverse the phenotype of experimental PAH in animal models and improve symptoms in human IPAH patients (Andrae *et al*, 2008), suggesting that increased PDGF signalling in vSMCs contributes to development of IPAH. Our result indicates that hypoxia induces miR-24 expression and downregulation of Trb3, suggesting that elevation of miR-24 might cause thickening of the medial layer as a result of inhibition of BMP signalling, similar to that in IPAH patients with BMPRII mutations. It is intriguing to speculate that the level of expression of miR-24 might be upregulated in the pulmonary vasculature of IPAH patients, in comparison with normal vasculature, with concurrent decrease in Trb3 expression. If aberrant expression of miR-24 in the vasculature of PAH or other cardiovascular diseases is confirmed, modulation of the miR-24 level *in vivo* by delivery of anti-miR-24 oligonucleotides could be considered a novel therapy.

Materials and methods

Cell culture

Human primary PASMCs were purchased from Lonza (#CC-2581) and were maintained in Sm-GM2 media (Lonza) containing 5% FBS. Early-passage (passage 4–7) PASMCs were used for this study. PAC1, C3H10T1/2, P19, mink lung epithelial (MV1Lu), and C2C12 cell lines were purchased from ATCC and maintained in Dulbecco's modified Eagle's medium supplemented with 10% fetal calf serum (FCS; Sigma). Recombinant human BMP4, PDGF-BB, and TGFβ1 were purchased from R&D Systems. Cells were treated with 3 nM BMP4, 20 ng/ml PDGF-BB, or 100 pM TGFβ1 alone or a combination of these factors under starvation conditions (0.2% FBS) as described (Lagna *et al*, 2007).

RNA preparation and real-time RT–PCR

Total RNA was extracted by TRIzol (Invitrogen). For detection of mRNAs, 1 μg of RNA was subjected to RT reaction using the first-strand cDNA synthesis kit (Invitrogen) according to the manufacturer's instructions. Quantitative analysis of the change in expression levels was performed using a real-time PCR machine (iQ5; Bio-Rad) PCR cycling conditions were 94°C for 3 min and 40 cycles of (94°C for 15 s, 60°C for 20 s, and 72°C for 40 s). For detection of mature miRNAs, the TaqMan MicroRNA assay kit (Applied Biosystems) was used according to the manufacturer's instructions. Data analysis was performed by comparative C_t method using the Bio-Rad software. The average of three experiments each performed in triplicate along with their standard errors are presented. The sequences of RT–PCR primers can be found in the Supplementary data.

miRNA mimic

Chemically modified double-stranded RNAs designed to mimic endogenous mature miR-24, miR-221, and negative-control miRNA were purchased from Ambion. miRNA mimics were transfected using RNAi Max (Invitrogen) according to the manufacturer's directions at 0.3 or 3 nM as indicated.

Anti-miRNA oligonucleotides
2′-*O*-methyl-modified RNA oligonucleotides complementary to the miRNA or GFP (control) sequence were purchased from IDT and transfected as previously reported (Davis *et al*, 2008, 2009).

RNA interference
Synthetic siRNAs targeting human Trb3 or mouse Trb3 were purchased from Dharmacon as described previously (Chan *et al*, 2007). An siRNA with a non-targeting sequence (scramble siRNA; Dharmacon) was used as negative control. The siRNAs were transfected at 50 nM using RNAi Max (Invitrogen) according to the manufacturer's directions. FITC-conjugated fluorescence oligonucleotides (Block-it; Invitrogen) were used to evaluate transfection efficiency.

Plasmid DNA transfection and cDNA expression constructs
Cells were transfected using Fugene6 (Roche) according to the manufacturer's protocol. Human Trb3 expression plasmid with the 3′-UTR was purchased from Origene (cat. no. SC112991). Full-length human Trb3 including the 2-kb 3′-UTR, which contains the miR-221-target sequence, was cloned into a pCMV6-XL4 vector. Human Trb3 expression plasmid without the 3′-UTR, SBE-Luc, BRE-Luc, Trb3-luc, and adenoviral Trb3 construct (Ad_Trb3), were previously described (Chan *et al*, 2007).

Immunoblot assay
Cells were lysed in TNE buffer and total cell lysates were separated by SDS–PAGE, transferred to PVDF membranes (Millipore), immunoblotted with antibodies, and visualized using an enhanced chemiluminescence detection system (Amersham Biosciences). Protein bands were quantitated by densitometry using the gel analysis software ImageJ (rsbweb.nih.gov/ij/). Antibodies used for immunoblotting were anti-GAPDH antibody (2E3-2E10; Abnova), anti phospho Smad1/5/8 (clone 47-258; Calbiochem), anti-Smad1 (Zymed), anti-Smad2/3 (#610843; BD Biosciences), anti-phospho-Smad2 (a kind gift from Dr ten Dijke), and anti-SMA (clone 1A4; Sigma). Anti-human and mouse Trb3 antibodies were previously described (Chan *et al*, 2007).

Immunofluorescence staining
PASMCs or PAC1 cells were fixed and permeabilized in a 50% acetone–50% methanol solution and stained using anti-SMA antibody (clone 1A4; Sigma) conjugated with FITC, anti-hTrb3 conjugated with Cy3, and 4′-6-diamidino-2-phenylindole (DAPI; Invitrogen).

Luciferase assay
The luciferase-reporter construct was transfected together with β-galactosidase (β-gal) plasmid as an internal transfection control. Luciferase assays were performed as described (Lagna *et al*, 2007).

Collagen matrix contraction assay
Collagen matrix contraction assay was performed as described in the Supplementary data (Neuman *et al*, 2009).

Animal study and immunohistochemistry
All experiments were performed in accordance with the guidelines and regulations of the Institutional Animal Care and Use Committee at Tufts Medical Center. Adult male Sprague–Dawley rats were randomized to 17 days of normoxia or hypobaric hypoxia as described previously (Preston *et al*, 2006). At the end of the exposure period, rats were killed and PAs were processed for paraffin embedding. Paraffin-embedded tissue sections (5-μm) were immunostained as described in the Supplementary data.

In situ hybridization of miRNA
Rat PA sections were hybridized with a miRCURY LNA detection probe for miR-24 (cat. no. 18121-01; Exiqon) or with a control scrambled control probe (cat. no. 99004-01; Exiqon), followed by treatment with anti-DIG-HRP antibody (antibody 6212; Abcam) and signal amplification by Tyramide Technology from Molecular Probes (Invitrogen).

Statistical analysis
The results presented are the average of at least three experiments each performed in triplicate along with the standard errors. Statistical analyses were performed by analysis of variance, followed by Tukey's multiple comparison test or Student's *t*-test as appropriate, using Prism 4 (GraphPad Software Inc.). *P*-values less than 0.05 were considered significant and are indicated by asterisks.

Supplementary data
Supplementary data are available at *The EMBO Journal* Online (http://www.embojournal.org).

Acknowledgements
We thank Dr P ten Dijke for antibodies and R Warburton and F Celestin for technical assistance. We also thank the members of the Hata and Lagna laboratory for critical discussion. This work was supported by grants from the National Institutes of Health (HD042149 and HL082854) to AH and (HL086572) to GL. M-CC is a recipient of a postdoctoral fellowship from the American Heart Association.

Conflict of interest
The authors declare that they have no conflict of interest.

References
Andrae J, Gallini R, Betsholtz C (2008) Role of platelet-derived growth factors in physiology and medicine. *Genes Dev* **22:** 1276–1312

Bezy O, Vernochet C, Gesta S, Farmer SR, Kahn CR (2007) TRB3 blocks adipocyte differentiation through the inhibition of C/EBPbeta transcriptional activity. *Mol Cell Biol* **27:** 6818–6831

Bowers AJ, Scully S, Boylan JF (2003) SKIP3, a novel *Drosophila* tribbles ortholog, is overexpressed in human tumors and is regulated by hypoxia. *Oncogene* **22:** 2823–2835

Chan MC, Nguyen PH, Davis BN, Ohoka N, Hayashi H, Du K, Lagna G, Hata A (2007) A novel regulatory mechanism of the bone morphogenetic protein (BMP) signaling pathway involving the carboxyl-terminal tail domain of BMP type II receptor. *Mol Cell Biol* **27:** 5776–5789

Davidson AJ, Zon LI (2000) Turning mesoderm into blood: the formation of hematopoietic stem cells during embryogenesis. *Curr Top Dev Biol* **50:** 45–60

Davis BN, Hilyard AC, Lagna G, Hata A (2008) SMAD proteins control DROSHA-mediated microRNA maturation. *Nature* **454:** 56–61

Davis BN, Hilyard AC, Nguyen PH, Lagna G, Hata A (2009) Induction of microRNA-221 by platelet-derived growth factor signaling is critical for modulation of vascular smooth muscle phenotype. *J Biol Chem* **284:** 3728–3738

Fulci V, Chiaretti S, Goldoni M, Azzalin G, Carucci N, Tavolaro S, Castellano L, Magrelli A, Citarella F, Messina M, Maggio R, Peragine N, Santangelo S, Mauro FR, Landgraf P, Tuschl T, Weir DB, Chien M, Russo JJ, Ju J *et al* (2007) Quantitative technologies establish a novel microRNA profile of chronic lymphocytic leukemia. *Blood* **109:** 4944–4951

Guo J, Sartor M, Karyala S, Medvedovic M, Kann S, Puga A, Ryan P, Tomlinson CR (2004) Expression of genes in the TGF-beta signaling pathway is significantly deregulated in smooth muscle cells from aorta of aryl hydrocarbon receptor knockout mice. *Toxicol Appl Pharmacol* **194:** 79–89

Huang S, He X, Ding J, Liang L, Zhao Y, Zhang Z, Yao X, Pan Z, Zhang P, Li J, Wan D, Gu J (2008) Upregulation of miR-23a ~27a ~24 decreases transforming growth factor-beta-induced tumor-suppressive activities in human hepatocellular carcinoma cells. *Int J Cancer* **123:** 972–978

Ku M, Howard S, Ni W, Lagna G, Hata A (2005) OAZ regulates BMP signaling through SMAD6 activation. *J Biol Chem* **281:** 5277–5287

Kuwahara K, Teg Pipes GC, McAnally J, Richardson JA, Hill JA, Bassel-Duby R, Olson EN (2007) Modulation of adverse cardiac remodeling by STARS, a mediator of MEF2 signaling and SRF activity. *J Clin Invest* **117:** 1324–1334

Lagna G, Ku MM, Nguyen PH, Neuman NA, Davis BN, Hata A (2007) Control of phenotypic plasticity of smooth muscle cells by BMP signaling through the myocardin-related transcription factors. *J Biol Chem* **282:** 37244–37255

Lee EJ, Gusev Y, Jiang J, Nuovo GJ, Lerner MR, Frankel WL, Morgan DL, Postier RG, Brackett DJ, Schmittgen TD (2007) Expression profiling identifies microRNA signature in pancreatic cancer. *Int J Cancer* **120:** 1046–1054

Li S, Chang S, Qi X, Richardson JA, Olson EN (2006) Requirement of a myocardin-related transcription factor for development of mammary myoepithelial cells. *Mol Cell Biol* **26:** 5797–5808

Mattie MD, Benz CC, Bowers J, Sensinger K, Wong L, Scott GK, Fedele V, Ginzinger D, Getts R, Haqq C (2006) Optimized high-throughput microRNA expression profiling provides novel biomarker assessment of clinical prostate and breast cancer biopsies. *Mol Cancer* **5:** 24

McNamara CA, Sarembock IJ, Bachhuber BG, Stouffer GA, Ragosta M, Barry W, Gimple LW, Powers ER, Owens GK (1996) Thrombin and vascular smooth muscle cell proliferation: implications for atherosclerosis and restenosis. *Semin Thromb Hemost* **22:** 139–144

Medjkane S, Perez-Sanchez C, Gaggioli C, Sahai E, Treisman R (2009) Myocardin-related transcription factors and SRF are required for cytoskeletal dynamics and experimental metastasis. *Nat Cell Biol* **11:** 257–268

Meng F, Henson R, Lang M, Wehbe H, Maheshwari S, Mendell JT, Jiang J, Schmittgen TD, Patel T (2006) Involvement of human micro-RNA in growth and response to chemotherapy in human cholangiocarcinoma cell lines. *Gastroenterology* **130:** 2113–2129

Misiakos EP, Kouraklis G, Agapitos E, Perrea D, Karatzas G, Boudoulas H, Karayannakos PE (2001) Expression of PDGF-A, TGFb and VCAM-1 during the developmental stages of experimental atherosclerosis. *Eur Surg Res* **33:** 264–269

Monzen K, Nagai R, Komuro I (2002) A role for bone morphogenetic protein signaling in cardiomyocyte differentiation. *Trends Cardiovasc Med* **12:** 263–269

Moser M, Patterson C (2005) Bone morphogenetic proteins and vascular differentiation: BMPing up vasculogenesis. *Thromb Haemost* **94:** 713–718

Neuman NA, Ma S, Schnitzler GR, Zhu Y, Lagna G, Hata A (2009) The four-and-a-half LIM domain protein 2 regulates vascular smooth muscle phenotype and vascular tone. *J Biol Chem* **284:** 13202–13212

Ohoka N, Yoshii S, Hattori T, Onozaki K, Hayashi H (2005) TRB3, a novel ER stress-inducible gene, is induced via ATF4–CHOP pathway and is involved in cell death. *EMBO J* **24:** 1243–1255

Owens G (1995) Regulation of differentiation of vascular smooth muscle cells. *Physiol Rev* **75:** 487–517

Owens GK, Kumar MS, Wamhoff BR (2004) Molecular regulation of vascular smooth muscle cell differentiation in development and disease. *Physiol Rev* **84:** 767–801

Preston IR, Hill NS, Warburton RR, Fanburg BL (2006) Role of 12-lipoxygenase in hypoxia-induced rat pulmonary artery smooth muscle cell proliferation. *Am J Physiol Lung Cell Mol Physiol* **290:** L367–L374

Qi L, Heredia JE, Altarejos JY, Screaton R, Goebel N, Niessen S, Macleod IX, Liew CW, Kulkarni RN, Bain J, Newgard C, Nelson M, Evans RM, Yates J, Montminy M (2006) TRB3 links the E3 ubiquitin ligase COP1 to lipid metabolism. *Science* **312:** 1763–1766

Schneider MD, Gaussin V, Lyons KM (2003) Tempting fate: BMP signals for cardiac morphogenesis. *Cytokine Growth Factor Rev* **14:** 1–4

Smith P, Heath D, Yacoub M, Madden B, Caslin A, Gosney J (1990) The ultrastructure of plexogenic pulmonary arteriopathy. *J Pathol* **160:** 111–121

Sun F, Wang J, Pan Q, Yu Y, Zhang Y, Wan Y, Li X, Hong A (2009) Characterization of function and regulation of miR-24-1 and miR-31. *Biochem Biophys Res Commun* **380:** 660–665

Sun Q, Zhang Y, Yang G, Chen X, Cao G, Wang J, Sun Y, Zhang P, Fan M, Shao N, Yang X (2008) Transforming growth factor-beta-regulated miR-24 promotes skeletal muscle differentiation. *Nucleic Acids Res* **36:** 2690–2699

Suzuki C, Murakami G, Fukuchi M, Shimanuki T, Shikauchi Y, Imamura T, Miyazono K (2002) Smurf1 regulates the inhibitory activity of Smad7 by targeting Smad7 to the plasma membrane. *J Biol Chem* **277:** 39919–39925

Takahashi Y, Ohoka N, Hayashi H, Sato R (2008) TRB3 suppresses adipocyte differentiation by negatively regulating PPARgamma transcriptional activity. *J Lipid Res* **49:** 880–892

ten Dijke P, Arthur HM (2007) Extracellular control of TGFb signalling in vascular development and disease. *Nature Rev Mol Cell Biol* **8:** 857–868

Wang HR, Ogunjimi AA, Zhang Y, Ozdamar B, Bose R, Wrana JL (2006) Degradation of RhoA by Smurf1 ubiquitin ligase. *Methods Enzymol* **406:** 437–447

Wang Q, Huang Z, Xue H, Jin C, Ju XL, Han JD, Chen YG (2008) MicroRNA miR-24 inhibits erythropoiesis by targeting activin type I receptor ALK4. *Blood* **111:** 588–595

Wang T, Zhang X, Obijuru L, Laser J, Aris V, Lee P, Mittal K, Soteropoulos P, Wei JJ (2007) A micro-RNA signature associated with race, tumor size, and target gene activity in human uterine leiomyomas. *Genes Chromosomes Cancer* **46:** 336–347

Yang X, Long L, Southwood M, Rudarakanchana N, Upton PD, Jeffery TK, Atkinson C, Chen H, Trembath RC, Morrell NW (2005) Dysfunctional Smad signaling contributes to abnormal smooth muscle cell proliferation in familial pulmonary arterial hypertension. *Circ Res* **96:** 1053–1063

Yi ES, Kim H, Ahn H, Strother J, Morris T, Masliah E, Hansen LA, Park K, Friedman PJ (2000) Distribution of obstructive intimal lesions and their cellular phenotypes in chronic pulmonary hypertension. A morphometric and immunohistochemical study. *Am J Respir Crit Care Med* **162** (4 Part 1)**:** 1577–1586

Yoshida T, Gan Q, Shang Y, Owens GK (2007) Platelet-derived growth factor-BB represses smooth muscle cell marker genes via changes in binding of MKL factors and histone deacetylases to their promoters. *Am J Physiol Cell Physiol* **292:** C886–C895